System Identification and Control Systems Engineering Approaches for Optimal and Practical Personalized mHealth Interventions for Physical Activity

by

Mohamed El Mistiri

A Dissertation Presented in Partial Fulfillment
of the Requirements for the Degree
Doctor of Philosophy

Approved April 2024 by the
Graduate Supervisory Committee:

Daniel E. Rivera, Chair
Shuguang Deng
Christopher Muhich
Theodore P. Pavlic
Wenlong Zhang

ARIZONA STATE UNIVERSITY

May 2024

ABSTRACT

Physical inactivity is a major contributor to chronic illnesses and mortality globally. However, most interventions to address it rely on static, aggregate models that overlook idiographic (i.e., individual-level) dynamics, limiting intervention effectiveness. Leveraging mobile technology and control systems engineering principles, this dissertation provides a novel, comprehensive framework for personalized behavioral interventions that have been tested experimentally under the Control Optimization Trial (COT) paradigm. Through careful design of experiments, elaborate signal processing and model estimation, and judicious formulation of behavior intervention optimization as a control system problem, this dissertation develops tools to overcome challenges faced in the large-scale dissemination of mobile health (mHealth) interventions. A novel Three-Degrees-of-Freedom Kalman Filter-based Hybrid Model Predictive Control (3DoF-KF HMPC) controller is formulated for physical activity interventions and evaluated in a clinical trial, demonstrating its effectiveness.

Furthermore, this dissertation expands on understanding the underlying dynamics influencing behavior change. Engineering principles are applied to develop a conceptual approach to generate dynamic hypotheses and translate these into first-principle dynamic models. The generated models are used in concert with system identification principles to enhance the design of experiments that yield dynamically informative data sets for behavioral medicine applications. Additionally, sophisticated search, filtering, and model estimation algorithms are applied to optimize and personalize model structures and estimate dynamic models that account for nonlinearities and "Just-in-Time" (JIT; moments of need, receptivity, and opportunity) context in behavior change systems. In addition, the pervasive issue of data missingness in interventions is addressed by integrating system identification principles with a Bayesian inference model-based technique for data imputation. The findings in this dissertation

extend beyond physical activity, offering insights for promoting healthy behaviors in other applications, such as smoking cessation and weight management.

The integration of control systems engineering in behavioral medicine research, as demonstrated in this dissertation, offers broad impacts by advancing the field's understanding of behavior change dynamics, enhancing accessibility to personalized behavioral health interventions, and improving patient outcomes. This research has the potential to radically improve behavioral interventions, increase affordability and accessibility, inspire interdisciplinary collaboration, and provide behavioral scientists with tools capable of addressing societal challenges in mHealth and preventive medicine.

To my family, for all their love, support, and patience throughout my life, and especially through graduate school.

To my parents, Dr. Mufid and Dr. Hekmet. Since a young age, you have been role models for me, with your dedication and passion for helping your patients and expanding knowledge.

To my grandparents, who called me their "young scientists" for as long as I can recall. Although they may no longer be with us, their passion for science, curiosity, and exploring new paths continues to live on through me.

ACKNOWLEDGEMENT

First and foremost, I would like to express my deepest gratitude to my advisor Dr. Daniel E. Rivera. I have been a part of the Control Systems Engineering Lab (CSEL) under Dr. Rivera's supervision, since 2020. During these four years, I have grown into the engineer and researcher I am today. Dr. Rivera's knowledge, dedication, and approach to research and problem-solving have been fundamental to my learning and success in finishing this work. Dr. Rivera has also been a mentor for me on a personal level, providing guidance and support and leading by example with his inspirational hard work, extraordinary work ethic, and professionalism. I would like to thank him for his guidance and understanding during these years.

I have been fortunate to collaborate with remarkable researchers on this work, to whom I extend my sincere gratitude. I would like to thank Drs. Christopher Muhich, Theodore P. Pavlic, Shuguang Deng, and Wenlong Zhang for serving on my graduate committee, offering their time, and sharing their comments and knowledge to guide and expand my research. Additionally, I express my special thanks to Drs. Eric Hekler and Predrag Klasnja for their support and for sharing their passion and vision for enhancing the efficacy and accessibility of preventive behavioral interventions to improve public health. Their generosity with their knowledge in behavioral science has been instrumental in shaping my understanding of behavior change theories and the design of the experiments for the studies explored in this work. I am also very grateful to Drs. Steven De La Torre, Donna Spruijt-Metz, Benjamin M. Marlin, and Misha Pavel for their guidance and insights regarding missing data imputation and modeling changes in engagement in behavior change interventions.

In addition, I wish to extend my deepest gratitude to current and past members of CSEL at Arizona State University and the Design Lab at the University of California

San Diego: Drs. Naresh N. Nandola, Ceśar A. Martin, Owais Khan and Meelim Kim, as well as, Junghwan Park, Rachael T. Kha, and Sarasij Banerjee. You have all brightened my journey and I appreciate all the personal and professional relationships we have built.

Last but not least, I have been blessed by growing up in a supportive family, with a tremendous appreciation for science and research. To my parents, Drs. Mufid El Mistiri and Hekmet Bugrein, words cannot express how grateful I am for all your support over the years and for instilling in me the values of integrity, hard work, and passion for benefiting society through science. To my sister, Dr. Sara El Mistiri, witnessing your resilience and determination in overcoming all the challenges in medical school has motivated me to reach excellence in my own pursuits. To my younger brother, Jamal El Mistiri, you have always been supportive and there to cheer me with all the good vibes. Your belief in me has always inspired me to set a good example. I am certain you will accomplish all your goals and become an aspiring young engineer.

This work would have not been possible without the financial support of multiple parts from the National Institutes of Health (NIH), particularly, the National Cancer Institute (NCI) through grants U01 CA229445 and R01 CA244777 and the National Library of Medicine (NLM) through grant R01 LM013107. The opinions in this dissertation are my own and not necessarily those of NIH.

TABLE OF CONTENTS

Page

LIST OF TABLES xii

LIST OF FIGURES xiii

CHAPTER

1 INTRODUCTION 1

1.1 Motivation 1

1.2 Personalized Input Signal Design 9

1.3 Modeling Physical Activity Behavior Change 13

1.4 Control Strategies for Personalized Optimal Adaptive Behavioral Interventions 18

1.5 Data Missingness and Imputation 21

1.6 Contributions of The Dissertation 23

1.7 Dissertation Outline 26

1.8 Publications Summary 29

2 ENHANCED SOCIAL COGNITIVE THEORY DYNAMIC MODELING AND SIMULATION TOWARDS IMPROVING THE ESTIMATION OF "JUST-IN-TIME" STATES 34

2.1 Introduction 34

2.2 Social Cognitive Theory (SCT) 37

2.3 Intervention Design: *JustWalk JITAI* 39

2.4 Input Signal Design 42

2.5 Simulation Results & Discussion 46

2.5.1 Adherent participant: No Disturbances 47

2.5.2 Adherent Participant: With Disturbances 50

2.5.3 Non-adherent Participant: No Disturbances 53

CHAPTER Page

2.5.4 Non-adherent Participant: With Disturbances 54
2.6 Conclusions 57
3 SYSTEM IDENTIFICATION AND SIGNAL PROCESSING IN UNDERSTANDING "JUST-IN-TIME" STATES FOR PHYSICAL ACTIVITY: ANALYSIS OF THE *JUSTWALK JITAI* INTERVENTION 59
3.1 Introduction 59
3.2 Study Description & Input Signal Design 61
3.3 Model-on-Demand (MoD) 63
3.4 Noise Reduction & Signal Separability: Singular Spectrum Analysis (SSA) 68
3.5 Results & Discussion 71
3.5.1 SSA: Noise Reduction and Signal Separability 71
3.5.2 Model Estimation and cross-validation 75
3.5.3 MoD: Analyzing Behavior in Context 85
3.6 Conclusions & Future Work 87
4 MODEL PREDICTIVE CONTROL IN MHEALTH: A DECISION FRAMEWORK FOR OPTIMIZED PERSONALIZED PHYSICAL ACTIVITY INTERVENTIONS 89
4.1 Introduction 89
4.2 Simulation Model & Intervention Design 93
4.2.1 Social Cognitive Theory (SCT) 94
4.2.2 Fluid Analogy Formulation for SCT 94
4.2.3 Intervention Design & Development 96

CHAPTER Page

4.3 Results and Discussion 99
4.3.1 Participant A: Adherent Participant 100
4.3.2 Non-Adherent Participant 118
4.4 Summary and Conclusions 124
5 SYSTEM IDENTIFICATION AND HYBRID MODEL PREDICTIVE CONTROL IN PERSONALIZED MHEALTH INTERVENTIONS FOR PHYSICAL ACTIVITY 127
5.1 Introduction 127
5.2 SCT-based adaptive behavioral intervention 131
5.3 *JustWalk* Intervention 135
5.3.1 *JustWalk* Input Signal Design 136
5.3.2 ARX Model Structure Estimation & Validation 139
5.4 HMPC formulation for adaptive PA intervention 147
5.4.1 3DoF-KF HMPC Framework 148
5.4.2 Logical and Discrete Constraints 162
5.4.3 Maintenance Phase 164
5.5 Results and Discussion 165
5.5.1 Nominal Case 167
5.5.2 Robustness Analysis 169
5.6 Conclusions and Future Work 172

CHAPTER Page

6 INPUT SIGNAL DESIGN, MODEL ESTIMATION, AND HYBRID MODEL PREDICTIVE CONTROL STRATEGIES IN THE CONTROL OPTIMIZATION TRIAL FRAMEWORK: ANALYSIS OF *YOURMOVE*, A PHYSICAL ACTIVITY INTERVENTION 174

6.1 Introduction 174

6.2 *YourMove* Intervention 177

6.3 *YourMove* Input Signal Design 182

6.3.1 Zippered Multisine 184

6.3.2 Shifted Multisine 187

6.3.3 Selection of Input Signal Approach 190

6.3.4 Personalization of the Input Signals 193

6.4 *YourMove* Idiographic Modeling for a Generalized Intervention Structure 195

6.4.1 DSPSA in Estimating Individualized ARX Models 196

6.4.2 Generalized Predictive Model for HMPC 206

6.4.3 Missingness and Data Imputation 209

6.5 Control Strategies 209

6.5.1 Default Tuning 210

6.5.2 Maintenance Reconfiguration 213

6.5.3 Stagnation in Disturbance Measurements 214

6.5.4 "Open-Loop" Policy 217

6.5.5 GA Constraints Tightening 219

6.5.6 Expected Points Reconfiguration 222

CHAPTER Page

6.5.7 Transitioning Back to Default Tuning 223
6.6 Preliminary Results 224
6.6.1 Participant A 225
6.6.2 Participant B 232
6.6.3 Participant C 237
6.7 Preliminary Findings & Future Work 243
7 MODELING AND SYSTEM IDENTIFICATION OF USER ENGAGEMENT IN MHEALTH INTERVENTIONS USING A BAYESIAN APPROACH FOR MISSING DATA IMPUTATION 248
7.1 Introduction 248
7.2 Materials and Methods 251
7.2.1 HearSteps II 251
7.2.2 Theory-Based Dynamic Modeling 254
7.2.3 Bayesian-Based Data Imputation 256
7.2.4 Data Analysis 259
7.3 Results 263
7.4 Discussion 266
7.5 Conclusions 274
8 SUMMARY, CONCLUSIONS AND FUTURE WORK 275
8.1 Summary and Conclusions 275
8.2 Future Research Directions 280
8.2.1 Within-day Models 280
8.2.2 *YourMove JITAI* 281

CHAPTER Page

8.2.3 Semiphysical Modeling 284

REFERENCES 286

APPENDIX

A CONSENT FOR ACADEMIC USE OF COLLABORATIVE WORK 299

LIST OF TABLES

Table Page

2.1 List of the SCT Inputs and Outputs Considered in This Chapter from. 39

2.2 Notification Rates (in Notifications/day) for Each Decision Rule Per Scenario. 49

3.1 Summary of the NRMSE Fit Indices of the MoD and ARX-Based Estimators for Each of the Reconstructed Uncorrelated SSA Components of *Step Count*. 79

3.2 Summary of the NRMSE Fit Indices of the MoD and ARX-Based Estimators for Each of the Reconstructed Uncorrelated SSA Components of *Step Count*. 84

5.1 List of Measured Signals Included in the Estimated ARX Model and Their Correspondence with the Variables in the SCT Model. 142

5.2 Table Summarizing ARX Orders Obtained for All the Possible Combinations of Estimation and Validation Cycles, with a Minimum of Two Estimation Cycles. 144

6.1 EMA Survey Questions Used in *YourMove* Study, Along with Their Respective Behavioral Constructs. 180

6.2 DSPSA Parameters Used in *YourMove* Study. 206

6.3 Default Control Design Parameters for *YourMove*. 214

7.1 *HeartSteps II* Construct and Variables. 253

7.2 Performance of the Four Examined Imputation Methods: Mean Realization of the Bayesian Inference Approach, Forward-fill, Backward-fill, and Linear Interpolation. 264

7.3 Summary of the Fit Indices of the ARX Models Estimated from the Raw Data and Data Imputed By Four Different Methods. 265

LIST OF FIGURES

Figure Page

1.1 Simulation Results Illustrating the Proposed Control Optimization Trial (COT) Behavioral Intervention Phases, Based on a Representative Participant from *JustWalk*. 6

1.2 Schematic Depicting the Proposed Structure for Control Optimization Trial (COT) Behavioral Interventions, and Their Relation to the Chapters in This Dissertation. 7

1.3 Depicts the Hypothesized Relationship Between Steady-State Goals and Daily Step Counts, Based on the Baseline Performance Prior to the Intervention. 11

1.4 Combined PRBS and RMLS That Defines the Decision Rule Signal for *JustWalk JITAI*. 12

1.5 Schematic Depicting the Fluid Analogy of a Simplified SCT Model in an Open-Loop Setting. 15

1.6 Block Diagram Schematic Depicting the Proposed Three-Degrees-Of-Freedom By Means of Kalman Filter HMPC (3DoF-KF HMPC) Structure, Aiming to Achieve Setpoint Tracking While Effectively Accounting for Both Measured and Unmeasured Disturbances. 20

2.1 Schematic Illustrating the Fluid Analogy of the Social Cognitive Theory Model. 38

2.2 Multisine Base Cycle for the Goal Setting Input Signal in the Time Domain (Top) Along with Its Spectral Power Density (Bottom). 43

2.3 Base PRBS Signal for the Decision Rules Signal in *JustWalk JITAI*. . . . 44

2.4 Combined PRBS and RMLS Constructing the Decision Rule Signal in *JustWalk JITAI*. 46

Figure Page

2.5 Simulated Results Illustrating the Response of an Adherent Participant to the Designed Input Signals, in the Absence of Any Disturbances. ... 48

2.6 Simulation That Illustrates the Response of an Adherent Participant to the Designed Input Signals, in the Presence of Disturbances in the Form of *Perceived Barriers/Obstacles* and Bad *Environmental Context.* 51

2.7 Notifications Sent Throughout the Intervention (Middle), the Decision Rules (Bottom) and *Goal Attainment* (Top) Associated with Notifications Sent Each Day for the Adherent Participant in the Presence of the Disturbances. 52

2.8 Simulation Illustrating the Response of a Non-Adherent Participant to the Designed Input Signals, in the Absence of Disturbances..... 54

2.9 Simulation Illustrating the Response of a Non-Adherent Participant to the Designed Input Signals, in the Presence of Disturbances in the Form of *Perceived Barriers/obstacles* and Bad *Environmental Context.*. 55

2.10 Notifications Sent Throughout the Intervention (Middle), the Decision Rules (Bottom) and *Goal Attainment* (Top) Associated with Notifications Sent Each Day for the Non-Adherent Participant in the Presence of the Disturbances. 56

3.1 Schematic Illustrating MoD Adaptive Selection of Regressor Neighborhood Size At an Operating Point. 64

3.2 (A) Time Series, (b) Spectral Power Density of the *Step Count* Components ($\hat{Y}_i \ \forall \ 1 \leq i \leq L$) Decomposed By SSA, Along with Their Relevance (r_i). 72

Figure Page

3.3 Original (Y) and SSA-Filtered (Y_{SSA}) Daily *Step Count* Signals in Steps/day, Along with Residuals. 73

3.4 Reconstructed Signals of Uncorrelated Groups of SSA Components for *Step Count*. 74

3.5 Case I Simulation Results for MoD and ARX-Based Estimators Compared to the Unfiltered *Step Count* Signal Y. 77

3.6 Case II Simulation Results for MoD and ARX-Based Estimators for Each of the Uncorrelated Reconstructed SSA Components (Trend, Seasonality 1, Seasonality 2). 78

3.7 Case II Simulation Results of the Combined Model Estimated Using the MoD and ARX-Based Estimators Compared to (a) the SSA-Filtered *Step Count* Signal Y_{SSA}, And (b) the Unfiltered *Step Count* Signal Y. 81

3.8 Case III Simulation Results of the Combined Model Estimated Using the MoD and ARX-Based Estimators Compared to (a) the SSA-Filtered *Step Count* Signal Y_{SSA}, And (b) the Unfiltered *Step Count* Signal Y. 82

3.9 Impulse Responses for MoD and ARX-Based Estimators in a Simulated Hypothetical Scenario Illustrating the Change in MoD Responses for a Representative *JustWalk JITAI* Participant At Different Operating Conditions. 86

4.1 Schematic Illustrating the Receding Horizon Strategy for MPC. 91

Figure Page

4.2 Schematic Depicting the Fluid Analogy of the SCT Model for an Operant Learning-Self-Efficacy (OLSE) System in an Intervention Setting Including the Implementation of MPC Controller. 95

4.3 Simulation Results from Applying an Unconstrained MPC Controller on the Self-Efficacy Loop for an Adherent Participant. 102

4.4 Simulation Results from Applying a Constrained MPC Controller on the Self-Efficacy Loop for an Adherent Participant, with a Lower Bound Constraint on *Self-Efficacy*. 104

4.5 Simulation Results from Applying a Constrained MPC Controller on the Self-Efficacy Loop for an Adherent Participant, with a Lower Bound Constraint Applied on Goal Attainment. 106

4.6 Simulation Results from Applying a Constrained MPC Controller on OLSE System for an Adherent Participant, in the Presence of a Measured Random Disturbance (Deviations of the Average Daily Temperature from the Participant's Preference). 108

4.7 Schematic Illustrating an Operant-Learning Loop Illustrating Dual (and Competing) Behavioral Outcome Dynamics, with *Fitness* and *Fatigue* in the Loop. 110

4.8 Simulation Results from Applying Constrained MPC on Dual BO Dynamics OLSE System for an Adherent Participant in the Presence of a Measured Random Disturbance (Deviations of the Average Daily Temperature from the Participant's Preference). 112

Figure Page

4.9 Simulation Results for an Adherent Participant Illustrating the Closed-Loop Responses of *Fitness*, *Fatigue*, and *Behavioral Outcomes* Performance for the Adherent Participant. 113

4.10 Simulation Results from Applying Constrained MPC on Dual BO Dynamics OLSE System for an Adherent Participant, in the Presence of Nonlinearity and a Measured Random Disturbance. 115

4.11 Simulation Results from Applying Constrained MPC on Dual BO Dynamics OLSE System for an Adherent Participant, in the Presence of Nonlinearity and a Measured Random Disturbance. 117

4.12 Simulation Results from Applying Constrained MPC on Dual BO Dynamics OLSE System for a Non-Adherent Participant, in the Presence of a Measured Random Disturbance (Deviations of the Average Daily Temperature from the Participant's Preference). 120

4.13 Simulation Results from Applying Constrained MPC on Dual BO Dynamics OLSE System for a Non-Adherent Participant, in the Presence of Nonlinearity and a Measured Random Disturbance (Deviations of the Average Daily Temperature from the Participant's Preference). 123

5.1 Simulation Illustrating Control Optimization Trial (COT) Behavioral Intervention Phases. 129

5.2 Simplified SCT Model in a Fluid Analogy 132

5.3 Schematic Depicting a Personalized PA Intervention Based on a Participant-Specific Model, as Used in *JustWalk* and *YourMove*. 134

5.4 The *JustWalk* App Interface. 136

Figure Page

5.5 Representation of a "Zippered" Spectra Design for Number of Designed Inputs $n_u = 2$, and $n_s = 3$ Excited Harmonic Frequencies Per Input Channel. 138

5.6 Table Summarizing ARX Orders Obtained for All the Possible Combinations of Estimation and Validation Cycles, with a Minimum of Two Estimation Cycles. 145

5.7 Step Responses of the 5-Input Model Estimated for a Representative *JustWalk* Participant. 147

5.8 Block Diagram Schematic Depicting the Proposed Three-Degrees-Of-Freedom By Means of Kalman Filtering HMPC Structure, Aiming to Achieve Setpoint Tracking While Effectively Accounting for Both Measured and Unmeasured Disturbances. 149

5.9 Closed-Loop Simulation Results from the Implementation of HMPC in a Personalized Intervention for a Representative *JustWalk* Participant, in the Presence of Measured Disturbances (Temperature and Weekend/Weekday) and Unmeasured Stochastic Disturbance. 168

5.10 Closed-Loop Monte Carlo Simulation Results from the Implementation of HMPC in a Personalized Intervention for *JustWalk* Participant A, in the Presence of Measured Disturbances (Temperature and Weekend/Weekday) and Unmeasured Stochastic Disturbance. 171

6.1 Simulation Results Illustrating the Stages of the Control Optimization Trial (COT) Behavioral Intervention, Based on a Representative Participant from *JustWalk*. 177

Figure Page

6.2 Examples of the Custom Watch-Face Variations Provided to Participants in *YourMove*. 179

6.3 Schematic Illustrating the Common Practice in Multisine Input Signal Design Where the Relative Amplitude for Harmonics Past ω^* is 0. 185

6.4 Power Spectral Density of the Designed Inputs in a Two-Channel Signal, Illustrating the Alternating Harmonics in the Zippered Spectra Approach. 186

6.5 Time-domain Depiction of the Designed Zippered Input Signals (u_8, u_9) in *YourMove*. 187

6.6 Cross-correlation Coefficients for Zippered Signals for the First 40 Lags, with Standard Error Bounds of 3σ. 188

6.7 Time-domain Depiction of the Designed Shifted Signal in Two Input Channels (u_8, u_9). 189

6.8 Cross-correlation Coefficients for the Designed Shifted Input Signals for the First 20 Lags, with Confidence Bounds of $3\sigma^2$. 190

6.9 Power Spectral Density of the Designed Shifted Input Signal for Two Channels Illustrating the Overlap in the Harmonics. 191

6.10 Depicts a Stochastic Algorithm Minimizing a Loss Function. 199

6.11 Flowchart Summarizing the Algorithm Followed in Tuning the Controller Based on the Participant's Performance. 215

6.12 Participant A Data for the Three COT Stages of *YourMove* Study. The Open-Loop Stages (Consisting of Baseline and System Identification Stages) Are Highlighted in Red and Cyan, Respectively. 227

Figure Page

6.13 Unit Step Responses for the Estimated Model Dynamics for Participant A, Along with Their Respective Steady-state Gains. 228

6.14 Participant B Data for the Three COT Stages of *YourMove* Study. The Open-Loop Stages (Consisting of Baseline and System Identification Stages) Are Highlighted in Red and Cyan, Respectively. 233

6.15 Unit Step Responses for the Estimated Model Dynamics for Participant B, Along with Their Respective Steady-state Gains. 235

6.16 Participant C Data for the Three COT Phases of *YourMove* Study. Baseline, System Identification, and Maintenance Phases Are Highlighted in Red, Cyan, and Green, Respectively. 239

6.17 Unit Step Responses for the Estimated Model Dynamics for Participant C, Along with Their Respective Steady-state Gains. 240

7.1 Fluid Analogy Representation of the Hypothesized DBCI App Engagement Model. 255

7.2 Graphic Representation of the Dynamic Bayesian Network Model Representation of the Hypothesized Model, Used to Impute Missing Data Points in a Markov Chain Monte Carlo Sampling Approach. 258

7.3 Unit Step Responses of the 5-Input ARX Model Estimated from the Raw Data, Along with Their Steady-State Gains. 267

7.4 Time Series Plot Representing the Results of the Estimated ARX Models for a Representative *HeartSteps II* Participant Utilizing Raw Data and the Mean Realization of the Bayesian Inference Imputation for the Case of 3.97% Missingness. 268

Figure Page

7.5 Time Series Plot Representing the Results of the Estimated ARX Models for a Representative *HeartSteps II* Participant Utilizing Raw Data and the Mean Realization of the Bayesian Inference Imputation for the Case of 33.73% Missingness (Withholding Data Points on 75 Days). . . . 270

7.6 Unit Step Responses of the 5-Input ARX Models Estimated from the Raw Data and the Imputed Data Sets in the Case of 3.97% Missingness. 272

7.7 Unit Step Responses of the 5-Input ARX Models Estimated from the Raw Data and the Imputed Data Sets in the Case of 33.73% Missingness. 273

8.1 Block Diagram Schematic Representing a Proposed MoD-Based 3DoF-KF MPC for Setpoint Tracking of a Process Subject to Constraints, Measured and Unmeasured Disturbances. 283

Chapter 1

INTRODUCTION

1.1 Motivation

Significant advances in technology in recent decades have ushered the development of sophisticated computational and mathematical tools, which have resulted in an improved understanding of many scientific phenomena through control theory and systems approaches (Luenberger, 2012; Åström and Murray, 2021). Specifically, the scope and applications of control system engineering principles have expanded beyond traditional engineering applications like aerospace (Eren *et al.*, 2017), chemical processes (Ogunnaike and Ray, 1995; Prett and García, 1988), and power systems (Liu *et al.*, 2016); control engineering principles have been applied to solve challenging problems in social and natural sciences including economic, environmental, robotic, and biomedical systems (Leonard *et al.*, 1992; Ford and Ford, 1999; de Wit *et al.*, 2012; Kurzhanski and Vályi, 1997). This is a consequence of the methodical approach that control system engineering provides, with the capability of identifying a dynamical model for the system of interest and designing a model-based controller to achieve a desired magnitude, speed, and shape of response while abiding by system restrictions and operational constraints.

An exciting and growing application of control systems engineering lies in the medical field. Traditionally, healthcare-oriented studies focus on generalized reductionist statistical analysis over a population (or subgroups of populations) which are effective to an extent yet lack the capability of exploring dynamic responses on an individualized level (Cloutier and Wang, 2011; Hekler *et al.*, 2013). In light of the ad-

vances in sensors and methods to gather "intensive" temporally dense data sets, there is recognition in the behavioral and medical fields for the need for computational dynamic models that can lead to a better understanding of phenomena and determine treatment delivery at an individual level. Control systems engineering principles provide formal approaches to analyze time-series data and shift the paradigm towards personalized, data-centric treatment strategies that maximize desired outcomes for each individual while minimizing risks (Kitano, 2002; Ahn *et al.*, 2006). Such goals must be achieved while taking into account system limitations and restrictions due to medical and logistical constraints.

The application of control systems in data-driven personalized healthcare can be split into two main categories: clinical applications aiding in the treatment of chronic illnesses and disorders (O'Shea, 2012), and behavioral medicine aiming to prevent or delay and manage the onset of chronic and relapsing disorders through adaptive interventions (Collins *et al.*, 2004; Rivera *et al.*, 2007b, 2018). Examples in this significant field of application can be found in diverse settings. On the clinical side, examples of efforts in the last decades include: directing chemotherapy towards tumors, to reduce the side effects of the treatment (Nacev *et al.*, 2012); MPC-based controller in optimal delivery of insulin to diabetic patients through an "artificial pancreas", to reduce the adverse effects of high or low glucose blood levels and bring normalcy to the patient's life (Gondhalekar *et al.*, 2016); and optimizing drug delivery and dosage in the treatment of fibromyalgia (Deshpande *et al.*, 2014).

With regards to behavioral medicine, it has been established that unhealthy habits such as smoking, poor diet, and physical inactivity are major contributors to chronic illnesses including cancer, cardiovascular disease, arthritis, and Type 2 diabetes (Fielding, 1985; Booth *et al.*, 2012; Saint-Maurice *et al.*, 2020). The impact of chronic illnesses on society, in terms of healthcare expenditure and reduced pro-

ductivity, is quite vast; it has been estimated that annual costs of smoking in the US are in the proximity of 300 billion dollars (US Department of Health and Human Services and others, 2014; Klein *et al.*, 2021). Moreover, such conditions reduce the quality of life of patients and have been estimated to contribute more than 50% to preventable deaths (Hekler *et al.*, 2013). Taking these facts into consideration, this work is focused on the application of control systems engineering principles in behavioral medicine, with the aim of the dissemination of preventive interventions on a large scale to improve individual and public health. The main goals proposed in this dissertation include: assessing the effectiveness of dynamical systems modeling in capturing human behavior, improving the effectiveness of system identification experimental design and dynamic modeling approaches in behavioral interventions with human subjects, and establishing a framework to deploy Model Predictive Control (MPC) strategies and evaluate these online, in real-world settings. In support of the concepts in this dissertation, there are efforts in establishing the control optimization trial (COT; Hekler *et al.* (2018)) framework for automated, personalized, optimal behavioral interventions and studies such as *YourMove* (R01CA244777, 2020) and *JustWalk Just-In-Time-Adaptive-Intervention* (JITAI; R01LM013107 (2020)) provide the means to validate the proposed work in experimental settings.

There have been a number of significant contributions to the application of control systems engineering principles in behavioral medicine that have taken place in recent years. In Rivera *et al.* (2018), a general outline for procedures to construct control-oriented dynamic models and design adaptive behavioral interventions was presented. Such procedures are inspired by the work done to obtain dynamical models for the Theory of Planned Behavior (TPB; Navarro-Barrientos *et al.* (2011)), and Social Cognitive Theory (SCT; Martín *et al.* (2014, 2020); Martín (2016)), which are highly regarded theories of behavior change and have been applied in behavioral

interventions for gestational weight gain (Dong *et al.*, 2012, 2013; Dong, 2014; Guo, 2018; Guo *et al.*, 2020) and physical activity (Martín *et al.*, 2015a; Martín *et al.*, 2016a,b) respectively. Other studies in this area have also explored the application of control systems engineering principles to gain insights into the dynamics of smoking cessation and to optimize behavioral interventions for this purpose (Timms *et al.*, 2013, 2014a,b,c,d; Timms, 2014).

In understanding problems related to physical activity (PA) behavior change and adaptive interventions, the use of fluid analogies (Rivera *et al.*, 2018) has led to the interpretation of behavior change theories like SCT into a semi-physical dynamic system that can be computationally modeled using engineering principles such as mass conservation (Martín *et al.*, 2020; El Mistiri *et al.*, 2022b). In previous work, system identification principles have been applied in experiment design for the *JustWalk* intervention and model estimation from the experimental data (Freigoun *et al.*, 2017; Martín, 2016). Furthermore, control strategies have been studied to deliver adaptive behavioral interventions using three-degree-of-freedom Hybrid Model Predictive Control (HMPC; Nandola and Rivera (2013)). However, the work has been limited to hypothetical representative models (Martín *et al.*, 2016a) and black-box dynamic models estimated from *JustWalk* data (Cevallos *et al.*, 2022; Khan *et al.*, 2022; El Mistiri *et al.*, 2023), which did not cover the full scope of the problem due to limitations of the original *JustWalk* study. These include the lack of *a priori* knowledge of the system in terms of the dominant time constant, as well as the absence of continuous measurements for SCT constructs of interest (where five-point Likert scales used to represent each construct did not provide sufficient variability in the measurements). Moreover, the prior work on PA behavioral interventions focused on behavior on a daily level and left much to be desired with regard to understanding multi-timescale dynamics and Just-In-Time (JIT) states associated with behavior change.

In this work, we leverage the prior knowledge from earlier research to advance the understanding of dynamical process systems associated with human behavior and behavior change, especially for PA interventions. Analysis of the previous *JustWalk* experimental data provides a solid foundation to improve and enhance the experimental design and input signals designed for the ongoing behavioral interventions promoting PA: control optimization trial *YourMove*, and *JustWalk JITAI*; these interventions focus on promoting higher levels of PA, in the form of the number of steps walked daily, for sedentary adults. Additionally, this dissertation presents data analysis for the micro-randomized trial (MRT) study under the name of *HeartSteps II*, focusing particularly on hypothesizing dynamic models for engagement in PA interventions and addressing the common challenge of missing data in behavioral interventions. The work presented in this dissertation plays a vital role in the development of the control optimization trial (COT) framework, in which a comprehensive approach to developing personalized optimal interventions is established, from system identification experiment design and individualized model estimation to control system design and implementation, as shown in Fig. 1.1 and Fig. 1.2.

In Chapter 4, closed-loop MPC strategies to overcome challenges with the lack of consistent measurements, while providing personalized PA interventions are presented. In *YourMove*, significantly improved experiment design, model estimation, and HMPC strategies are based on the observations made from analyzing *JustWalk* data, as shown in Chapters 5 and 6 of this dissertation. The psychoactive behavioral constructs of interest in the interventions are self-perceived and measured through means of self-reporting and self-reflection. These constructs have proven to be difficult to measure consistently, which can have a major impact on data analysis, estimated models accuracy, and the degree to which behavioral interventions can be personalized. Methods to elicit greater variability in the measurements are considered in this

work, as well as the approach followed to address missing data points in *YourMove*, as discussed in Chapter 6. The culmination of research efforts over the last years in the application of system identification and control systems engineering principles in adaptive behavioral interventions have come to fruition with the proposed strategies in one of the first of its kind large-scale clinical trials involving HMPC closed-loop adaptive intervention promoting PA in *YourMove*.

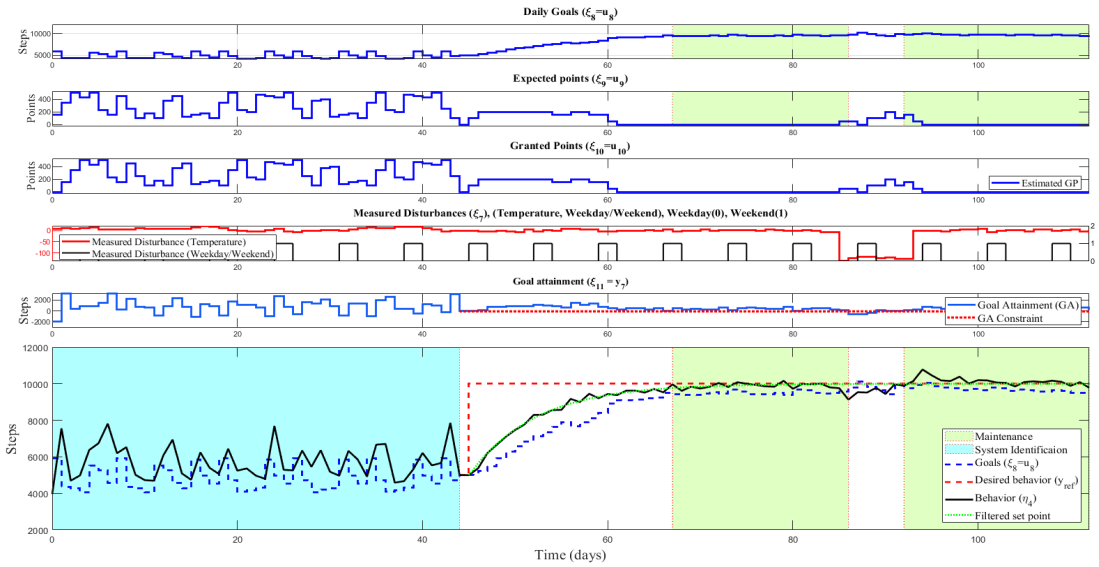

Figure 1.1: Simulation Results Illustrating the Proposed Control Optimization Trial (COT) Behavioral Intervention Phases, Based on a Representative Participant from *JustWalk*. Highlighted in Cyan is the System Identification Phase, and in Green is the Maintenance Phase, While the Unhighlighted Areas Represent the Initiation Phase. Aspects of the COT Are Discussed in Chapters 4, 5, and 6.

The concept of just-in-time adaptive intervention (JITAI; Perski *et al.* (2022); Klasnja *et al.* (2015); Nahum-Shani *et al.* (2015)) has been introduced in the field of behavioral science to address a key gap in the field's understanding of dynamic processes of behavior change. Therefore, in *JustWalk JITAI* an unconventional in-

put signal design is introduced to identify and model the multi-timescale dynamics (within-day and on a daily level) associated with PA behavior change and JIT states. JIT states are hypothesized to present conditions where the provision of support is only administered when it is expected to yield favorable results to counter notification fatigue experienced by participants; this is presented in Chapter 2. As described in Chapter 3, singular spectrum analysis (SSA; Golyandina *et al.* (2001)) is used to study the separability of the output signal into uncorrelated components that describe the idiosyncratic forces influencing behavior change at different time scales. Additionally, a nonlinear black-box modeling technique is examined in the form of Model-on-Demand (MoD; Stenman (1999)) to identify and model JIT states and multi-timescale dynamics.

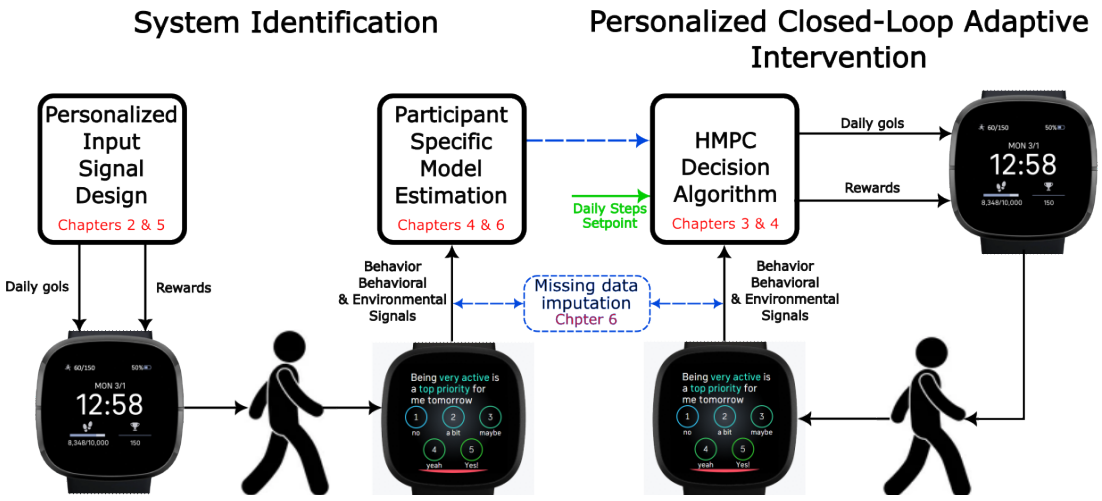

Figure 1.2: Schematic Depicting the Proposed Structure for Control Optimization Trial (COT) Behavioral Interventions, and Their Relation to the Chapters in This Dissertation.

In MRTs, such as *HeartSteps II*, input signal design is substituted by fully randomizing the selection of intervention components to yield data informative of the effect of these components under different conditions. In this work, analysis of the

HeartSteps II data focuses on utilizing fluid analogies to generate a dynamic hypothesis describing engagement in PA interventions and then translating it to a dynamic model. The developed model is utilized in implementing model-based Bayesian inference methods for data imputation, as presented in Chapter 7.

Fundamental and practical questions addressed in this dissertation to further our understanding of behavior change dynamics, develop controllers/decision policies, and the ability to disseminate personalized optimal mHealth intervention as a part of the COT framework include:

1. What system identification experiment's design is needed to estimate and validate useful dynamic models for behavior change? What is the proper amount of excitation needed from the input signal design? What magnitudes and duration of the input signals are needed to obtain informative data while keeping participants engaged?

2. What are the advantages and disadvantages of linear dynamical models for behavior change? When do nonlinear modeling techniques perform more effectively? Can nonlinear modeling techniques capture idiosyncrasies in behavior change dynamics in the context of JIT states?

3. How can the SCT fluid analogy model be enhanced to represent separate and possibly competing dynamics for constructs?

4. How can control strategies be developed to personalize PA interventions based on objectively measured signals while minimizing the effect of missingness (when data imputation is not possible)?

5. How to best formulate a generalized robust predictive controller that can implement the logical conditions in intervention components? How can a controller

be personalized for each individual without the need to significantly adjust the controller structure?

6. How can one best determine the appropriate features and regressor orders for dynamic model estimation, and do so in an efficient manner?

7. How can a systematic and practical tuning approach be developed to independently meet requirements for setpoint tracking, measured, and unmeasured disturbance rejection? The tuning approach must be intuitive to help in the dissemination of personalized closed-loop interventions on a large scale.

8. What are the proper approaches to impute missing data, and mitigate the negative impact of missingness on estimated models?

1.2 Personalized Input Signal Design

Mobile health (mHealth) and wireless behavioral interventions focus on delivering intervention components to users in context (Hekler *et al.*, 2013). This has been made possible through the advances in sensor technology and the popularity of smart devices (smartphones and smartwatches), as they provide access to temporally dense behavioral data, especially in terms of physical activity (Hekler *et al.*, 2016). However, not all data sets are created alike; data sets may not be informative because of the lack of proper excitation. In system identification, input signal design plays an essential role in experimental design that leads to the generation of informative data sets, which can be used to estimate control-oriented dynamic models (Rivera *et al.*, 2002). This is done by assuring the manipulated variables in the system are changed in a way that excites harmonics in the frequency domain covering a desired bandwidth, while abiding by operational and logistical limitations. Consequently, input signal design can be formulated as an optimization problem, where frequency and time domain

requirements serve as constraints.

There is a growing interest in applying system identification approaches, including experimental design, in behavioral health and medicine (Hekler *et al.*, 2016; Martín *et al.*, 2015b; Galvanin *et al.*, 2011). Such a task must be done judiciously, as most input signal design methods are developed with industrial applications in mind, and do not take into account the intricacies of human subjects and personalized adaptive behavioral interventions. The goal of model estimation is to obtain idiographic (i.e., individual) control-oriented dynamic models that can be used to deliver personalized interventions. Therefore, input signals must be designed for each participant to account for the individual's uniqueness and limitations.

The concept of "plant-friendly" input signal design has been introduced in Rivera *et al.* (2002) for industrial applications, where operational requirements including signal duration, amplitude, and rate of change for chemical processes are considered as part of the time domain constraints for multisine signals. Plant-friendliness has then been extended to "patient-friendly" input signal design in Deshpande *et al.* (2014) for applications in clinical trials in the treatment of fibromyalgia. The application of this concept was examined in the input signal design for *JustWalk* (Martín *et al.*, 2015a,b; Riley *et al.*, 2015; Freigoun *et al.*, 2017), where the input signals were designed with limited *a priori* knowledge of the dynamics associated with PA behavior change. In this dissertation, knowledge gained from *JustWalk* data analysis is leveraged to guide the efforts in designing input signals for the ongoing PA behavioral interventions *YourMove* and *JustWalk JITAI*. For both interventions multisine input signals are designed (to define the daily goals given to participants in the intervention) based on a predetermined desired range of effective frequencies, where the signal's distribution and phases are selected based on the solution to the optimization problem that minimizes certain signal aspects like its crest factor, (Guillaume *et al.*, 1991).

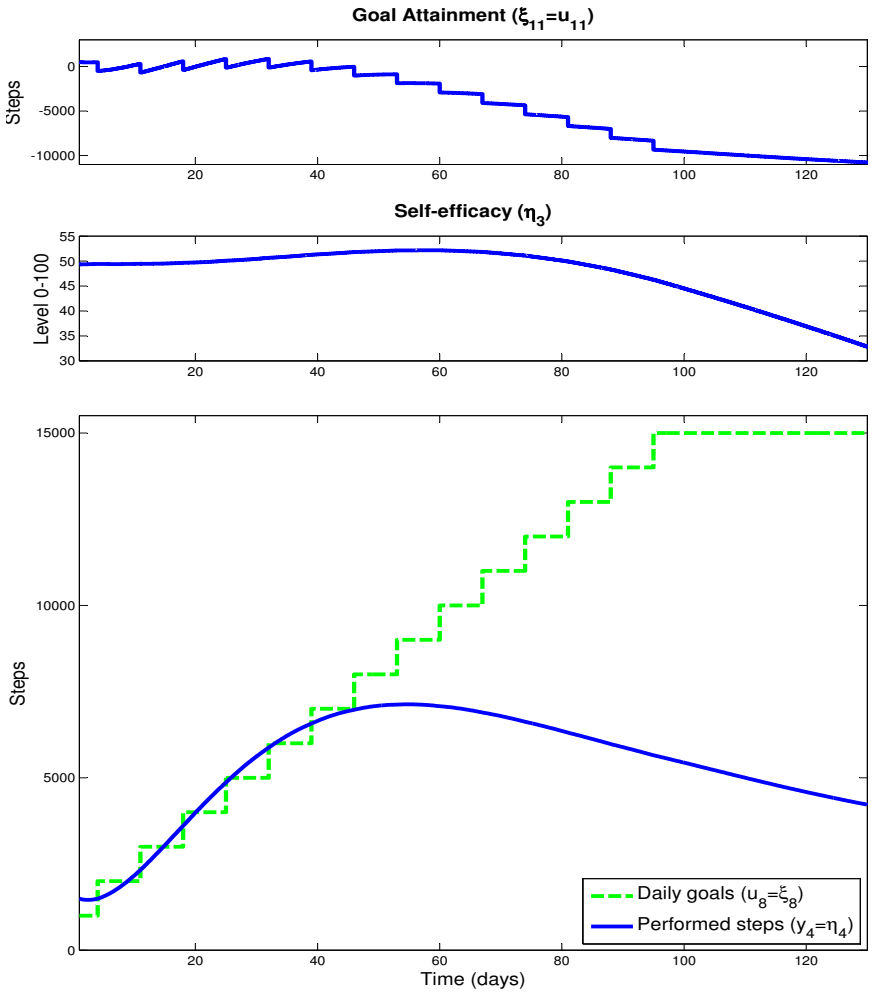

Figure 1.3: Depicts the Hypothesized Relationship Between Steady-State Goals and Daily Step Counts, Based on the Baseline Performance Prior to the Intervention, (Martín *et al.*, 2020).

One of the main observations made from analyzing *JustWalk* experimental data is the significant impact of the daily goals range on the estimated models. It hypothesizes that the relationship between daily goals and the performance of the participant is nonlinear, following an "inverted U" shape as shown in Fig. 1.3 (Martín *et al.*, 2020). This means that the goals given on a certain day must be deemed ambitious but doable by the participant, in order to maximize the benefits of the intervention. As the con-

cept of "ambitious yet achievable" goals depends on the participant's perception and performance, it is important to design the input signals in an individualized manner.

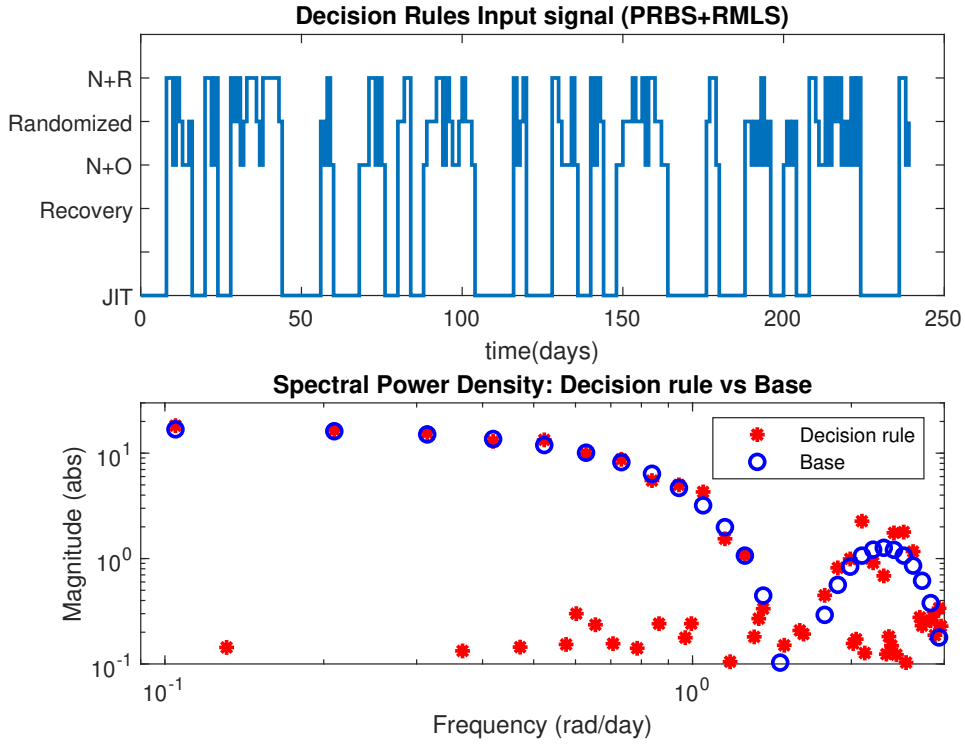

Figure 1.4: Combined PRBS and RMLS That Defines the Decision Rule Signal for *JustWalk JITAI* in the Time Domain (Top). The Spectral Power Density of the Final Decision Rules Signal (Bottom) in Comparison to the PRBS Base.

To personalize daily goals, the signal is scaled based on the average performance of the participant, which can be accomplished in different manners. For example, in *YourMove* the goal range for all cycles is defined based on the average performance of the participant in a baseline stage; this is discussed in more detail in Chapter 6. On the other hand, in *JustWalk JITAI* (presented in Chapter 2) the highest goal given in an input signal cycle varies based on the average performance in the previous cycle. This is a non-conventional approach in input signal design and is done to capture

the hypothesized nonlinearity in the system. Moreover, the proposed input signals for *JustWalk JITAI*, include a modified Pseudo-Random Binary Sequence (PRBS) with a three-level Multi-Level Random Sequence (MLRS) to provide variance and excitation needed in identifying JIT states, as illustrated in Fig. 1.4. A detailed description of the input signal design for *JustWalk JITAI* is provided in Chapter 2.

1.3 Modeling Physical Activity Behavior Change

Theories of behavior change, such as Social Cognitive Theory (SCT; Bandura (1986)) and Self-Determination Theory (SDT; Deci and Ryan (2012)), are conceptual postulations of the interrelations between personal and environmental factors influencing behavior. Such theories provide a detailed narrative description of the hypothesized interconnections between the various constructs shaping human behavior. This narrative description is equivalent to a conceptual model that can be interpreted into a computational model through various statistical modeling techniques, especially with the underlying assumption of the linearity of the relations between the constructs. Various modeling techniques have been applied in the past, including Structural Equation Modeling (SEM; Bollen (1989)) which proved to be effective in modeling steady-state behavior and developing path analysis diagrams for a visual representation of the conceptual model. However, SEM models represent static systems and do not capture the dynamic nature of the system's responses to changes over time. In Rivera *et al.* (2007b), the concept of fluid analogy was introduced as the means to obtain dynamic process models for behavior change systems that are akin to inventory systems in supply chain management (Schwartz *et al.*, 2006). This approach has shown great promise in dynamically modeling theories of behavior change like the Theory of Planned Behavior (TPB) based on a path diagram (Navarro-Barrientos *et al.*, 2011). The derived TPB dynamic model along with a

physiological energy balance model has been applied as the basis for behavioral interventions for weight loss and body composition change, particularly in the case of gestational weight gain problems (Navarro-Barrientos *et al.*, 2011; Dong *et al.*, 2012, 2014; Guo, 2018; Guo *et al.*, 2020).

Social Cognitive Theory (SCT) is a well-regarded theory of behavior change; many behavioral interventions have been developed based on SCT (Lopez *et al.*, 2011), including mHealth interventions for eating habits and physical activity (Norman *et al.*, 2007). SCT is the result of decades of work by behavioral scientists, starting with social learning theory (Bandura and Walters, 1963), which expanded on the learning theory beyond conditioning to clarify social factors like observational learning, and social support that influence acquiring new behaviors or concepts. Self-Efficacy Theory (Bandura, 1977) was then introduced to explain elements of cognition like self-regulation, and self-reflection that can influence behavior based on an individual's perception, which served as the foundation for SCT (Bandura, 1986). What distinguishes SCT is the reciprocity of influence between self-efficacy, social learning elements, and behavior, where the interrelations between the various constructs can sway behavior through nested loops.

In Martín *et al.* (2020), the fluid analogy approach has been applied to obtain a dynamic model for a theory of behavior change, consistent with SCT. A fluid analogy representation of a subsection of SCT is shown in Fig 1.5. In this context, η_i represents the level in inventory i, γ_{ij} represents the gain between inventory i and the inflow/outflow j, β_{iz} denotes the gain in inventory i due to changes in inventory z, and ζ_i is for unmeasured disturbances, where i, j, z are integers. The principle of mass conservation is then applied to each inventory to obtain a dynamic model representation of the system where

$$\text{Accumulation} = \text{Inflow} - \text{Outflow} \tag{1.1}$$

This hypothesized fluid analogy SCT dynamic model served as the basis for the *JustWalk* intervention, which was a physical activity behavioral intervention promoting healthy levels of daily steps to sedentary adults (Riley *et al.*, 2015; Martín, 2016; Freigoun *et al.*, 2017; Phatak *et al.*, 2018; Korinek *et al.*, 2018).

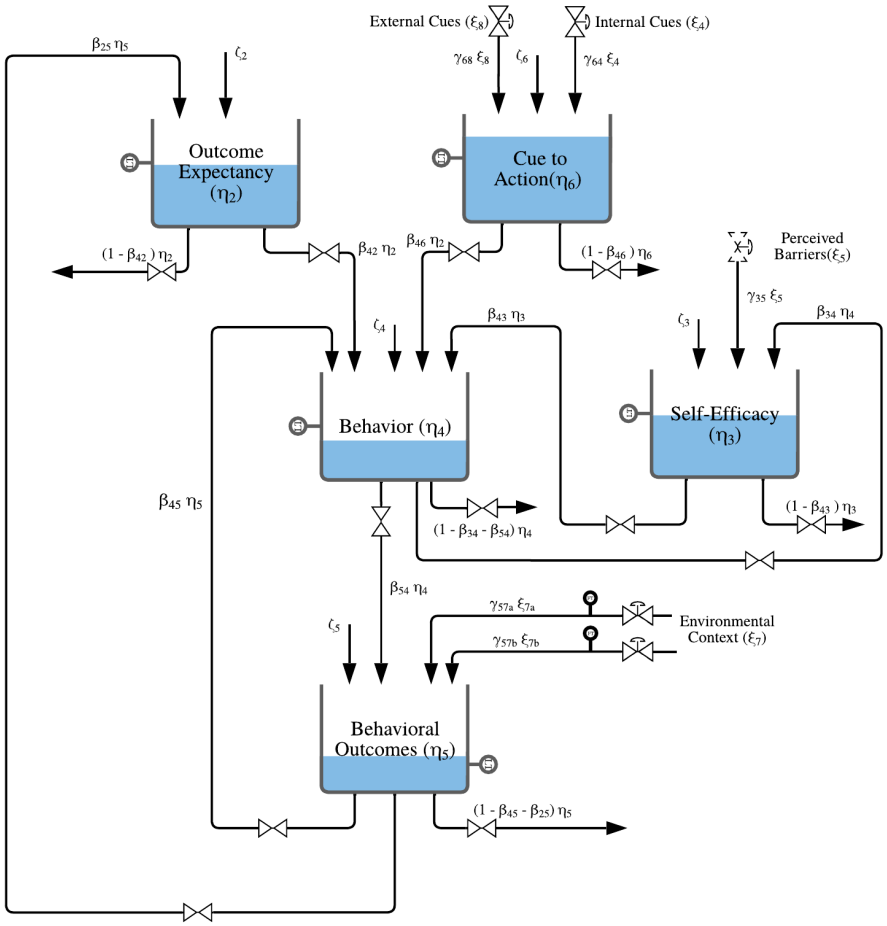

Figure 1.5: Schematic Depicting the Fluid Analogy of a Simplified SCT Model in an Open-Loop Setting, Adapted from Martín *et al.* (2020).

In this dissertation, the focus is on the Operant-Learning Self-Efficacy (OLSE) subsystem of the SCT. The OLSE subsystem consists of the Operant-Learning (OL) recycle loop between *Behavior* (η_4) and *Behavioral Outcomes* (η_5), and the Self-Efficacy (SE) recycle loop including *Behavior* and *Self-Efficacy* (η_3). A hypothetical

representation of the OLSE subsystem is utilized as the basis for simulations to improve control strategies for PA behavioral interventions (Chapter 4). One of the goals of the ongoing experiments is to validate the OLSE subsystem model through grey-box modeling techniques (Bohlin, 1994), expand on the fluid analogy model in collaboration with behavioral scientists, and establish a control framework to deliver optimal individualized PA interventions. In order to validate the model, an improved input signal design is devised, utilizing the knowledge gained from *JustWalk*, to generate more informative data sets. As the system of interest includes psychoactive behavioral constructs, elaborate techniques are applied to collect adequate measurements of the behavioral constructs of interest (i.e., not limited to a five-point Likert scale), which are described in Chapter 6. These should increase compliance from the participants with measurements, and elicit greater variability in the collected data.

One of the hypotheses when modeling PA behavior change systems is the separate and distinct (possibly competing) impact different facets of constructs like *Behavioral Outcomes* (e.g., fitness and fatigue) can have on PA levels. To mimic such dynamics, separate inventories can be designated for each of the expected behavioral outcomes. This results in the ability to model a variety of higher-order dynamics (e.g., underdamped, inverse response) based on the gains and time constants for each inventory. This approach can be applied to estimate models of the different behavioral outcomes of interest separately, depending on the considered behavior and the ability to measure each behavioral outcome independently, as detailed in Chapter 4. In the ongoing SCT-inspired PA behavioral interventions, efforts to separately measure fatigue and fitness as behavioral outcomes are underway. In the same principle, other constructs in SCT can be partitioned into distinct inventories to model hypothesized higher-order dynamics associated with the construct.

Additionally, in this dissertation, the use of fluid analogies as a tool to generate

dynamic hypotheses and models is expanded. In collaboration with behavioral scientists, an SDT-inspired fluid analogy model describing engagement in the *HeartSteps II* intervention is constructed. To address the prevalent issue of missingness in behavioral interventions, this hypothesized model is used as the basis for a model-based Bayesian inference imputation approach, which allows quantifying the uncertainty from both data imputation and scarcity, as detailed in Chapter 7.

One of the challenges faced in the dissemination of large-scale behavior change interventions is the uniqueness of the responses from each individual to the different intervention components and exogenous factors. To overcome this challenge in this work, a stochastic search algorithm is used to optimize the model structure for each individual in a timely manner and seamlessly deploy the closed-loop intervention phase of the experiment. Particularly, discrete Simultaneous Perturbation Stochastic Approximation (DSPSA; Wang and Spall (2011)) is utilized for both feature and order selection in model estimation for each participant in *YourMove*. The effectiveness of this approach is detailed in Chapter 6, along with the proposed mechanism to fit the estimated individualized models into a generalized model structure that is utilized in the predictive model structure in the HMPC-based closed-loop intervention stages.

The main aims of the *JustWalk JITAI* study involve the identification of JIT states and the multi-timescale dynamics associated with PA behavior change. This imposes new challenges in modeling the system. To overcome such challenges, sophisticated signal processing and modeling techniques are utilized to decompose the output signal into its components, reduce noise, and capture the system's nonlinearities with respect to the JIT context. Particularly, SSA is used to study the separability of *Behavior* into components, and then reconstruct the *Behavior* signal without noise components. Additionally, MoD is implemented as a data-centric modeling approach combining local and global model estimation to capture the nonlinearities in systems associated

with PA behavior change. A detailed account of these techniques and an analysis of the obtained results from *JustWalk JITAI* are presented in Chapter 3.

1.4 Control Strategies for Personalized Optimal Adaptive Behavioral Interventions

Prior work at Arizona State University's Control Systems Engineering Lab (CSEL) in the *JustWalk* study (in collaboration with behavioral scientists), has provided a good foundation for understanding behavior change associated with PA interventions (Riley *et al.*, 2015; Freigoun *et al.*, 2017; Phatak *et al.*, 2018; Korinek *et al.*, 2018; Kha *et al.*, 2022). While the experimental data in *JustWalk* was not adequate to validate aspects of the semi-physical SCT model (for reasons that included the inability to measure behavioral constructs of interest beyond a five-point Likert scale for each construct and lackluster compliance by the participants in responding to the daily surveys used to measure psychological constructs), the knowledge obtained from the data analysis was still of a great value. *JustWalk* has led to: 1) an improved input signal design based on *a priori* knowledge; 2) refined measurement collection methods related to the psychoactive constructs of interest, to elicit more variability as well as higher participant compliance; 3) partial validation of the SCT fluid analogy structure (much of the model remains unfalsified); 4) an insight into the best approaches to utilize black-box modeling techniques in estimating models to predict the daily step count (Freigoun *et al.*, 2017; Kha *et al.*, 2022); and 5) the ability to test HMPC formulation and control strategies, based on the modeled participant behavior, in simulation (Cevallos *et al.*, 2022; Khan *et al.*, 2022; El Mistiri *et al.*, 2023). All of these have played an essential role in the design and implementation of the ongoing PA-oriented behavioral interventions (*JustWalk JITAI* and *YourMove*).

One of the main takeaways from the *JustWalk* study is the importance of personalization of the daily step targets, with respect to what a participant would deem

"ambitious yet achievable". In this dissertation, control strategies to bring this concept into application in a closed-loop behavioral intervention setting are presented. The proposed closed-loop control strategies can be applied to various types of participants, depending on the participant's level of compliance with the daily surveys utilized to measure self-reported psychoactive constructs, yielding different levels of personalization. The main aim of the closed-loop control scheme is to personalize the intervention and provide each participant with ambitious enough daily step goals guiding them towards the desired intervention outcome of 10,000 steps per day while mitigating the probability of disengagement and dropping out of the intervention because of extremely ambitious goals. The proposed MPC strategies provide the main framework for the personalization of the interventions through controller tuning and constraint enforcement. To individualize the intervention without relying on self-reported measurements, the state-space representation of the SCT model has been manipulated to augment *Goal Attainment* as an output. This allows for imposing output constraints on the *Goal Attainment*, to ensure providing achievable goals by the controller.

Initially, the developed closed-loop control strategies are evaluated utilizing a hypothetical representation of a subsystem in the SCT semi-physical model. This is an essential step toward the implementation of closed-loop behavioral interventions on a large scale. Chapter 4 presents a detailed account of the devised control strategies, for different levels of complexity and individualization of the closed-loop system. Furthermore, Auto Regressive with eXogenic inputs (ARX; Ljung (1999)) model estimation has been performed on experimental *JustWalk* data, to obtain participant-specific models. Estimated models for representative *JustWalk* participants are utilized to evaluate the validity of the devised control strategies in a robust three-degrees-of-freedom Kalman filter-based Hybrid Model Predictive Control (3DoF-KF HMPC;

depicted in Fig. 1.6) formulation for a participant-based PA intervention, in a simulation environment. Simulation results for a representative participant illustrating the performance of the devised controller formulation in setpoint tracking and disturbance rejection are presented in Chapter 5 of this dissertation. Additionally, in this chapter, the robustness of the proposed 3DoF-KF HMPC is evaluated using Monte Carlo simulation.

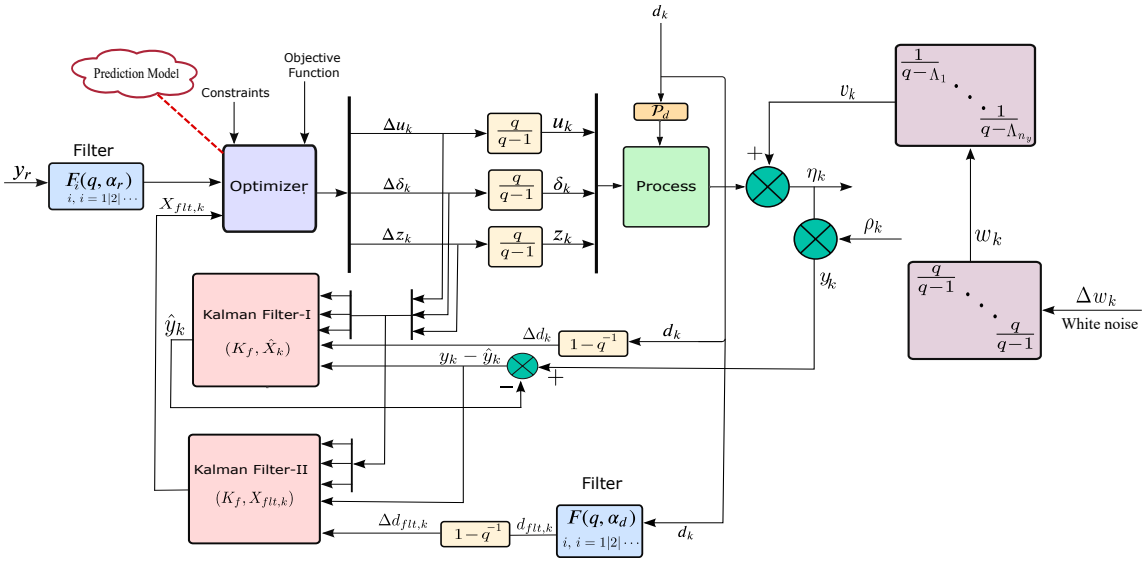

Figure 1.6: Block Diagram Schematic Depicting the Proposed Three-Degrees-Of-Freedom By Means of Kalman Filter HMPC (3DoF-KF HMPC) Structure, Aiming to Achieve Setpoint Tracking While Effectively Accounting for Both Measured and Unmeasured Disturbances. The Controller Utilizes External Filters to Adjust the Speed of Response for Measured Disturbances Rejection and Setpoint Tracking. Additionally, Nested Kalman Filters Are Utilized to Tune for Unmeasured Disturbances Separately (Khan *et al.*, 2022).

The devised closed-loop control strategies for PA interventions are adopted and meticulously refined in *YourMove*, to accommodate for unforeseen conditions encountered in a real-world implementation. This is an iterative process, which resulted in

what is dubbed the "digital PA coach tuning" control strategy. A detailed account of the algorithm followed in adaptively adjusting controller tuning and controller reconfiguration, along with clinical trial results for the first of its kind COT study (*YourMove*) are presented in Chapter 6.

1.5 Data Missingness and Imputation

Missing data is a prevalent issue in randomized controlled trials (RCTs) in both medical and behavioral intervention studies (Jakobsen *et al.*, 2017; Bell *et al.*, 2014a). In work done by Rioux and Little (2021), 96% of reviewed studies between 2015 and 2019 reported a degree of missing data that impacted outcomes. The best approach in intervention studies is to mitigate data loss by experiment design. Despite any measures taken to limit missingness, the loss of data points in such studies is typically unavoidable, due to low levels of participant compliance, technical issues, or participant dropout. Moreover, improper handling of the missing data points can add bias to the data and reduce variance. The ramifications of data loss can be quite significant, particularly in longitudinal studies, as it can cloud conclusions and reduce the quality of estimated models, especially when the duration of the experiment is limited. Note that MATLAB's System Identification toolbox does not support model estimation with missing data points or provide sophisticated data imputation tools. The impact of missing data points can be even more severe when real-time decision-making is done based on feedback measurements of the outputs of interest. Consequently, the loss of any measurement can render the optimization problem in the decision-making algorithm unsolvable and halt the intervention. This is indeed the case in the HMPC-guided closed-loop portion of *YourMove* intervention.

To reduce data loss in the ongoing behavioral interventions, positive reinforcement and participant compliance monitoring policies are followed, along with other

measures. The proposed measures include:

- The use of smartwatches (Fitbit Versa 3) as the device to measure the daily step count, which is the most significant output signal in the intervention.
- Positive reinforcement for compliance, where participants will be financially rewarded with gift cards for completing the self-reported surveys used to measure the psychoactive constructs of interest.
- Automated monitoring for compliance levels of the participants, where text messages and notifications are sent to participants whose compliance level is low to nudge them to partake in the daily surveys and wear the measuring device more consistently.
- Minimizing the burden associated with responding to the daily surveys, by reducing the number of questions in each survey. Furthermore, survey questions are worded carefully in an easy-to-read manner, and are mainly focused on the two psychological constructs relevant to the OLSE subsystem of the SCT model (*Self-Efficacy* and *Behavioral Outcomes*).
- In *YourMove*, the daily surveys are provided to the participants through the smartwatch watchface, which is expected to reduce the burden of answering the surveys as questions are now present on the participant's wrist.

In principle, the measures taken above should reduce missing data points. However, a degree of loss is expected in the experimental data. Therefore, policies to handle missing data points, and methods for data imputation must be considered as a part of the data analysis, not only to interpolate missing data points within a set but also to extrapolate incidents of data loss online. This is particularly significant for the

closed-loop control stages of *YourMove*, as data imputation must be conducted in real-time to allow for the intervention to proceed uninterrupted.

In this dissertation, a sophisticated model-based Markov Chain Monte Carlo (MCMC) Bayesian inference approach for data imputation is explored. Particularly, this approach is studied in imputing missing data points as a part of data analysis for the *HeartSteps II* study. Details regarding the model used in this Bayesian inference imputation approach and results highlighting its capability of propagating and quantifying uncertainty due to data imputation are presented in Chapter 7. On the other hand, for *YourMove* a simple rolling average approach is utilized to impute missing data points, as described in Chapter 6. This is done because of limitations faced in the available computational power and time to impute missing data points online in the closed-loop stages of the study.

1.6 Contributions of The Dissertation

This dissertation presents a comprehensive control optimization trial (COT) framework for the delivery of optimal personalized behavior interventions based on system identification and control systems engineering principles. Moreover, this dissertation validates the effectiveness of this comprehensive approach through a unique clinical trial, providing unprecedented results and insights. In this dissertation prior knowledge is leveraged to design improved input signals for system identification in PA interventions, providing more informative data sets. Additionally, novel signal processing and modeling approaches are utilized to further the understanding of behavior change idiosyncrasies in the context of JIT states. Finally, a sophisticated model-based approach for data imputation is evaluated to address the ubiquitous problem of data loss in behavior change interventions.

The contributions of this dissertation in terms of designing informative open-

loop system identification experiments for physical activity (PA) behavior change interventions and modeling behavior change systems related to physical activity are summarized as follows:

- Design of input signals to generate informative experimental data to identify and estimate just-in-time (JIT) states and the multi-timescale dynamics associated with behavior change in PA-oriented interventions. This input signal design is based on a novel unconventional method aimed at identifying JIT states, as a part of the *Just Walk JITAI* intervention.

- Development and evaluation of improved approaches to personalize input signal design for the goal-setting component in PA behavioral interventions. Two proposed approaches are tested in real-world settings as a part of *YourMove* and *JustWalk JITAI*.

- Enhancement of the dynamical systems model for Social Cognitive Theory (SCT) to incorporate separate and possibly competing dynamics for different facets of behavioral constructs. This improvement to SCT produces higher-order systems and can mimic different observed phenomena in behavior change systems.

- Development of a computational dynamical systems model for participant engagement in mHealth interventions.

- Application of a signal processing technique, particularly Singular Spectrum Analysis (SSA), to study the separability of behavior into its uncorrelated components covering different frequencies and remove noise in an informed manner. This provides the means to study idiosyncratic forces influencing behavior change at different time scales.

- Integration of input signal design in *JustWalk JITAI*, SSA, and Model-on-Demand (MoD) in a novel approach to capture nonlinearities associated with behavior change at different frequencies of interest and in context of JIT states.

- Implementation of the Discrete Simultaneous Perturbation Stochastic Approximation (DSPSA) algorithm to optimize model order and features in an ARX structure in an idiographic manner. This allows for the estimation of participant-specific models (online) within the limited time available for model estimation in *YourMove*.

The contributions of this dissertation in terms of closed-loop optimal personalized behavior change interventions, particularly for the physical inactivity problem, are summarized as follows:

- Development of MPC-based closed-loop control strategies to deliver optimal personalized behavioral interventions promoting healthy levels of PA, even under circumstances with limited measurement capabilities and plant-model mismatch.

- Expanding the mixed logical dynamical (MLD) structure implementation in behavior change interventions to include logical conditions based on decisions made in previous instances of the intervention. This is particularly formulated to incorporate granting financial rewards as part of the optimization objective function over the entirety of the move horizon.

- Extension of the devised control strategies and integrating them with a robust three-degrees-of-freedom Kalman filter-based Hybrid Model Predictive Control (3DoF-KF HMPC) formulation.

- Evaluation of the efficacy of the synergism between the devised system identification experiment, formulated 3DoF-KF HMPC, and control strategies in delivering personalized closed-loop PA interventions in real-world settings. This is done as a part of a first-of-its-kind COT study, under the name of *YourMove*.

Last but not least, this dissertation contributes to solving the problem of data loss and missingness commonly faced in behavior change interventions. This is done through the evaluation of a model-based Bayesian inference data imputation approach, utilizing Markov Chain Monte Carlo methods to propagate and quantify the combined uncertainty due to data scarcity as well as data imputation.

1.7 Dissertation Outline

After this introductory chapter, the dissertation continues in Chapter 2 with a detailed description of the SCT dynamical systems model. The translation of the fluid analogy model of SCT into a system of differential equations is presented and explained. In addition, the operationalization of JIT state conditions is explained and the design of the *JustWalk JITAI* (R01LM013107, 2020) study is described, including the two main intervention components (goal setting and inspiring bouts). Additionally, this chapter illustrates the integration of the intervention components into the SCT model, highlighting the within-day component in the form of bouts of notifications aimed to inspire the participant to engage in PA. This chapter presents an innovative input signal design for the *JustWalk JITAI* intervention components, allowing the operationalization of JIT into a decision rules signal that dictates the conditions under which notifications can be sent. The proposed input signal design also provides an adaptive approach for the personalization of the goal-setting intervention component. Chapter 2 highlights the use of simulations based on the developed SCT model to guide elements of the input signals design for *JustWalk JITAI*.

Chapter 3 presents a detailed description of a novel signal processing and model estimation method that can be used to understand and model idiosyncrasies in behavior change systems in the context of JIT states. Particularly, SSA is utilized to study the separability of the output signal into different groups of uncorrelated components, decompose the signal into its components, and then construct a filtered output signal from its most relevant components excluding noise. In addition, this chapter introduces MoD and highlights its capability of estimating localized models under a global structure, which can be utilized to capture nonlinearities associated with behavior change systems in the context of JIT states. Results for a representative *JustWalk JITAI* participant presented in Chapter 3 serve as proof of concept for the effectiveness of this method in analyzing and modeling the impact of exogenous signals on behavior change systems at different time-scales, while taking into account JIT state conditions.

Chapters 4 and 5 focus on the development of closed-loop framework and control strategies promoting PA. In Chapter 4, a reduced SCT model (focusing on the OLSE subsystem) is utilized to study and develop control strategies that deliver personalized closed-loop interventions, while considering possible limitations faced in the availability of reliable measurements for psychoactive SCT constructs, and plant-model mismatch. The control strategies presented in Chapter 4 apply a classical MPC formulation and are based on hypothetical participants representing extreme ends at the spectrum of possible participant adherence in PA-oriented interventions. These control strategies are further examined in Chapter 5 in a simulation setting, utilizing a HMPC formulation and a participant-specific black-box model estimated for a representative *JustWalk* participant. In Chapter 5, details regarding the estimation of the participant-specific ARX model are provided. In addition, the 3DoF-KF HMPC controller formulation is presented, highlighting its capability to make deci-

sions based on categorical and logical conditions. This is particularly important for granting rewards as a part of the positive reinforcement component of the intervention, where financial rewards are granted based on the participant's performance with respect to controller decisions made at the previous sampling instance. Furthermore, in Chapter 5 Monte Carlo simulations are utilized to examine the robustness of the devised 3DoF-KF HMPC formulation in the face of plant-model mismatch.

Chapter 6 in this dissertation is dedicated to the real-world implementation of the first COT study, *YourMove* (R01CA244777, 2020). In this chapter, the unique aspects of *YourMove* are highlighted along with the challenges faced and the methods devised to overcome them. Chapter 6 presents refinements to the input signal design used in the *YourMove* as a part of the system identification stage. Additionally, as *YourMove* is a large-scale study (including 190+ participants in the closed-loop intervention) a stochastic search algorithm is utilized, which allows for the estimation of idiographic models that can be fixed in a generalized structure for all participants through state-space model manipulation. This generalized model structure serves as the predictive model structure in the 3DoF-KF HMPC controller formulation for all participants, yet allows the personalization of the closed-loop intervention for each participant through the estimated participant-specific model parameters, tuning, and constraints assignment. Furthermore, in Chapter 6 a detailed account of the adaptive controller tuning and reconfiguration strategies, dubbed "digital PA coach tuning", is provided. Unprecedented results from the ongoing *YourMove* study are presented and discussed in Chapter 6 for representative participants, along with preliminary findings and lessons learned from *YourMove* to date.

In Chapter 7 a dynamic model for engagement in physical activity interventions is hypothesized and a sophisticated model-based data imputation approach is evaluated. Particularly, the hypothesized model aims to provide a theoretical background for

modeling engagement in PA interventions, in light of the available *HeartSteps II* data. In this chapter, the use of fluid analogy as a tool for hypothesis generation is highlighted. Moreover, the hypothesized model serves as the basis for a Bayesian inference technique to handle data loss, allowing informed imputation of missing data points while propagating uncertainty due to data imputation and scarcity into estimated models.

Chapter 8 concludes this dissertation with a summary of the important conclusions and the advances achieved through real-world implementation of control systems engineering principles in behavior change interventions. This chapter also presents recommendations regarding future directions for the research. Chapters in this dissertation are written in the form of stand-alone papers based on published and submitted papers.

1.8 Publications Summary

The dissertation has resulted in a series of contributions to the literature (published, in review, in press, or in preparation). Journal papers published to date relating to work done in this dissertation are listed below:

1. Spruijt-Metz, D., B. M. Marlin, M. Pavel, D. E. Rivera, E. Hekler, S. De La Torre, **M. El Mistiri**, et al. "Advancing Behavioral Intervention and Theory Development for Mobile Health: The *Heartsteps II* Protocol," *International Journal of Environmental Research and Public Health* 19, no. 4 (2022): 2267

2. Cevallos, Daniel, Cèsar A. Martin, **M. El Mistiri**, Daniel E. Rivera, and Eric Hekler. "Un esquema de decisiones para intervenciones adaptativas comportamentales de actividad física basado en control predictivo por modelo híbrido: ilustración con *Just Walk*," *Revista Iberoamericana de Automatica e Informatica*

Industrial 19, no. 3 (2022): 297-308. **(Joint First Authorship)**.

3. Park, J., M. Kim, **M. El Mistiri**, R. Kha, S. Banerjee, L. Gotzian, G. Chevance, D. E. Rivera, P. Klasnja, and E. Hekler "Advancing Understanding of Just-in-Time States for Supporting Physical Activity (Project *JustWalk JITAI*): Protocol for a System ID Study of Just-in-Time Adaptive Interventions," *Journal of Medical Internet Research (JMIR)* 12.1 (2023): e52161.

Journal papers that are currently in review or in preparation based on work related to this dissertation are as follows:

4. **El Mistiri, M.**, D. E. Rivera, P. Klasnja, J. Park, and E. Hekler. "Model Predictive Control Strategies in mHealth: Optimal Personalized Physical Activity Interventions," *Journal of Process Control.* **(In Review)**

5. **El Mistiri, M.**, S. De La Torre, K. Tung, B. Marlin, M. Pavel, P. Klasnja, D. Spruijt-Metz, an D. E. Rivera. "System Identification of Engagement in mHealth Intervention with a Bayesian Approach for Missing Data Imputation," *IEEE Open Journal of Engineering in Medicine and Biology.* **(In Review)**

6. De La Torre, S., **M. El Mistiri**, E. Hekler, P. Klasnja, B. Marlin, M. Pavel, D. Spruijt-Metz, and D. E. Rivera. "Modeling Engagement with A Digital Behavior Change Intervention (*HeartSteps II*): A System Identification Approach," *Journal of Biomedical Informatics (JBI).* **(Preliminary Acceptance/Under Revision; Joint First Authorship)**

7. **El Mistiri, M.**, O. Khan, D. E. Rivera, C. Martin, and E. Hekler. "Data-Driven mHealth Interventions: System Identification and Hybrid Model Predictive Control to Deliver Optimal Personalized Physical Activity Interventions," *IEEE Open Journal of Control Systems.* **(In Preparation)**

8. Khan, O., **M. El Mistiri**, S. Banerjee, D. E. Rivera, and E. Hekler, "3DoF-KF HMPC: A Kalman filter-based Hybrid Model Predictive Control Algorithm for Mixed Logical Dynamical Systems," *Control Engineering Practice.* **(In Preparation)**

9. Kim, M, S. Assi, **M. El Mistiri**, J. Park, S. Banerjee, D. E. Rivera, P. Klasnja, and E. Hekler. "Optimizing and Validating Individualized and Adaptive mHealth Digital Health Interventions via Control Systems Engineering Methods: Protocol of a Randomized Controlled Trial," *Journal of Medical Internet Research (JMIR).* **(In Preparation)**

10. Banerjee, S., O. Khan, **M. El Mistiri**, N. N. Nandola, E. Hekler, and D. E. Rivera. "Data-Driven Control of Nonlinear Systems using a Three-Degree-of-Freedom Model-on-Demand Model Predictive Control Framework," **(In Preparation)**

Additionally, the following refereed conference proceedings papers relating to this dissertation have been published:

11. **El Mistiri, M.**, D. E. Rivera, P. Klasnja, J. Park and E. Hekler, "Model Predictive Control Strategies for Optimized mHealth Interventions for Physical Activity," *Proceedings of the 2022 American Control Conference,* Atlanta, GA, June 8 – 10, 2022, pgs. 1392 – 1397.

12. **El Mistiri, M.**, D. E. Rivera, P. Klasnja, J. Park and E. Hekler, "Enhanced Social Cognitive Theory Dynamic Modeling and Simulation Towards Improving the Estimation of 'Just-In-Time' States," *Proceedings of the 2022 American Control Conference*, Atlanta, GA, June 8 – 10, 2022, pgs. 468 - 473.

13. Khan, O., **M. El Mistiri**, D. E. Rivera, C. A. Martin, and E. Hekler. "A Kalman filter-based Hybrid Model Predictive Control Algorithm for Mixed Logical Dynamical Systems: Application to Optimized Interventions for Physical Activity," *61st IEEE Conference on Decision and Control,* Cancún, Mexico, Dec. 6-9, 2022, pp. 2586-2593. IEEE, 2022.

14. K. Tung, S. De La Torre, **M. El Mistiri**, R. Braga de Braganca, E. Hekler, M. Pavel, D.E. Rivera, P. Klasjna, D. Spruij-Metz, and B.M. Marlin "BayesLDM: A Domain-specific Modeling Language for Probabilistic Modeling of Longitudinal Data," *2022 IEEE/ACM Conference on Connected Health: Applications, Systems and Engineering Technologies (CHASE),* Arlington, VA, USA, 2022, pp. 78-90.

15. **El Mistiri**, M., O. Khan, D.E. Rivera, and E. Hekler, "System identification and hybrid model predictive control in personalized mHealth interventions for physical activity," *2023 American Control Conference,* San Diego, CA, May 30 – June 2, 2023, pgs. 2240 – 2245

The following conference papers are based on the work presented in this dissertation, have been accepted and are currently in press:

16. **El Mistiri, M.**, S. Banerjee, D. E. Rivera, P. Klasnja, J. Park, and E. Hekler. "Understanding 'Just-in-Time' States in Behavioral Interventions using System Identification and Data Science Methods," *IFAC Symposium on System Identification (SYSID 2024)*, Boston, USA, July 17-19, 2024. **(Accepted; In Press)**

17. **El Mistiri, M.**, S. De La Torre, K. Tung, B. Marlin, M. Pavel, P. Klasnja, D. Spruijt-Metz, an D. E. Rivera. "System Identification of User Engagement in mHealth Behavioral Interventions," *IFAC Symposium on System Identification*

(SYSID 2024), Boston, USA, July 17-19, 2024. **(Accepted; In Press)**

Chapter 2

ENHANCED SOCIAL COGNITIVE THEORY DYNAMIC MODELING AND SIMULATION TOWARDS IMPROVING THE ESTIMATION OF "JUST-IN-TIME" STATES

2.1 Introduction

Inactivity has led to an increase in chronic diseases within populations (Booth *et al.*, 2012). Physical inactivity causes an increased deterioration of body functions resulting in various illnesses like obesity, diabetes, heart disease, cancer, rheumatoid arthritis, and more. On the other hand, maintaining healthy levels of physical activity (PA) can work as a preventive measure against all of these illnesses, or at least delay their onset (Booth *et al.*, 2012; Saint-Maurice *et al.*, 2020); an increase from 4,000 to 8,000 steps/day reduces the risk for all-cause mortality by 51% for adults. Despite the various public physical activity awareness campaigns over the years, there is a low prevalence of healthy PA levels in the general population; about 80% of adults in the US do not meet the recommended CDC guidelines of 150 minutes of moderate to vigorous physical activity exercises (Olson *et al.*, 2018). Thus, the question is not if PA is beneficial for health, but rather how to support people to engage and sustain healthy PA levels. Control systems engineering has proven to be very beneficial in many fields, and the adoption of system identification and dynamic control strategies in the behavioral medicine field is an area of significant promise in research (Rivera *et al.*, 2018; Hekler *et al.*, 2016). Prospects include the dissemination of interventions on a large scale to the general population, that can help fight addiction and adopt healthy behavior.

One of the reasons the field of behavioral medicine struggles to help people be active is because of limited understanding of the dynamic processes that occur in real-world contexts that facilitate or hinder a person's ability to be active (Hekler *et al.*, 2016; Kessler and Glasgow, 2011). Much of behavioral intervention development relies on relatively static theoretical models and corresponding interventions. While "tailoring" is a key concept for behavioral interventions, which in the field involves defining if/then rules to adjust the provision of support to a person based on some assessment of that person in a given instance, the field has largely moved forward improving knowledge about processes using methods designed more to test if interventions or intervention components work or not, on average for a population. These methods, particularly if used on data sets that only have snapshots of data (e.g., data gathered once every 3 months, which is still common in the field), produce limited to no insights about dynamic processes, particularly as they manifest in real-world contexts. Thus, the field's dominant methods and approaches provide only limited insights into dynamical processes.

With the increased availability of temporally dense data afforded by digital technologies, there has been a re-emergence of the use of *idiographic* methods, which refers to data analysis explicitly designed to study predictions and patterns within time series data corresponding to a single individual. These temporally dense time series data have also enabled the use of control systems methods, such as dynamical systems modeling, system identification, and controller design to guide dynamic decision-making. In particular, prior work has illustrated the value of dynamical systems modeling for specifying dynamic predictions relevant to behavior change in context (Martín *et al.*, 2020), the value of system identification for producing informative data about dynamic processes related to behavior change (Hekler *et al.*, 2016), and the possibility of creating controllers to drive digital health interventions (Martín

et al., 2016a).

Building on this prior work, a key gap in the field's understanding of dynamic processes of behavior exists with regard to multi-timescale prediction and, by extension, decision-making. In particular, the field has advanced the concept of a just-in-time adaptive intervention (JITAI; Perski *et al.* (2022); Klasnja *et al.* (2015); Nahum-Shani *et al.* (2015)), which involves both provision of support when a person has the need for a specific type of support, the opportunity to respond favorably to the support, and receptivity to receiving the support, which can then contribute to adaptations over time that results in meaningful behavior change (e.g., meeting and sustaining behavioral targets). Thus, it is not only important to provide good "just-in-time" support, but to also make sure said support is contributing towards meaningful behavior change over time. This issue could be conceptualized as a multi-timescale problem in that robust prediction and decision-making are needed both in shorter timescale (e.g., deciding whether to send a notification to invite a person to plan a bout of walking in the next 3 hours) and longer timescales (e.g., establishing "ambitious but doable" step goals in a given day that can facilitate gradual increases towards clinically meaningful targets).

The purpose of this chapter is to describe and design innovative input signals design to study multi-timescale dynamics that are part of a digital health intervention, *JustWalk JITAI*. This work leverages prior work, particularly a dynamical model of the Social Cognitive Theory (SCT), that encapsulates prior domain knowledge about behavioral processes that influence physical activity. Specifically, we use SCT to simulate plausible responses of participants to different signal design processes to estimate the plausible data quality that will be produced from the input signal design.

The chapter is organized as follows: Section 2.2 gives a brief description of SCT. Section 2.3 presents components and the thought process for the behavior change

experiment. Section 2.4 details the input signal design, while in Section 2.5 simulation results of the examined case studies are presented and discussed. Section 2.6 provides conclusions along with implications for future work.

2.2 Social Cognitive Theory (SCT)

Theories of behavior change like SCT utilize psychological constructs to hypothesize how different factors may impact behavior. SCT allows for the prediction of the ability of an individual to engage in determined behavior, by explaining the interconnections between various factors influencing behavior, including previous experience (Bandura, 1989). The constructs in the SCT can be measured using sensors or inferred from other signals. Fluid analogies utilize engineering principles, such as the conservation of mass, to represent theories of behavior change like SCT as dynamic mathematical models. The work done in Martín *et al.* (2020) describes a dynamical model for the SCT which can be seen in Fig. 2.1 in a fluid analogy representation.

Table 2.1 lists the SCT components considered in this chapter along with their associated symbols. In the fluid analogy, the main SCT behavioral constructs are considered as inventories (tanks) in an inventory system with the level inside each vessel representing system outputs. Brief descriptions of the main system outputs included in this work are as follows:

1. *Self-efficacy*: The perceived capability and desire to engage in a targeted behavior, given constraints, obstacles, and demands.

2. *Outcome Expectancies*: The perceived chance that engaging in behavior will lead to certain outcomes.

3. *Behavioral Outcomes*: The outcomes (e.g. fatigue, fitness) resulting from engagement in a certain behavior.

4. *Behavior*: The actual behavior of interest. This can represent different characteristics of behavior (e.g. frequency, intensity, duration). For this study, the behavior of interest is the amount of steps taken per day.

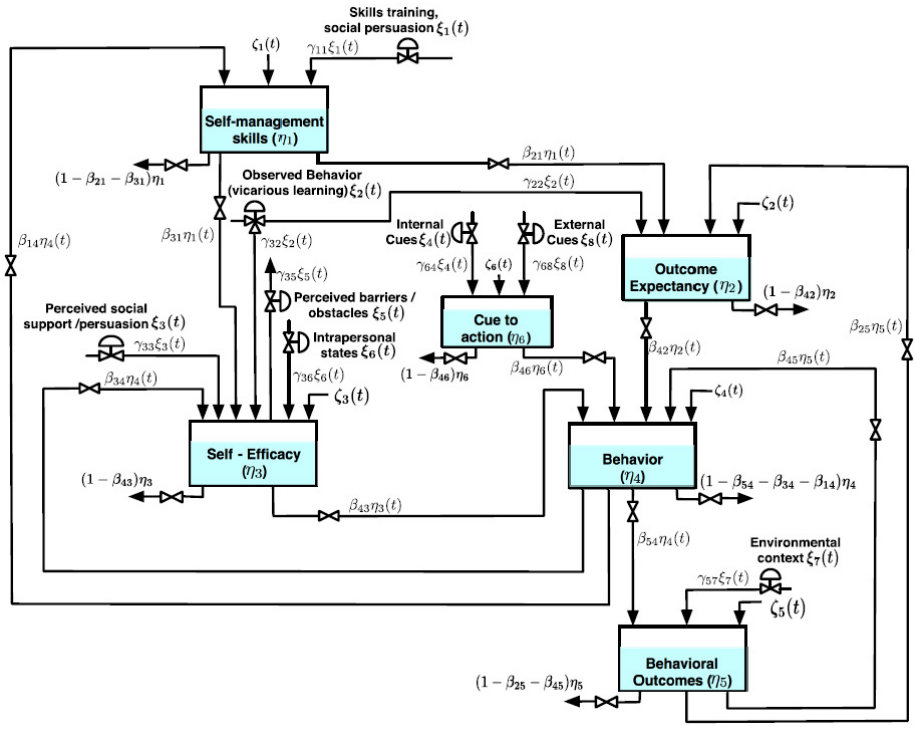

Figure 2.1: Schematic Illustrating the Fluid Analogy of the Social Cognitive Theory Model (Rivera *et al.*, 2018; Martín *et al.*, 2020).

Based on SCT, behavioral constructs are influenced by exterior stimuli from various factors as well as from interactions between the constructs, which is depicted by how inventory levels change over time based on influences of inflows/outflows into the system (system inputs) and deviations in connected inventories. The inputs considered in this work are described below:

1. *External Cues*: Represents exogenous stimuli to the system (e.g. assigned goals, a friend's invite) which triggers *Behavior* or *Behavior* increase.

2. *Perceived barriers and obstacles*: Represents external conditions that directly impact *Self-Efficacy* (e.g. busyness, seasonal illness).

3. *Environmental context*: External and environmental conditions that can have a positive or negative impact on the experience at which *Behavior* occur and the *Behavioral Outcomes* as a consequence (e.g. weather, weekday vs weekend).

Table 2.1: List of the SCT Inputs and Outputs Considered in This Chapter from Martín *et al.* (2020).

Name	**Symbol**
Inflows/Outflows (system inputs)	
Perceived barriers and obstacles	ξ_5
Environmental context	ξ_7
External Cues	ξ_8
Inventory levels (system outputs)	
Outcome expectancies	η_2
Self-efficacy	η_3
Behavior	η_4
Behavioral outcomes	η_5
Cues to action	η_6

2.3 Intervention Design: *JustWalk JITAI*

JustWalk JITAI intervention design follows a similar structure to the previous behavior change experiment (*JustWalk*) in the goal-setting component, where in an open-loop setting participants are given a specific amount of steps to walk each day

as the daily goal (Martín *et al.*, 2020). In an extension to what was done in *JustWalk*, in this intervention the maximum and minimum values of the daily goals in each cycle are adjusted based on the average performance of the previous cycle. For the initial cycle of the intervention, the maximum and minimum values are decided based on the participant's performance at the baseline period, where the behavior of the participant is measured before the intervention starts. This allows for maintaining ambitious yet achievable daily goals personalized for each participant for each cycle.

The second component of *JustWalk JITAI* is the walking notifications, which consist of within-day messages designed to inspire a person to take a short (e.g., 10 minutes) walk. This intervention component is designed with a focus on studying the notion of a just-in-time (JIT) state, which involves the degree to which the notification is well-matched to a particular moment. To operationalize this, three conditions about the current moment are taken into account:

- *Need* (N): Whether the participant has not met or progressed enough towards the given daily goal.
- *Opportunity* (O): Whether the participant has a window of opportunity to go on a walk within the upcoming sampling period (based on calendar input or recognized patterns).
- *Receptivity* (R): If the participant has received less than 3 messages within the day.

Three combinations of the conditions are chosen as the decision rules for the walking notifications component: 1) N+O, 2) N+R, 3) N+O+R also known as the JIT decision rule.

The premise of the walking notifications component is to examine the dynamic responses to the provision of support within moments that are more or less likely to

be "just-in-time"; meaning a moment when a person has the need, opportunity, and receptivity to a given intervention. By nudging participants to plan for PA when they are in "just-in-time states" the yield of the walking notifications should increase while maintaining a minimal burden on participants. Theoretically, this should maximize walking notifications benefits and minimize notification fatigue.

Participants in the intervention are given a Fitbit Versa 3 device to track their daily step count. Daily goals are delivered through a smartphone application that syncs with the Fitbit device to obtain measurements and store them in a database on a secure server. Measurement of other output psychological constructs like *Self-Efficacy* (η_3), and *Behavioral Outcomes* (η_5) are taken through surveys known as ecological momentary assessments (EMAs; Shiffman *et al.* (2008)) provided to participants at different times of the day. Multiple specifically articulated survey questions are designed to assess each construct and the average score is utilized.

In this chapter, the SCT model is simplified by excluding the *Self-Management Skills* inventory (η_1). Moreover, only *Perceived barriers/obstacles* (ξ_5) and *Environmental contexts* (ξ_7) are considered as disturbances out of the system's exogenous inputs. As per exogenous inputs, only *External Cues* (ξ_8) are considered including both intervention components: goal setting (ξ_8^{gs}) and walking notifications (ξ_8^{ib}). This yields a simplified system of ordinary differential equations (ODEs) that can be seen in (2.1-2.5) below:

$$\tau_2 \frac{d\eta_2}{dt} = \beta_{25}\, \eta_5(t) - \eta_2(t) + \zeta_2(t) \tag{2.1}$$

$$\tau_3 \frac{d\eta_3}{dt} = \gamma_{35}\, \xi_5(t) + \gamma_{311}\, \xi_{11}(t) + \beta_{34}\, \eta_4(t) - \eta_3(t) + \zeta_3(t) \tag{2.2}$$

$$\tau_4 \frac{d\eta_4}{dt} = \beta_{42}\, \eta_2(t) + \beta_{43}\, \eta_3(t) + \beta_{45}\, \eta_5(t) + \beta_{46}\, \eta_6(t) - \eta_4(t) + \zeta_4(t) \tag{2.3}$$

$$\tau_5 \frac{d\eta_5}{dt} = \gamma_{57}\, \xi_7(t) + \beta_{54}\, \eta_4(t) - \eta_5(t) + \zeta_5(t) \tag{2.4}$$

$$\tau_6 \frac{d\eta_6}{dt} = \gamma_{68}^{gs}\, \xi_8^{gs}(t) + \gamma_{68}^{ib}\, \xi_8^{ib}(t) - \eta_6(t) + \zeta_6(t) \tag{2.5}$$

In a departure from previous work, the SCT model in equations (2.3) - (2.5) has been modified to accommodate for within-day effects (like walking notifications) on the numerical solution generated during integration. This is essential in the simulations presented in this chapter, where the model is used to achieve an informative input signal design for the system of interest. The process of input signal design is iterative by nature, and the built simulation allows for examining different designs on hypothetical participants to set expectations and validate decisions made in the design. For instance, by simulating extreme scenarios, a rough estimate of the amount of notifications being sent to a participant throughout the intervention is obtained. This allows for the assessment of the expected notification burden associated with each decision rule.

2.4 Input Signal Design

To elicit dynamic responses over the timescales of interest, two different input signals are designed in *JustWalk JITAI* for the separate components of the intervention: goal setting and walking notifications. All designed signals follow the guidelines presented in Gaikwad and Rivera (1996), and Rivera *et al.* (2002), in which equation (2.6) is highlighted to define the effective frequency range of the input signal based on a *a priori* knowledge and estimates of the dominant system time constant.

$$\omega_* = \frac{1}{\beta_s \tau_{dom}^H} \leq \omega \leq \frac{\alpha_s}{\tau_{dom}^L} = \omega^* \tag{2.6}$$

τ_{dom}^L and τ_{dom}^H represent the higher and lower bounds for the estimated dominant time constant of the system. α_s and β_s dictate the input signal's content of high and low frequency respectively.

For goal setting, a multisine (MS) signal is utilized. The input signal design parameters shown in (2.7) are chosen based on obtained knowledge from previous

work (see Section 5.3.2 and El Mistiri *et al.* (2023)).

$$\tau_{dom}^{L} = 1 \text{ days}, \ \tau_{dom}^{H} = 2 \text{ days}, \ \alpha_s = 2, \ \beta_s = 2 \tag{2.7}$$

The design parameters lead to a cycle length of 26 days as seen in Fig. 2.2. The MS signal determines the daily goals given to participants throughout the 260 days intervention, in 10 cycles. For each cycle the lower bound in goals is determined by the average steps taken per day from the previous cycle with a 2,000 steps/day range. This design is expected to generate an added transient in the output signals, which will have to be accounted for in the subsequent analysis of the experimental data.

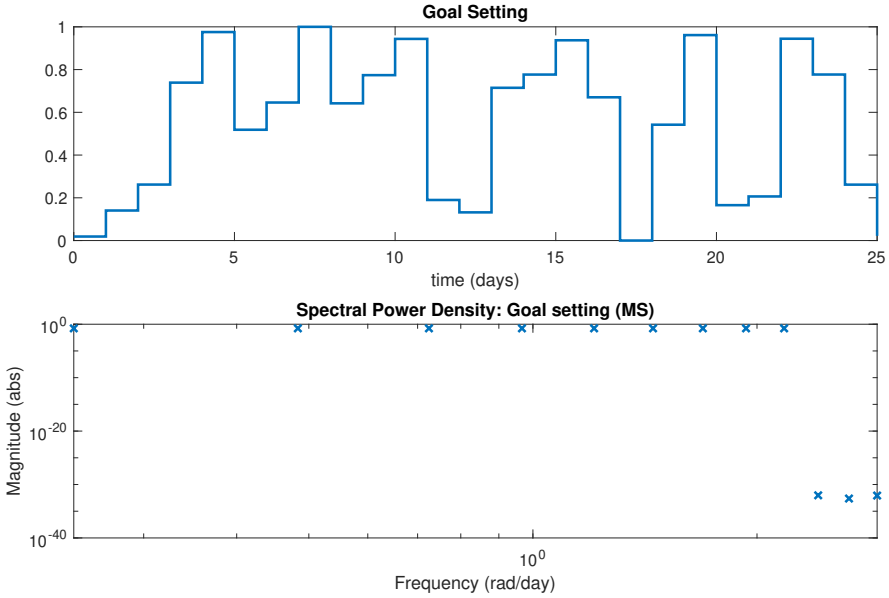

Figure 2.2: Multisine Base Cycle for the Goal Setting Input Signal in the Time Domain (Top) Along with Its Spectral Power Density (Bottom).

The effective frequency range of the signal is related to the design parameters through (2.6). This yields persistence of excitation between $\omega_* \approx 0.25$ rad/day to $\omega_* \approx 2$ rad/day for the designed MS signal, as it is highlighted in the power spectrum of the signal seen in Fig. 2.2.

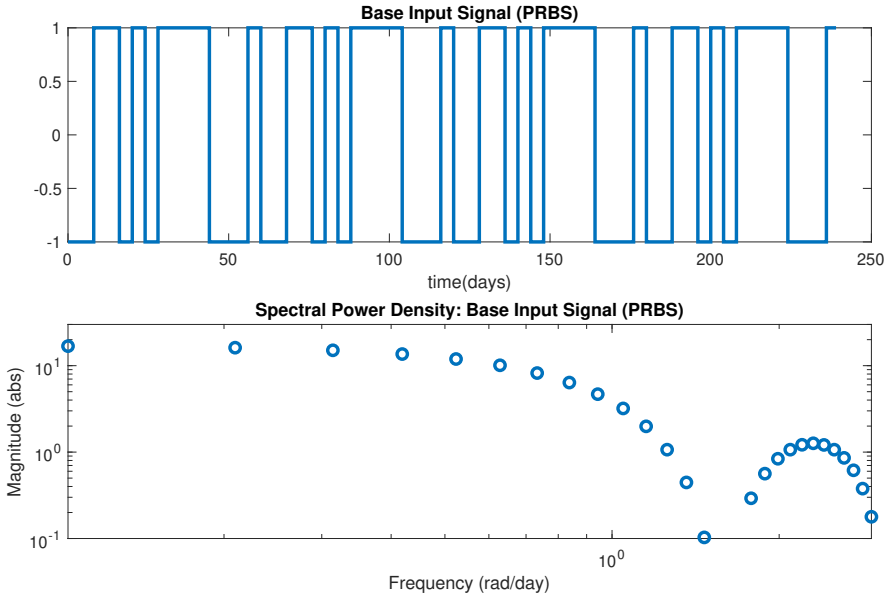

Figure 2.3: Base PRBS Signal for the Decision Rules Signal in the Time Domain (Top). Spectral Density of the Base PRBS Signal (Bottom).

For the walking notifications component, the three decision rules for sending prompts to participants are tested against fully randomized prompts, to study the effectiveness and dynamics of the decision rules. The purpose of the decision rules is to minimize the burden on participants and notification fatigue by prompting engagement in PA when participants are most likely to respond. To construct this categorical four-level input signal an innovative method is used where a pseudo-random binary sequence (PRBS) is utilized as the base for the design. Then, a random multi-level sequence (RMLS) is superimposed over one of PRBS's binary levels. Input signal design parameters for the PRBS are chosen as seen in (2.8).

$$\tau_{dom}^{L} = 3 \text{ days}, \ \tau_{dom}^{H} = 3.5 \text{ days}, \ \alpha_s = 2, \ \beta_s = 2 \tag{2.8}$$

This results in a 60 days cycle with $n_r = 4$ shift registers and switching time $T_{sw} = 4$ days, as can be seen in Fig. 2.3. The parameters are chosen to cover the most

important dynamics of the system by introducing variability in a sufficient frequency without allowing the system to settle. Four cycles of the designed PRBS signal are needed to cover 240 days of the study; then the walking notifications element is taken offline for the remainder of the experiment.

Fig. 2.3 provides further confirmation regarding the chosen guidelines for the base PRBS input signal, as it can be seen that the spectral power density contains sufficient persistent excitation by the number of harmonics included in the effective frequency range between $\omega_* \approx 0.14$ rad/day to $\omega^* \approx 0.67$ rad/day.

A uniformly distributed RMLS with three levels is superimposed over the base PRBS signal, where the signal equals 1. The three-level RMLS is generated with a different realization at each instant that the PRBS signal switches to 1. This allows for superimposing a new random sequence at each instant it is needed, without any repetitions across cycles as can be seen in Fig. 2.4, which reduces the bias from the possibility of participants recognizing any repetitive patterns.

The switching time for the RMLS signal is one day, enabling the introduction of more variability at a higher frequency to the decision rules input signal. This adds persistence of excitation to the high frequencies while maintaining the excitation in the lower frequencies at the effective frequency range as Fig. 2.4 illustrates. Moreover, the decision framework of the walking notifications component allows for identification of higher frequency dynamics through the effect of the notifications sent to participants within-day.

The utilization of the decision rule input signal for the walking notifications component, along with the goals signal for the goal setting component assures covering a wide range of system dynamics over the different time scales of interest. Despite the overlap in the effective frequency ranges of the designed input signals, each of them is unique in the component it covers, and the two signals are orthogonal to

one another in nature. This can be confirmed by applying cross-correlation analysis to the designed input signals. The input signal design is made with the purpose of providing persistence of excitation across both low and high frequency and generating dynamically informative experimental data suitable for various modeling approaches.

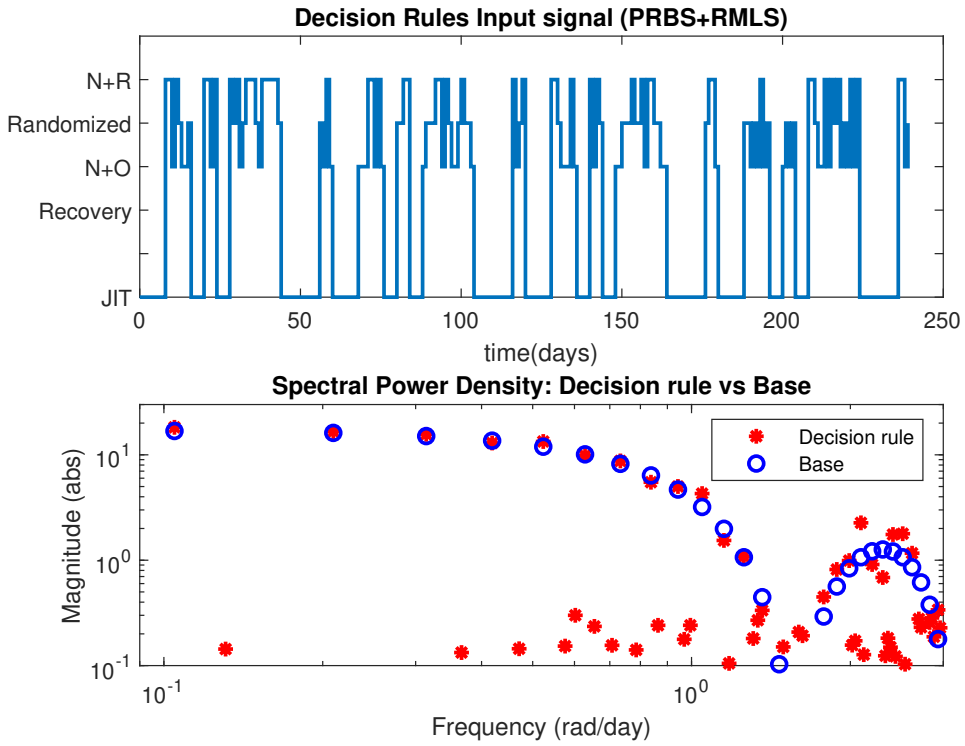

Figure 2.4: Combined PRBS and RMLS Constructing the Decision Rule Signal in the Time Domain (Top). Spectral Power Density of the Final Decision Rules Signal in Comparison to the PRBS Base (Bottom).

2.5 Simulation Results & Discussion

The SCT model presented above is utilized to simulate the designed intervention on two types of hypothetical participants: an adherent (ideal) participant, and

a non-adherent participant. The simulations also cover two different scenarios per participant: intervention without the presence of perceived barriers and unpleasant experiences versus when such disturbances occur. The goal of the intervention is to increase the amount of steps participants take per day, and ideally reach 10,000 steps/day. All simulations assume inactive participants with 2,000 steps/day as the baseline and the intervention starting at day zero. High-frequency noise is added to the behavior as part of the system, to mimic the variability in the amount of steps taken per day, as observed in previous work. Other stochastic conditions are incorporated into the simulation through the unmeasured disturbances at each inventory. In this section, the results obtained for each of the scenarios are presented and the insights they provide into the intervention and input signal design are discussed.

To account for the opportunity condition in simulations, a calendar signal is developed with a hypothetical schedule for the participants. The time within-day is divided into eight periods of three hours, where the first two periods and the last period of the day are excluded to avoid sending prompts while participants are asleep. The availability of the participant in the remaining five periods within the day is randomly generated. This calendar signal is utilized in all simulations when the opportunity is considered in the decision rules.

2.5.1 Adherent participant: No Disturbances

In this scenario, the participant is very adherent to the given goals, as the *Cues to action* level sharply increases with the increase in the daily goals. This participant can be classified as an overachiever; behavior levels significantly exceed the given goals on the majority of the intervention days. This can be also observed in the *Goal Attainment* signal, as the signal is positive for most of the intervention (approximately 71.2% of the intervention days). This leads to the progression in the daily

goals towards the target of 10,000 steps/day based on the previous cycle's average performance. The majority of the significantly negative *Goal Attainment* values are associated with the beginning of a new cycle of goal setting as a result of the higher values for daily goals. Consequently, it is observed that the participant's *Self-Efficacy* decreases upon significant increases in the goals in a new MS cycle. This particular observation helped inform the decision on an ambitious yet achievable upper bound for goals in each cycle. This particular participant does not take long to adjust their behavior and reach an average behavior level that meets or exceeds the given goals.

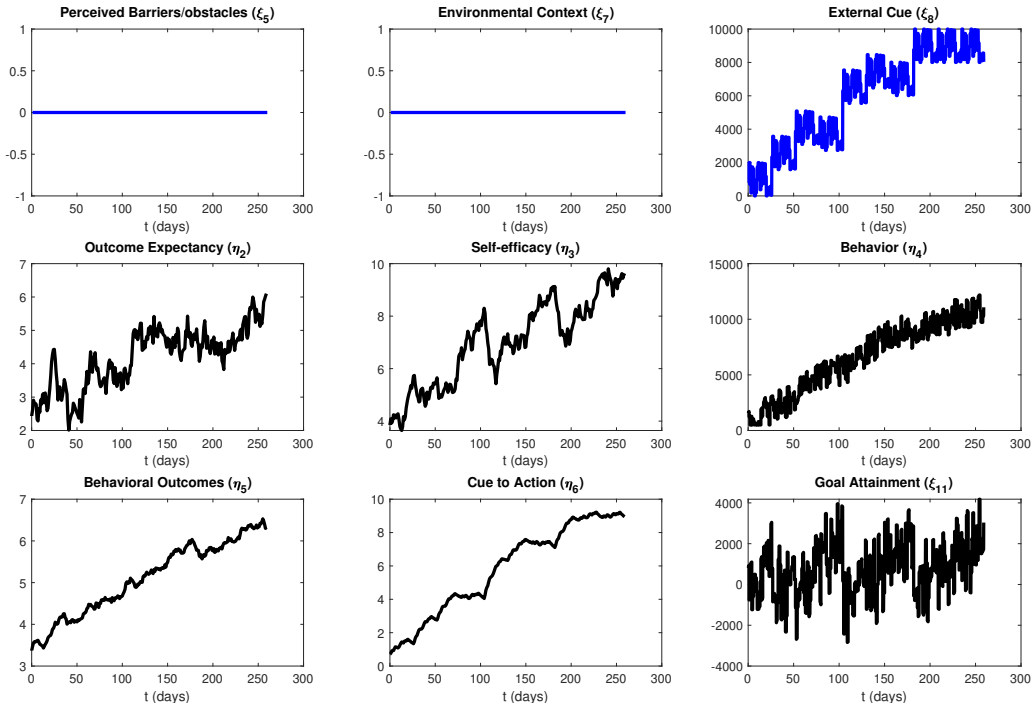

Figure 2.5: Simulated Results Illustrating the Response of an Adherent Participant to the Designed Input Signals, in the Absence of Any Disturbances.

The *Self-Efficacy* of this adherent participant increases over time as behavior increases closer to the desired intervention outcome. This adds to the participant's ability to engage in PA and walk more steps per day, which contributes to the participant overachieving the upper range of their given goals in each cycle. At the peaks

of *Self-Efficacy* the participant exceeds the daily goals by close to 4,000 steps per day increasing the average step count for that cycle, just before a new cycle with significantly higher goals is introduced. The observed trend in the *Behavioral Outcomes* and *Outcome Expectancies* is a gradual increase with the increase in *Behavior*, which is slower than what is observed with *Self-Efficacy*. *Behavioral Outcomes* increase as the benefits of the increased PA levels are observed by the participant, and higher *Outcome Expectancies* follow. This contributes to *Behavior* itself as part of the Operant-Learning (OL) loop.

Table 2.2: Notification Rates (in Notifications/day) for Each Decision Rule Per Scenario.

Scenario	**N+O**	**N+R**	**JIT**
Adherent with no disturbances	0.52	0.67	0.33
Adherent with disturbances	0.50	0.84	0.51
Non-Adherent with no disturbances	1.7	1.7	1.2
Non-Adherent with disturbances	1.8	1.8	1.3

This scenario illustrates an adherent participant who would be able to meet the daily goals most of the time, therefore, not satisfying the need condition in the decision rules for majority of the intervention. This is indeed the case observed in the simulation results where the total amount of notifications sent to this participant is the least out of all presented scenarios, at 236 (144 randomized and 92 non-randomized notifications). It is also observed that the decision rules work as they are designed; the JIT decision rule offers the least amount of burden when a participant meets the daily goals as observed in Table 2.2. The second lowest notification rate in this scenario is achieved when the need and opportunity decision rule (N+O) is enforced.

Lastly, when the need and receptivity decision rule (N+R) is followed, the notification rate is approximately double what is seen in the JIT rule. In all decision rules, the observed daily notifications rate and the amount of notifications sent in total are significantly less than the randomized notifications periods.

2.5.2 Adherent Participant: With Disturbances

In this scenario, the response of the same adherent hypothetical overachiever is simulated when the participant faces challenges. Such challenges are demonstrated by the exogenous disturbances in the form of *Perceived Obstacles & Barriers*, and *Environmental Context*. This is done to mimic real-life situations where undesired environmental factors like weather (i.e., rain, heat waves, etc.) might not allow participants to exercise or walk in their normal routine. Another exogenous factor that can impact engagement in PA is in the form of daily life obstacles participants perceive and face, like coming down with a seasonal illness or having to accommodate for unforeseen work/school/social life demands. In Fig. 2.6 it is observed that this participant's response in this scenario is very similar to the previous case. The main differences are seen in the *Self-Efficacy* and *Behavioral Outcomes* as they are negatively impacted by the *Perceived Barriers*, and the bad *Environmental Contexts* respectively. Consequently, *Outcome Expectancies* and *Behavior* are at lower levels than what is seen in Section 2.5.1.

Despite the negative impact of the considered exogenous disturbances, this participant still manages to adapt to higher goals quite effectively. The participant overachieves the daily goals by a decent margin as illustrated in Fig. 2.6 by the *Goal Attainment* signal; this participant meets or exceeds the daily goals for 63.5% of the intervention. Based on this described nature of the *Behavior*, this participant can be classified as a goal-oriented, determined person who is not easily deterred by any

obstacles or inconveniences.

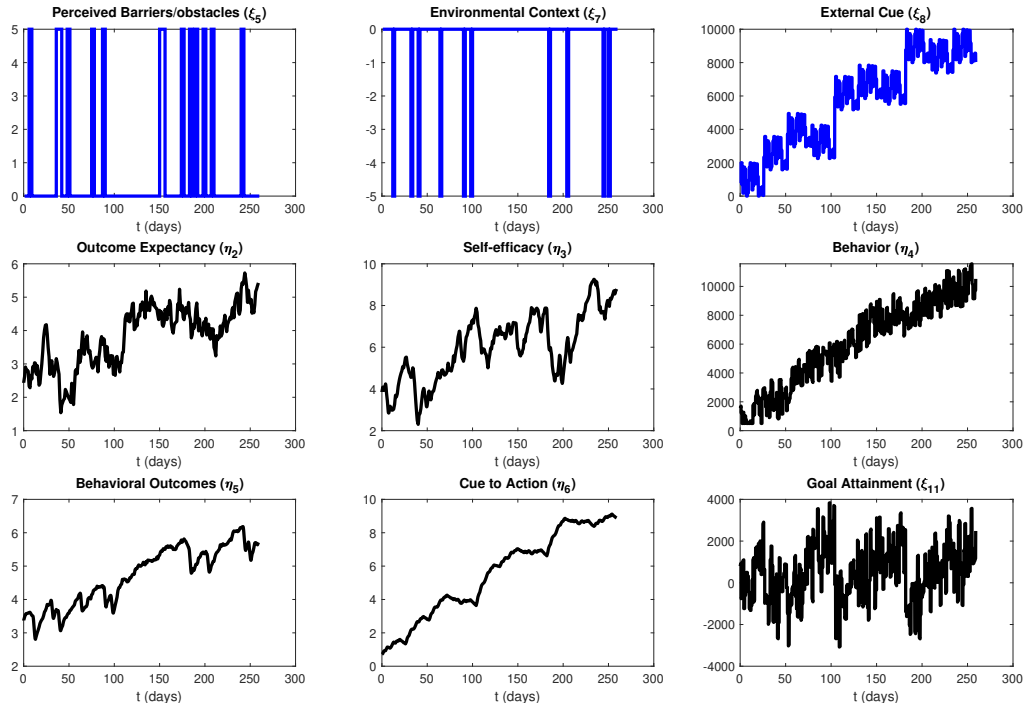

Figure 2.6: Simulation That Illustrates the Response of an Adherent Participant to the Designed Input Signals, in the Presence of Disturbances in the Form of *Perceived Barriers/Obstacles* and Bad *Environmental Context*.

Positive *Goal Attainment* in this scenario is lower than what is seen in the previous case, as a result, more inspiring bout prompts are sent to the participant, due to meeting the need condition more frequently. The participant receives 263 total notifications in this simulation (144 randomized and 119 non-randomized notifications). The rates of notifications for the decision rules change when disturbances occur in contrast to the case seen in Section 2.5.1. Table 2.2 shows that the highest increase in notification rates is seen in the N+R decision rule periods. The notification rate for the JIT rule also increases when exogenous disturbances occur. Surprisingly, the rate of notifications for the N+O decision rule decreases in this scenario. This implies that the differences between the two scenarios for the adherent participant are not

only limited to the levels of the considered constructs; there is a shift in the periods at which goals are met as well as the percentage of days the behavior exceeds the given goals.

Figure 2.7: Notifications Sent Throughout the Intervention (Middle), the Decision Rules (Bottom) and *Goal Attainment* (Top) Associated with Notifications Sent Each Day for the Adherent Participant in the Presence of the Disturbances.

2.5.3 Non-adherent Participant: No Disturbances

In this scenario, the participant is not adherent to the given goals, which is evident in the *Cues to action* levels. The participant fails to achieve the desired 10,000 steps per day target, yet is more active by the end of the intervention. As it can be seen in Fig. 2.8 the average level for behavior increases overall, however, the *Goal Attainment* is progressively negative. This participant managed to meet or exceed daily goals only for 34.6% of the intervention. Due to underperformance by this participant, the given goals never reach 10,000 steps per day as intended by design, and the maximum value for the given goals is around 6,500 steps/day. The negative *Goal Attainment* values lead to a significant decrease in the *Self-Efficacy* levels for this participant. Such low levels negatively impact the participant's drive to meet the daily goals and most likely will lead to the participant dropping out of the intervention, or becoming absolutely disengaged with the goals and daily EMAs. The disengagement scenarios have not been included in this chapter and will be pursued in future work for more representational simulations.

Behavioral Outcomes and *Outcome Expectancies* increase at a very high rate for the first half of the intervention. For the second half of the intervention, the rate of change in both constructs decreases and is negative by the end of the intervention. The sustained gains in *Behavioral Outcomes* and outcome expectancies are the main contributors to the increase in this participant's average daily step count. Therefore, this participant can be classified as an experience-oriented participant rather than goal-oriented.

The amount of walking notifications sent in this scenario is 428 notifications in total (144 randomized and 284 non-randomized notifications). In this scenario, there is an increase in the notification rates for each of the examined decision rules, as

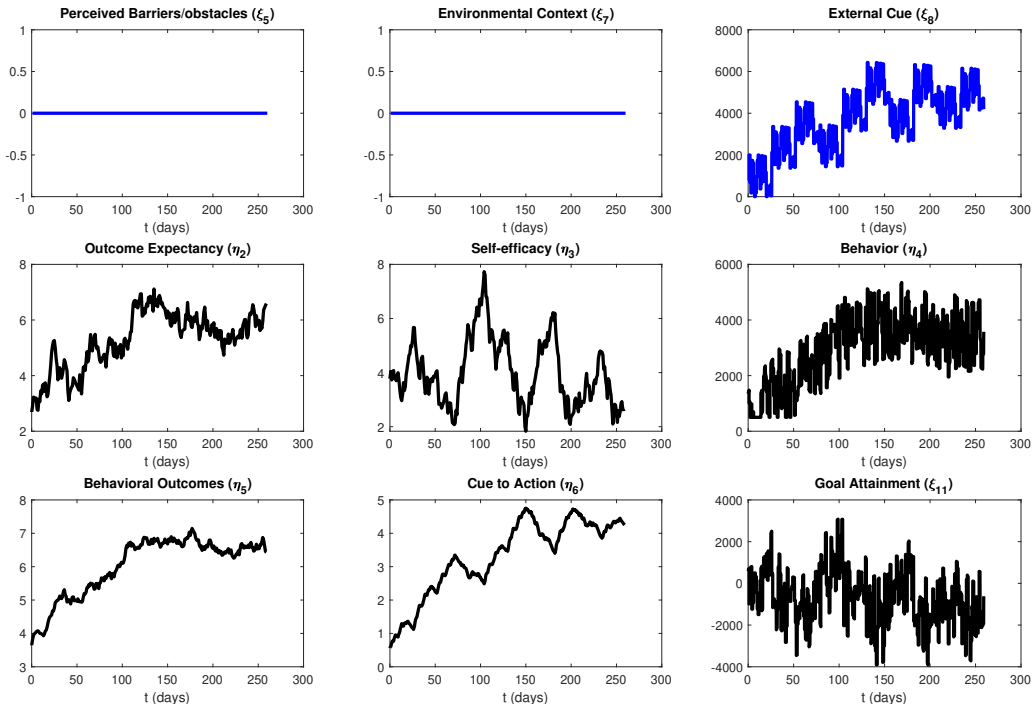

Figure 2.8: Simulation Illustrating the Response of a Non-Adherent Participant to the Designed Input Signals, in the Absence of Disturbances.

expected, because of the negative *Goal Attainment* for most of the intervention. As can be seen in Table 2.2 the biggest increase in the notification rates compared to the adherent participant scenarios is observed in the N+O decision rule periods, followed by the increase in notification rate for N+R decision rule, which is significantly higher than the adherent participant cases. The JIT decision rule shows the minimum increase in this scenario.

2.5.4 Non-adherent Participant: With Disturbances

The non-adherent participant performs worse from an intervention standpoint when faced with exogenous disturbances. The same changes in *Perceived Barriers/Obstacles* and *Environmental Contexts* as the ones examined in Section 2.5.2 are applied in this scenario. As a result, the average step-count for this participant only

slightly increases above the baseline by the end of the intervention. As expected from this non-adherent participant, the 10,000 steps/day target is never reached and the highest given daily goal is close to 5,700 steps/day in this scenario. The lower daily goals are a result of the participant having negative *Goal Attainment* for 31.2% of the intervention. The negative *Goal Attainment* values lead to lower *Self-Efficacy* and reduced PA levels as a consequence; the *Self-Efficacy* levels are the lowest out of all examined scenarios. It can also be observed in Fig. 2.9 that the non-adherent participant is more sensitive to exogenous disturbances than the adherent participant; *Self-Efficacy* and *Behavioral Outcomes* drop more significantly when inconvenient circumstances occur.

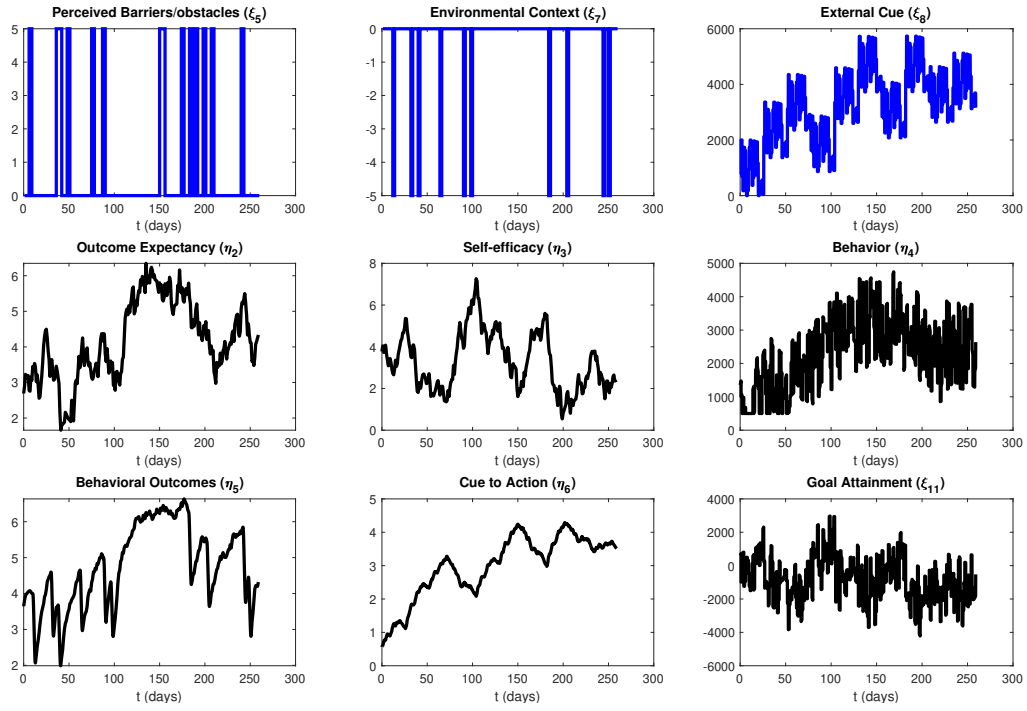

Figure 2.9: Simulation Illustrating the Response of a Non-Adherent Participant to the Designed Input Signals, in the Presence of Disturbances in the Form of *Perceived Barriers/obstacles* and Bad *Environmental Context*.

As this participant is experience-oriented, the significant decrease in the *Behav-*

ioral Outcomes as a result of bad *Environmental contexts* leads to noticeably lower levels in *Outcome Expectancies* than the case for this participant without disturbances. Consequently, the contribution of the OL loop to the *Behavior* levels is minimal. This leads to the average level of *Behavior* decreasing closer to the baseline value towards the end of the intervention. This underperforming non-adherent participant is more likely to drop out of the study due to the negative impact on *Self-Efficacy* as well as the lower values of *Behavioral Outcomes* and *Outcome Expectancies*.

Figure 2.10: Notifications Sent Throughout the Intervention (Middle), the Decision Rules (Bottom) and *Goal Attainment* (Top) Associated with Notifications Sent Each Day for the Non-Adherent Participant in the Presence of the Disturbances.

The overall amount of notifications sent in this scenario is the highest at 459 notifications with 144 randomized notifications and 315 non-randomized notifications. This is to be expected as the participant does not manage to meet the goals for the majority of the intervention. Consequently, the highest notification rates for all decision rules are observed in this scenario. The most significant increase in the notification rates is observed for the N+O decision rule, as shown in Table 2.2. The second highest increase is observed in the N+R rule. Also, the highest notification rate for the JIT decision rule is seen in this scenario. The notification rates for the three decision rules are all substantially lower than those of the randomized periods for all simulated scenarios, which shows that the decision rules are working as designed.

The simulation results shown above are a major factor in shaping the specifics of the decision rules and having rough expectations of what is to come when the intervention goes online. By examining hypothetical participants ranging in behavior from being highly adherent to absolutely non-adherent, an informative, balanced intervention can be achieved. This should result in insightful experimental data that allows for modeling the interesting multi-timescale dynamics of behavior change.

2.6 Conclusions

This chapter serves as a proof of concept of the effectiveness of system identification approaches in input signal design for behavioral intervention experiments. Through the utilization of *a priori* knowledge from previous work and simulation, the iterative input signal design process can be optimized to establish behavioral interventions, which provide dynamically informative experimental data covering the important multi-timescale dynamics associated with behavior change. This is the aim of the *JustWalk JITAI*, where the innovative design of the input signals for goal setting and walking notifications allow for systematic examination of behavior change

dynamics at high frequencies (e.g. within-day) while maintaining a low burden on participants. To reduce the burden on participants even further, in future work methods such as pattern recognition will be utilized for the opportunity condition, rather than an external calendar signal. The measured experimental data should allow for estimation and validation of control-oriented models through sophisticated system identification methods including grey-box approaches and black-box approaches in the form of Auto Regressive with eXogenic inputs (ARX; Ljung (1999)) and Model-on-Demand (MoD; Stenman (1999)). The obtained idiographic dynamical models can be applied in optimal personalized behavioral interventions through sophisticated control algorithms like model predictive control (MPC). Furthermore, the estimated models provide insight into the best control strategies per individual even in cases where measurements of some of the psychological constructs are not easily attainable.

The adoption of system identification approaches in behavioral science can lead to a better understanding of the multi-timescale dynamic processes of behavior on an idiographic level, that allows for personalized provision of intervention support following the notions of just-in-time state. This should maximize the gains from behavioral interventions and allow for fostering healthy behavior in participants. The implementation of judiciously designed, personalized JITAIs for PA on a large scale should improve the quality of life and life expectancy of both participants and the community overall.

Chapter 3

SYSTEM IDENTIFICATION AND SIGNAL PROCESSING IN UNDERSTANDING "JUST-IN-TIME" STATES FOR PHYSICAL ACTIVITY: ANALYSIS OF THE *JUSTWALK JITAI* INTERVENTION

3.1 Introduction

The benefits of physical activity (PA) to health are numerous; an increase from 4,000 to 8,000 steps/day is linked to the reduction of all causes of mortality by 51% (Saint-Maurice *et al.*, 2020). However, the majority of the population does not meet the recommended CDC guidelines for PA, therefore most people do not reap the benefits of healthy levels of PA (Olson *et al.*, 2018). Although digital behavior change interventions (DBCIs) have demonstrated their potential in promoting healthy behaviors including PA, the efficiency of classical DBCIs is hurdled by various obstacles (Schoeppe *et al.*, 2016). Much of traditional behavior medicine focuses on static models on a nomothetic level (i.e., group or population level), that only examine if an intervention component has positive outcomes without explaining the dynamics and drivers behind behavior change. Consequently, traditional studies do not take into account idiosyncrasies within a group or a population, and on a deeper level idiosyncrasies within an individual over time. Hence, there is a lack of understanding of the dynamic and possibly context-varying nature of systems associated with behavior change, especially on an individual level. Therefore, the delivery of behavioral interventions is not personalized or optimized to ensure the effectiveness of DBCIs in promoting sustained healthy behavior.

The availability of temporally dense PA data afforded by advances in and pop-

ularity of wearable technologies that track PA levels (e.g., FitBit) has set the stage for the re-emergence of idiographic data analysis methods. Such methods are particularly geared towards understanding behavior change dynamics on an individual level, by analyzing and predicting patterns within time series data corresponding to each individual. These temporally dense longitudinal data sets provide unprecedented opportunities to apply system identification, and control systems engineering principles to implement data-driven solutions to problems faced in behavioral medicine, in terms of optimization and personalization of decision-making in an intervention (Hekler *et al.*, 2016). However, many challenges are faced in extracting value out of data, both on exploratory and predictive levels. Hence, it is particularly important to focus on 1) the design of experiments to provide dynamically informative data sets; and 2) developing and improving signal processing and model estimation methods that can capture nonlinearities of the system and idiosyncrasies in context.

In behavioral medicine, the concept of "just-in-time" adaptive interventions (JITAIs) has been introduced to improve the understanding of the impact of context and multi-timescale dynamics associated with behavior change, and by extension increase the efficiency of decision-making. The essence of JITAIs is in the provision of support only when a participant has the need for a certain kind of support, the opportunity to act on the support, and the receptivity to respond positively to that support. This can result in meaningful and sustained adaptations of healthy behavior over time in what is known as "just-in-time" (JIT) states. Therefore, it is imperative to understand the JIT context to address JITAIs as an optimization problem, where robust prediction and decision-making are needed to provide the support that contributes towards sustainable healthy behavior change. In pursuit of exploring and understanding these concepts, a digital health intervention study (*JustWalk JITAI*; Park *et al.* (2023)) has been developed, and the results of these are presented in this chapter.

JustWalk JITAI is one of the first empirical studies of JIT states based on system identification principles. To facilitate understanding and analyzing such complex dynamic phenomena, innovative input signals are designed and implemented in the design of experiment, and advanced data-driven modeling techniques are utilized in a comprehensive approach. This chapter provides a brief overview of elements comprising the proposed approach and examines its application on a representative *JustWalk JITAI* participant. The results presented demonstrate the significant potential of a comprehensive system identification approach in improving the understanding of behavior change systems, in context.

This chapter is arranged as follows. Section 3.2 provides a brief description of the *JustWalk JITAI* study and the input signal design. Section 3.3 details the implemented estimator, and its advantages in terms of modeling behavior change in context, while in Section 3.4 a brief summary of Singular Spectrum Analysis (SSA) is provided. In Section 3.5, results of the proposed approach are presented and discussed for a representative participant. Section 3.6 provides conclusions along with implications for future work.

3.2 Study Description & Input Signal Design

JustWalk JITAI is an NIH-funded study aimed at advancing the understanding of multi-timescale dynamics and JIT states context for supporting PA, in the form of daily *Step Count*. As this is a unique study, addressing advanced problems in behavioral science, a new and innovative design of experiments is introduced. The intervention was designed to provide informative data on short and long-timescale dynamics in behavior change systems related to PA, within-day, and between-day respectively. This is essential in operationalizing JITAIs as a multi-timescale robust optimization problem, where support is only provided at JIT states, in a manner

that ensures the provided support contributes towards sustained behavior change. To accomplish this, two intervention components are utilized: 1) adaptive daily goals and 2) walking notifications (see Chapter 2).

In the adaptive daily goals component, each participant is given daily targets of the number of steps they should meet on a given day, to help them move towards eventually meeting national PA recommendations, which were dictated by a personalized realization of the designed multisine signal for this component. To adapt the signal to the performance of each participant, the maximum and minimum amount of daily step goals in each cycle are adjusted based on the performance in the previous cycle. Consequently, this intervention component is further personalized to each participant, by providing ambitious yet achievable goals. This aspect of the design produces informative data that captures the longer-term dynamics at high and low participant performance.

The walking notifications component of the *JustWalk JITAI* focuses on within-day dynamics and JIT states. This component consists of inspiring messages sent to participants within-day on 4 decision points (once every 3 hours starting at 7 am), to invite them to go on a short walk (e.g., 10 minutes). The decision on whether to send a notification or not at every decision point is dictated by a decision rules signal designed for this intervention component. This input signal is designed to test the effectiveness of notifications sent on what is perceived as full or partial JIT states in comparison to fully randomized notifications. To operationalize this, three conditions about the current moment are taken into account:

- *Need* (N): If the participant is not on track to meet the given daily goal.
- *Opportunity* (O): Whether the next 3-hour window is predicted to be an opportune window for the participant to engage in PA, based on a previously

developed algorithm .

- *Receptivity* (R): If the participant has received less than 6 notifications, and responded favorably (i.e., walked) to half of the notifications sent to them in the last 72 hours.

Three different combinations of the JIT conditions to send notifications are chosen as the decision rules in the intervention: 1) N+R, 2) N+O, 3) N+O+R which is labeled as the JIT decision rule. These three combinations are compared to fully randomized decisions.

To design a categorical input signal for the walking notifications component, the approach described in Chapter 2 is followed: a pseudo-random binary sequence (PRBS) is generated to serve as the base signal. Then, a three-level uniformly distributed random multi-level sequence (RMLS) is superimposed on one of the binary levels in the PRBS signal. This is done to evaluate the impact of the different JIT states combinations in comparison to fully randomized notifications, as well as to study the dynamic nature of the response to the notifications under different conditions. A detailed description of the input signal design is provided in Chapter 2 and El Mistiri *et al.* (2022a); details regarding the study design and experimental protocol are published in Park *et al.* (2023).

3.3 Model-on-Demand (MoD)

One of the main objectives of the *JustWalk JITAI* is to explore the multi-timescale dynamics and the dynamic impact of JIT states on PA behavior change. In this chapter, the focus is on understanding the dynamic nature of the system in the context of JIT states. To reach this aim, Model-on-Demand (MoD; Braun *et al.* (2001)) is utilized, which is a sophisticated data-centric modeling approach. MoD is an adap-

tive modeling approach, which does not rely on a global model, making it a perfect candidate to explore and explain JIT states. As demonstrated in Fig. 3.1, in MoD a weighted least-squares regression problem in (3.2) is solved to fit the data in a bounded neighborhood around each operating point k, under a specified global regressor structure $[n_a\, n_b\, n_k]$. Therefore, MoD combines both local and global modeling. Hence, in MoD, the estimation data is not discarded, rather a subset of the data is used to estimate a local model at each operating point on demand.

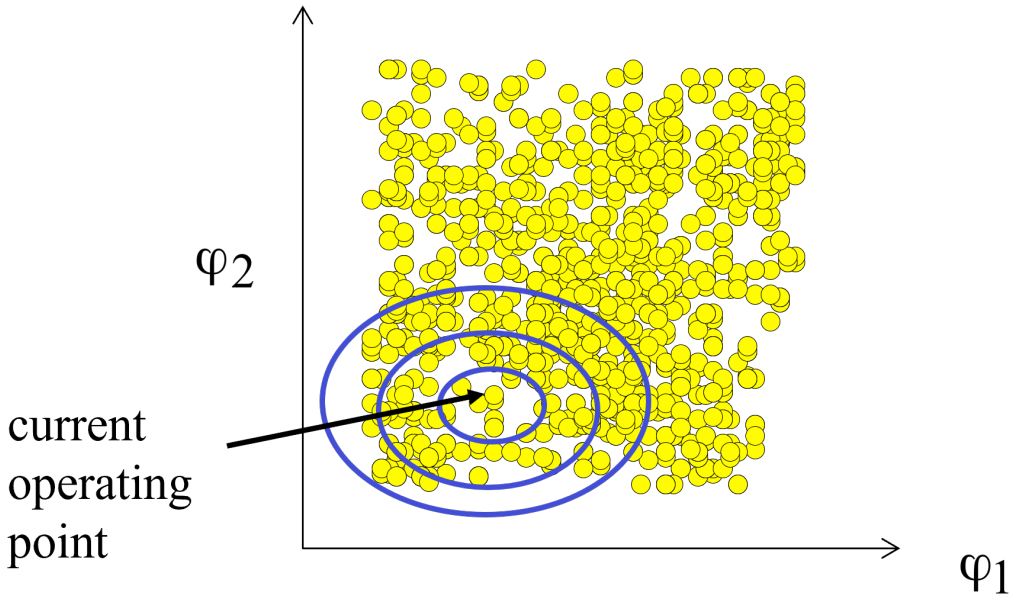

Figure 3.1: Schematic Illustrating MoD Adaptive Selection of Regressor Neighborhood Size At an Operating Point, (Braun, 2001).

In this chapter, MoD formulation is described for a single input single output (SISO) system, however, the same formulation can be extended to multi input multi output (MIMO) systems (Braun *et al.*, 2001). For a SISO process with a nonlinear structure:

$$y_k = m(\varphi_k) + e_k \tag{3.1}$$

where $m(\cdot)$ is an unknown nonlinear mapping and e_k is an error term. The error is

modeled as a random signal with zero mean and variance σ_k^2. The MoD predictor estimates output predictions, $\hat{y}_k$, based on a local neighborhood of the regressor space φ, as depicted in Fig. 3.1. This is done by solving the optimization problem in (3.2), at each operating point k.

$$\hat{\theta} = \arg \min_{\theta} \sum_{i=1}^{N} \ell \left(y_i - \hat{m}(\varphi_i, \theta) \right) K_h \left(\frac{\|\varphi_i - \varphi_k\|_M}{h} \right) \tag{3.2}$$

where

$$\hat{\theta} = [\hat{\theta}_0 \ \hat{\theta}_1 \ \hat{\theta}_2 \ \cdots \ \hat{\theta}_{p_{reg}}] \tag{3.3}$$

represents parameters of the local polynomial model of the regressors, and φ_* is the regressor vector at the point $* \in \{i, k\}$, which can be defined differently for different model structures. Nonlinear and linear model structures can be used to define the local model in (3.2). Due to the computational simplicity of estimating parameters for linear or quadratic model structures, as they are linear in the unknown parameters, in this chapter a model structure akin to a linear ARX is utilized:

$$\varphi_* = [y_{*-1} \cdots y_{*-n_a} \, u_{1,*-n_{k_1}} \ \cdots \ u_{1,*-n_{b_1}-n_{k_1}+1} \cdots u_{n_u,*-n_{k_{n_u}}} \ \cdots \ u_{n_u,*-n_{b_{n_u}}-n_{k_{n_u}}+1}]^T$$

where n_a denotes the output order in the regressor (as in the number of previous output lags), n_b denotes the number of previous lags in the input, and n_k denotes the input delay in the model. For a MIMO system, n_a is specified for each output in a matrix reflecting interactions between outputs, and n_b and n_k are specified for each input-output combination. i is the sample instance from the estimation database of length N. The length of the parameter vector p_{reg} is determined by the length of the regressor vector d_{reg}, where $p_{reg} = d_{reg}$ for the linear case, and $p_{reg} = d_{reg} + d_{reg}(d_{reg} + 1)/2$ for the quadratic case. The weighting of the data points in the neighborhood of k is performed through a kernel-based function $K_h(\cdot)$, where higher weights are given to points closer to c based on their scaled distance in regressor space and bandwidth h.

The distance scaling function is defined as

$$\|\tilde{\varphi}\|_M = \sqrt{\tilde{\varphi}^T M \tilde{\varphi}} \tag{3.4}$$

where $\tilde{\varphi} = \varphi_i - \varphi_k$, and M is the scaling matrix obtained from the inverse covariance of the regressors. The bandwidth h is selected adaptively through an iterative process to optimize over local information criteria (e.g., AIC, GCV), within a user-defined range $[i_{min},\, i_{max}]$ for neighborhood size.

Assuming a local model structure that is linear in the unknown parameters a MoD estimate is computed through least squares regression.

$$m(\varphi_k, \theta) = \theta_0 + \theta_1^T(\varphi_i - \varphi_k) \tag{3.5}$$

where θ_0 and θ_1 are the minimizers estimated by solving the least squares problem expressed in (3.2), utilizing the model structure presented in (3.5). The one-step-ahead prediction is therefore given by

$$\hat{y_k} = \alpha + \hat{\theta}_1^T \varphi_i \tag{3.6}$$

where

$$\alpha = \hat{\theta}_0 - \hat{\theta}_1^T \varphi_k \tag{3.7}$$

Solving the local regression problem around the neighborhood of k produces a single prediction $\hat{y}_k$ corresponding to the current operating conditions defined by the regressor φ_k. To obtain a prediction at other operating points in the regressor space, the estimation database is called again and both the relative weights and the selection of data are updated to optimize a new local model at the new operating point. This distinguishes MoD from global modeling techniques in which the model is estimated for the overall data only once, and then the data is discarded. Additionally, the adaptive computation of bandwidth h, which governs the trade-off between bias and

variance errors in model estimation, has a significant impact on the estimated linear local models.

In MoD, the regressor structure used in $\varphi(t)$, the local polynomial order that approximates $m(\cdot)$, k_{min}, k_{max}, and the goodness-of-fit (GoF) criterion can be specified to influence the estimated model; these variables impact the size of the neighborhood chosen to fit the local model. Additionally, the window function is also specified by the user, a tricube window function is most commonly used as it has attractive features like being continuously differentiable and a known value of zero at the boundaries (Braun, 2001). It is important to select a minimum neighborhood size i_{min} sufficiently large to avoid ill conditions in parameter estimation. On the other hand, i_{max} can be set as the entirety of the data set length, however, that can lead to a high computational for large data sets. Hence, informed decisions are necessary in the selection of the neighborhood range, to assure the efficiency of model estimation. Moreover, optimizing over the local information criteria in selecting the optimal neighborhood size i_{opt} represents a classic trade-off between bias and variance; a large neighborhood size reduces variance-induced error while increasing error due to bias from fitting a local model over a large data set.

The MoD approach fits perfectly with understanding the dynamics of JIT states, as the estimated local models depend on the operating condition at each point. Five input signals ($n_u = 5$) are utilized to define conditions in regressor space, including designed intervention components and other exogenous signals, as follows:

- *Step Goals* (u_1): the daily step goal given to a participant, as described in Section 3.2.

- *Decision Rules* (u_2): defines the utilized JIT rule for sending notifications on a specific day, as defined in Section 3.2.

- *Viewed Walking Notifications* (u_3): number of walking notifications viewed by the participant on a day.
- *Temperature* (u_4): the recorded highest daily temperature.
- *Weekend* (u_5): a binary signal representing whether a given day is a weekend (1) or a weekday (0).

The modeled output of interest is PA behavior y, in terms of daily *Step Count*, which also serves as part of the regressor φ_k to define context at each point.

3.4 Noise Reduction & Signal Separability: Singular Spectrum Analysis (SSA)

There are several challenges faced in analyzing data related to PA behavior systems. For instance, the accuracy of the measurements can be heavily influenced by the quality of the sensors used in activity tracking, and the algorithms utilized to filter the raw data (Bender *et al.*, 2017). In addition, the availability of the measurement and its quality are predicated on participants' adherence to wearing the measurement device. As a result, missingness can exist on no wear days and measurement levels can be significantly low on low wear-time days, which does not represent the actual behavior. Additionally, the collected *Step Count* signal represents the aggregate impact of idiosyncratic forces impacting behavior on different timescales. For example, life rhythms (e.g., work, weekends) can contribute to the daily *Step Count* in a periodic manner, which is independent of the overall trend caused by intentional engagement in PA. Hence, to understand PA behavior change in context, it is desired to reduce the noise in the measurement and analyze the different components that constitute the overall measurement.

In this work, we rely on Singular Spectrum Analysis (SSA) to reduce noise in the *Step Count* measurement and study its separability. SSA is a Singular Value

Decomposition (SVD) based nonparametric technique for signal processing and time series analysis. SSA is beneficial in analyzing different aspects of the system, like investigating the separability of the measured signal to its components, filtering measurement noise, and studying causality (Hassani and Zhigljavsky, 2009). In SSA, time series data is decomposed into a sum of its components by performing SVD on the Hankle matrix of the original data. Each component in the sum is then designated into groups of trend, periodic, quasi-periodic, or noise components. Moreover, cross-correlated components can be grouped and summed to capture their collective characteristics. Finally, the filtered output signal is constructed through the sum of the most relevant system components, excluding noise.

The Hankel matrix H is constructed by transferring the one-dimensional output signal $Y = [y_1\, y_2\, \ldots\, y_N]$ of length N into a series of L-lagged vectors as follows:

$$H = [h_1\, h_2\, \ldots\, h_M] = \begin{bmatrix} y_1 & y_2 & \cdots & y_M \\ y_2 & y_3 & \cdots & y_{M+1} \\ \vdots & \vdots & \ddots & \vdots \\ y_L & y_{L+1} & \cdots & y_N \end{bmatrix} \tag{3.8}$$

where $M = N - L + 1$, and L is an integer such that $2 \leq L < N$ which represents the window length utilized to construct the Hankel matrix. L is a user-selected parameter and must be sufficiently large to capture important system dynamics. In this work, the window length L is selected based on the periodicity observed in the autocovariance of the output signal. This is done by obtaining the mean distance between lags at which peaks in the autocovariance occur. L is then selected to include all lags within twice the mean distance between peaks.

SVD is then performed on H to decompose it into a total of L rank-one bi-orthogonal elementary matrices. The eigenvalues of HH^T are represented by λ_i in descending order ($\lambda_1 \geq \lambda_2 \geq \cdots \geq \lambda_L \geq 0$), while their corresponding or-

thonormal left and right eigenvectors are denoted by U_i and V_i respectively, where $i = 1, \cdots, L$. Therefore, the Hankel matrix can be re-written as the linear combination of L matrices

$$H = \sum_{i=1}^{L} H_i \tag{3.9}$$

where

$$H_i = \sqrt{\lambda_i} U_i V_i^T \tag{3.10}$$

Each matrix H_i represents a component of the output signal, which is then Hankelized into $\hat{H}_i$ by calculating the antidiagonal average. Consequently, the summation of the Hankel matrices of all output signal components $\hat{H}_i$ represents the Hankel matrix of the original signal H. Time series signals $Y_{SSA,i}$ for each component i are then extracted from each Hankelized component matrix $\hat{H}_i$. As a result, the original signal is the summation of the reconstructed components

$$H = \sum_{i=1}^{L} \hat{H}_i \Rightarrow Y = \sum_{i=1}^{L} \hat{Y}_i \tag{3.11}$$

The relevance of each component r_i is determined by its contribution to the sum of all real singular values

$$r_i = 100 \frac{\sqrt{\lambda_i}}{\sum_{i=1}^{L} \sqrt{\lambda_i}} \tag{3.12}$$

A threshold value Th is selected to filter out the least relevant components, where the subset of the selected important components is of size d, where

$$d = \max(i \ \mid \ r_i > Th \ \forall \ i = 1, \cdots, L) \tag{3.13}$$

Because of SSA's formulation, high-frequency components -which are often associated with noise- represent the least contribution to the total of the singular values ($\sum_{i=1}^{L} \sqrt{\lambda_i}$). Therefore, this step effectively represents noise reduction in the reconstruction of the filtered output signal Y_{SSA}.

$$Y_{SSA} = \sum_{i=1}^{d} \hat{Y}_i \tag{3.14}$$

Subsequently, cross-correlated signals from the selected reconstructed components $(\hat{Y}_1, \ldots, \hat{Y}_d)$ are aggregated to represent their collective impact in each group (e.g., trend, seasonality 1) at its respective frequency range.

3.5 Results & Discussion

In this section, results for the implementation of the proposed signal processing and model estimation approach on data for a representative *JustWalk JITAI* participant are presented and discussed. The separability of the *Step Count* signal is demonstrated by analyzing the SSA decomposed signal components. Moreover, the effectiveness of MoD in modeling behavior change in context is illustrated.

3.5.1 SSA: Noise Reduction and Signal Separability

The autocovariance function of the measured *Step Count* signal for this participant indicated a periodicity of seven lags. Consequently, a window length of $L = 15$ days is utilized. This results in the decomposition of the system into 15 different components, the time series and spectral power densities of which are presented in Fig. 3.2a and Fig. 3.2b, respectively. By analyzing the amplified frequencies in the spectral power density of each component and their patterns in the time domain, a threshold value $Th = 4\%$ is utilized to filter out higher-frequency components. This results in reducing the number of relevant components to $d = 5$. These components are used to reconstruct the SSA-filtered output signal shown in Fig. 3.3. The normalized root mean square error (NRMSE) of the SSA-filtered output signal is 45.3%, illustrating that it captures most of the important system dynamics.

Results in Fig. 3.3 demonstrate the effectiveness of SSA in noise reduction. This is evident in how the SSA-filtered signal appears as a smoothed version of the original signal; maintaining important dynamics, while excluding high-frequency changes that

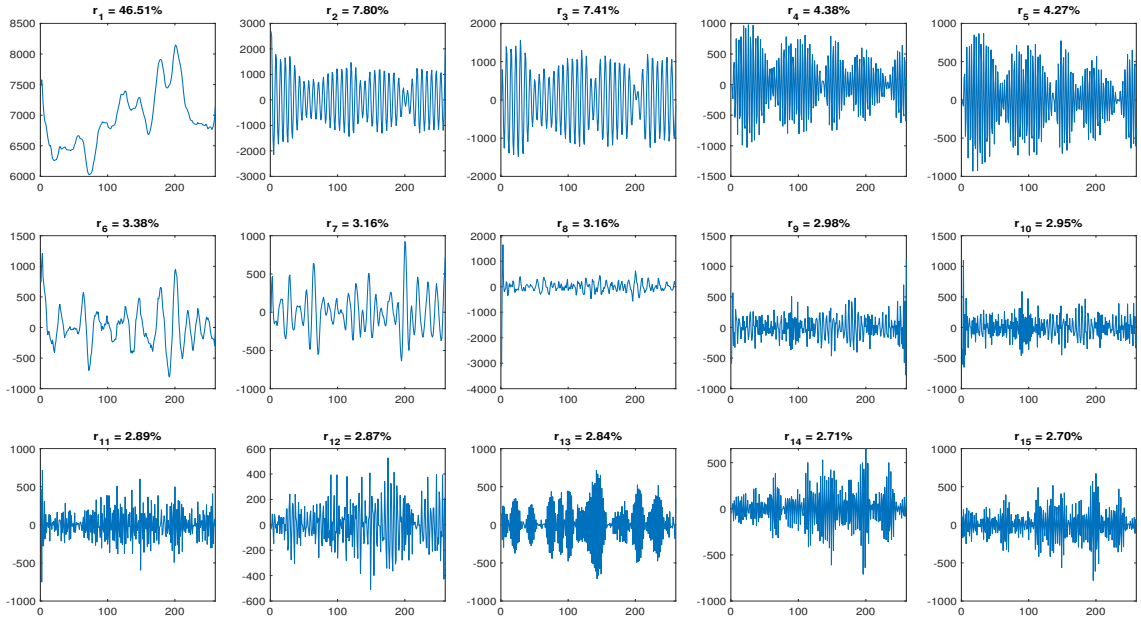

(a) Time series

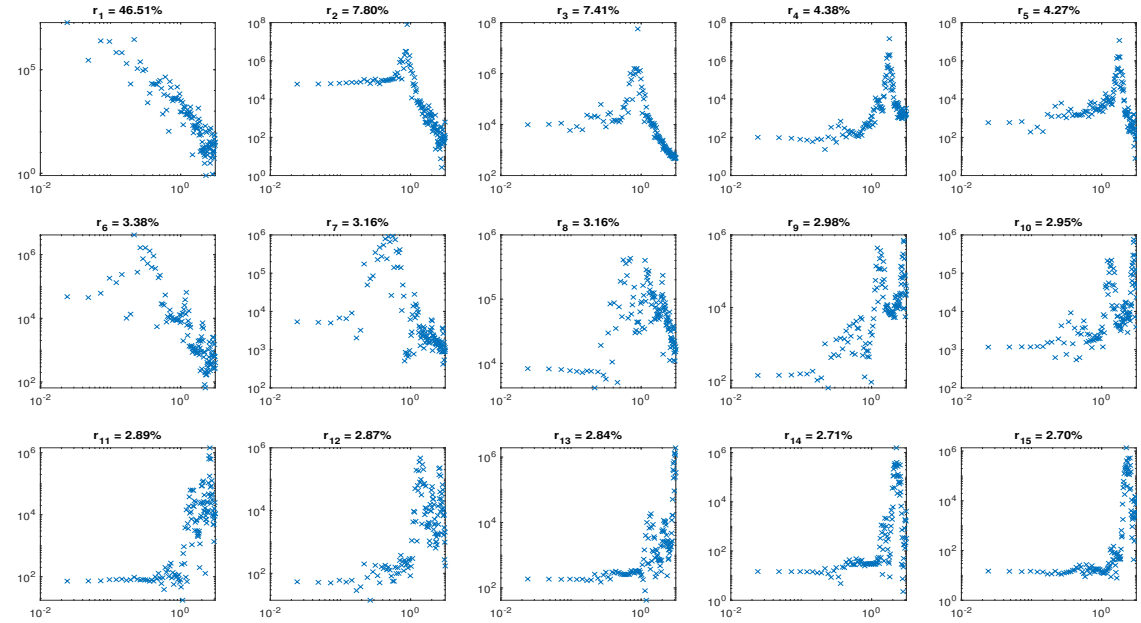

(b) Spectral power density

Figure 3.2: (A) Time Series, (b) Spectral Power Density of the *Step Count* Components ($\hat{Y}_i \ \forall \ 1 \leq i \leq L$) Decomposed By SSA, Along with Their Relevance (r_i).

can be attributed to noise. Moreover, the impact of significantly high and low data points, which can be considered outliers that do not represent the actual system dynamics, is reduced in the SSA-filtered time series.

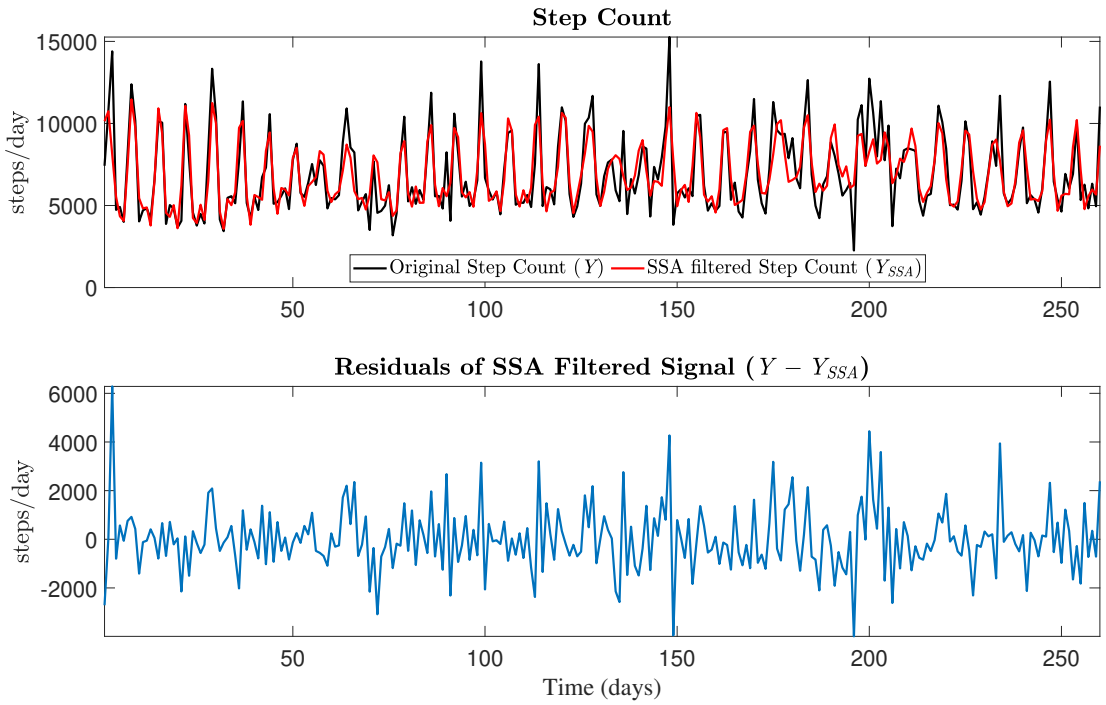

Figure 3.3: Original (Y) and SSA-Filtered (Y_{SSA}) Daily *Step Count* Signals in Steps/day, Along with Residuals.

By analyzing the cross-correlation between the relevant components, they are found to form three distinct groups, with each group covering a different frequency range:

1. *Trend*: contains the first component, which covers low frequencies and represents the underlying slower dynamics of changes in the *Step Count* trend.

2. *Seasonality 1*: consistent of the second and third components. This group covers intermediate frequencies, where periodicity is observed in a 7 days pattern.

3. *Seasonality 2*: covers higher frequencies, with an observed periodicity over 3-4 days span. The fourth and fifth components are grouped in this set.

The reconstructed signals for each group are presented in Fig. 3.4. The obtained results illustrate that the collected daily *Step Count* signal is separable. Additionally, these results demonstrate that the benefit of SSA goes beyond noise reduction; SSA breaks down time series data components into uncorrelated groups that capture different features of the overall behavior. Consequently, each component can be modeled independently to help understand the dynamic nature of the idiosyncratic forces influencing behavior change in context, at different frequencies.

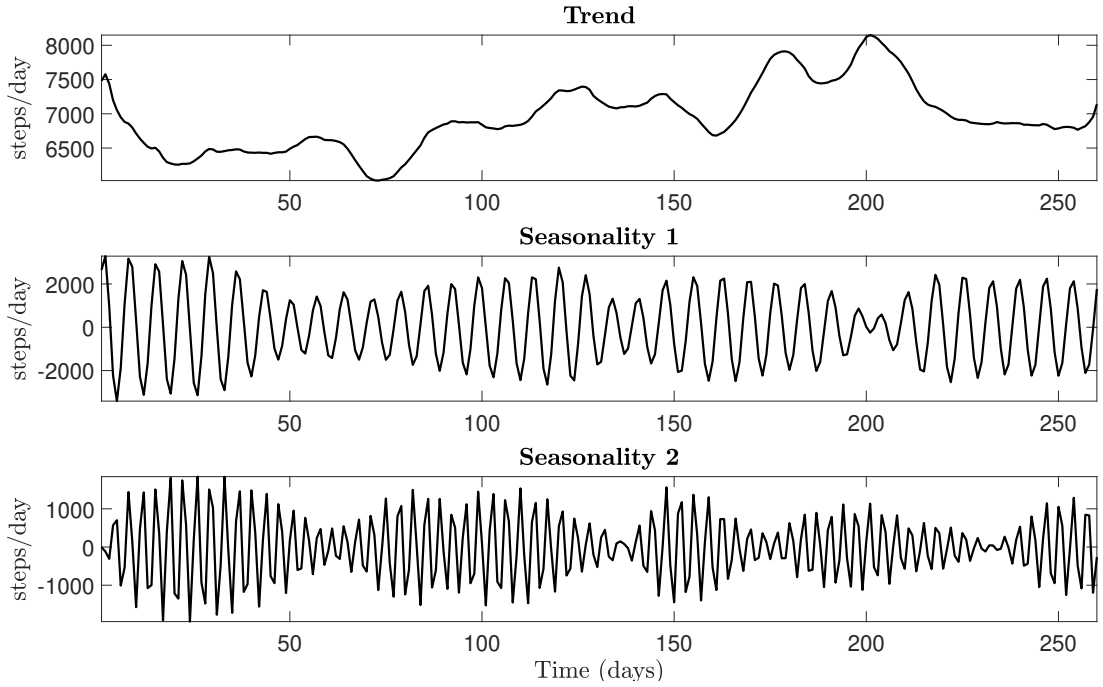

Figure 3.4: Reconstructed Signals of Uncorrelated Groups of SSA Components for *Step Count*. The Reconstructed Groups Are Arranged from Top to Bottom Based on Their Increasing Covered Frequencies.

3.5.2 Model Estimation and cross-validation

As illustrated in the previous section, SSA is effective in noise reduction and decomposing the *Step Count* signal into uncorrelated groups of components that cover different frequencies. In combination with MoD, this provides the opportunity to analyze and model the idiosyncracies that influence change in the walking behavior of the participant, at their respective frequencies, by performing model estimation on each group of components (trend, seasonality 1, and seasonality 2) separately. To investigate the added benefit of this approach, in this section, the MoD estimator is utilized to model 1) the raw unfiltered *Step Count*, 2) the SSA-filtered signal, and 3) the grouped SSA reconstructed components. In addition, to evaluate the added benefit of the MoD estimator, we contrast its performance in each of these scenarios against a global ARX model of the same regressor structure.

To compare the estimated models across the three cases mentioned above on common ground, the following data preprocessing and model estimation procedure is utilized for each case. First of all, the data is standardized to ensure well-conditioned matrices in model estimation. The data is then segmented into sub-experiments, where each experiment contains two consecutive goal-setting cycles. Consequently, five different sub-experiments are constructed, with 52 days of the intervention in each sub-experiment. The selected regressor order is $[n_a\, n_b\, n_k] = [4\ 4\ 1]$ for both the MoD and ARX estimators. Data for each sub-experiment is then transferred to regressor space φ, reducing the number of data points available in each sub-experiment to 48. The sub-experiments are then grouped into estimation and validation data groups, where four sub-experiments are designated for estimation, and one is for validation, yielding a total of five possible combinations. Sub-experiments' data in regressor space is then merged based on their group to allow for model estimation and cross-validation

across all possible combinations, following the approach in Section 5.3.2, where the combination with the highest weighted NRMSE fit index is selected (El Mistiri *et al.*, 2023).

A linear local polynomial is utilized in the MoD estimator for all examined cases. Additionally, Akaike Information Criterion (AIC) is utilized as a GoF measure for the localized models, with a variance penalty of 3. Because of data scarcity, the neighborhood size has been fixed to the maximum number of available data points in regressor space, which is done by selecting $i_{min} = i_{max} = 192$. Consequently, the variations in the local models are only dependent on the kernel-based weighting function of the relevance of points in the neighborhood around k, which is selected as a tricube kernel.

Case I: Model Estimation Based on Raw Data

Simulation results for the estimated models utilizing the unfiltered *Step Count* signal in the estimation database are presented in Fig. 3.5. As illustrated in Fig. 3.5, the combination of estimation validation/estimation data that resulted in the highest weighted average NRMSE fit for the MoD estimator utilizes the last four sub-experiments for estimation, while the first sub-experiment is designated for validation. The obtained results demonstrate that both models underestimate the performance of the participant, as they do not follow the peaks in the *Step Count* Y. This can be attributed to a possible exogenous signal that is not included in the model structure. Therefore, further analyses, including feature selection, are needed to examine possible improvements to the black box-model structure by incorporating behavioral constructs such as *Perceived Busyness* and *Environmental Context*. In this case, the MoD estimator outperforms the ARX-based estimator as illustrated by NRMSE fit indices for the estimation and overall data. However, the MoD estimator underper-

forms the ARX-based estimator in cross-validation, as evident by the lower NRMSE fit index for the MoD estimator over the validation data (21.61% for MoD vs 30.18% for ARX).

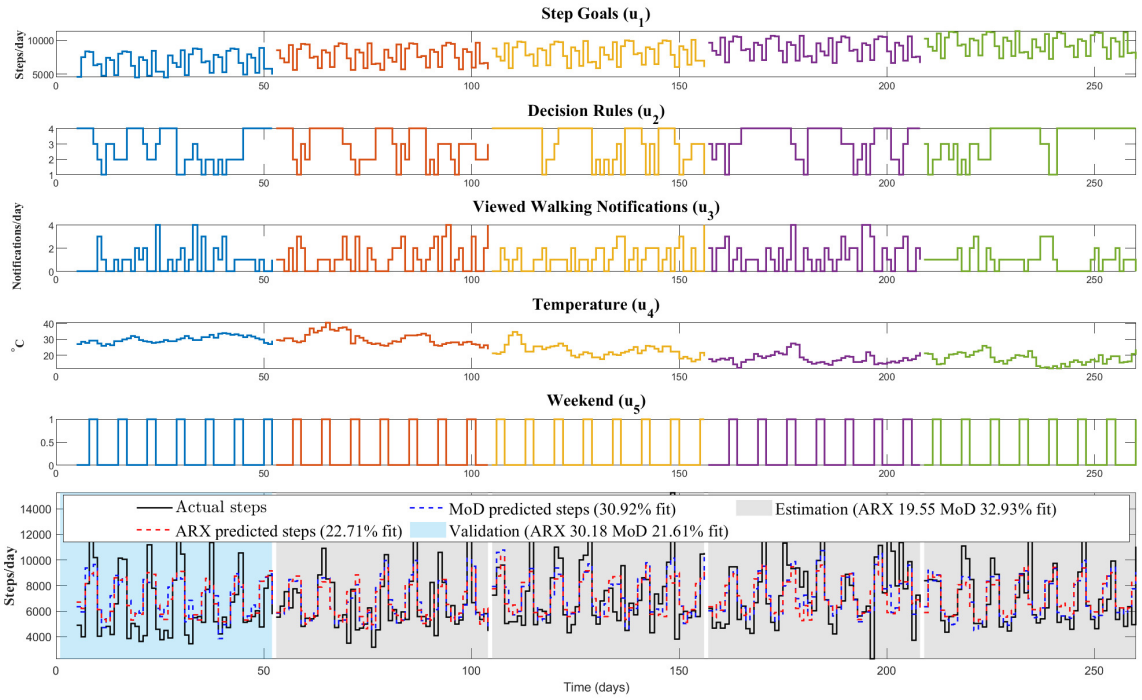

Figure 3.5: Case I Simulation Results for MoD and ARX-Based Estimators Compared to the Unfiltered *Step Count* Signal Y. Estimation Sub-Experiments Are Highlighted in Grey, Whereas the Validation Sub-Experiment is Highlighted in Cyan.

Case II: Model Estimation Based on SSA Reconstructed Components

In this case, the procedure described above is repeated for each of the reconstructed correlated SSA components presented in Fig. 3.2 (Trend, Seasonality 1, Seasonality 2). As the three reconstructed components are not correlated, no interactions between the outputs are included in model estimation. Hence, each of the outputs is estimated independently, then they are augmented to provide the overall model. Furthermore, as described in (3.14) the SSA-filtered signal Y_{SSA} is constructed as the summation

of the reconstructed relevant components. Therefore, the augmented model can be manipulated to predict the SSA-filtered *Step Count* signal Y_{SSA}.

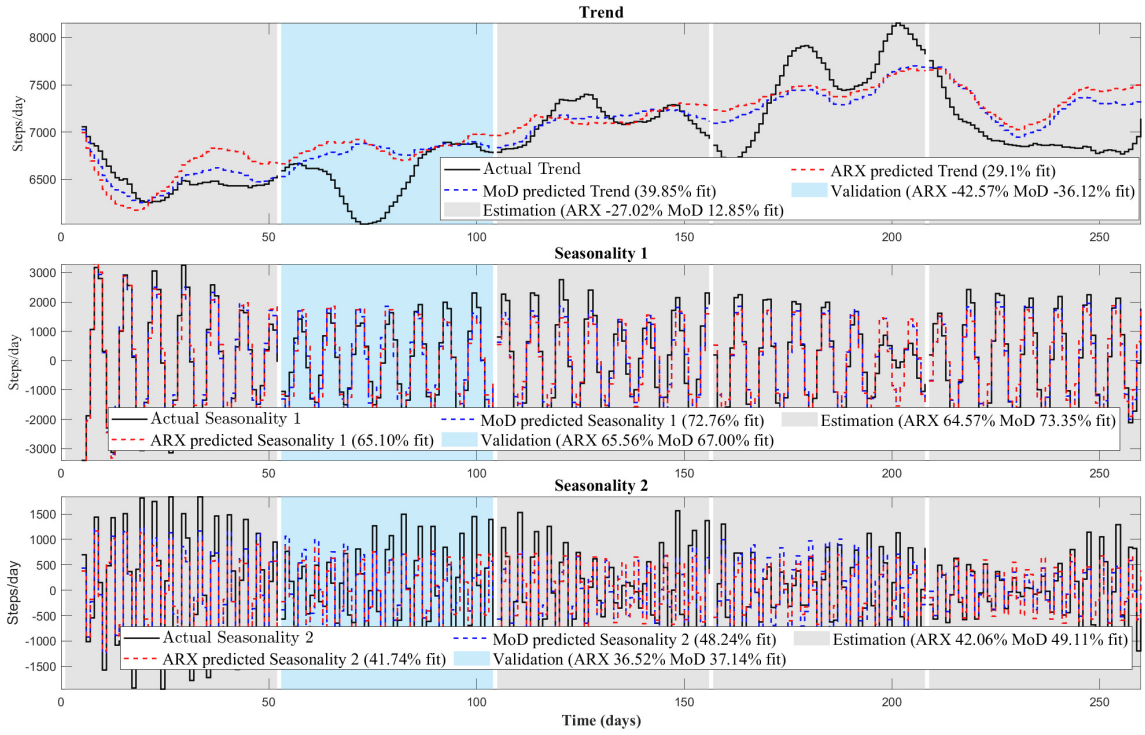

Figure 3.6: Case II Simulation Results for MoD and ARX-Based Estimators for Each of the Uncorrelated Reconstructed SSA Components (Trend, Seasonality 1, Seasonality 2). Estimation Sub-Experiments Are Highlighted in Grey, Whereas the Validation Sub-Experiment is Highlighted in Cyan.

Simulation results for the estimated models for this case are presented in Fig. 3.6. The Trend component represents the longer-term underlying dynamics behind behavior change. Therefore, this component is used in selecting the combination of estimation/validation sub-experiments in model estimation, where the combination that yields the highest weighted average NRMSE fit for the validation and overall data in the Trend component is selected. As a result, the second sub-experiment is utilized for validation while the first, third, fourth, and fifth sub-experiments are

designated for model estimation. As demonstrated in Fig. 3.6, both the MoD and ARX-based estimators perform well in capturing the periodic dynamics in the Seasonality 1 and Seasonality 2 signals, with a slight advantage to MoD as illustrated by the NRMSE fits summarized in table 3.1.

Table 3.1: Summary of the NRMSE Fit Indices of the MoD and ARX-Based Estimators for Each of the Reconstructed Uncorrelated SSA Components of *Step Count*.

Method	**Estimation Fit (%)**	**Validation Fit (%)**	**Overall Fit (%)**
		Trend	
MoD	12.85	-36.12	39.85
ARX	-27.02	-42.57	29.10
		Seasonality 1	
MoD	73.35	67.00	72.76
ARX	64.57	65.56	65.10
		Seasonality 2	
MoD	49.11	37.14	48.24
ARX	42.06	36.52	41.74

As evident in table 3.1 and Fig. 3.6, both estimators do not perform very well in modeling the trend component. This is especially the case for the second subexperiment, which is utilized for cross-validation. It is worth noting that the NRMSE fit indices for the estimation and overall data for the MoD estimator are decently high, illustrating its outperformance over the ARX-based estimator. Despite the low cross-validation NRMSE fit for the trend component, the combined model for all components performs well in terms of capturing the dynamics of the SSA-filtered *Step*

Count signal Y_{SSA} and therefore the actual *Step Count* Y, as illustrated in Fig. 3.7.

While utilizing SSA components in the estimation database is effective in modeling the unfiltered *Step Count* Y (as evident in Fig. 3.7b) this approach yields slightly lower NRMSE fits for both of the MoD and ARX-based estimators when utilizing the unfiltered *Step Count* Y in the estimation database. The added benefit of utilizing the reconstructed signals from uncorrelated SSA components in the estimation database is that it allows analyzing and studying each component separately. As a result, it sheds light on the unique dynamic changes of each component in response to changes in the exogenous inputs. To improve results from this approach and reach its full potential feature and order selection need to be optimized for each component separately, instead of using the same inputs and orders for all reconstructed components, which will be examined in future work.

Case III: Model Estimation Based on SSA-filtered *Step Count*

In this case, the model estimation procedure described above is applied with the SSA-filtered *Step Count* signal Y_{SSA} as the only output in the estimation database. Therefore, the estimated models are less impacted by the noise in the measured output. Fig. 3.8 illustrates the performance of both the MoD and ARX-based estimators of the same regressor orders in a simulation setting, over both estimation and validation data. As evident in Fig. 3.8a, MoD produces better results than the ARX-based global model in predicting the SSA-filtered *Step Count* based on the presented NRMSE fit indices. The outperformance of the MoD estimator, utilizing the SSA-filtered output signal Y_{SSA} in the estimation database, is further highlighted in comparison with the unfiltered *Step Count* Y, as demonstrated in Fig. 3.8b.

Note that both estimators, in this case, yielded sufficiently high NRMSE fit indices for cross-validation against unfiltered *Step Count* signal Y. Matter of fact, the cross-

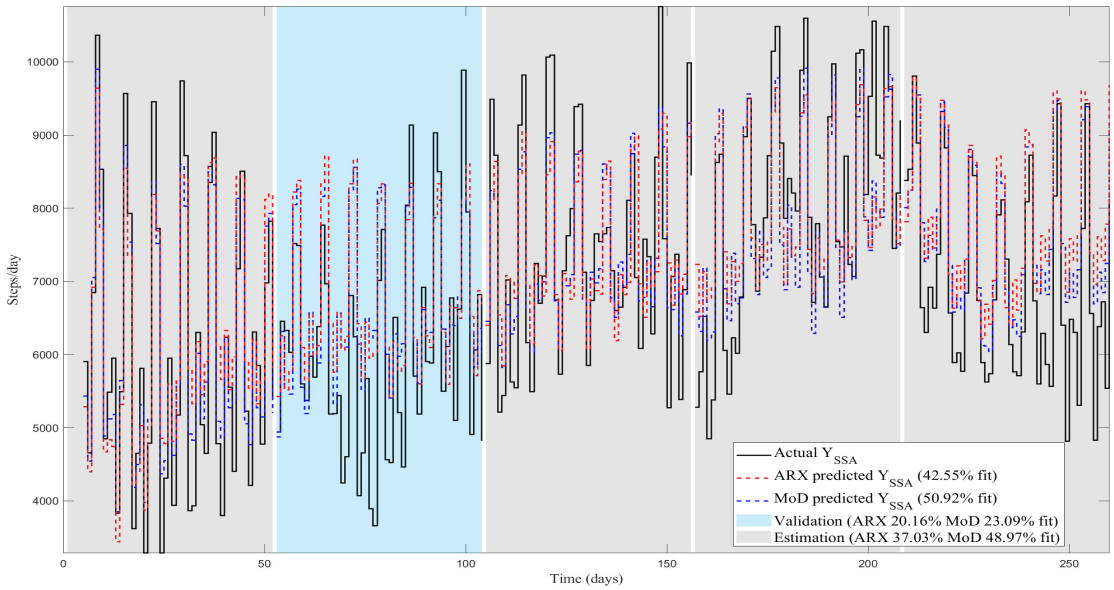

(a) SSA-filtered *Step Count* Y_{SSA}

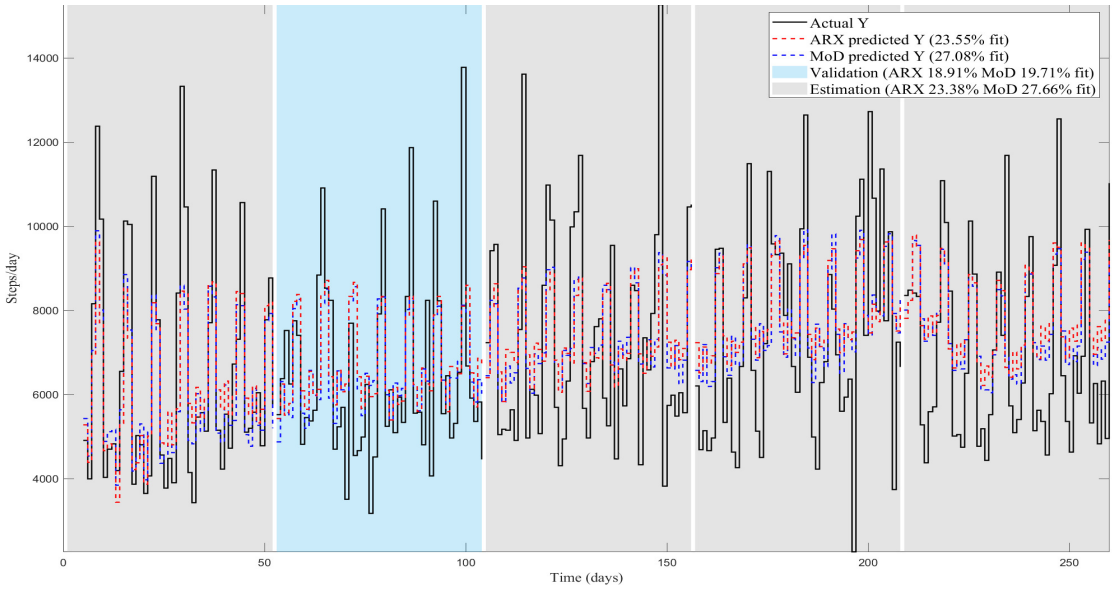

(b) Unfiltered *Step Count* Y

Figure 3.7: Case II Simulation Results of the Combined Model Estimated Using the MoD and ARX-Based Estimators Compared to (a) the SSA-Filtered *Step Count* Signal Y_{SSA}, And (b) the Unfiltered *Step Count* Signal Y. Estimation Sub-Experiments Are Highlighted in Grey. The Validation Sub-Experiment is Highlighted in Cyan.

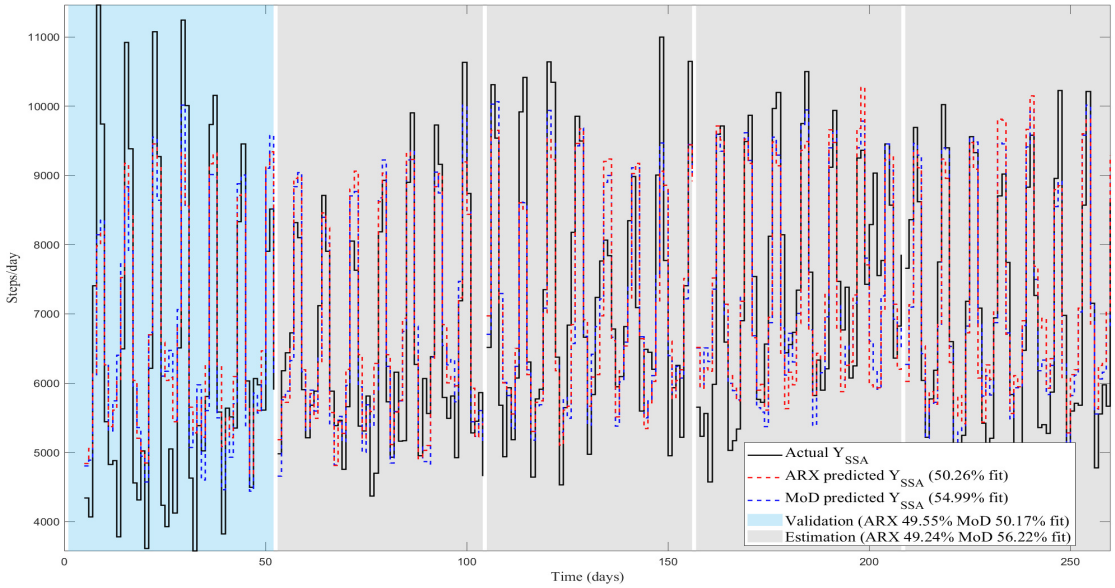

(a) SSA-filtered *Step Count* Y_{SSA}

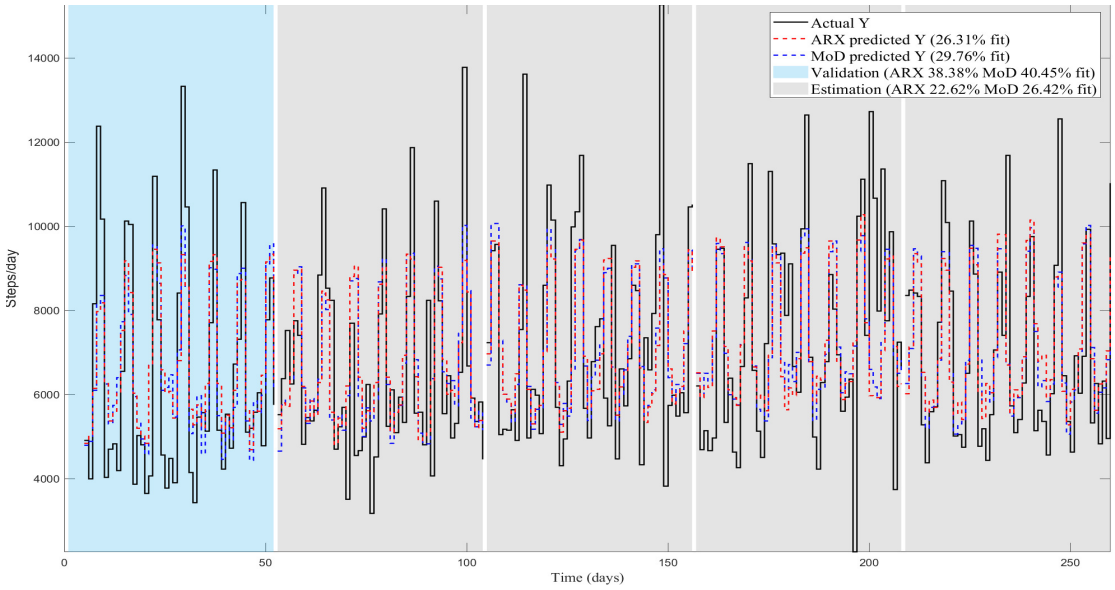

(b) Unfiltered *Step Count* Y

Figure 3.8: Case III Simulation Results of the Combined Model Estimated Using the MoD and ARX-Based Estimators Compared to (a) the SSA-Filtered *Step Count* Signal Y_{SSA}, And (b) the Unfiltered *Step Count* Signal Y. Estimation Sub-Experiments Are Highlighted in Grey. The Validation Sub-Experiment is Highlighted in Cyan.

validation fit indices, in this case, are higher than the estimators of the same structure in Case I (relying on the unfiltered *Step Count* signal in the estimation database). This is significant, as it illustrates the effectiveness of the proposed SSA approach in noise reduction. SSA filters out noise components from the output measurement in a systematic manner, which allows for modeling and analyzing the underlying dynamics behind behavior change without being overshadowed by high-magnitude noise in the output measurement. Another important takeaway is that SSA noise reduction has a more significant impact on the performance of MoD. This is evident in the cross-validation fit which almost doubles in Case III when compared to Case I, see table 3.2. The sensitivity of the MoD estimator to noise is believed to be caused by its reliance on localized model estimation. At each operating point, MoD estimates coefficients for the model parameters, within the global structure, based on data in the neighborhood of the operating condition. Hence, the localized models are heavily impacted by measurement noise. Consequently, when the impact of noise on the localized models is reduced, MoD is capable of estimating local models that predict the unfiltered output signal Y with higher NRMSE fits, in comparison to the same estimator utilizing unfiltered Step Counts Y in the estimation database.

While improvements from using MoD might seem small in terms of NRMSE fit indices, the real added benefit of the MoD estimator is that it optimizes over localized models under a global structure. Therefore, MoD yields improved global fits with local models that vary in dynamics with respect to the operating conditions. This provides the framework needed to analyze idiosyncrasies in a participant's behavior in context.

Overall, the obtained models illustrate the effectiveness of the proposed input signal design in providing dynamically informative data sets. This is particularly evident in the obtained NRMSE fits, which are sufficiently high for all examined cases, despite the high magnitude noise in systems associated with behavior change. Addi-

tionally, signal processing through SSA successfully decomposes behavior signal into independent components at different frequencies and reduces noise. The integration of innovative input signal design, SSA, and MoD provides a sophisticated approach to model, analyze, and understand behavior change systems in context of JIT states and at different frequencies. The effectiveness of this approach is asserted by the performance of the presented estimators in predicting the unfiltered *Step Count* Y, as summarized in Table 3.2.

Table 3.2: Summary of the NRMSE Fit Indices of the MoD and ARX-Based Estimators for Each of the Reconstructed Uncorrelated SSA Components of *Step Count*.

Method	*Step Count* Y		SSA-filtered *Step Count* Y_{SSA}	
	Validation Fit (%)	Overall fit (%)	Validation Fit (%)	Overall fit (%)
Case I				
MoD	21.61	30.92	N/A	N/A
ARX	30.18	22.71	N/A	N/A
Case II				
MoD	19.71	27.08	23.09	50.92
ARX	18.91	23.55	20.16	42.55
Case III				
MoD	40.45	29.76	50.17	54.99
ARX	38.38	26.31	49.55	50.26

3.5.3 MoD: Analyzing Behavior in Context

Having validated the MoD estimator, in this section, the benefit of the estimator in explaining PA behavior change in context is explored. To allow for more data points to be included in estimating localized models, the entirety of the available data is included in the MoD estimation database. Consequently, the total length of the MoD estimator's database is $N = 256$ in regressor space. The neighborhood range is updated accordingly to $k_{min} = k_{max} = 256$. The MoD estimator is then implemented in simulation for hypothetical scenarios, to illustrate the impact of changing operating conditions on the obtained responses.

To showcase the difference between the MoD and ARX-based estimators, the simulation conditions are fixed for the exogenous environmental inputs, while some intervention components are manipulated. In this scenario, Temperature is held constant at $u_4 = 30°C$, and it is assumed that the intervention occurs on a weekday $u_5 = 0$. As per intervention components, the JIT decision rule is implemented, while Step Goals start initially at an ambitious level $u_1 = 10,000$ steps/day, then are reduced to a less challenging level $u_1 = 6,000$ steps/day. During the periods of ambitious and non-ambitious goals, an impulse of walking suggestions is sent to the participant and assumed to be viewed, $u_3 = 3$ notifications/day for five consecutive days.

As illustrated in Fig. 3.9 impulse responses for the MoD estimator vary significantly based on operating conditions. During the first impulse of notifications, the Step Goal signal is at an ambitious level relative to the steady state value of the *Step Count*. Under such operating conditions, the sent walking suggestions have a significant positive impact on the *Step Count*. The daily *Step Count* increases by a factor of 930 steps/day at the peak, due to the Viewed Walking Notifications u_3. Meanwhile, the second impulse of notifications, with the same magnitude and duration, has a di-

minished effect on the system. Viewed Walking Suggestions in this case, contribute to an increase of only 285 steps/day when the given goal is lower than the steady-state value of the *Step Count*. Moreover, variations in MoD's impulse responses extend beyond the magnitude of the gain, and include the speed and shape of response as seen in Fig. 3.9. On the other hand, the ARX-based estimated model yields the same impulse responses, regardless of the operating conditions.

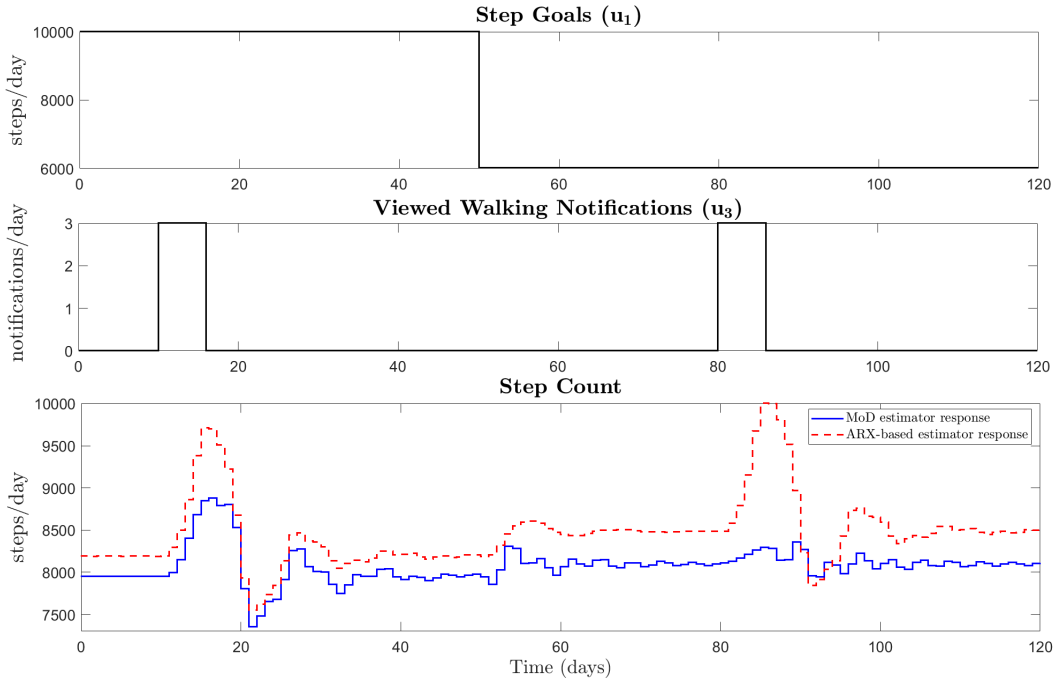

Figure 3.9: Impulse Responses for MoD and ARX-Based Estimators in a Simulated Hypothetical Scenario Illustrating the Change in MoD Responses for a Representative *JustWalk JITAI* Participant At Different Operating Conditions.

From a behavioral science perspective, variations in responses to the same impulse of notifications can be attributed to the participant's perception of the utility of the received notification with respect to the context at which the notifications are received. For instance, if the support through the notification is provided while the goal is not achieved (i.e., there is a need for support) then it is of high utility.

Therefore, the participant acts upon the viewed notifications, and they materialize as efforts toward the goal. Conversely, when support is provided without the need for it (e.g., when the given goals are easily attainable), then its perceived value diminishes and it can be burdensome for the participant. Hence, it does not lead to the intended positive outcomes. Therefore, the obtained MoD simulation results for these hypothetical scenarios, presented in Fig. 3.9, fit perfectly within JIT concepts and explain idiosyncrasies in the responses of this representative *JustWalk JITAI* participant to walking suggestions based on context. The same analysis can be extended to various scenarios, including at different Decision Rules u_2, to study and predict their impact.

3.6 Conclusions & Future Work

In this work, a comprehensive system identification approach to studying PA behavior change is presented based on experimental results from *JustWalk JITAI*. This approach includes: informed input signal design, signal processing, and noise reduction, as well as a data-driven model estimator geared towards capturing nonlinearities in the system based on operating conditions. The findings in this chapter illustrate the cumulative effect of this approach in analyzing and understating idiosyncrasies in the dynamics of PA-related behavior change, based on context.

The input signal design is based on *a priori* knowledge and provides dynamically informative data sets at frequencies of interest. Furthermore, SSA utilization in *Step Count* time series analysis is remarkably effective in reducing measurement noise in an informed manner, and studying the separability of the measured output signal. The analysis shows that the daily *Step Count* has separable uncorrelated groups of components that can be analyzed independently. Finally, MoD is an excellent alternative approach to global modeling that captures nonlinearities associated with behavior change systems and JIT states. The full potential of this approach culminates in

the development of efficient personalized JITAIs within the control optimization trial (COT; see Chapter5 and Chapter 6) framework, which can be disseminated on a large scale to reduce physical inactivity and improve public health.

Future efforts will include further personalization of the MoD estimator for each participant, through the incorporation of algorithms to optimize over input and order selection for the global MoD estimator structure. Similarly, feature and order selection algorithms will be explored in optimizing the global model structure for each of the reconstructed signals of uncorrelated groups of SSA components for *Step Count*, to reach the full benefit of this approach. Furthermore, the presented comprehensive system identification approach will be applied to intraday data (i.e., sampled at 3 hours intervals) to help understand the multi-timescale dynamics associated with JIT states and PA behavior change.

Chapter 4

MODEL PREDICTIVE CONTROL IN MHEALTH: A DECISION FRAMEWORK FOR OPTIMIZED PERSONALIZED PHYSICAL ACTIVITY INTERVENTIONS

4.1 Introduction

Physical activity (PA) offers enormous benefits to both personal and public health. According to a study by Saint-Maurice *et al.* (2020), an increase in daily steps from 4,000 to 8,000 steps/day can reduce the risk for all-cause mortality by 51% in adults; including reduced risk of cancer and heart disease. Notwithstanding, the prevalence of those who engage in regular physical activity in the general population is low; about 53% of adults in the US, 44% in Australia, and 40% in the UK are sedentary (Centers for Disease Control and Prevention, 2021; Australian Government Department of Health, 2021; Department for Digital Culture, 2017). Over the years, extensive research has been conducted to explore the most effective approaches for implementing behavioral interventions. However, the translation of these interventions into large-scale, impactful initiatives have faced significant challenges. Nonetheless, there is hope for affordable real-world interventions that can improve public health. Control systems engineering principles have been applied to solve challenging problems in social and natural sciences including economic, environmental, robotic, and biomedical systems (Leonard *et al.*, 1992; Ford and Ford, 1999; de Wit *et al.*, 2012; Kurzhanski and Vályi, 1997). Particularly for healthcare systems, areas for research for control systems engineering can be split to two categories: 1) clinical application in terms of automation of treatment dosage and delivery, especially in cases of chronic illnesses like diabetes and fibromyalgia (Gondhalekar *et al.*, 2016; Deshpande *et al.*, 2014).

2) behavioral medicine aiming to prevent or delay and manage the onset of chronic and relapsing disorders (Collins *et al.*, 2004; Rivera *et al.*, 2007b). Based on recent advances in digital technology and the availability of PA data through smartphones and other devices, control systems engineering has emerged as a promising tool in this regard, leveraging the availability of physical activity data to design and implement effective interventions (Hekler *et al.*, 2016; Conroy *et al.*, 2011). By harnessing the power of technology and principles of system identification and control systems engineering, mobile health (mHealth) interventions can be tailored to individual needs and delivered in a way that maximizes their impact. Because of the importance of modeling to control engineering, it is essential to choose appropriate health behavior theories and apply a sound dynamical systems methodology to generate meaningful, and ultimately useful, control-oriented models.

A sound behavioral theory provides guidance regarding the underlying forces and factors that drive a particular behavior (e.g., walking) and the interconnections between behavior and its various influences. These theories elucidate behavior through various psychological constructs, which in principle are akin to latent variables used in the chemical processing industry. A specific construct may not be measured, yet its dynamics can be inferred by examining its interrelationships with measurable components (Tham *et al.*, 1991). Examining such constructs from this prism can lead to a deeper understanding of behavior change and facilitate effective interventions. Social Cognitive Theory (SCT; Bandura (1986)) has been regarded as one of the most influential theories of behavior change, and has been widely used in health behavior; the dynamical model for SCT developed in Martín *et al.* (2020) is considered in this work.

Model Predictive Control (MPC) is widely popular in chemical process industries and beyond, including various other domains. This is mainly due to its versatility,

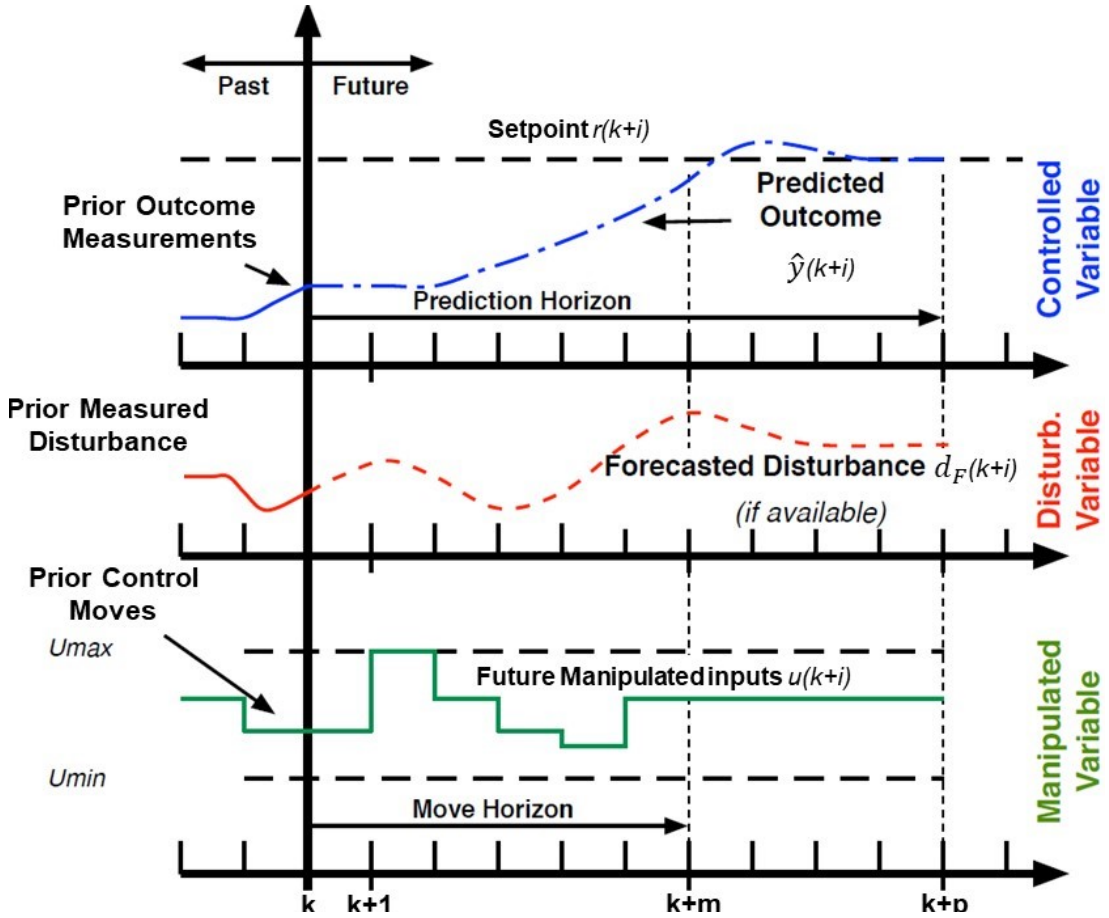

Figure 4.1: Schematic Illustrating the Receding Horizon Strategy for MPC. Adapted from Rivera *et al.* (2018).

simplicity, and capability to optimize control decisions under constraints (Bordons and Camacho, 2007; Prett and García, 1988; García *et al.*, 1989). In MPC a receding horizon algorithm is implemented, where a model of the system is utilized to forecast the impact of future changes in manipulated variables on system states and outputs over a prediction horizon p (Figure 4.1). By solving the optimization problem in (4.1), future moves in the manipulated variables $\Delta u(k)$ are determined over a move horizon m subject to specified constraints. Subsequently, only the first move in the manipulated variables is implemented and the computations are repeated at each

sampling instant utilizing feedback measurements from the current state of the process (García *et al.*, 1989).

$$\begin{aligned}\min_{[\Delta u(k),\ldots,\Delta u(k+m)]} \sum_{l=1}^{p} ||\Gamma_l^Y (y(k+l|k) - r(k+1))||_2^2 + \sum_{l=1}^{m} ||\Gamma_l^u u(k+l-1) - u_r||_2^2 \\ + \sum_{l=1}^{m} ||\Gamma_l^{\Delta u} \Delta u(k+l-1)||_2^2\end{aligned} \tag{4.1}$$

where u_r denotes setpoint targets for manipulated variables, and y_r represents the desired setpoint for the output y. Γ^Y, Γ^u and $\Gamma^{\Delta u}$ represent controlled variable, manipulated variable, and move suppression weight matrices, respectively. Γ^Y, Γ^u, $\Gamma^{\Delta u}$, p and m are adjustable controller parameters. MPC enables the enforcement of constraints on controlled (y), manipulated (u), and move size (Δu) variables:

$$y_{min} \leq y(k+i) \leq y_{max} \; \forall \; 1 \leq i \leq p \tag{4.2}$$

$$u_{min} \leq u(k+i) \leq u_{max} \; \forall \; 0 \leq i \leq m-1 \tag{4.3}$$

$$\Delta u_{min} \leq \Delta u(k+i) \leq \Delta u_{max} \; \forall \; 0 \leq i \leq m-1 \tag{4.4}$$

In the unconstrained scenario, the optimization problem highlighted in (4.1) is simplified to a linear system of equations ($Ax = b$) that can be solved with a closed-form solution. Conversely, when constraints are introduced, the optimization problem defined by (4.1)-(4.4) forms a quadratic objective function with linear inequality constraints, which is a readily solvable Quadratic Programming (QP) problem (García *et al.*, 1989).

The work presented in Rivera *et al.* (2017) introduced hybrid model predictive control (HMPC) as an approach with significant potential to deliver PA behavioral interventions. The sole output of interest was walking behavior (measured with steps per day), while manipulated variables, namely goals and expected reward points in the intervention, were limited to predefined discrete levels. In this chapter, the hybrid formulation is set aside and instead, emphasis is placed on exploring diverse

control strategies with continuous variables to determine if these result in desired intervention outcomes. The findings in this chapter demonstrate that judicious problem formulation and constraint enforcement can guide the controller toward making user-friendly decisions; maximizing the benefits of the intervention while minimizing the risk of participant disengagement and dropouts. Furthermore, in this chapter, we investigate MPC strategies using an enhanced SCT model that takes into account the possibility of dual, competing behavioral outcomes, such as fitness and fatigue. Both the modeling of this phenomenon and the suitability of MPC-based strategies under these conditions are examined.

The conclusions and diverse insights developed in this chapter have significant implications for the design of the *YourMove* intervention, which is being developed in collaboration with the Design Lab at the University of California San Diego (UCSD) as part of the activities conducted under the NIH grant R01CA244777 (R01CA244777, 2020). The chapter is organized as follows: Section 4.2 describes the simulation model and intervention design, Section 4.3 presents and discusses simulation results for the various optimization problem formulations, while Section 4.4 ends with conclusions and implications for future work.

4.2 Simulation Model & Intervention Design

This section describes a fluid analogy process model that serves as the basis for the computational analysis performed in this work, along with some of the details of control-oriented behavioral interventions for physical activity, which is reflected in current efforts such as *YourMove*.

4.2.1 Social Cognitive Theory (SCT)

In SCT, it is postulated that behavior interacts with personal and environmental factors in nested loops, allowing the possibility to predict the ability of an individual to engage in a certain behavior based on endogenous and exogenous factors. Some constructs in SCT are self-perceived and subjective, which are measured through Ecological Momentary Assessment (EMA; Shiffman *et al.* (2008)) surveys provided to participants daily. On the other hand, other constructs, such as steps per day, can be directly measured (Martín, 2016). The work done by Martín *et al.* (2020) describes a fluid analogy process model for the main constructs of SCT , which is amenable to closed-loop control approaches. In this chapter, the SCT subsystem involving *Self-Efficacy* (η_3), *Behavior* (η_4), and *Behavioral Outcomes* (η_5), depicted in Figure 4.2, is considered. This subsystem is comprised of Operant Learning (OL) and Self-Efficacy (SE) loops (Loeber *et al.*, 2006), which is subsequently referred to in this chapter as an OLSE system.

4.2.2 Fluid Analogy Formulation for SCT

The fluid analogy relates to the dynamic interrelations of SCT components over time. In this analogy, the main SCT constructs are modeled as tanks (inventories), while the other components are treated as inflows/outflows to the inventory system. The fluid analogy provides a structure and framework to readily obtain a mathematical model from the SCT following conservation principles such as mass conservation (Hekler *et al.*, 2016; Martín, 2016; Navarro-Barrientos *et al.*, 2011; Spruijt-Metz *et al.*, 2015a). By applying conservation of mass to each inventory, a system of ODEs is obtained to represent the schematic shown in Figure 4.2.

$$\tau_3 \frac{d\eta_3}{dt} = \gamma_{311}\, \xi_{11}(t) + \beta_{34}\, \eta_4(t)\eta_3(t) + \zeta_3(t) \tag{4.5}$$

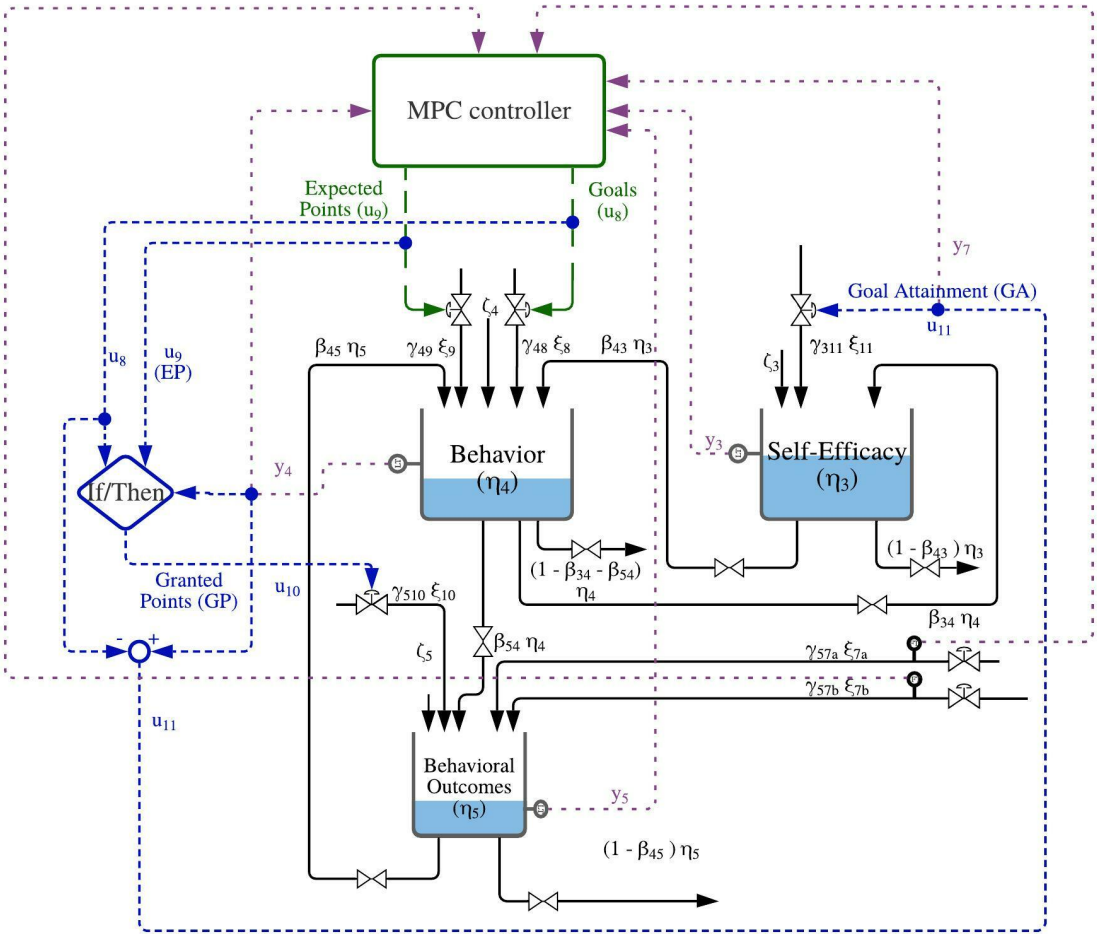

Figure 4.2: Schematic Depicting the Fluid Analogy of the SCT Model for an Operant Learning-Self-Efficacy (OLSE) System in an Intervention Setting Including the Implementation of MPC Controller. Adapted from Martín *et al.* (2020)

$$\tau_4 \frac{d\eta_4}{dt} = \gamma_{48}\ \xi_8(t) + \gamma_{49}\ \xi_9(t) + \beta_{43}\ \eta_3(t) + \beta_{45}\ \eta_5(t) - \eta_4(t) + \zeta_4(t) \tag{4.6}$$

$$\tau_5 \frac{d\eta_5}{dt} = \gamma_{510}\ \xi_{10}(t) + \gamma_{57}\ \xi_7(t) + \beta_{54}\ \eta_4(t) - \eta_5(t) + \zeta_5(t) \tag{4.7}$$

τ_i represents the time constant for inventory i, γ_{ij} represents the gain between inventory i and the inflow/outflow j, β_{iz} denotes the gain in inventory i for changes in inventory z, and ζ_i is for unmeasured disturbances, where i, j, z are integers. To ensure the outflows from each inventory are physically realizable, the following constraints

are needed:

$$0 \leq \quad \beta_{43} \quad < 1 \tag{4.8}$$

$$0 \leq \quad \beta_{45} \quad < 1 \tag{4.9}$$

$$0 \leq \beta_{34} + \beta_{54} < 1 \tag{4.10}$$

The primary inventory for the intervention is *Behavior* (η_4), which is measured in the form of daily step-count in steps/day. This construct can encompass various characteristics (e.g., duration, frequency, and type) and their fluctuations over time (Martín, 2016; Martín *et al.*, 2020). In this study, the chosen time frame is on a daily level. However, it is important to note that this framework can be extended to different temporal granularities (e.g., weekly level) based on the behavior of interest. *Self-efficacy* (SE; η_3) is a fundamental component of SCT and represents the individual's perceived capability to engage in the behavior of interest. The level of SE can fluctuate over time depending on other main constructs in the SCT model (e.g., *Behavior*) as well as other exogenous variables. Understanding the dynamic relationship between SE and the other constructs is essential in comprehending the factors that impact an individual's motivation and ability to engage in desired behaviors. Another significant construct in SCT is *Behavioral Outcomes* (BO; η_5), which depicts the physical and psychological consequences of engaging in a particular behavior. These *Behavioral Outcomes* can include aspects such as fatigue and positive reinforcement. BO can be influenced by external factors including environmental context and the presence of financial or psychological incentives.

4.2.3 Intervention Design & Development

In an intervention setting like the one being implemented in *YourMove*, individualized goal targets are given to participants on a daily basis (Hekler, 2021;

R01CA244777, 2020). Participants who successfully meet their daily goals earn points, which can be accumulated and later exchanged with financial rewards in the form of gift cards. The number of expected points for each day and the daily step goals are communicated to participants through a digital user platform, such as a smartphone. To integrate the intervention into the SCT system the following signals (which correspond to inflows and outflows in Figure 4.2) are included.

- *Goals* (ξ_8; u_8): These represent the daily step target given to a participant and directly influence *Behavior*.

- *Expected Points* (EP; ξ_9; u_9): The number of points a participant expects to earn, should they meet the daily target. EP is hypothesized to serve as motivation to meet the given daily goal. A maximum of 500 points/day can be earned.

- *Granted Points* (GP; ξ_{10}): The amount of granted points, which is equivalent to ξ_9 when a participant achieves the daily step goal. This is accomplished through the following condition:

$$\delta_{GA} = 1 \Leftrightarrow y_4 \geq u_8;\ \xi_{10} = \delta_{GA} u_9 \tag{4.11}$$

- *Goal Attainment* (GA; y_7; ξ_{11}): The difference between the behavior and given goal:

$$y_7 = \xi_{11} = \eta_4 - \xi_8 \tag{4.12}$$

Goals and EP can be independently manipulated, whereas GP and GA depend on meeting the daily goal as expressed in (4.11) and (4.12) respectively. GP signal provides positive reinforcement for meeting the given daily goal and influences BO (η_5). It is important to recognize that GA can serve as both an inflow (when behavior

surpasses the given goal) and as an outflow (when the goal is not achieved); this signal has a significant impact SE. The main exogenous input to the system in this work is *Environmental Context* (ξ_7), which represents environmental factors that can influence *Behavior* through the OL loop. In the context of this chapter, one particular exogenous input taken into account is ambient temperature. This stochastic signal is considered as a measured disturbance that can impact *Behavior* by deviating from the participant's ideal temperature to exercise, directly impacting BO, and therefore influencing engagement in PA.

MATLAB and Simulink are utilized to implement the simplified SCT model and MPC controller depicted in Figure 4.2 in a simulation environment. A state-space representation of the system shown in equations (4.5) - (4.7) and (4.12) is utilized to design the controller. MATLAB's Model Predictive Control toolbox is used to implement the various control strategies proposed in this chapter, through the different tools provided by the toolbox like slack and dynamic constraint implementation. Hypothetical models postulated in this work represent two different expected types of participants:

1. Participant A: An adherent participant, who responds well to the given daily goals.

2. Participant B: A non-adherent participant, who is not goal-oriented, and may not follow the daily goals.

It is worth mentioning that these two types of participants (A and B) represent extreme and opposing ends of the spectrum of possible responses expected from participants in the intervention. The majority of people should exhibit behavior in between the examined extremes. Moreover, a participant's response to the intervention is not fixed and can move across the spectrum over time due to various personal

and environmental factors (e.g., seasonality, sickness, busyness).

The purpose of the simulations in this work is to explore different MPC strategies, starting with the simplest case and then introducing more sufficient problem specifications based on behavioral scientists' feedback on the feasibility and likely limitations. Furthermore, simulations are implemented to gain insight in terms of the response of the hypothetical participants to the devised control strategy and tuning, and the robustness of the controller in cases of plant-model mismatch.

4.3 Results and Discussion

In this section, control strategies supported by simulation results for the hypothetical (adherent and non-adherent) participants are presented and discussed. The control strategy is built based on the hypothetical adherent participant with six different scenarios that increase in complexity:

1. SE loop unconstrained.
2. SE loop with constraints on SE.
3. SE loop with constraints on GA.
4. OLSE system with constraints on GA and the presence of disturbances.
5. A dual competing dynamics behavioral outcomes OLSE system with constraints on GA and stochastic disturbances.
6. A dual competing dynamics behavioral outcomes OLSE system with constraints on GA and stochastic disturbances in the presence of nonlinearity that introduces plant-model mismatch.

Subsequently, to test the performance of the devised control strategy under conditions of plant limitations and plant-model mismatch, it is evaluated on the hypothet-

ical non-adherent participant for the case of a dual competing dynamics behavioral outcomes OLSE system with constraints on GA and stochastic disturbances, as well as in the presence of nonlinearities in the model that lead to plant-model mismatch. In all conducted simulations an initial goal level of $\xi_{8initial} = 1,000$ steps/day is assumed as a baseline. While this value may seem relatively low, it provides insights into the performance of the control strategies at extreme initial conditions. The desired outcome of the simulated intervention strategies and scenarios is to achieve a sustained level of 10,000 steps/day for the behavior of the participants. The findings from each of the cases are discussed, along with their implications for future work.

4.3.1 Participant A: Adherent Participant

An adherent participant follows step goals and overcomes obstacles to meet them on daily basis. In mathematical terms, this translates to a gain greater than or equal to one between the *Goals* and *Behavior*. To simulate this expected behavior from adherent participants the following model parameters are utilized:

- $\tau_3 = 1,\ \tau_4 = 2,\ \tau_5 = 5.$
- $\gamma_{311} = 1.3,\ \gamma_{48} = 1,\ \gamma_{49} = 0.3,\ \gamma_{57} = 4,\ \gamma_{510} = 5.$
- $\beta_{34} = 0.5,\ \beta_{43} = 0.2,\ \beta_{45} = 0.2,\ \beta_{54} = 0.4.$

The combination of model parameters shown above results in a gain between *Goals* and *Behavior* of approximately 1.26, which is similar to the gain estimated from system identification analysis for a representative *Just Walk* participant as presented in Section 5.3.2 and in El Mistiri *et al.* (2023).

Self-Efficacy (SE) loop: Unconstrained Case

This initial case represents the least amount of problem specification. The control strategy does not include constraint enforcement, with move suppressive weights set at $\Gamma^{\Delta u} = \text{diag}(1, 1)$. As the main output of interest is *Behavior*, weights on setpoint tracking for the controlled variables are selected as ($\Gamma^{Y} = \text{diag}(0, 1, 0)$), while no target tracking for the manipulated variables is implemented ($\Gamma^{u} = 0$). As a result, many issues arise from this inadequate problem specification. As evident in Figure 4.3, significant moves occur in the manipulated variables. These large moves, especially in the *Goals*, imply assigning very ambitious goals that cannot be immediately achieved. Consequently, this leads to largely negative GA at the beginning of the intervention, resulting in a notable decline in SE.

This scenario illustrates a short and excessively ambitious intervention, which may not be a successful approach for promoting the adoption of sustained healthy behavior. While *Behavior* rapidly increases to surpass the given goals by the 5th day of the intervention, the demanding nature of the intervention causes the observed significant drop in SE, and can potentially result in participant disengagement and dropout (Hekler, 2021; Klasnja, 2021). Moreover, the observed extensive use of EP in this control strategy suggests its overreliance on financial rewards to encourage the participant to achieve the given daily goals. Thus, this control strategy is deemed impractical for its excessive usage of EP, which exceeds the maximum allowable amount of points per day.

The results obtained in this scenario highlight the importance of judicious formulation of the optimization problem, and the need for imposing sensible constraints in such interventions, on both controlled and manipulated variables. To successfully implement MPC in PA behavioral interventions, it is essential to recognize that there

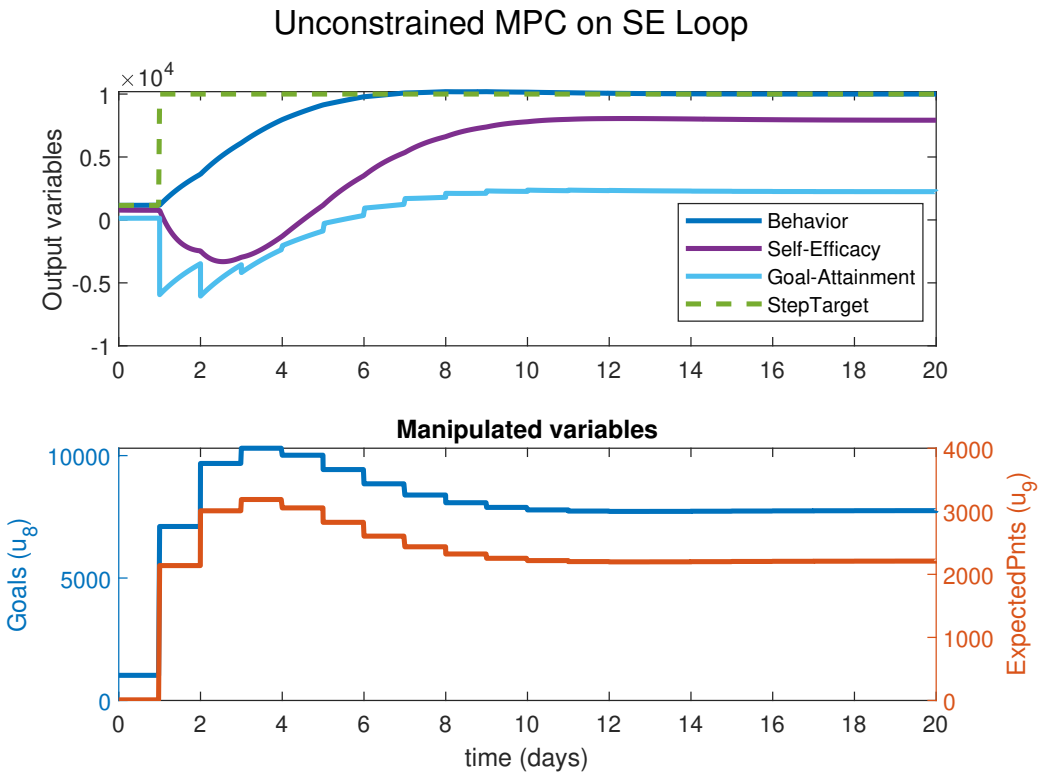

Figure 4.3: Simulation Results from Applying an Unconstrained MPC Controller on the Self-Efficacy Loop for an Adherent Participant. The Controller Parameters Are: $p = 100$, $m = 50$, $\Gamma^Y = \text{diag}(0, 1, 0)$, $\Gamma^u = 0$, $\Gamma^{\Delta u} = \text{diag}(1, 1)$.

are physical and budgetary limitations associated with the manipulated variables. For example, a participant can only walk a finite amount of steps within a day, and only a certain amount of EP can be awarded on a given day to abide by an affordable budget for the intervention. These limitations are comparable to limitations faced in chemical processes, such as limits in the opening of a valve, or safety limits on an exothermic reaction. It is crucial to address these constraints to ensure that the intervention is practical and feasible, as presented in subsequent scenarios.

Self-Efficacy (SE) loop: Constrained Self-Efficacy

To account for the physical and financial limitations of the system, constraints are applied to the manipulated variables. These constraints, as described in (4.13) and (4.14), are applied to all the constrained cases presented in this work.

$$0 \leq u_8(k+i) \leq 15000 \text{ [steps/day]}, \quad \forall\ 0 \leq i \leq m-1 \tag{4.13}$$

$$0 \leq u_9(k+i) \leq 500 \text{ [points/day]}, \quad \forall\ 0 \leq i \leq m-1 \tag{4.14}$$

Maintaining a sufficient level of SE is imperative to mitigate participant dropout. Hence, a SE output is constrained at a specified level below its initial value, as follows:

$$\eta_{3initial} - 500 \leq y_3(k+i) \leq \infty\ \forall\ 0 \leq i \leq p \tag{4.15}$$

The results presented in Figure 4.4 provide interesting insights into the impact of the implemented constraints and tuning. Despite the lower move suppression weights ($\Gamma^{\Delta u} = \text{diag}(0.1, 0.1)$), the intervention in this constrained scenario takes approximately 11 days for the controlled variable response to settle, which is twice as long as the unconstrained case. This slower response is a direct consequence of constraint enforcement, where moves in the manipulated variables are obtained through an optimal solution of the QP problem. As a result, initial manipulated variables moves are significantly lower than the unconstrained case. Figure 4.4 illustrates the application of the constraints on both EP and SE. Although EP is changed abruptly by the controller, the constraint is not violated and the EP signal is phased off by the end of the intervention.

Despite improved controller performance, this case demonstrates an idealistic scenario, where measurements of *Self-Efficacy* are available at all times. In real life situations, missingness in measurements for behavioral constructs is commonplace due to participants' lack of compliance with EMAs. Additionally, in this case, the increase

in the daily goals is quite rapid. This is specifically evident in the initially negative GA values, which progressively decrease until the *Behavior* response is around the settling time. To overcome this issue the controller can be tuned for higher move suppression weights, especially for *Goals*.

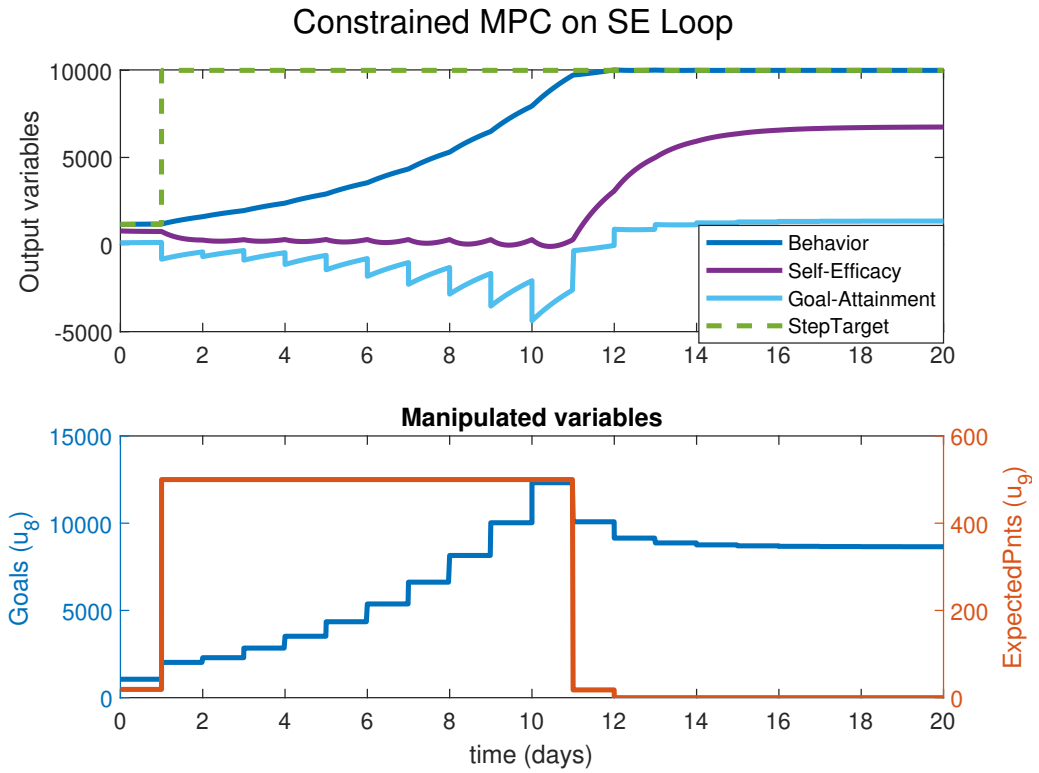

Figure 4.4: Simulation Results from Applying a Constrained MPC Controller on the Self-Efficacy Loop for an Adherent Participant, with a Lower Bound Constraint on *Self-Efficacy*. Controller Parameters Are: $p = 100$, $m = 50$, $\Gamma^Y = \text{diag}(0, 1, 0)$, $\Gamma^u = 0$, and $\Gamma^{\Delta u} = \text{diag}(0.1, 0.1)$. Enforced Constraints Are: 0 steps/day $\leq u_8 \leq$ 15000 steps/day, 0 points/day $\leq u_9 \leq$ 500 points/day, and $\eta_{3i} - 500 \leq y_3 \leq \infty$. All Results Are in Terms of Deviation from Steady-state.

Self-Efficacy (SE) loop: Constrained Goal Attainment

A practical shortcoming of the scenario shown in Section 4.3.1 is that the *Self-Efficacy* is a behavioral construct perceived by the participant, and cannot be easily measured; continuous measurements are not available for this construct, as its values are restricted to discrete Likert scale through the EMA answers. Another challenge faced in measuring behavioral constructs like SE is the prevalence of missing data points throughout the intervention, as participants can be inconsistent with answering EMA surveys daily. In cases of unreliable SE measurement, alternative signals can be used by the controller to infer SE levels. In this case, GA is utilized as it is an input to the SE inventory in (4.5), and can be readily estimated through (4.12).

In this control strategy, several adjustments are made to formulate the optimization problem more sufficiently. Firstly, to mitigate the negative impact of negative *Goal Attainment* on SE a lower bound of -100 steps/day is placed on the GA output. This is done to guide the participant toward providing "ambitious yet achievable" goals. Additionally, to steer clear of reliance on financial rewards, $u_{9_r} = 0$ points/day is set as a target for EP, with an associated weight $\Gamma^u(2,2) = 1$. The remaining tuning parameters and constraints are maintained the same as in Section 4.3.1. The control strategy and tuning implemented in this case are highly effective in attaining the desired outcome. As illustrated in Figure 4.5, the controlled variable response reaches 95% settling time approximately by day 32 of the intervention, which is significantly slower than the previous cases. However, this slower settling time is achieved by making modest changes in the goals over a longer timeframe to reach steady-state. As a result, GA signal is positive throughout the intervention, without violating the enforced lower constraint, which is a clear indication of the effectiveness of this control strategy and tuning. This successful constraint enforcement prevents any significant

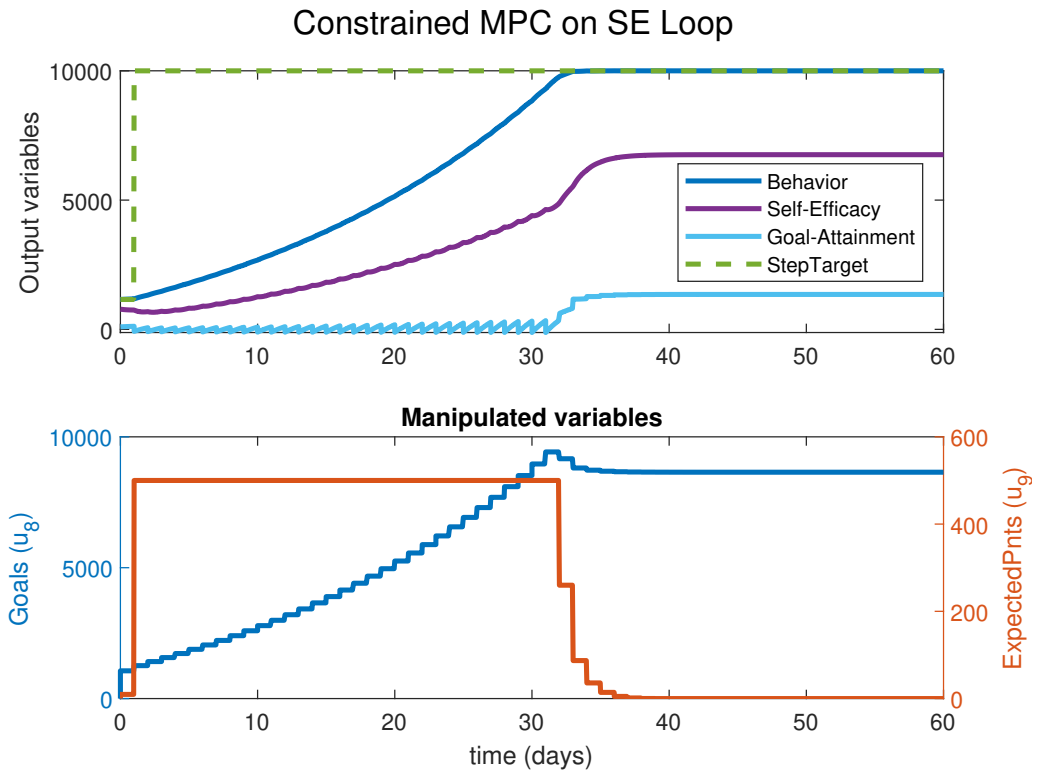

Figure 4.5: Simulation Results from Applying a Constrained MPC Controller on the Self-Efficacy Loop for an Adherent Participant, with a Lower Bound Constraint Applied on Goal Attainment. Controller Parameters Are: $p = 100$, $m = 50$, $\Gamma^Y = \text{diag}(0, 1, 0)$, $\Gamma^u(2, 2) = 1$, and $\Gamma^{\Delta u} = \text{diag}(0.1, 0.1)$. Enforced Constraints Are: $0 \leq u_8 \leq 15000$ steps/day, $0 \leq u_9 \leq 500$ points/day, and $-100 \leq y_7 \leq \infty$ steps/day. All Results Are in Terms of Deviation from Steady-state.

drops in SE, demonstrating the positive impact of incorporating constraints on the readily available GA signal. Additionally, the use of EP remains within the upper constraint of 500 points/day and follows the 0 points/day target, after the desired level of *Behavior* is reached. This approach avoids any potential financial dependency on EP to maintain healthy levels of PA.

OLSE System: Constrained Goal Attainment with Disturbances

In this scenario, the scope of the simulation is broadened by including the *Behavioral Outcomes* inventory to conform to the full OLSE system shown in Figure 4.2. This increases problem complexity through: 1) nonlinearity resulting from the conditionality of awarding granted points based on the feedback signal of participant's behavior, and 2) additional (higher-order) dynamics. This scenario further illustrates the controller's ability to operate under stochastic conditions, as a random temperature disturbance is introduced on day 40. The constraints from the prior case are applied in this scenario, with the addition of 50 points/day as an upper move size constraint for change in EP (Δu_9). The GP signal is provided to the controller as a measured disturbance.

This case shows the ability of the controller to maintain specifications and effectively control a more complex system in the presence of stochastic disturbances. The controlled variable response settles within 20 days, which is faster than the case in Section 4.3.1 due to the added gains from the OL loop. All constraints are maintained throughout the simulation, as seen in Figure 4.6. EP increases up until the large increase in GA, around day 20. After that point, EP use is close to 0 points/day following the set manipulated variable target, to the instant the random temperature disturbance is introduced at day 40. Consequently, EP is minimally utilized to maintain behavior at the desired levels. The concept of the "transfer of variance" is observed in the fluctuations in the manipulated variables after the introduction of the noisy temperature disturbance; the controller effectively maintains the desired behavior setpoint by optimally adjusting the manipulated variables in response to changes in ΔT.

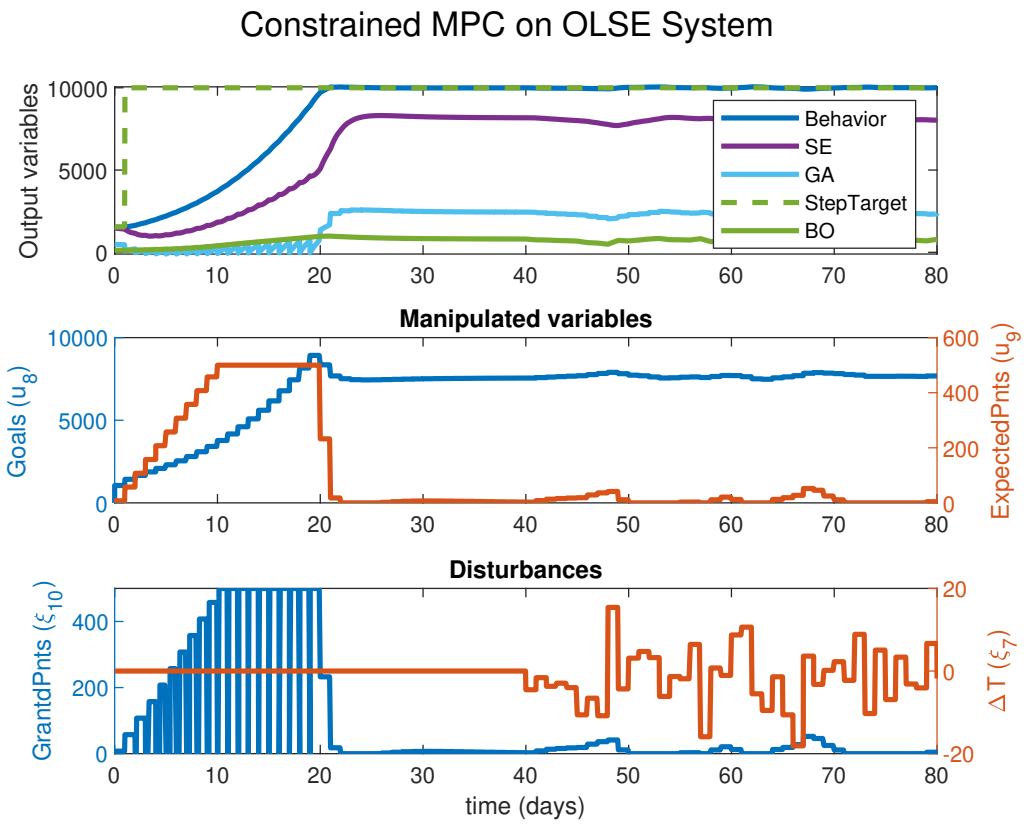

Figure 4.6: Simulation Results from Applying a Constrained MPC Controller on OLSE System for an Adherent Participant, in the Presence of a Measured Random Disturbance (Deviations of the Average Daily Temperature from the Participant's Preference). Controller Parameters Are: $p = 100$, $m = 50$, $\Gamma^Y = \text{diag}(0, 1, 0, 0)$, $\Gamma^u(2, 2) = 1$, and $\Gamma^{\Delta u} = \text{diag}(0.1, 0.1)$. The Following Constraints Are Applied: $0 \leq u_8 \leq 15000$ steps/day, $0 \leq u_9 \leq 500$ points/day, $-\infty \leq \Delta u_9 \leq 50$ points/day , and $-100 \leq y_7 \leq \infty$ steps/day. All Results Are in Terms of Deviation from Steady-state.

Dual Behavioral Outcomes Dynamics OLSE System: Constrained Goal Attainment with Disturbances

In real-world circumstances, multiple behavioral outcomes can exist with different speeds and distinct impacts on *Behavior*. For instance, when initially engaging in

PA *Fatigue* may be more prominent. However, over time *Fatigue* impact diminishes while *Fitness* takes effect, especially if the participant maintains engagement in the intervention and PA. To model these separate and potentially competing dynamics of *Behavioral Outcomes*, an enhancement is made to the SCT model. This enhancement involves the inclusion of separate inventories for the mentioned expected outcomes (*Fatigue*; η_5^{ftg}, and *Fitness*; η_5^{fit}). Figure 4.7 provides a visual representation of the corresponding fluid analogy for the Operant-Learning recycle loop, incorporating these two outcomes. To model the dual dynamics on behavioral outcomes, equation (4.7) is replaced with a set of ODEs (4.16)-(4.18) representing the system. These equations capture the distinct dynamics and interactions between *Fatigue* and *Fitness*, acknowledging their distinct dynamics and impacts on BO, and by extension on *Behavior*.

$$\tau_5^{fit}\frac{d\eta_5^{fit}}{dt} = \gamma_{510}\ \xi_{10}(t) + \beta_{54}^{fit}\ \eta_4(t) - \eta_5^{fit}(t) + \zeta_5^{fit}(t) \tag{4.16}$$

$$\tau_5^{ftg}\frac{d\eta_5^{ftg}}{dt} = \gamma_{57}\ \xi_7(t) + \beta_{54}^{ftg}\ \eta_4(t) - \eta_5^{ftg}(t) + \zeta_5^{ftg}(t) \tag{4.17}$$

$$\tau_5\frac{d\eta_5}{dt} = \beta_{45}^{fit}\ \eta_5^{fit} - \beta_{45}^{ftg}\ \eta_5^{ftg} - \eta_5(t) + \zeta_5(t) \tag{4.18}$$

Assuming an instantaneous effect of *Fatigue* and *Fitness* on the overall *Behavioral Outcome* (i.e., *Behavioral Outcome Performance*), $\tau_5 = 0$, which simplifies (4.18) as follows.

$$\eta_5 = \beta_{45}^{fit}\ \eta_5^{fit} - \beta_{45}^{ftg}\ \eta_5^{ftg} + \zeta_5(t) \tag{4.19}$$

This dual *Behavioral Outcomes* Operant-Learning subsystem is of a second-order and can yield a variety of BO dynamic responses (e.g., underdamped, overshoot, inverse response). The specific dynamic characteristics of the response are dependent on the choice of participant parameters. The selected coefficients for the added

OL subsystem components in the presented simulations for both participants are as follows:

1. $\tau_5^{fit} = 2,\ \tau_5^{ftg} = 1,\ \tau_5 \approx 0.$

2. $\gamma_{57} = 4,\ \gamma_{510} = 5.$

3. $\beta_{45}^{fit} = 0.5,\ \beta_{45}^{ftg} = 0.2,\ \beta_{45} = 0.2,\ \beta_{54}^{fit} = 0.8,\ \beta_{54}^{ftg} = 0.7.$

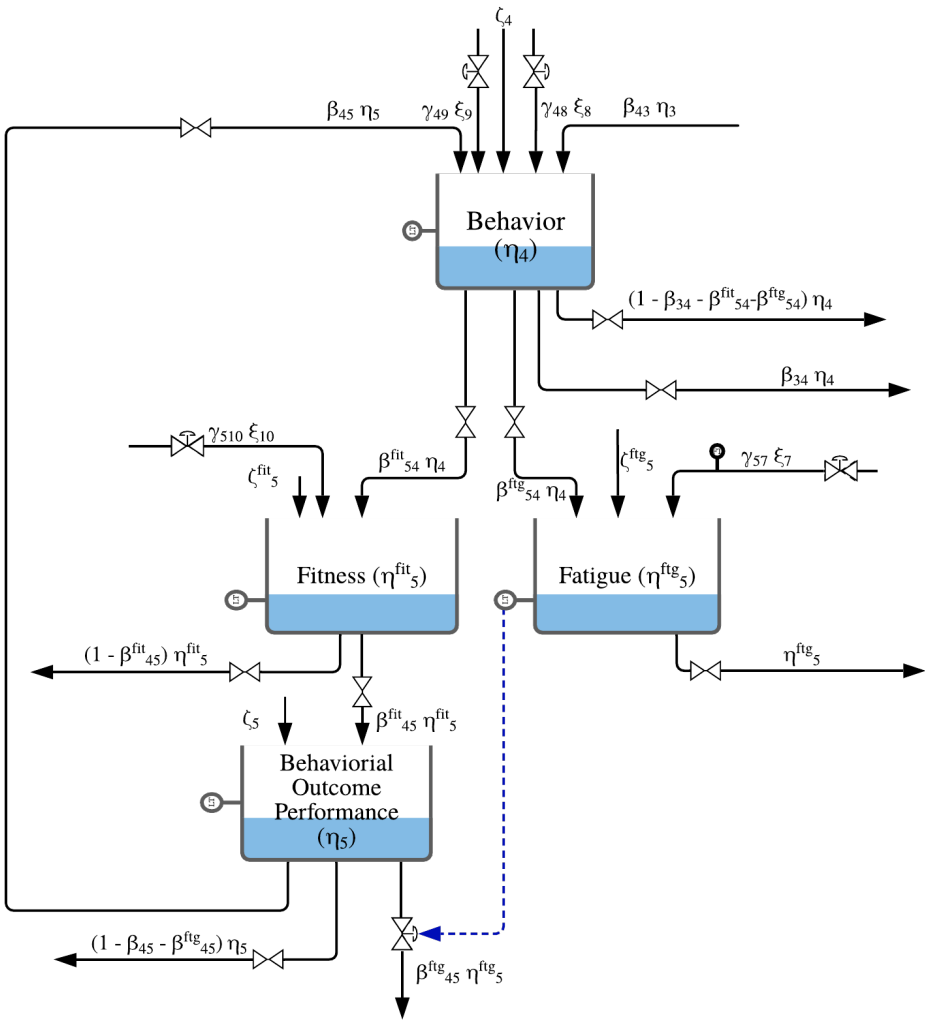

Figure 4.7: Schematic Illustrating an Operant-Learning Loop Illustrating Dual (and Competing) Behavioral Outcome Dynamics, with *Fitness* and *Fatigue* in the Loop.

The incorporation of the dual dynamics of *Bheavioral Outcomes* in the OL recycle loop introduces a higher-order SCT system, which increases the complexity of the system presented in Section 4.3.1. In this scenario, the same control strategy and controller tuning presented in Section 4.3.1 are implemented, with the main distinction being the inclusion of *Fatigue* and *Fitness* BO dynamics in the controller's internal model. Additionally, on day 50 of the intervention a random temperature disturbance is introduced in this scenario. The obtained simulation results provide further evidence of the controller's effectiveness in handling stochastic conditions within a complex system.

As demonstrated in Figure 4.8, the response of the controlled variable settles within the span of approximately 24 days from the beginning of the intervention. This is longer than what is seen in the previous case, because of the initial negative effect of *Fatigue* on the amount of daily steps count. Consequently, the participant struggles to meet their assigned daily goals initially, resulting in low GA values at the beginning of the intervention. However, GA remains above the lower constraint of -100 steps/day constraint and progressively increases along with the *Behavior* over time. More importantly, the initial low GA values do not lead to a significant decrease in SE levels. This indicates that the participant's perceived capability in achieving the provided goals is not significantly impacted, despite the initial challenges. All enforced constraints are satisfied including the constraint on the move size for EP at 50 points/day. Additionally, EP usage is within budget, following constraints, and is phased off to minimal utilization after reaching the 10,000 steps/day setpoint. The inclusion of a manipulated variable target on EP proves to be highly effective in maintaining EP close to 0 points/day, even under stochastic conditions after day 50. The controller only utilizes EP when necessary, which is essential to avoid financial rewards utilization as the main driver for maintaining healthy behavior. Additionally,

this demonstrates the feasibility of such control strategies, making them a viable option for the dissemination of such interventions on a large scale.

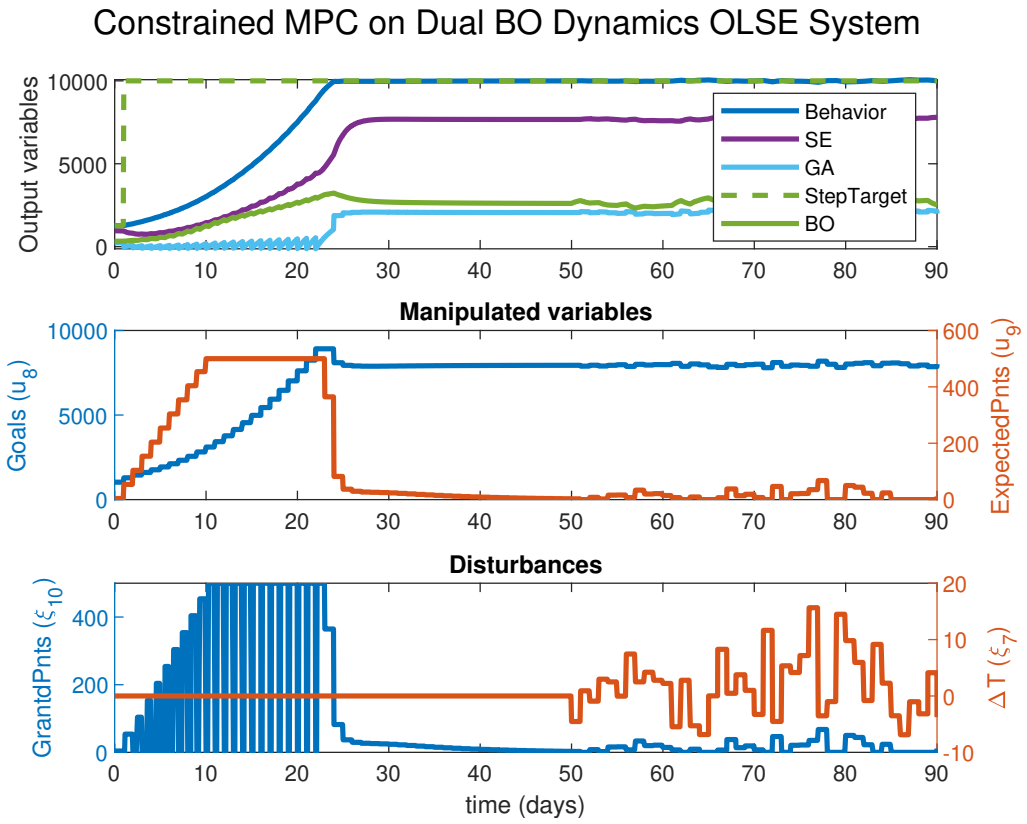

Figure 4.8: Simulation Results from Applying Constrained MPC on Dual BO Dynamics OLSE System for an Adherent Participant in the Presence of a Measured Random Disturbance (Deviations of the Average Daily Temperature from the Participant's Preference). A Low Bound is Applied on Goal Attainment. The Controller Parameters Are: $p = 100$, $m = 50$, $\Gamma^Y = \text{diag}(0, 1, 0, 0, 0)$, $\Gamma^u(2, 2) = 1$, and $\Gamma^{\Delta u} = \text{diag}(0.1, 0.1)$. The Following Constraints Are Applied: $0 \leq u_8 \leq 15000$ steps/day, $0 \leq u_9 \leq 500$ points/day, $-\infty \leq \Delta u_9 \leq 50$ points/day , and $-100 \leq y_7 \leq \infty$ steps/day. All Results Are in Terms of Deviation from Steady-state.

Figure 4.9 demonstrates the higher-order dynamics of the OL loop in this scenario.

This is evident in the overshoot observed in the close-loop response. This figure also illustrates the different and competing components of *Behavioral Outcomes*, and their impact on the dynamic response in terms of both speed and shape of response. For instance, in this scenario *Behavioral Outcomes Performance* settles within 27 days from the beginning of the intervention, which is slower than the previous case which settled within 21 days. This is due to the slower fitness (η_5^{fit}) response, and the nature of the competing components.

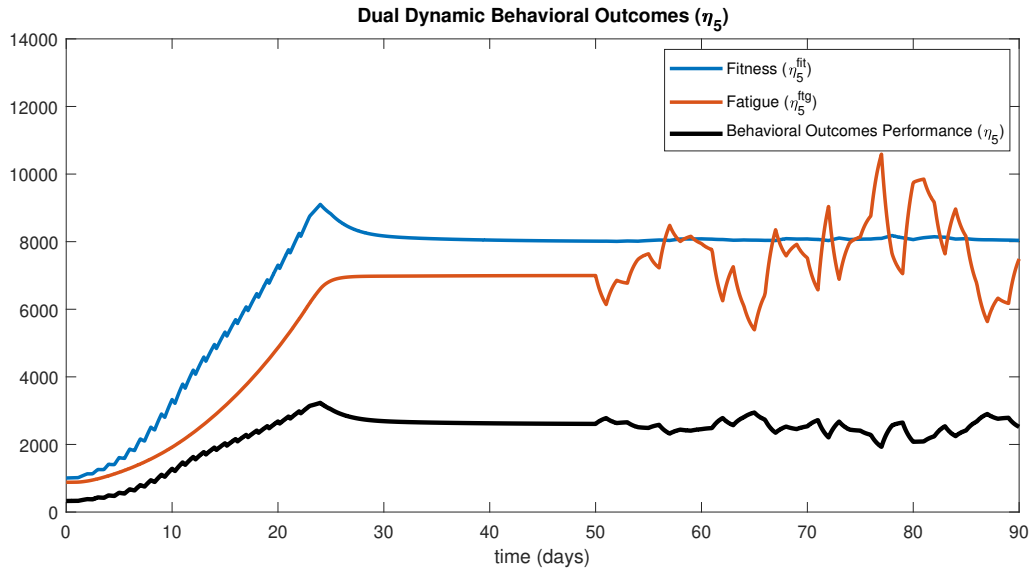

Figure 4.9: Simulation Results for an Adherent Participant Illustrating the Closed-Loop Responses of *Fitness*, *Fatigue*, and *Behavioral Outcomes* Performance for the Adherent Participant.

Dual Behavioral Outcomes Dynamics OLSE System with Nonlinearity: Constrained Goal Attainment with Disturbances

In real-world interventions, the difficulty in reaching higher levels of PA increases as *Behavior* levels increase; when participants reach a certain threshold in their daily

step count, it becomes more challenging to increase PA levels in terms of daily steps. This can be attributed to many factors, like busyness and not being able to designate more time to exercise or walk. Up until this point in the chapter, the majority of cases examined have involved linear, time-invariant models. However, it is essential to consider cases of nonlinearity. Therefore, to model such nonlinear dynamics in this scenario, the gain γ_{48} varies exponentially with respect to the difference between *Behavior* (η_4) and the threshold as a fraction of the desired outcome of 10,000 steps/day as follows:

$$\gamma_{48}(t) = c + be^{-\alpha(\eta_4(t)-TH)/10000} \tag{4.20}$$

where

$$b = \frac{\gamma_{48_f} - \gamma_{48_i}}{e^{-\alpha} - 1}, \text{ and } c = \gamma_{48i} - b \tag{4.21}$$

The threshold level selected in this simulation is $TH = 8,000$ steps/day, with the initial value of the gain parameter representing this hypothetical adherent participant at $\gamma_{48_i} = 1$, and the final value $\gamma_{48_f} = 0.6$. This yields an exponential decay in the overall system gain between *Behavior* and *Goals* from 1.26 to 0.58. Consequently, a gradual change in the participant's behavior occurs past the selected threshold: from being able to meet and overachieve the goals by 26%, to only being able to accomplish 58% of a goal given to them on a certain day.

As a result of this nonlinearity in the participant's behavior model, a mismatch between the plant and controller model occurs once the *Behavior* levels reach the defined threshold. In closed-loop simulation results for this scenario, shown in Figure 4.10 below, the impact of the nonlinearity can be clearly observed after the participant surpasses the threshold of 8,000 steps/day on the 21st day of the intervention. The rate of the increase in *Behavior* decreases rapidly, which leads to the controller increasing the daily goals, surpassing 10,000 steps/day. In this scenario, the controlled

variable reaches 95% of the desired target on the 30th day of the intervention.

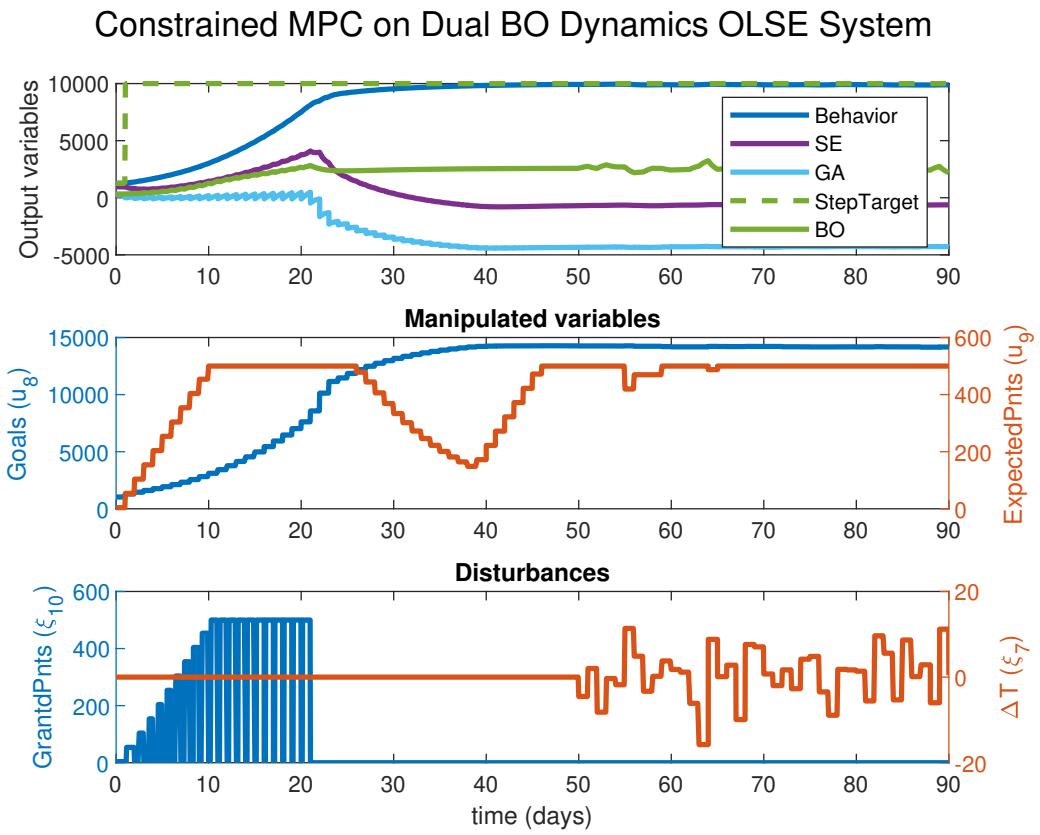

Figure 4.10: Simulation Results from Applying Constrained MPC on Dual BO Dynamics OLSE System for an Adherent Participant, in the Presence of Nonlinearity and a Measured Random Disturbance. A Low Bound is Applied on Goal Attainment. The Controller Parameters Are: $p = 100$, $m = 50$, $\Gamma^Y(2,2) = 1$, $\Gamma^u(2,2) = 1$, and $\Gamma^{\Delta u} = \text{diag}(0.1, 0.1)$. The Following Constraints Are Applied: $0 \leq u_8 \leq 15000$ steps/day, $0 \leq u_9 \leq 500$ points/day, and $-\infty \leq \Delta u_9 \leq 50$ points/day . Adaptive Lower Constraint is Applied on GA Starting with -100 steps/day $\leq y_7$, Then Gradually Decreasing to -5000 steps/day $\leq y_7$. All Results Are in Terms of Deviation from Steady-state.

Note the GA signal is positive throughout the first 20 days of the intervention. Afterward, as the system gains change, the participant is not able to meet the daily goals,

which results in negative GA from day 21 and on-words. To avoid an offset in the controlled variable due to the output constraints on SE and GA, dynamic constraints are implemented in this case: after the *Behavior* level surpasses the threshold, the lower constraint on SE and GA are gradually relaxed (from -100 to -5000 steps/day for GA). This allows the controller to increase the daily goals higher, close to 15,000 steps/day by the end of the intervention, to guide the participant towards the set-point. Consequently, GA values progressively decrease through the simulation. The sustained negative values of GA lead to the observed significant drop in SE levels. EP utilization in this scenario does not violate the defined upper bound and move size constraints. However, EP usage is close to the maximum allowed value for the majority of the simulation and is not phased off when the participant reaches the setpoint.

This control strategy introduces adaptive constraint enforcement in a behavioral intervention setting. While such a strategy guides the participant to the desired setpoint (which is considered a success from a control engineering standpoint), it has significant drawbacks from a behavioral science perspective. The significantly and sustainably negative values of GA, as well as the substantial drop in SE can have a negative impact on the participant and increase the possibility of participant disengagement and dropout. Moreover, the sustained utilization of EP throughout the intervention, even after *Behavior* levels settle at the setpoint, may form dependency of the participant on the financial incentives. Hence, this control strategy is not ideal for dealing with cases similar to the one explored in this scenario; from a behavior intervention standpoint, providing "ambitious yet achievable" goals is more important than reaching the desired setpoint.

An alternative approach to easing the lower bounds on GA and SA is the utilization of slack variables as a part of the optimization objective function. Through this

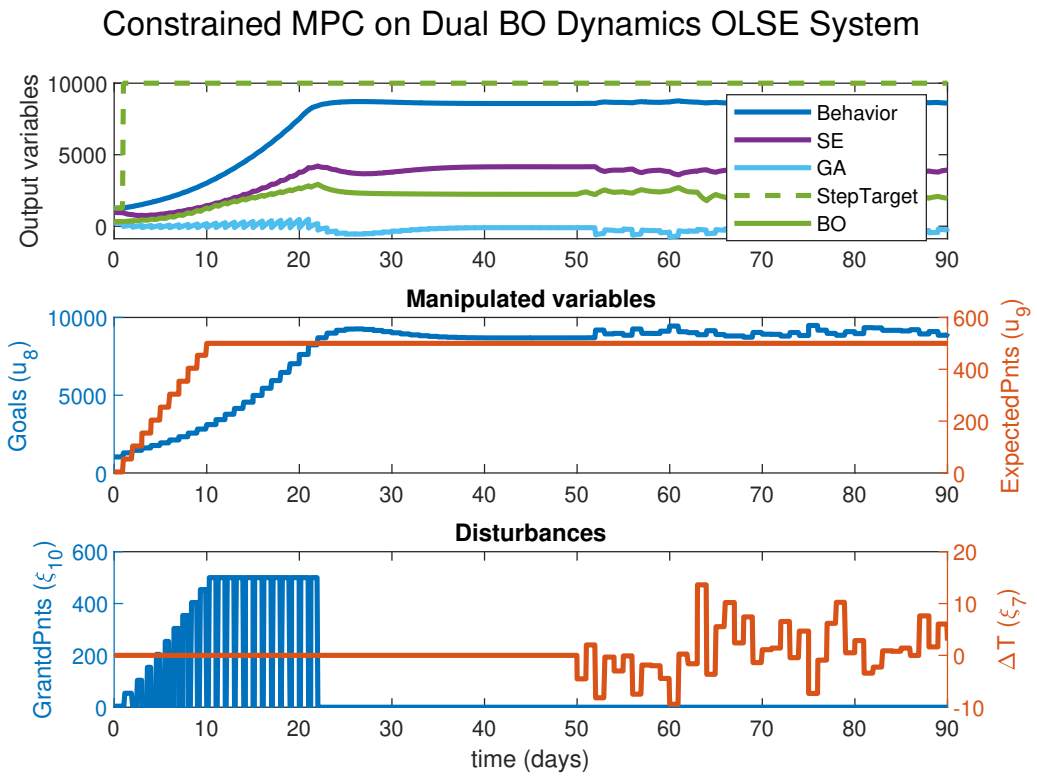

Figure 4.11: Simulation Results from Applying Constrained MPC on Dual BO Dynamics OLSE System for an Adherent Participant, in the Presence of Nonlinearity and a Measured Random Disturbance. A Low Bound is Applied on Goal Attainment. The Controller Parameters Are: $p = 100$, $m = 50$, $\Gamma^Y(2,2) = 1$, $\Gamma^u(2,2) = 1$, and $\Gamma^{\Delta u} = \text{diag}(0.1, 0.1)$. The Following Constraints Are Applied: $0 \leq u_8 \leq 15000$ steps/day, $0 \leq u_9 \leq 500$ points/day, $-\infty \leq \Delta u_9 \leq 50$ points/day , and $-100 \leq y_7 \leq \infty$ steps/day. All Results Are in Terms of Deviation from Steady-state.

approach, lower output constraints can be "softened" through the inclusion of their respective slack variable values, which are determined as a part of the QP solution. In this approach, the lower constraint on GA and SE is optimally adjusted based on an assigned weight for the slack variable terms in the optimization function. Through

MATLAB's MPC toolbox, the slack weight for both SE and GE is set to 0.5 in this simulation, the results of which can be seen in Figure 4.11. The difference between the two constraint relaxation approaches can be clearly observed by comparing Figures 4.10 and 4.11 after the 21st day of the intervention, when the decrease in the gain between *Goals* and *Behavior* occurs. The use of low slack weights in the constraint softening approach leads to a clear offset between the controlled variable and the setpoint, where *Behavior* settles at close to 1400 steps/day shy from the setpoint. This is a result of enforcing "soft" lower bound constraints on both GA and SE, where it can be observed that the GA values slightly violate the lower constraint; GA reaches -500 steps/day when the overshoot happens in *Goals* between days 21 and 33.

The negative values of GA lead to a decrease in SE past the 21st day of the intervention. However, as GA values are only slightly negative in this simulation, the drop in SE levels is not very significant and does not violate the enforced constraint on SE. Therefore, the participant is less likely to disengage and drop out of the intervention with this control strategy. Moreover, the use of slack variables in this control strategy maintains the *Goals* signal at reasonable levels; the goals signal settles approximately at 8700 steps/day and the goals never exceed 10,000 steps on any day of the intervention. While this control strategy results in an offset, it is the more suitable strategy for closed-loop behavioral interventions, based on the feedback of behavioral scientists.

4.3.2 Non-Adherent Participant

In the previous subsections, control strategies for behavioral interventions aimed at improving physical activity levels for an adherent participant have been developed. However, not all participants involved in PA interventions will abide by the daily goals. Even adherent participants may enter into cycles of noncompliance due to

factors such as stress or busyness. Hence, it is important to test the performance of the proposed control strategy on simulation conditions for a non-adherent participant. The following model parameters are utilized to represent such a participant:

- $\tau_3 = 3,\ \tau_4 = 1,\ \tau_5 = 1.$
- $\gamma_{311} = 0.45,\ \gamma_{48} = 0.46,\ \gamma_{49} = 1.3,\ \gamma_{57} = 2,\ \gamma_{510} = 5.$
- $\beta_{34} = 0.5,\ \beta_{43} = 0.67,\ \beta_{45} = 0.25,\ \beta_{54} = 0.54.$

The combination of these parameters for the non-adherent participant yields a gain of 0.53 between *Goals* and *Behavior*. This translates to the participant not following goals closely, and most likely their inability to achieve the goals for the majority of the intervention. Hence, it is essential to examine the devised control strategies and assure their compatibility with non-adherent participants; in terms of delivering "ambitious yet achievable" goals and robustness to plant-model mismatch.

Dual Behavioral Outcomes Dynamics OLSE System: Constrained Goal Attainment with Disturbances and Plant Limitations

As can be seen in Figure 4.12 the devised strategy performs well in terms of increasing the number of daily steps in the case of the non-adherent participant. This is evident in the "ambitious yet achievable" goals given to the participant due to the constraint on GA of -100 steps/day. It is important to note that slack variables have been implemented in this case, to assure the feasibility of the optimization problem and 'soften' the constraints on both SE and GA. The utilized slack variable weight for both output constraints is at 0.5. The participant does not meet the daily goals within the first 6 days of the intervention, however, due to the increase in SE and BO, as a result of the accumulation of the benefits of fitness in the OL recycle loop, the participant achieves the daily goals from day 7 to day 27.

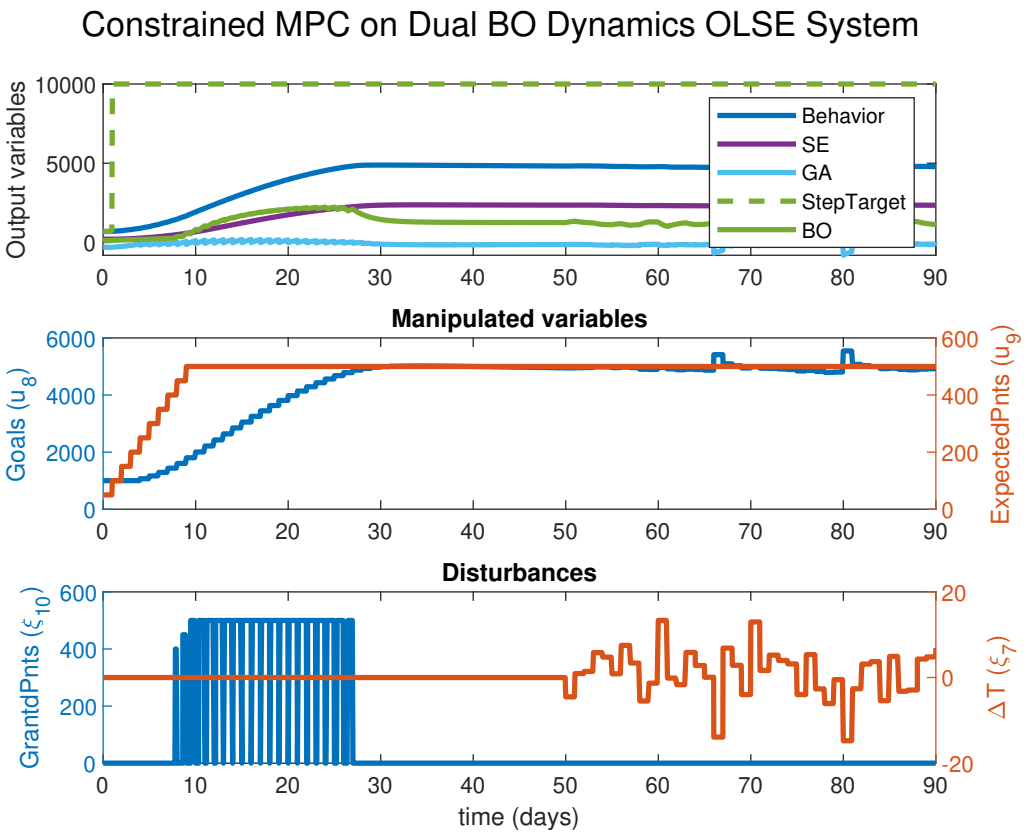

Figure 4.12: Simulation Results from Applying Constrained MPC on Dual BO Dynamics OLSE System for a Non-Adherent Participant, in the Presence of a Measured Random Disturbance (Deviations of the Average Daily Temperature from the Participant's Preference). A Low Bound is Applied on Goal Attainment. Controller Parameters Are: $p = 100$, $m = 50$, $\Gamma^Y = \text{diag}(0, 1, 0, 0, 0)$, $\Gamma^u(2, 2) = 1$, and $\Gamma^{\Delta u} = \text{diag}(0.1, 0.1)$. The Following Constraints Are Applied: $0 \leq u_8 \leq 15000$ steps/day, $0 \leq u_9 \leq 500$ points/day, $-\infty \leq \Delta u_9 \leq 50$ points/day , and $-100 \leq y_7 \leq \infty$ steps/day. All Results Are in Terms of Deviation from Steady-state.

Despite the controller's best effort to guide such a participant towards the setpoint of 10,000 steps/day, an offset between the setpoint and the number of daily steps is observed. The participant's behavior settles within 30 days from the beginning of

the intervention at a level a little below 5,000 steps/day. This is mainly due to plant limitations, where the overall gain between *Goals* and *Behavior* for this participant does not allow for achieving the desired setpoint, without significantly violating the GA constraint. Consequently, at steady state, GA is negative, and the GA constraint is not met due to the use of slack. This is indeed the case, despite the use of the EP and financial rewards to motivate the participant. While the utilization of EP abides by the upper constraint of 500 points/day and the move size constraint of 50 points/day, financial incentives are never phased off in this simulation because the participant never reaches the desired setpoint at any point of the intervention.

Dual Behavioral Outcomes Dynamics OLSE System with Nonlinearity: Constrained Goal Attainment with Disturbances

Human behavior is highly intricate and subject to time-varying dynamics and nonlinear changes, especially as individuals adapt to different situations and seek to improve their life conditions. As the aim of behavioral interventions is to aid participants in adopting healthier behaviors and facilitate such behavior change, it is imperative for the controller to be robust to changes in system dynamics and successfully guide participants toward the desired behavior in such situations. For instance, it is possible for an individual who started the intervention as a non-adherent and not goal oriented participant to change their response to the daily goals over time, because of the benefits they see from the intervention or changes in life rhythms leading to the individual having more time to engage in the intervention. Consequently, a plant-model mismatch would occur as system dynamics, especially gains would change over time.

In the simulation results shown in Figure 4.13 the controller response to nonlinear changes in system dynamics, leading to plant-model mismatch is presented. In this scenario, the gain between the daily goal and the *Behavior* inventory (γ_{48}) increases

exponentially with the increase of the output following the expression presented in (4.20). Initially, the same accumulative value for the gain between *Goals* and *Behavior* is the same as the previous case at 0.53, which is accomplished through the utilization of ($\gamma_{48_i} = 0.46$). This is the case until the participant reaches a threshold of 4500 steps/day. After this threshold, as the participant experiences the benefits of their increased walking behavior, the gain increases gradually to reach ($\gamma_{48_f} = 0.6$) resulting in an accumulative gain between *Goals* and *Behavior* of 1. Consequently, the participant overcomes all limitations and is able to meet and exceed the daily goals. While the plant model in this case exhibits nonlinear dynamics, the controller model is linear and is based on the initial gain value (γ_{48_i}).

As observed in Figure 4.13, the controller performs very well in terms of providing the participant with "ambitious yet achievable" goals throughout the majority of the intervention and guiding the participant to the desired intervention outcome. At the beginning of the intervention, it is seen that the closed-loop response is very similar to the case shown in Section 4.3.2, which is expected as the same model for the non-adherent participant is utilized initially. The controller gradually increases the daily goals while abiding by the lower bound output constraint on GA of -100 steps/day, and incrementally increasing the use of EP by 50 points/day until reaching the upper bound constraint of EP of 500 points/day. By day 10 of the intervention, EP are fully utilized and the participant starts achieving the daily goal and receiving financial rewards in the form of GP based on their increased daily step-count.

After day 20, the participant's *Behavior* surpasses the threshold of 4500 steps/day. As a result γ_{48} increases, therefore, increasing the influence of *Behavior* in the SE and OL recycle loops. With the observed benefits of the increased *Behavior* level and *Fitness* effects outweighing *Fatigue* in *Behavioral Outcomes*, the positive OL recycle loop contribution to the daily step-count increases. Moreover, the positive

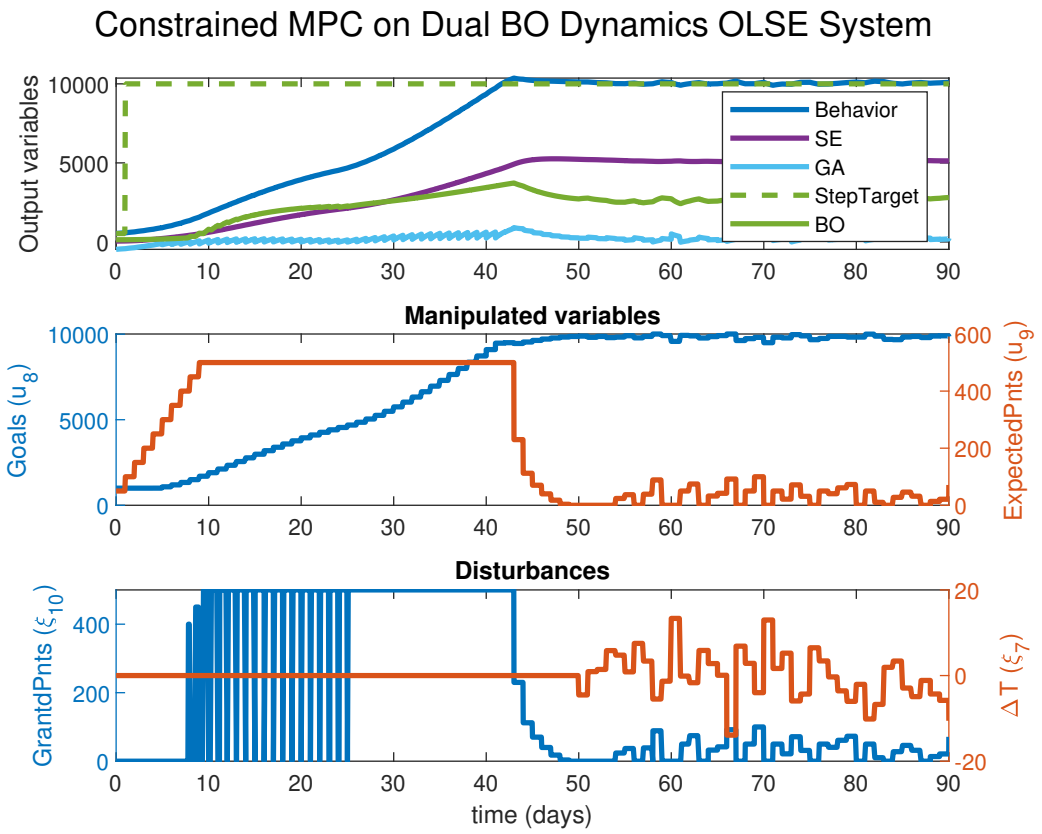

Figure 4.13: Simulation Results from Applying Constrained MPC on Dual BO Dynamics OLSE System for a Non-Adherent Participant, in the Presence of Non-linearity and a Measured Random Disturbance (Deviations of the Average Daily Temperature from the Participant's Preference). A Low Bound is Applied on Goal Attainment. Controller Parameters Are: $p = 100$, $m = 50$, $\Gamma^Y = \text{diag}(0, 1, 0, 0, 0)$, $\Gamma^u(2,2) = 1$, and $\Gamma^{\Delta u} = \text{diag}(0.1, 0.1)$. The Following Constraints Are Applied: $0 \leq u_8 \leq 15000$ steps/day, $0 \leq u_9 \leq 500$ points/day, $-\infty \leq \Delta u_9 \leq 50$ points/day , and $-100 \leq y_7 \leq \infty$ steps/day. All Results Are in Terms of Deviation from Steady-state.

Goal-Attainment yields higher SE levels, and subsequently higher SE recycle loop contribution to *Behavior*. This accumulative effect leads to a further rise in *Behavior* levels over the following days of the intervention, which in turn increases the gain

between *Goals* and *Behavior*. Therefore, the mismatch between the controller model and plant model becomes more prominent the further the participant progresses in the intervention.

Despite the mismatch between the plant and controller models, the closed-loop response seen in Figure 4.13 illustrates the effectiveness of the control strategy and the linear MPC in delivering a personalized optimal intervention. This is done while abiding by all the constraints enforced on SE and GA. Moreover, by the 44th day of the intervention, the output variable settles at the desired setpoint, and EP use is phased off following the set target on the manipulated variable to avoid financial dependency. Moreover, minimal EP use is observed after the introduction of the stochastic temperature disturbance on the 50th intervention day. The obtained simulation results serve as a proof of concept to the use of judiciously formulated linear MPC control strategies in delivering personalized optimal behavioral interventions, in spite of the nonlinearities that can be found in complex systems related to behavior change.

4.4 Summary and Conclusions

In this study, a variety of strategies for personalized PA behavioral interventions relying on MPC have been proposed and evaluated. The analysis is based on simulated models based on Social Cognitive Theory for adherent and non-adherent participants, representing expected extremes of behavior by intervention participants. The analysis begins with a simple unconstrained scenario for a SE loop subsystem, then develops into more complex higher-order systems including plant-model mismatch and nonlinearities. Through this process, significant decisions relating to problem specifications and constraint enforcement are made based on the expertise of behavioral scientists. An iterative approach is utilized, where feedback from experts guiding the increasing complexity of the system, as well as adjustments to the control strategy and tun-

ing, ensures the obtained applicability of the developed control strategies in real-life interventions.

The findings presented in this chapter illustrate the advantages of proper problem formulation and provide a proof of concept for the use of fluid analogies and MPC in operating behavioral interventions. The presented simulation results demonstrate that MPC, with sensibly formulated objective function and constraints, provides a compelling approach for delivering personalized physical activity interventions, even under circumstances with limited measurement capabilities and plant-model mismatch. The presented findings have played an essential role in furthering the exploration of control strategies for behavioral interventions, and have been implemented Three Degrees-of-Freedom Kalman Filter Hybrid Model Predictive Control (3DoF-KF HMPC) formulation as presented in Chapter 5, Khan *et al.* (2022) and El Mistiri *et al.* (2023). More details about the 3DoF-KF HMPC formulation and results of its implementation in a simulation setting for a representative *JustWalk* participant are presented in Chapter 5. The full potential of this research is realized through the integration of system identification and control in what is referred to as a "control optimization trial" (COT; Hekler *et al.* (2018)), which is part of the ongoing *YourMove* study (R01CA244777, 2020) (see Chapter 6). Using system identification concepts, especially input signal design and model structure selection, will enable estimating participant-specific parameters for the SCT model from dynamically informative experimental data (Rivera *et al.*, 2018). While the primary focus of this chapter is on deterministic conditions, the gained insights expand the comprehension of the impact and outcomes of various control strategies and have been applied in real-life stochastic conditions, in *YourMove*. The developed control strategies in this chapter are refined in *YourMove* based on participants' responses to the closed-loop intervention, as described in Section 6.5. In addition, preliminary results for repre-

sentative *YourMove* participants are presented in Chapter 6. The experimental data obtained from *YourMove* trial will aid in identifying the characteristics of noise and stochastic conditions associated with PA interventions, which will then be integrated into future simulations to further explore these different control strategies in more realistic conditions. Moreover, future efforts include formalizing and automating controller tuning to streamline personalized MPC-based interventions with minimal user involvement for the purpose of disseminating such interventions on a large scale and improving public health.

Chapter 5

SYSTEM IDENTIFICATION AND HYBRID MODEL PREDICTIVE CONTROL IN PERSONALIZED MHEALTH INTERVENTIONS FOR PHYSICAL ACTIVITY

5.1 Introduction

Various chronic health conditions, including cardiovascular disease, breast and colon cancer, obesity, diabetes, and arthritis are linked to insufficient levels of physical activity (McGinnis *et al.*, 2002). Such chronic conditions can reduce the quality of life for patients and may have fatal consequences. Physical activity (PA) can work as a preventative measure; recent studies show that walking 8,000 steps/day on average can reduce the risk of such conditions by 51% in comparison to averaging 4,000 steps/day (Booth *et al.*, 2012; Saint-Maurice *et al.*, 2020).

Despite this information being available to the public, many people do not meet the recommended guidelines for PA on a weekly basis (Olson *et al.*, 2018). Mobile health (mHealth) technologies provide new avenues to study behavior, especially related to PA through temporally rich data, and can deliver efficient, scalable, and user-friendly interventions to promote healthy behavior. Smart devices (e.g., smartphones, wearables) play an important role in terms of measuring PA levels and delivering intervention components at the right times and in the right context for users. Yet, the majority of mHealth PA interventions developed by researchers have only been evaluated in short-term trials (e.g., 4 weeks to 6 months) with moderate effects and limited scope (Payne *et al.*, 2015), lacking the ability to evaluate their effectiveness in real-world circumstances (Hekler *et al.*, 2016).

Systems related to behavior change are complex and involve both time-invariant

and time-varying dynamics, especially in the case of physical activity (Conroy *et al.*, 2011). However, traditional behavioral medicine approaches are centered around static modeling that does not encompass the full scope of the system (Hekler *et al.*, 2016). In recent years, the application of control system engineering principles in behavioral medicine brought about a paradigm shift in understanding the dynamic nature of behavior change and delivering behavioral interventions (Timms *et al.*, 2014b; Deshpande *et al.*, 2014; Guo *et al.*, 2020; Martín *et al.*, 2020). Goals include the development of a synergistic approach between system identification (to estimate individualized dynamic models for behavior change), and control design (to operationalize personalized decision-making framework for interventions) in what is known as the control-optimization-trial (COT; Hekler *et al.* (2018)). This approach is highly appealing, as it can be implemented to systematically guide participants toward attaining and sustaining healthy levels of PA.

One of the best-recognized theories of behavior change is Social Cognitive Theory (SCT; Bandura (1986)), which has been used as the basis for many behavioral interventions. SCT provides a causal framework to understand changes in behavior over time, as it relates personal and environmental factors to behavior and allows for predicting engagement in determined behavior. In the work done by Martín *et al.* (2020) a control-oriented dynamic model of the SCT was developed utilizing fluid analogy. To validate the hypothesized model structure and estimate parameters on an idiographic (i.e., individual) level, system identification experiments have been designed utilizing personalized input signals in an open-loop PA intervention setting (Martín *et al.*, 2015a,c). Based on these ideas, a pilot mHealth intervention called *JustWalk* has been developed with the analysis presented in various articles (Freigoun *et al.*, 2017; Korinek *et al.*, 2018; Phatak *et al.*, 2018), which illustrate the effectiveness of "ambitious yet achievable" daily goals and positive reinforcement of goal achievement

as intervention components to study and improve behavior.

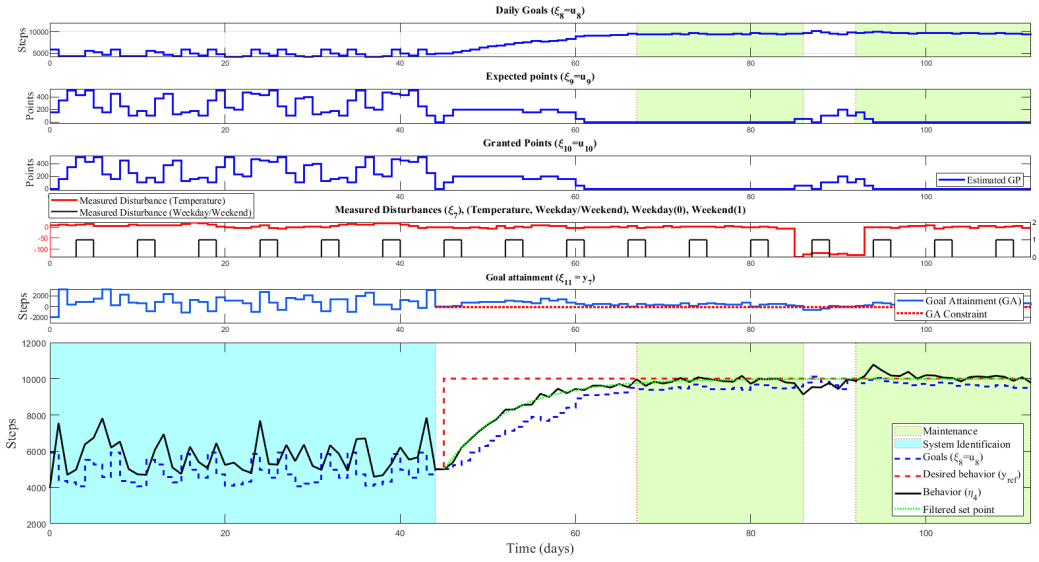

Figure 5.1: Simulation Illustrating Control Optimization Trial (COT) Behavioral Intervention Phases. Highlighted in Cyan is the System Identification Phase, and in Green is the Maintenance Phase, While the Unhighlighted Areas Represent the Initiation Phase.

In this work, black-box modeling techniques are examined in obtaining idiographic dynamic models for representative *JustWalk* participants. The estimated models are then utilized to test a developed decision-making algorithm for an adaptive mHealth intervention promoting PA (in terms of daily steps) among sedentary adults, in a simulation setting. Control strategies developed in Chapter 4 are utilized to ensure "ambitious yet achievable" daily goals in the simulated close-loop intervention (El Mistiri *et al.*, 2022b). This is done to evaluate the COT approach, with emphasis on system identification considerations, ahead of real-world implementation. Two intervention phases are included to ensure the longevity and success of the intervention results: 1) a behavioral initiation phase where individuals are progressively guided to desired healthy levels of PA through the introduction of daily step goals which are

reinforced by rewards, 2) a maintenance phase where rewards are gradually decreased based on the participant's enhanced ability to continue to engage in the desired behavior and to avoid dependency on the financial rewards in sustaining the healthy behavior.

In Chapter 4, a standard MPC formulation was implemented to devise control strategies for PA intervention, which were tested in simulation using the developed SCT-based model to represent hypothetical participants. These devised control strategies are expanded upon in this chapter, where the decision-making framework for intervention delivery is based on a hybrid model predictive control formulation (HMPC; Nandola and Rivera (2013); Khan *et al.* (2022)). In previous work, HMPC-based solutions were considered in behavioral health interventions for smoking cessation, fibromyalgia treatment, and gestational weight loss (Deshpande *et al.*, 2014; Timms *et al.*, 2014d; Dong *et al.*, 2014; Downs *et al.*, 2018). An initial formulation of HMPC for physical activity based on a hypothetical model of SCT is proposed in Martín *et al.* (2016a). Mixed logical dynamical (MLD) framework is utilized in the HMPC-based decision policy, to describe categorical and logical decisions associated with intervention components. Three-degree-of-freedom tuning is implemented to allow for adjusting the speed of response to setpoint tracking, measured, and unmeasured disturbance rejection independently. The controller is reconfigured through the adjustment of manipulated variable target weights, to operationalize the shift between initiation and maintenance phases. The obtained simulation results illustrate the effectiveness of the synergy between system identification (to estimate participant-specific models), and the devised controller formulation (to address hybrid system dynamics, setpoint tracking, disturbance rejection, and controller reconfiguration), in facilitating personalized optimal PA interventions. This is a vital step towards the dissemination of behavioral interventions promoting PA on a large scale.

This chapter is organized as follows: in Section 5.2 a description of SCT and the different components of the intervention is presented. Section 5.3 gives an overview of the design of the *JustWalk* intervention and the use of system identification methods to estimate a dynamic model using data from representative participants. Section 5.4 presents HMPC-based intervention controller formulation corresponding to the model estimated in Section 5.3, including discrete and logical constraints and controller reconfiguration. Section 5.5 presents a simulation study utilizing the estimated participant-specific models, to test the performance of the control strategy (based on Chapter 4) in guiding personalized PA interventions in the presence of disturbances. Finally, Section 5.6 provides a summary of the conclusions.

5.2 SCT-based adaptive behavioral intervention

The desired outcome of the intervention is to elevate physical activity levels, measured in the number of steps walked per day, among sedentary adults. This is achieved by reaching the recommended weekly average of 10,000 steps per day (or at least an increase of +3,000 steps per day from the baseline measurement). The design and implementation of the behavior change intervention are inspired by the aforementioned popular theory of behavior change SCT (Riley *et al.*, 2016; Phatak *et al.*, 2016). SCT is a well-substantiated behavioral theory, in which change in behavior is described through the interactions between behavior, psychoactive constructs, and environmental factors. In SCT human agency plays a significant role where individuals proactively self-reflect, self-regulate, and organize based on perceived outcomes, which allows for prediction of an individual's ability to engage in a determined behavior over time. Some of the prominent SCT constructs are:

- *Self-Efficacy* (η_3): represents the self-perceived capability to do what is needed to engage in a given behavior.

- *Behavior* (η_4): represents different characteristics of the behavior of interest (e.g., duration, frequency, and type), in this case, the number of daily steps.

- *Behavioral Outcomes* (η_5): represents the perceived psychological and physical outcomes (e.g., praise, fatigue) from engaging in the behavior.

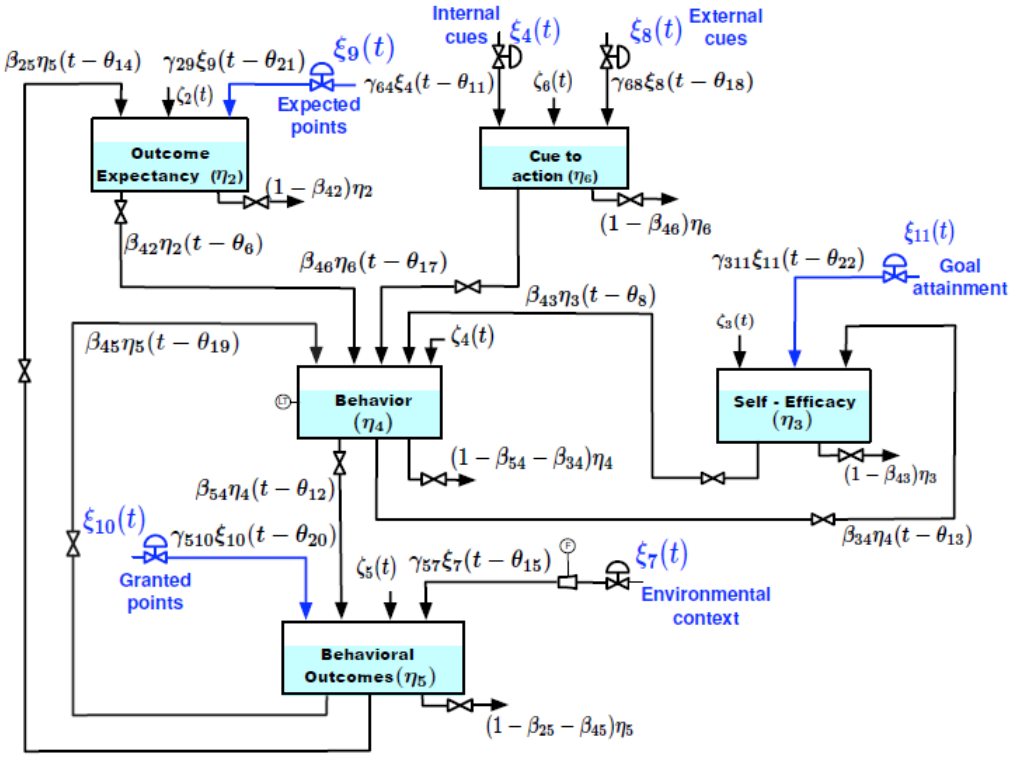

Figure 5.2: Simplified SCT Model in a Fluid Analogy, Based on (Martín *et al.*, 2020).

The work done in Martín *et al.* (2020) presents a dynamic model of SCT describing the constructs and their interconnections, which is derived based on a fluid analogy. Fig. 5.2 depicts a simplified version of the SCT model in a fluid analogy where each ξ_i represents an input (as inflow/outflow), η_i is an output (as an inventory level), γ_{ij} and β_{ij} represent the interrelational gains between the different various

inputs and inventories, ζ_i is an external disturbance and i, j are integers representing inventory and input numbers. By applying the conservation of mass on each inventory, the dynamic model of the system is described by the following ordinary differential equations:

$$\tau_2 \frac{d\eta_2}{dt} = \beta_{25}\ \eta_5(t) - \eta_2(t) + \zeta_2(t) \tag{5.1}$$

$$\tau_3 \frac{d\eta_3}{dt} = \gamma_{35}\ \xi_5(t) + \gamma_{311}\ \xi_{11}(t) + \beta_{34}\ \eta_4(t) - \eta_3(t) + \zeta_3(t) \tag{5.2}$$

$$\tau_4 \frac{d\eta_4}{dt} = \beta_{42}\ \eta_2(t) + \beta_{43}\ \eta_3(t) + \beta_{45}\ \eta_5(t) + \beta_{46}\ \eta_6(t) - \eta_4(t) + \zeta_4(t) \tag{5.3}$$

$$\tau_5 \frac{d\eta_5}{dt} = \gamma_{57}\ \xi_7(t) + \beta_{54}\ \eta_4(t) - \eta_5(t) + \zeta_5(t) \tag{5.4}$$

$$\tau_6 \frac{d\eta_6}{dt} = \gamma_{68}\ \xi_8(t) - \eta_6(t) + \zeta_6(t) \tag{5.5}$$

In an intervention setting, individualized daily goals are provided to participants aiming to increase their PA levels. Upon achieving the given daily goals, participants earn points which can be transferred to rewards chosen as part of a wellness program (e.g., water bottles, gift cards, etc). Daily step goals and expected points are delivered to the participants through a digital user platform, like a smartphone. To utilize the SCT model in the intervention, the following input signals are included:

- Goals (ξ_8; u_8): represent the daily step target and directly influence behavior.
- Expected Points (EP; ξ_9; u_9): the amount of points a participant expects to get, if they meet the daily target. A maximum of 500 points/day can be earned.
- Granted Points (GP; ξ_{10}): the amount of points granted, which is equivalent to ξ_9 when a participant meets or exceeds their step goal for the day.
- Goal Attainment (GA; y_7; ξ_{11}): represents the difference between the behavior and given goal.

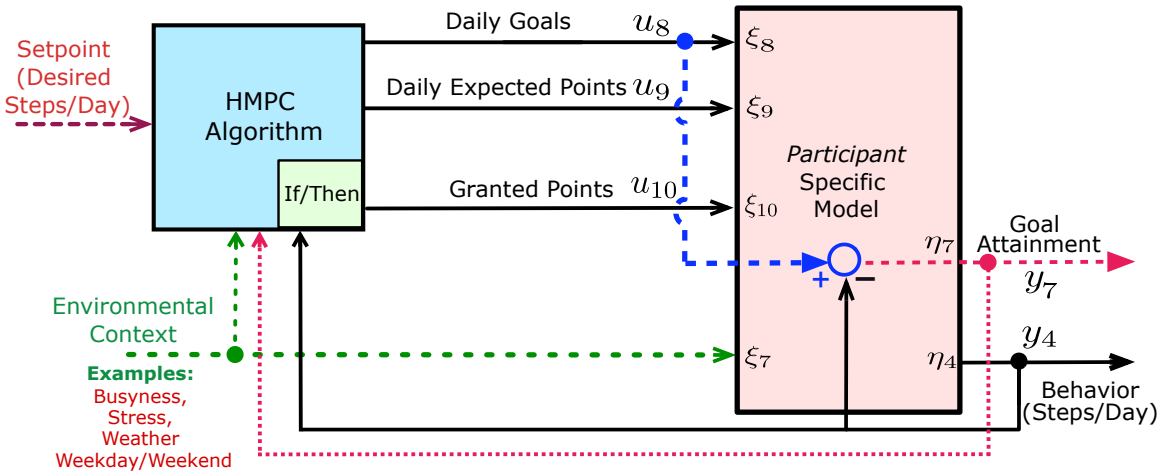

Figure 5.3: Schematic Depicting a Personalized PA Intervention Based on a Participant-Specific Model, as Used in *JustWalk* and *YourMove*.

$$y_7 = \xi_{11} = \eta_4 - \xi_8 \tag{5.6}$$

In Martín *et al.* (2016a), simulations are evaluated based on an enhanced SCT model with individualized self-regulation via internal cues, to mimic the process of the internalization of daily step goals (e.g., 10,000 steps) perceived as attainable by the individual. Self-regulatory mechanisms in human behavior can be modeled as a feedback process allowing for individuals to remain on track towards a defined goal, by the means of self-correcting and adjusting (Carver and Scheier, 1998). Internal model control (IMC; Morari and Zafiriou (1989)) is used to constitute an autoregulator through internalized cues to actions that depend on the transfer function between input ξ_4 and output η_4.

In this chapter, the use of *JustWalk* experimental data to estimate participant-specific models eliminates the need to define a self-regulator. Additionally, difficulties during *JustWalk* to obtain reliable measurements of the psychoactive constructs (*Self-Efficacy, Behavioral Outcomes*) motivate the use of the *Goal-Attainment* signal to infer whether intervention participants are reacting negatively to goals that are

extremely ambitious and unattainable. Insights provided in Chapter 4 form the basis for this work and are utilized to facilitate "ambitious yet achievable" goals (El Mistiri *et al.*, 2022b). The description of the *JustWalk* intervention and the use of system identification methods to obtain dynamic modeling are presented in the next section.

5.3 *JustWalk* Intervention

JustWalk was an SCT-based mHealth adaptive intervention application developed as a part of a study to promote PA for overweight sedentary adults. The main aim of the study was to understand dynamics associated with PA behavior change, through the estimation of individualized computational models utilizing system identification principles. To effectively measure PA levels (in terms of daily step count) a smartwatch activity tracker (Fitbit Zip, provided to participants as part of the study) was used as a part of the infrastructure to deliver the intervention. The tracker automatically synchronized with a front-end Android app, *JustWalk*. A back-end server was deployed to deliver daily goals and expected points and store the gathered data. Recruitment happened on a national level, for participants who fit the criteria of being generally healthy, inactive, 40 to 65 years of age, with a body mass index (BMI) of 25 to 45 kg/m^2, owned an Android phone compatible with Fitbit Zip and were willing to participate in the mHealth intervention for 14 weeks.

Participants in the walking intervention received daily step goals through the *JustWalk* app (presented in Fig. 5.4), and expected points which turned into daily granted points if the given goal was achieved that day. Upon accumulating the granted points past a certain threshold, participants were able to convert the points into Amazon gift cards. Throughout the study, participants were also nudged to complete a series of daily morning and evening ecological momentary assessment surveys (EMA; Shiffman *et al.* (2008)) to measure SCT constructs of interest (e.g., self-efficacy in the

Figure 5.4: The *JustWalk* App Interface.

achievement of the daily goal, quality of sleep, perceived busyness etc.).

The study lasted for 14 weeks, including a two-week baseline period, in which step goals were not provided to capture the participants' behavior prior to the introduction of intervention components. Individualized step goals were then given to participants based on their median daily step count calculated from the baseline period. This was done in an effort to incorporate a personalized "ambitious yet achievable" range of step goals in the input signal design. All the collected data was stored both locally and on the back-end server.

5.3.1 JustWalk Input Signal Design

Pseudo-random input signals were designed for the *JustWalk* intervention (Hekler, 2015), to generate data for system identification. A detailed account of the designed

multisine input signals for *Goals*, and *Expected Points* is covered in Martín *et al.* (2015b). A "zippered" approach (Rivera *et al.*, 2009) is followed to design input signals that are orthogonal in the frequency domain, therefore, they are uncorrelated. This allows for independently estimating transfer functions and uncertainty for the effect of each input on the outputs of interest. The multisine signals for the two manipulated inputs u_n were generated through (5.7), where $n = \{8, 9\}$.

$$u_n(k) = \lambda_n \sum_{j=1}^{N_s/2} \sqrt{2\alpha_{[n,j]}} \cos(\omega_j k T_s + \phi_{[n,j]}), \quad \omega_j = \frac{2\pi j}{N_s T_s}, \quad j = 1, \ldots, N_s \tag{5.7}$$

where λ_n is a factor for scaling the signal, N_s is the number of samples per period, T_s is the sampling time. For the j^{th} harmonic of the signal, each variable has the following meaning: $\alpha_{[n,j]}$ specifies the relative power of the harmonic, ω_j specifies the frequency, and $\phi_{[n,j]}$ is the phase. Factors $\alpha_{[n,j]}$ are chosen to assure orthogonality of the designed signals in the frequency domain; by assigning non-zero Fourier coefficient at a specific frequency in one signal, and a zero-valued Fourier coefficient at the same frequency for the other. This abides by the concept of the "zippered" input signal design (Rivera *et al.*, 2009), as can be seen in Fig. 5.5. For n_u input channels and n_s independently excited sinusoids, the Fourier coefficients are specified as

$$\alpha_{[n,j]} = \begin{cases} 1 & \text{if } j = n_u(i-1) + (n-7) \\ & \text{for } i = 1, 2, \ldots, n_s \\ 0 & \text{otherwise} \end{cases} \tag{5.8}$$

Following Nyquist-Shannon sampling theorem (Shannon, 1949), the bound for N_s is defined as:

$$N_s \geq 2 n_u n_s \tag{5.9}$$

For the selected $n_s = 3$ excited sinusoids in $n_u = 2$ input channels, (5.9) yields $N_s \geq 12$ days. $N_s = 16$ days was selected, which is a feasible duration for each cycle. The

intervention was designed to run for five cycles, resulting in designed input signals of 80 days overall. Minimal crest factor for the signal was obtained through the selection of phases $\phi_{[n,j]}$, following the approach illustrated in Guillaume *et al.* (1991).

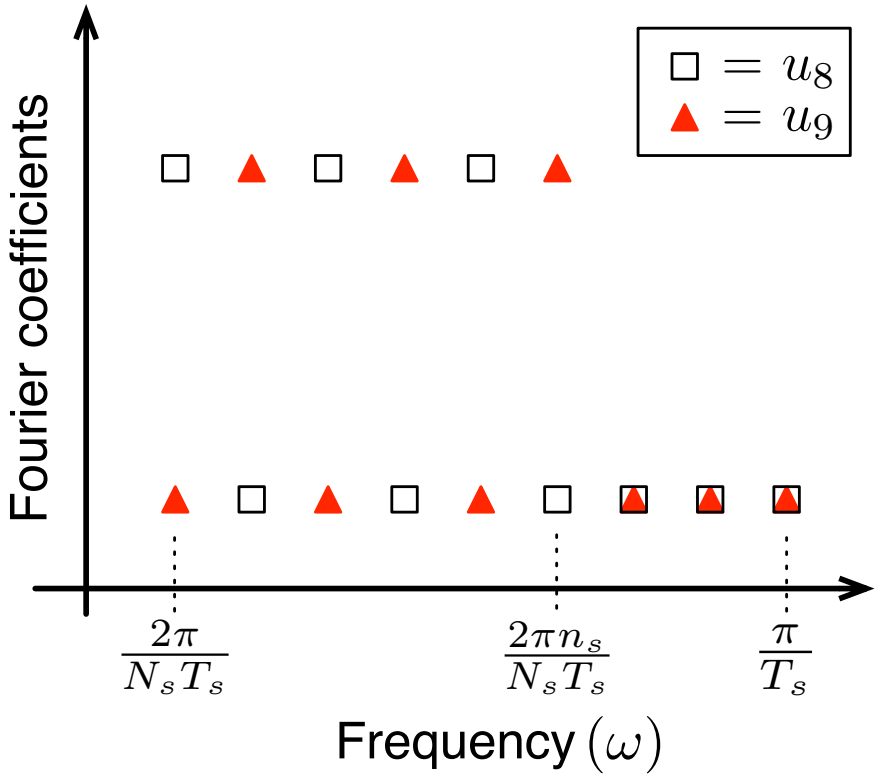

Figure 5.5: Representation of a "Zippered" Spectra Design for Number of Designed Inputs $n_u = 2$, and $n_s = 3$ Excited Harmonic Frequencies Per Input Channel.

The amplitudes of the designed input signals (u_8 and u_9 in Fig. 5.6) were chosen based on limited *a priori* knowledge available in literature (King *et al.*, 2013; Adams *et al.*, 2013). For the expected points, budgetary restrictions dictated the maximum number of possible points to grant on a given day; the signal was generated to be within the range of 0 to 500 points/day. The maximum step goal given to each participant was personalized based on the baseline performance in an attempt to give

ambitious, yet not overly ambitious goals. If the median baseline performance of the participant was below 3,000 steps/day, the factor utilized for the maximum step goals was 2.5 times the baseline median. On the other hand, if the median performance for the baseline period was above 7,500 steps/day, 1.75 was the factor utilized to avoid giving extremely ambitious goals (above 15,000 steps/day). For a participant with a median baseline performance between 3,000 and 7,500 steps/day, the used factor was 2. Other exogenous input signals were considered like perceived busyness, and average daily temperature, which were measured via EMA surveys and other means through the *JustWalk* app.

5.3.2 ARX Model Structure Estimation & Validation

In this section, model estimation strategies used on the *JustWalk* experimental data are described, and the obtained results of fitting Auto Regressive with eXogenic inputs (ARX; Ljung (1999)) dynamic models are presented. The use of black-box parametric modeling methods such as ARX plays a fundamental role in reaching the goal of identifying semi-physical (grey-box) personalized models that fit the SCT structure indicated in Section 5.2. Firstly, standard non-parametric estimation methods, like correlational analysis, were applied to provide insight into the correlation across the various combinations of input and output signals measured in the *JustWalk* study. While the effectiveness of the correlational analysis is hindered by the limited duration of the study, this initial step is still useful in terms of selecting the inputs and outputs to consider for the ARX model structure (Phatak *et al.*, 2018). Including all measured exogenous signals in the model estimation (specifically *Perceived Barriers* and *Perceived Busyness*) can be very computationally demanding and impose challenges. Such challenges include cross-correlation between such exogenous signals that can make model estimation difficult, and handling missing data points (due to

low compliance with the EMAs from participants). To address the aforementioned challenges, it is necessary to have access to extensive and informative datasets. However, acquiring such datasets in human subject research while minimizing participant burden can be challenging.

Least squares linear regression was performed, to minimize the model's predictive error based on the preprocessed data. Model structure can be abbreviated as ARX-$[n_a \quad n_{b_1},\ldots,n_{b_{n_\xi}} \quad n_{k_1},\ldots,n_{k_{n_\xi}}]$, where n_ξ is the number of considered inputs. A full expression of the ARX model is as follows:

$$y_k + \sum_{l=1}^{n_a} a_l y_{k-l} = \sum_{j=1}^{n_\xi} \sum_{i=0}^{n_{b_j}-1} b_{(i+1)(j)} \xi_{j,k-n_{k_j}-i} + e_k \tag{5.10}$$

where y_k is the output, $\xi_{j,k}$ is the measured input j, and e_k is the prediction error, all measured or estimated on day k. Moreover, regularization has been included in the least squares linear regression presented in (5.11), to assure the reduction of the impact of noise-induced variance (Pillonetto *et al.*, 2014; Ljung *et al.*, 2015)

$$\hat{\theta} = \arg\min_{\theta} \frac{1}{N} \sum_{k=1}^{N} (y_k - \hat{y}_{k|\theta})^2 + \lambda(\theta - \theta^*)^T R(\theta - \theta^*) \tag{5.11}$$

where θ represents model parameters, y_k and $\hat{y}_{k|\theta}$ are the measured and estimated output on day k, respectively. λ and R are regularization coefficients, and N represents the total duration of the data. Due to the limited duration of the input signal cycle, kernel regularization methods cannot be applied, and therefore, the regularization coefficients are manually chosen.

Data Preprocessing and Model Structure Selection

Accounting for missing data points through interpolation, shifting signals like *Behavior* and *Granted Points* by a sample to temporally align data, and mean subtraction are essential parts of data preprocessing. As the aim is to estimate idiographic models, the model orders for each input j (n_{b_j}) and the output (n_a) vary per participant.

To optimize the model orders, ARX order selection is evaluated. In this procedure, a range of orders for each input and output is specified, and then an exhaustive search over all the possible combinations ensues. Subsequently, the combination of orders that gives a stable ARX model with the lowest mean-square-error (MSE) over the validation data (reflecting on the model with the best predictive performance) is selected. This procedure can be computationally demanding, especially when considering a wide range of orders. The SCT fluid analogy model developed in Martín *et al.* (2020) and shown in Section 5.2, as well as the work done in Freigoun *et al.* (2017), imply that low-order models can adequately represent behavior change dynamics for PA interventions. Therefore, the order ranges chosen for the order selection are limited to $n_a, n_{b_j} \in \{1, 2, 3\}$ for all inputs and the output of interest. From inspecting the experimental data, the assumption of a basic unit input lag (i.e., $n_{k_j} = 1 \quad \forall j$) was determined to be reasonable. Moreover, because of the observed stationary nature of the data, noise characteristics over the course of the intervention are deduced to be stationary.

To determine the inputs to consider, extensive work has been done to evaluate all possible input combinations for each participant (Phatak *et al.*, 2018; Freigoun *et al.*, 2017). For the representative participant in Fig. 5.6, a 5-input model consisting of the signals in Table 5.1 is sufficient. It is important to note that *Goals* (u_8), and *Expected Points* (u_9) are statistically independent manipulated inputs, while *Granted Points* (u_{10}) depends on the fulfillment of the *Goals*. *Environmental Context: Temperature* (ξ_{7T}) presents an exogenous signal in the form of changes in the average daily temperature and *Environmental Context: Weekend* (ξ_{7wknd}) is a binary signal indicating if the day is a weekend day. Both signals correspond to measured disturbance variables.

Table 5.1: List of Measured Signals Included in the Estimated ARX Model and Their Correspondence with the Variables in the SCT Model According to Fig. 5.3. Goal-Attainment $\xi_{11} = y_7 = y_4 - u_8$ Can Be Considered as Both an Output and Input to the System and Can Be Estimated from the Available Signals.

Name	**Symbol**
Input Signals (inflows/outflows)	
Environmental Context (Temperature)	ξ_{7T}
Environmental Context (Weekend)	ξ_{7wknd}
Goals	u_8
Expected Points	u_9
Granted Points	u_{10}
Output Signals (inventory level)	
Behavior	$\eta_4 = y_4$

Estimation and Validation of Model Parameters

This subsection covers model estimation and the accompanying validation utilizing *Just Walk* experimental data and the 5-input ARX model structure presented above. Model validation is one of the most important aspects of system identification (Ljung, 1994), and it is constituted by a number of validation procedures. Cross-validation is one type of validation procedures in which the model fit percentage is evaluated over data that is not used in the estimation step. Traditionally in system identification, a certain percentage of the data is designated for estimation, and the remainder for validation. The underlying assumption behind this approach is that the noise characteristics of the system remain unchanged throughout the experiment. However,

in behavior interventions, it is expected that noise characteristics will change over time, due to seasonality (e.g., holidays, summer, etc) and life rhythms (e.g., work, vacation, school, intervention "fatigue" etc).

As mentioned in Section 5.3.1, the input signal consists of five repeated multi-sinusoids, where each cycle can be designated as a sub-experiment. The sub-experiments can then be partitioned into two groups of data (estimation and validation), with each combination containing two or three estimation sub-experiments, resulting in a total of 20 possible combinations to be evaluated. This approach is examined in this sub-section, where all possible combinations are evaluated for a representative *JustWalk* participant along with order selection. Normalized root mean square error (NRMSE) fit index (F) is used to compute a quantifiable measure of the goodness of the model

$$F = 100 \times \left(1 - \frac{||y_k - \hat{y}_k||_2}{||y_k - \bar{y}||_2}\right) \tag{5.12}$$

y_k is the measured output, $\hat{y}_k$ is the simulated output, $\bar{y}$ is the mean of all measured y_k values, and $||\cdot||_2$ indicates a vector l_2-norm.

NRMSE fits computed for each sub-experiment are averaged over the designated estimation and validation cycles to obtain a measure of the goodness of fit of the model on estimation (F_e) and validation (F_v) respectively. The overall fit percentage of the model (F_o) is calculated by applying (5.12) on the overall data, without partitioning it into sub-experiments. Subsequently, a weighted average F_{ave} of the obtained fit indices is utilized to select the best model.

$$F_{ave} = W_v F_v + W_o F_o \tag{5.13}$$

where W_v, W_o are the averaging weights for validation, and overall fit indices respectively. As the main focus of model estimation is to obtain the best predictive model for utilization as the internal model in a HMPC guided closed-loop intervention, the averaging weight for validation is selected to be the highest at $W_v = 0.6$.

Table 5.2: Table Summarizing ARX Orders Obtained for All the Possible Combinations of Estimation and Validation Cycles, with a Minimum of Two Estimation Cycles. For Each Combination, NRMSE Fit Percentage for Each Cycle is Shown and Highlighted with Magenta for Estimation, and Cyan for Validation, Along with the Average Overestimation and Validation Cycles (F_e and F_v), and the Overall Data Fit Percentage (F_o). The Selected Model is Based on the Maximum Weighted Average Fit Percentage (F_{ave}), Which is the Case for Row 13 (Highlighted in Yellow).

Row #	Est Cycles	Val Cycles	NRMSE Fit per Cycle (%)					Avg Est (%)	Avg Val (%)	Overall (%)	F_{avg} (%)	ARX Orders $[n_a, n_{b1}, n_{b2}, n_{b3}, n_{b4}, n_{b5}]$
			Cycle 1	Cycle 2	Cycle 3	Cycle 4	Cycle 5					
1	[1,2]	[3,4,5]	49.53%	44.99%	-10.43%	30.44%	-6.45%	47.26%	4.52%	19.76%	10.62%	[2,2,3,3,1,1]
2	[1,3]	[2,4,5]	42.69%	12.35%	33.44%	29.12%	-32.16%	38.07%	3.10%	19.06%	9.49%	[1,2,1,3,1,2]
3	[1,4]	[2,3,5]	47.62%	36.10%	4.18%	42.93%	3.98%	45.27%	14.76%	25.71%	19.14%	[1,1,3,3,1,1]
4	[1,5]	[2,3,4]	38.58%	39.24%	2.05%	35.48%	27.62%	33.10%	25.59%	25.61%	25.60%	[2,2,3,3,1,1]
5	[2,3]	[1,4,5]	44.99%	41.88%	19.78%	39.41%	10.67%	30.83%	31.69%	28.56%	30.44%	[1,1,3,3,1,1]
6	[2,4]	[1,3,5]	33.07%	45.04%	-3.62%	51.19%	12.74%	48.12%	14.06%	23.68%	17.91%	[1,1,1,3,3,1]
7	[2,5]	[1,3,4]	29.73%	44.69%	-3.04%	7.35%	27.78%	36.24%	11.35%	20.22%	14.90%	[1,3,1,3,3,1]
8	[3,4]	[1,2,5]	40.00%	23.30%	28.99%	42.21%	10.18%	35.60%	24.49%	25.53%	24.91%	[2,2,3,3,1,1]
9	[3,5]	[1,2,4]	25.78%	23.21%	19.89%	30.88%	29.81%	24.85%	26.62%	19.82%	23.90%	[2,1,3,3,1,1]
10	[4,5]	[1,2,3]	24.61%	35.74%	-2.74%	46.16%	34.56%	40.36%	19.20%	22.80%	20.64%	[3,1,3,3,3,1]
11	[3,4,5]	[1,2]	32.18%	28.44%	22.23%	40.56%	29.17%	30.65%	30.31%	25.43%	28.36%	[2,2,3,3,1,1]
12	[2,4,5]	[1,3]	28.23%	41.44%	-2.05%	48.87%	29.95%	40.09%	13.09%	23.86%	17.40%	[1,1,3,1,1,3]
13	[2,3,5]	[1,4]	36.34%	39.17%	10.58%	40.90%	29.57%	26.44%	38.62%	28.07%	34.40%	[1,1,3,3,1,1]
14	[2,3,4]	[1,5]	34.08%	40.50%	34.63%	51.66%	-0.45%	42.26%	16.81%	29.58%	21.92%	[3,3,2,3,1,2]
15	[1,4,5]	[2,3]	38.12%	41.55%	6.07%	42.48%	26.58%	35.73%	23.81%	26.95%	25.07%	[2,2,3,3,2,1]
16	[1,3,5]	[2,4]	40.86%	30.57%	21.81%	42.80%	11.18%	24.61%	36.69%	28.79%	33.53%	[1,1,1,3,1,2]
17	[1,3,4]	[2,5]	42.53%	10.25%	36.11%	39.37%	-5.79%	39.34%	2.23%	18.64%	8.79%	[3,2,3,3,1,1]
18	[1,2,5]	[3,4]	39.73%	44.45%	-2.68%	38.40%	26.25%	36.81%	17.86%	25.52%	20.92%	[2,2,3,3,1,1]
19	[1,2,4]	[3,5]	45.54%	49.87%	16.88%	40.64%	2.19%	45.35%	9.54%	27.59%	16.76%	[3,1,3,3,2,1]
20	[1,2,3]	[4,5]	50.07%	40.99%	16.96%	35.38%	-1.17%	36.01%	17.10%	28.19%	21.54%	[1,2,3,3,1,1]

Table 5.2 presents a summary of results obtained from this system identification approach with the 5-input ARX model for this representative participant. The best model is selected based on the weighted average fit percentage (the results for which are presented in row 13 -highlighted in yellow- in Table 5.2) which provides the selected model an edge in terms of prediction ability. On the other hand, if the best model was selected based on the overall fit only, the model summarized in row 14 would have been chosen, which lacks significantly in the validation fit. This is illustrated vividly by the NRSME fit percentage for the 5th cycle, where it is negative for the model in the 14th row (meaning it performs worse than the average of the data in that cycle).

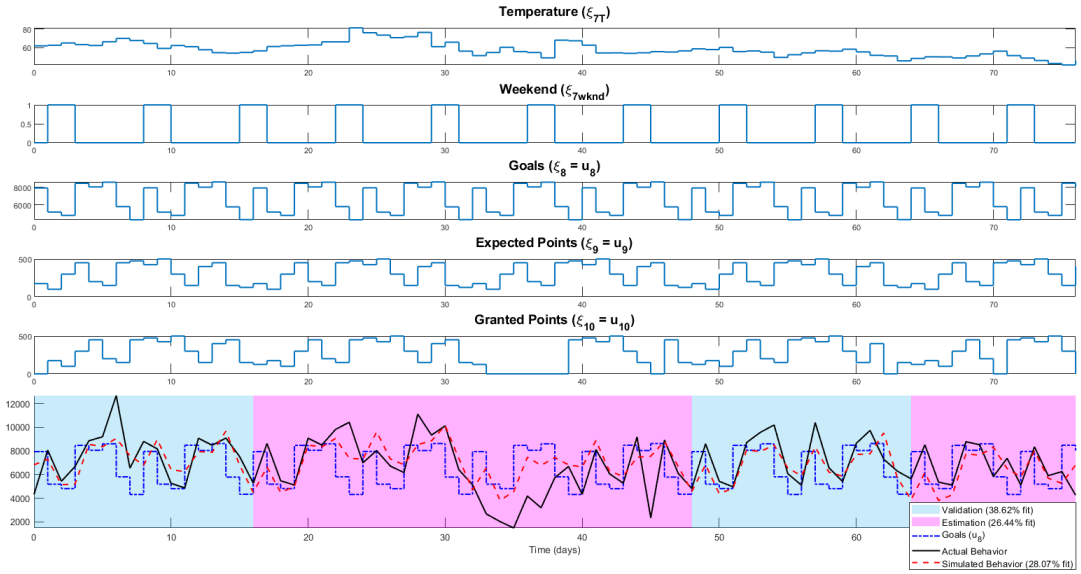

Figure 5.6: Time Series Plot Representing the Results of the Estimated ARX Model for This Representative Participant. Five Input Sequences Corresponding to Measured Disturbances (*Temperature* and *Weekend*) and Manipulated Variables (*Goals*, *Expected Points* and *Granted Points*) Are Shown from the Top. The Bottom Plot Includes Simulated *Behavior* (Estimated from an ARX Model with Regularization), Actual *Behavior* and Daily *Goals* (All in steps/day). Estimation and Validation Data Regions Are Highlighted in Magenta and Cyan, Respectively. The Overall NRMSE Fit Percentage is 28.07% (with 26.44% Fit for Estimation Regions and 38.62% Fit for Validation Regions). The ARX Model is Estimated Through Regularized Least-Squares Regression, Based on the Model Order Obtained Through Order Selection $n_a = 1$, $n_b = [1\ 3\ 3\ 1\ 1]$, $n_k = [1\ 1\ 1\ 1\ 1]$. Regularization Parameters $\lambda = 10^2$ and $R = 1$.

Fig. 5.6 illustrates the difference between actual output measurements and the prediction from a 5-input ARX model with the structure in (5.10). As shown in the figure with the magenta highlighted regions of the plot, the cycles selected to estimate

the model are the 2nd, 3rd, and 5th cycles, while cycles 1 and 4 are validation cycles. order selection yielded: $n_a = 1$, $n_b = [1\ 3\ 3\ 1\ 1]$, with fixed values for the delays at $n_k = [1\ 1\ 1\ 1\ 1]$, while the selected regularization parameters are $\lambda = 10^2$ and $R = 1$. The estimated model reflects, in addition to a good fit to validation data, a good fit for the entire data set (consisting of both estimation and validation data). The estimated regularized ARX model of the 5-input system yields an overall NRMSE index at 28.07% (an average of 38.62% fit over the validation sub-experiments and 26.44% for estimation sub-experiments). By integrating the overall fit criterion with the fit to cross-validation data, a balance is achieved between accurate prediction and model precision across the entire data set.

Assessment of Participant Characteristics

The estimated ARX model provides the basis for simulation as the plant and the controller model. It is essential that the estimated model not only provides a good fit to the data, yet it should be control-oriented and provide important insight regarding the most impactful signals for a specific participant to personalize the intervention. Step responses from the idiographic ARX models represent another validation procedure that can be used to confirm or rebuke hypotheses and reveal precise participant-specific information about the response dynamics including directionality, magnitude, and speed of response.

For instance, from Fig. 5.7, one can predict that this representative *JustWalk* will typically reach approximately 85% of the desired daily step goals within the first day of goal announcement. *Expected Points* input has the most significant impact on the number of steps walked out of the manipulated variables, while *Goals* have the lowest gain magnitude (which balances out as *Goals* are on average an order of magnitude higher than *Expected* and *Granted Points*). The direction of the gains

in the obtained step responses agree with behavioral scientists' expectations, which increases the confidence in the estimated model.

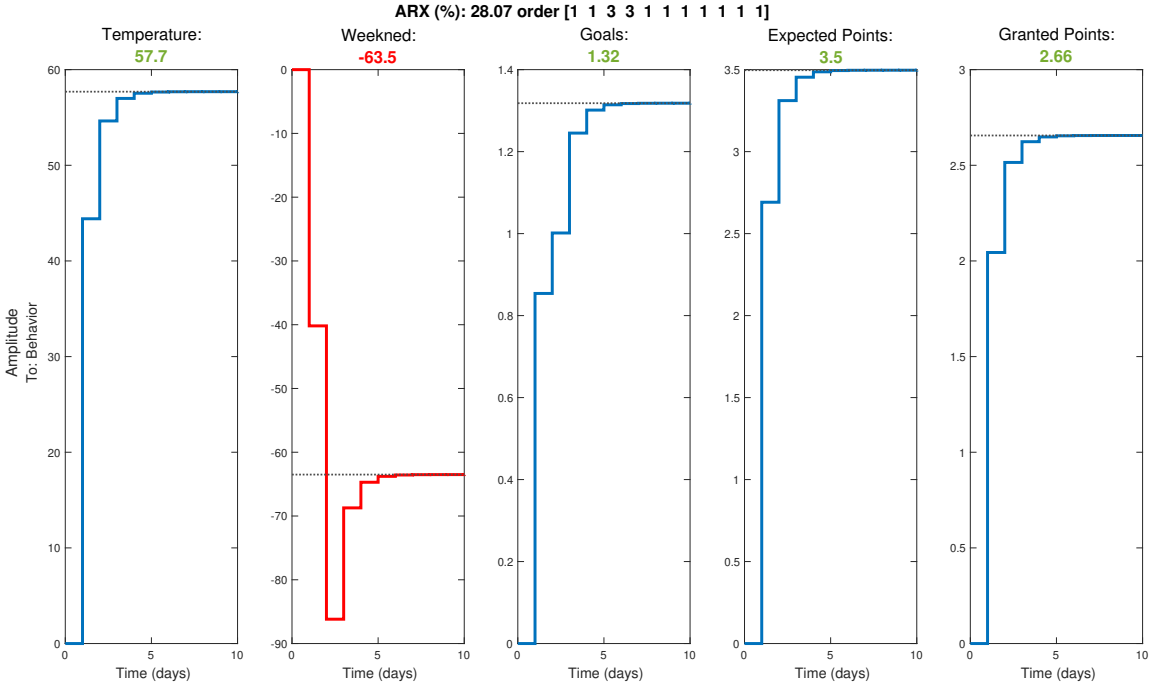

Figure 5.7: Step Responses of the 5-Input Model Estimated for a Representative *JustWalk* Participant. Steady-State Gains for Each Input Are Highlighted At the Top of Each Step Response. The Unit Step Responses Are Arranged Left to Right as *Temperature*, *Weekend*, *Goals*, *Expected Points*, and *Granted Points* with Steady-State Gains of 57.70, -63.50, 1.32, 3.5, and 2.66 Respectively.

5.4 HMPC formulation for adaptive PA intervention

The aim of the adaptive intervention is to guide people towards achieving and maintaining a desired level of 10,000 daily steps, while abiding by some important physical and operational restrictions, such as:

- Upper and lower constraints for goals and points (u_8, u_9, and u_{10}) are determined based on personalized conditions for each participant and budgetary restrictions.

- The ability to reconfigure the intervention online to enforce different phases. During different phases, some of the intervention components can be partially activated or deactivated. For example, in the maintenance phase of the intervention, which is reached by achieving and maintaining the desired behavior target for a period of time, the positive reinforcement component of the intervention through financial rewards (in the form of points) can be gradually reduced and taken offline.

A detailed description of the HMPC formulation along with the decision policy for the intervention is provided in the following subsections.

5.4.1 3DoF-KF HMPC Framework

The control strategy for the PA behavioral intervention must satisfy all the requirements, constraints, and intricacies associated with the intervention as part of the objective function formulation over the prediction and move horizons. Hence, a hybrid model predictive control (HMPC) strategy (Nandola and Rivera, 2013; Khan *et al.*, 2022) is examined and applied to this problem (depicted in Fig. 5.8), as it accounts for hybrid dynamics via mixed logical dynamic (MLD) representation; this allows for incorporating the natural constraints and logical arguments associated with the problem as part of the prediction model and objective function. In hybrid dynamical systems, both discrete and continuous events can occur simultaneously and can be modeled by a combination of differential (or difference) equations and logical conditions. This enables obtaining dynamic responses to continuous, categorical, or binary changes. The controller is designed with the ability to handle the following tasks, and tune the response to each independently:

- **Setpoint Tracking:** *Goals* and *Expected Points* are assigned to guide the

participant toward reaching the overall target of 10,000 daily steps.

- **Measured Disturbance Rejection:** The controller effectively adjusts the *Goals* and *Expected Points* to mitigate the effect of measured external disturbances. (e.g., *Environmental Context*).

- **Unmeasured Disturbance Rejection:** Moves in the manipulated variables are optimized to counter the effect of unknown (hence, unmodeled) external influences (e.g., illness, social life events, etc).

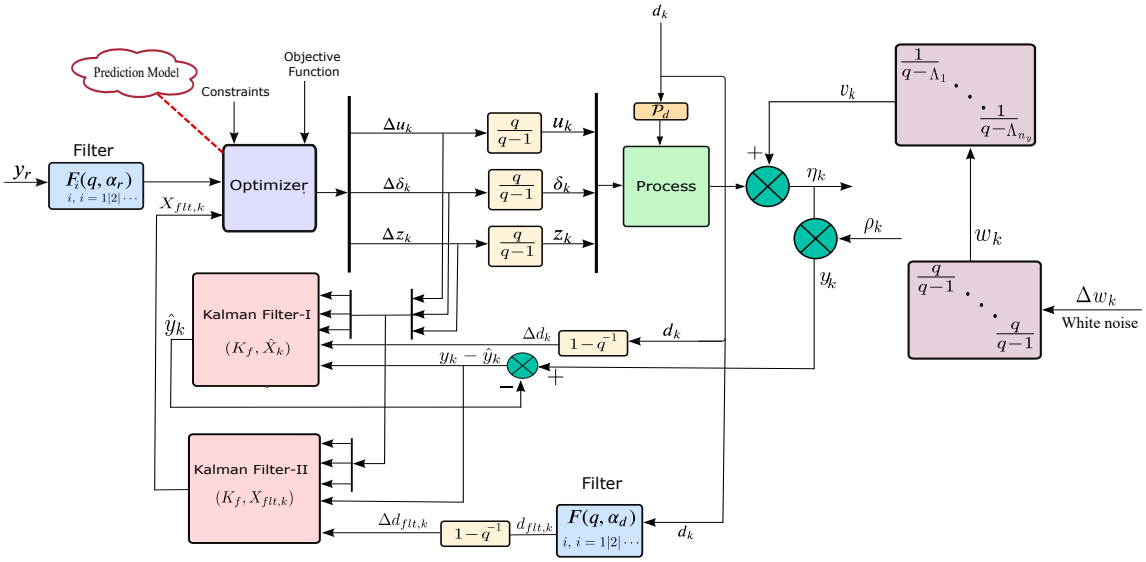

Figure 5.8: Block Diagram Schematic Depicting the Proposed Three-Degrees-Of-Freedom By Means of Kalman Filtering HMPC Structure, Aiming to Achieve Setpoint Tracking While Effectively Accounting for Both Measured and Unmeasured Disturbances. The Controller Utilizes External Filters to Adjust the Speed of Response for Measured Disturbances Rejection and Setpoint Tracking. Additionally, Nested Kalman Filters Are Utilized to Tune for Unmeasured Disturbances Separately (Khan *et al.*, 2022).

In model predictive control a receding horizon algorithm is followed, in which values of the manipulated variables over a given move horizon are determined online by solving an optimization problem. To solve the optimization problem and obtain the control movements over the move horizon a predictive model of the system is utilized. The same model is then used to compute system outputs over a prediction horizon with the current plant state estimate (i.e., output measurements) serving as the initial state for prediction. At each sampling instant, only the first move in the manipulated variables is applied, and then the whole process is repeated over the shifted move and prediction horizons.

The HMPC controller in this work utilizes the state-space structure seen below:

$$x_{k+1} = Ax_k + B_1u_k + B_2\delta_k + B_3z_k + B_dd_k \tag{5.14}$$

$$y_k = Cx_k + d'_k + v_k \tag{5.15}$$

$$E_5 \geq E_2\delta_k - E_4y_k - E_1u_k + E_3z_k + E_dd_k - E_6u_{k-1} - E_7y_{k-1} \tag{5.16}$$

where $x = [x_c^T \quad x_d^T]^T, x_c \in \mathbb{R}^{n_x^c}, x_d \in \{0,1\}^{n_x^d}$, and $u = [u_c^T \quad u_d^T]^T, u_c \in \mathbb{R}^{n_u^c}, u_d \in \{0,1\}^{n_u^d}$ are system states and inputs with continuous and discrete elements; $y \in \mathbb{R}^{n_y}$ is the output vector; d, d', and v are measured disturbances, unmeasured disturbances, and measurement noise, respectively. $\delta \in \{0,1\}^{n_\delta}$ and $z \in \mathbb{R}^{n_z}$ are binary and discrete auxiliary variables that serve the purpose of converting discrete and logical decisions into their equivalent linear inequality constraints represented in (5.16). $n_x = n_x^c + n_x^d$, $n_u = n_u^c + n_u^d$, n_{dist}, and n_y are the total number of states, inputs, measured disturbances and outputs, respectively. The impact of unmeasured disturbances is considered on the outputs only. Assuming that the system of interest is open-loop stable, the unmeasured disturbances (d') are considered as a stochastic signal described by the following model:

$$\zeta_{k+1} = A_w\zeta_k + B_ww_k \tag{5.17}$$

$$d'_k = C_w \zeta_k \tag{5.18}$$

where the eigenvalues of A_w are all inside the unit circle, and w_k is an integrated white noise. Assuming that the unmeasured disturbance signal consists of uncorrelated components, therefore, $B_w = C_w = I$ and $A_w = \text{diag}\{\Lambda_1, \cdots, \Lambda_{n_y}\}$, where $\Lambda_i = 0, \forall i$ for single-integrating disturbances (i.e., Type I) and $\Lambda_i = 1, \forall i$ for double-integrating disturbances (i.e., Type II). The model for the unmeasured disturbances is then augmented into the state-space model system as follows:

$$X_{k+1} = \mathcal{A}X_k + \mathcal{B}_1 \Delta u_k + \mathcal{B}_2 \Delta \delta_k + \mathcal{B}_3 \Delta z_k + \mathcal{B}_d \Delta d_k + \mathcal{B}_w \Delta w_k \tag{5.19}$$

$$y_k = \mathcal{C}X_k + v_k \tag{5.20}$$

where,

$$X_k = [\Delta x_k^T \quad \Delta \zeta_k^T \quad \eta_k^T]^T, \quad \mathcal{A} = \begin{bmatrix} A & B_v C_w & 0 \\ 0 & A_w & 0 \\ CA & CB_v C_w + D_v C_w A_w & I \end{bmatrix}$$

$$\mathcal{B}_i = \begin{bmatrix} B_i \\ 0 \\ CB_i \end{bmatrix}, \mathcal{B}_w = \begin{bmatrix} 0 \\ B_w \\ D_v C_w B_w \end{bmatrix}, \quad \mathcal{C} = \begin{bmatrix} 0 & 0 & I \end{bmatrix}, \; i = 1, 2, 3, d$$

For the objective function, a standard quadratic cost function is used to compute the moves in the manipulated variables through the optimization problem as

$$\begin{aligned} J \triangleq & \sum_{i=1}^{p} \|y_{k+i} - y_r\|^2_{W_y} + \sum_{i=0}^{m-1} \|\Delta u_{k+i}\|^2_{W_{\Delta u}} + \sum_{i=0}^{m-1} \|u_{k+i} - u_r\|^2_{W_u} \\ & + \sum_{i=0}^{p-1} \|\delta_{k+i} - \delta_r\|^2_{W_\delta} + \sum_{i=0}^{p-1} \|z_{k+i} - z_r\|^2_{W_z} \end{aligned} \tag{5.21}$$

where m and p are the move and prediction horizons, respectively. The matrices W_y, and $W_{\Delta u}$ are the penalty weights on the error, and move size, while W_u, W_δ, and

W_z are the penalty weights on manipulated variables, auxiliary binary variables, and auxiliary discrete variables targets respectively. The problem is formulated as a tracking control system where y_r, u_r, δ_r, and z_r are the references for the outputs, inputs, binary and discrete auxiliary variables, respectively. The solution of the optimization problem is obtained by finding the sequences of control actions that minimize J as

$$\min_{\substack{[\delta_{k+i}]_{i=0}^{p-1},[z_{k+i}]_{i=0}^{p-1} \\ [u_{k+i}]_{i=0}^{m-1},[\psi_{k+i}]_{i=1}^{p},}} J + \sum_{i=1}^{p} \|\psi_{k+i}\|_{W_s}^2 \tag{5.22}$$

subject to the logical constraints described in (5.16) and the following input/output constraints:

$$\begin{aligned} y_{min} - \psi_{k+i} \leq y_{k+i} \leq y_{max} + \psi_{k+i}, 1 \leq i \leq p \\ u_{min} \leq u_{k+i} \leq u_{max}, \quad 0 \leq i \leq m-1 \\ \Delta u_{min} \leq \Delta u_{k+i} \leq \Delta u_{max}, \ 0 \leq i \leq m-1 \\ \psi_{k+i} \geq 0, \qquad 1 \leq i \leq p \end{aligned} \tag{5.23}$$

$\psi \in \mathbb{R}^{n_y}$ is a vector for slack variables, and W_s is the slack weights matrix. Output constraints are softened as their respective weights in W_s approach zero, and become "hard" constraints as their weights are close to infinity. The capability of the framework to allow for "soft" constraint enforcement is essential in assuring obtaining a feasible solution at each sampling instance, especially with the presence of unpredictable events that can significantly impact the outputs.

In this work, a three-degree-of-freedom (3DoF) tuning structure is incorporated into the HMPC formulation. This assures the ability to tune the speed of response for setpoint tracking, measured and unmeasured disturbance rejection independently by selecting the parameters α_r^j, α_d^l and $f_a^j \in [0\ 1]$, for $j = 1, \cdots, n_y$, and $l = 1, \cdots, n_{dist}$. A filter matrix $F(q, \alpha_r)$ for setpoint tracking is defined as

$$F(q, \alpha_r) = \text{diag}\{f(q, \alpha_r^1), \cdots, f(q, \alpha_r^{n_y})\} \tag{5.24}$$

where each element can be implemented as a Type I or Type II discrete-time filter. In this work, only step changes are considered for setpoints. Hence, Type I filter is used for all elements:

$$f(q, \alpha_r^j) = \frac{(1-\alpha_r^j)q}{q-\alpha_r^j}, \quad j = 1, \cdots, n_y \tag{5.25}$$

For the measured disturbances rejection, measured and forecasted disturbances are independently processed through the filter matrix $F(q, \alpha_d)$. Based on the observed dynamics of the system and the lack of double-integrated disturbances, Type I filters are deemed sufficient:

$$F(q, \alpha_d) = \text{diag}\{f(q, \alpha_d^1), \cdots, f(q, \alpha_d^{n_{dist}})\} \tag{5.26}$$

$$f(q, \alpha_d^l) = \frac{(1-\alpha_d^l)q}{q-\alpha_d^l}, \quad l = 1, \cdots, n_{dist} \tag{5.27}$$

This structure of the separate filters for setpoint tracking and measured disturbance rejection constitutes two degrees of freedom. In both setpoint tracking and measured disturbance rejection, the speed of response can be adjusted for each output j and each measured disturbance l independently, by adjusting their respective filter time-constant α_r^j and α_d^l; a lower value for the filter time-constant results in a quicker response, while a time-constant closer to one corresponds to a slower response.

For the third degree of freedom, a Kalman filter is utilized to compute future states based on the system's model and current feedback measurements y_k. To decouple the dynamics of measured and unmeasured disturbances, the Kalman filter is utilized in two stages as presented in Nandola and Rivera (2013), and Khan *et al.* (2022). In the first stage, the actual states X_k are estimated as $\hat{X}_k$ by considering both measured disturbances d_k and unmeasured disturbances, as described in (5.28) and (5.29).

$$\hat{X}_{k|k-1} = \mathcal{A}\hat{X}_{k-1|k-1} + \mathcal{B}_1\Delta u_{k-1} + \mathcal{B}_2\Delta\delta_{k-1} + \mathcal{B}_3\Delta z_{k-1} + \mathcal{B}_d\Delta d_{k-1} \tag{5.28}$$

$$\hat{X}_{k|k} = \hat{X}_{k|k-1} + K_f(y_k - \mathcal{C}\hat{X}_{k|k-1}) \tag{5.29}$$

where $\hat{X}_{k|k-1}$ is the estimated value of $\hat{X}$ at sampling instant k based on $k-1$, and $\hat{X}_{k|k}$ is the corrected value at instant k given the feedback measurement y_k. As the measured disturbances signal d_k is included in (5.28), the correction term in equation (5.29) accounts for the impact of unmeasured disturbances. The gain matrix K_f directly impacts the correction term, and therefore, the speed of response in the unmeasured disturbance. Finally, the estimated filtered states X_{filt} utilized in the objective function for the controller incorporate the impact of both filtered measured disturbances $d_{filt,k}$ and unmeasured disturbances. This is done by utilizing the prediction error resulting from equations (5.28)-(5.29).

$$X_{filt,k|k-1} = \mathcal{A}X_{filt,k-1|k-1} + \mathcal{B}_1\Delta u_{k-1} + \mathcal{B}_2\Delta\delta_{k-1} + \mathcal{B}_3\Delta z_{k-1} + \mathcal{B}_d\Delta d_{filt,k-1} \quad (5.30)$$

$$X_{filt,k|k} = X_{filt,k|k-1} + K_f(y_k - \mathcal{C}\hat{X}_{k|k-1}) \quad (5.31)$$

where $X_{filt,k|k-1}$ is the estimated value of X_{filt} at sampling instant k based on $k-1$, and $X_{filt,k|k}$ is the corrected value at instant k given the feedback measurement y_k. The terms in equation (5.31), excluding the final term, capture the effect of the filtered measured disturbances. Whereas, the correction term in equation (5.29) accounts for the impact of the unmeasured disturbances. This ensures that the designated tuning for measured disturbance rejection, represented by α_d^j, is decoupled from unmeasured disturbance rejection. In the same manner, the effect of unmeasured disturbances on each output is tuned separately through the gain matrix K_f.

$$K_f = [0 \quad F_b^T \quad F_a^T]^T \quad (5.32)$$

where,

$$F_a = \text{diag}\left\{ f_a^1, \quad \cdots, \quad f_a^{n_y} \right\}$$

$$F_b = \text{diag}\left\{ f_b^1, \quad \cdots, \quad f_b^{n_y} \right\}$$

$$f_b^j = \frac{\left(f_a^j\right)^2}{1 + \Lambda_j - \Lambda_j f_a^j},\ 1 \leq j \leq n_y \tag{5.33}$$

and

$$f_a^j \to 0 \quad \text{as} \quad \omega_j/\sigma_j \to 0 \tag{5.34}$$

$$f_a^j \to 1 \quad \text{as} \quad \omega_j/\sigma_j \to \infty \tag{5.35}$$

This parameterization of K_f does not require solving the Riccati equation to obtain an optimal value for the filter gains, hence, estimating covariance matrices for unmeasured disturbances is not needed. Furthermore, the work done in Lee *et al.* (1994) and Lee and Yu (1994) shows direct links to robustness. Moreover, through this parameterization, the impact of unmeasured disturbance on each output j can be tuned separately by adjusting the parameter f_a^j, where F_a corresponds to the outputs, and F_b corresponds to the augmented estimated unmeasured disturbance states, as described in (5.19). For the coefficients of the unmeasured disturbance filter f_a^j, a smaller value indicates a slower response. On the other hand, as the value is closer to 1 a faster response is expected. The gain matrix K_f is also important in terms of handling plant-model mismatch through the control system feedback.

By applying 3DoF filtering and propagating the filtered states and signals over the prediction horizon p, two separate output prediction signals are obtained as expressed in equations (5.36) and (5.37).

$$\begin{aligned}\mathcal{Y}_{filt,k+1} = {} & \Phi X_{filt,k} + \mathcal{H}_1 \mathcal{U}_k + \mathcal{H}_2 \bar{\delta}_k + \mathcal{H}_3 \mathcal{Z}_k + \mathcal{H}_d \mathcal{D}_{filt,k} - \mathcal{H}_{11} u_{k-1} - \mathcal{H}_{21} \delta_{k-1} \\ & - \mathcal{H}_{31} z_{k-1} - \mathcal{H}_{d1} d_{filt,k-1}\end{aligned} \tag{5.36}$$

$$\begin{aligned}\mathcal{Y}_{k+1} = {} & \Phi \hat{X}_k + \mathcal{H}_1 \mathcal{U}_k + \mathcal{H}_2 \bar{\delta}_k + \mathcal{H}_3 \mathcal{Z}_k + \mathcal{H}_d \mathcal{D}_k - \mathcal{H}_{11} u_{k-1} - \mathcal{H}_{21} \delta_{k-1} \\ & - \mathcal{H}_{31} z_{k-1} - \mathcal{H}_{d1} d_{k-1}\end{aligned} \tag{5.37}$$

$\mathcal{Y}_{filt,k+1}$ is the output prediction vector accounting for the effects of the filtered measured disturbance d_{filt} and is used to formulate the objective function. Whereas,

$\mathcal{Y}_{k+1}$ is used in enforcing equality and inequality constraints as it accounts for the unfiltered measured disturbance d through the estimated state $\hat{X}_k$, where

$$\mathcal{Y}_{k+1} = \begin{bmatrix} y_{k+1} \\ y_{k+2} \\ \vdots \\ y_{k+p} \end{bmatrix}, \quad \mathcal{U}_k = \begin{bmatrix} u_k \\ u_{k+1} \\ \vdots \\ u_{k+m-1} \end{bmatrix}, \quad \bar{\delta}_k = \begin{bmatrix} \delta_k \\ \delta_{k+1} \\ \vdots \\ \delta_{k+p-1} \end{bmatrix}, \quad \mathcal{Z}_k = \begin{bmatrix} z_k \\ z_{k+1} \\ \vdots \\ z_{k+p-1} \end{bmatrix}$$

$$\mathcal{D}_{filt,k} = \begin{bmatrix} d_{filt,k} \\ d_{filt,k+1} \\ \vdots \\ d_{filt,k+p-1} \end{bmatrix}, \quad \mathcal{Y}_{filt,k+1} = \begin{bmatrix} y_{filt,k+1} \\ y_{filt,k+2} \\ \vdots \\ y_{filtk+p} \end{bmatrix}, \quad \mathcal{D}_k = \begin{bmatrix} d_k \\ d_{k+1} \\ \vdots \\ d_{k+p-1} \end{bmatrix}$$

$$\mathcal{H}_i = \begin{bmatrix} \mathcal{C}\mathcal{B}_i & 0 & \cdots & 0 & 0 \\ \mathcal{C}\mathcal{A}\mathcal{B}_i - \mathcal{C}\mathcal{B}_i & \mathcal{C}\mathcal{B}_i & \cdots & 0 & 0 \\ \mathcal{C}\mathcal{A}^2\mathcal{B}_i - \mathcal{C}\mathcal{A}\mathcal{B}_i & \mathcal{C}\mathcal{A}\mathcal{B}_i - \mathcal{C}\mathcal{B}_i & \cdots & \vdots & \vdots \\ \vdots & \vdots & \ddots & \vdots & \vdots \\ \mathcal{C}\mathcal{A}^{p-1}\mathcal{B}_i - \mathcal{C}\mathcal{A}^{p-2}\mathcal{B}_i & \mathcal{C}\mathcal{A}^{p-2}\mathcal{B}_i - \mathcal{C}\mathcal{A}^{p-3}\mathcal{B}_i & \cdots & \mathcal{C}\mathcal{A}\mathcal{B}_i - \mathcal{C}\mathcal{B}_i & \mathcal{C}\mathcal{B}_i \end{bmatrix}$$

$$\Phi = \begin{bmatrix} \mathcal{C}\mathcal{A} \\ \vdots \\ \mathcal{C}\mathcal{A}^p \end{bmatrix}, \quad H_{i1} = \begin{bmatrix} \mathcal{C}\mathcal{B}_i \\ \mathcal{C}\mathcal{A}\mathcal{B}_i \\ \vdots \\ \mathcal{C}\mathcal{A}^{p-1}\mathcal{B}_i \end{bmatrix}, \quad i = 2,\ 3,\ d$$

$$\mathcal{H}_1 = \begin{bmatrix} \mathcal{C}\mathcal{B}_1 & 0 & \cdots & 0 & 0 \\ \mathcal{C}\mathcal{A}\mathcal{B}_1 - \mathcal{C}\mathcal{B}_1 & \mathcal{C}\mathcal{B}_1 & \cdots & 0 & 0 \\ \mathcal{C}\mathcal{A}^2\mathcal{B}_1 - \mathcal{C}\mathcal{A}\mathcal{B}_1 & \mathcal{C}\mathcal{A}\mathcal{B}_1 - \mathcal{C}\mathcal{B}_1 & \ddots & \vdots & \vdots \\ \vdots & \vdots & \ddots & \mathcal{C}\mathcal{B}_1 & \vdots \\ \mathcal{C}\mathcal{A}^{m-1}\mathcal{B}_1 - \mathcal{C}\mathcal{A}^{m-2}\mathcal{B}_1 & \mathcal{C}\mathcal{A}^{m-2}\mathcal{B}_1 - \mathcal{C}\mathcal{A}^{m-1}\mathcal{B}_1 & \cdots & \mathcal{C}\mathcal{A}\mathcal{B}_1 - \mathcal{C}\mathcal{B}_1 & \mathcal{C}\mathcal{B}_1 \\ \mathcal{C}\mathcal{A}^{m}\mathcal{B}_1 - \mathcal{C}\mathcal{A}^{m-1}\mathcal{B}_1 & \mathcal{C}\mathcal{A}^{m-1}\mathcal{B}_1 - \mathcal{C}\mathcal{A}^{m-2}\mathcal{B}_1 & \cdots & \mathcal{C}\mathcal{A}^2\mathcal{B}_1 - \mathcal{C}\mathcal{A}\mathcal{B}_1 & \mathcal{C}\mathcal{A}\mathcal{B}_1 \\ \vdots & \vdots & \vdots & \vdots & \vdots \\ \mathcal{C}\mathcal{A}^{p-1}\mathcal{B}_1 - \mathcal{C}\mathcal{A}^{p-2}\mathcal{B}_1 & \mathcal{C}\mathcal{A}^{p-2}\mathcal{B}_1 - \mathcal{C}\mathcal{A}^{p-1}\mathcal{B}_1 & \cdots & \mathcal{C}\mathcal{A}^{p-m+1}\mathcal{B}_1 - \mathcal{C}\mathcal{A}^{p-m}\mathcal{B}_1 & \mathcal{C}\mathcal{A}^{p-m}\mathcal{B}_1 \end{bmatrix}$$

The inequality constraints representing logical conditions expressed in (5.16) are propagated p steps ahead. For $1 \leq \ i \ \leq \ m$

$$E_5 \geq E_2\delta_{k+i-1} - E_4 y_{k+i-1} - E_1 u_{k+i-1} + E_3 z_{k+i-1} + E_d d_{k+i-1} - E_6 u_{k+i-2} - E_7 y_{k+i-2}$$

For $i = m + 1$

$$E_5 \geq E_2\delta_{k+m} - E_4 y_{k+m} - E_1 u_{k+m-1} + E_3 z_{k+m} + E_d d_{k+m} - E_6 u_{k+m-1} - E_7 y_{k+m-1}$$

For $m + 1 < i \leq p$

$$E_5 \geq E_2\delta_{k+i-1} - E_4 y_{k+i-1} - E_1 u_{k+m-1} + E_3 z_{k+i-1} + E_d d_{k+i-1} - E_6 u_{k+m-1} - E_7 y_{k+i-2}$$

As a result,

$$\bar{E}_5 \geq \bar{E}_2\bar{\delta}_k + \bar{E}_3\mathcal{Z}_k + \bar{E}_1\mathcal{U}_k + \bar{E}_4\mathcal{Y}_k + \bar{E}_d\mathcal{D}_k + \bar{E}_6 u_{k-1} + \bar{E}_7 y_{k-1} \tag{5.38}$$

where

$$\bar{E}_i = \text{diag}\{E_i, \cdots, E_i\},\ i = 2,\ 3,\ d, \quad \bar{E}_j = \begin{bmatrix} -E_j & 0 & \cdots & 0 \end{bmatrix}^T,\ j = 6, 7$$

$$\bar{E}_5 = \begin{bmatrix} E_5 \\ E_5 \\ \vdots \\ E_5 \end{bmatrix}, \quad \bar{E}_1 = \begin{bmatrix} -E_1 & 0 & \cdots & 0 \\ -E_6 & \ddots & \ddots & 0 \\ 0 & \ddots & \ddots & \vdots \\ 0 & \ddots & -E_6 & -E_1 \\ 0 & \ddots & 0 & -E_6 - E_1 \\ \vdots & \vdots & 0 & \vdots \\ 0 & \cdots & \cdots & -E_6 - E_1 \end{bmatrix}, \quad \bar{E}_4 = \begin{bmatrix} -E_4 & 0 & \cdots & 0 \\ -E_7 & -E_4 & \ddots & 0 \\ 0 & \ddots & \ddots & \vdots \\ \vdots & \ddots & -E_7 & -E_4 \end{bmatrix}$$

Equation (5.38) is simplified by substituting $\mathcal{Y}_k$ from (5.37), then it is rewritten as follows:

$$\begin{aligned} \mathcal{E}_5 \geq \mathcal{E}_2\bar{\delta}_k + \mathcal{E}_3\mathcal{Z}_k + \mathcal{E}_1\mathcal{U}_k + \mathcal{E}_d\mathcal{D}_k + \mathcal{E}_4\hat{X}_k - \mathcal{E}_{41}u_{k-1} - \mathcal{E}_{42}\delta_{k-1} - \mathcal{E}_{43}z_{k-1} \\ - \mathcal{E}_{4d}d_{k-1} + \mathcal{E}_6u_{k-1} + \mathcal{E}_7y_{k-1} \end{aligned} \tag{5.39}$$

where

$$\mathcal{E}_i = \left(\bar{E}_i + \bar{E}_4\bar{\mathcal{H}}_i\right), \quad \mathcal{E}_4 = \bar{E}_4\bar{\Phi}, \quad \mathcal{E}_j = \bar{E}_j, \quad j = 5,\ 6,\ 7, \quad \mathcal{E}_{4i} = \bar{E}_4\bar{\mathcal{H}}_{i1}, \quad i = 1,\ 2,\ 3,\ d$$

$$\bar{\Phi} = \begin{bmatrix} \mathcal{C} \\ \Phi(1:(p-1)n_y, :) \end{bmatrix}, \quad \bar{\mathcal{H}}_i = \begin{bmatrix} [0]_{n_y} \\ \mathcal{H}_i(1:(p-1)n_y, :) \end{bmatrix}, \quad i = 1, 2, 3, d, 11, 21, 31, d1$$

Here n_y is number of outputs, $[0]_{n_y}$ denotes matrix with n_y rows that has all the elements 0 and $*(1:(p-1)n_y, :)$ represents the rows from row 1 to row $(p-1)n_y$ of the matrix $*$ including all its columns.

The objective function in (5.22) can be written in vector format, utilizing $\mathcal{Y}_{filt,k+1}$ from (5.36).

$$\begin{aligned} \min_{\substack{\mathcal{U}_k,\, \bar{\delta}_k, \\ \mathcal{Z}_k,\, \Psi_{k+1}}} \quad J \triangleq & ||\mathcal{Y}_{filt,k+1} - \mathcal{Y}_{r,filt,k+1}||^2_{\widehat{W}_y} + ||\mathcal{U}_k - \mathcal{U}_r||^2_{\widehat{W}_u} + ||\bar{\delta}_k - \bar{\delta}_r||^2_{\widehat{W}_d} \\ & + ||\mathcal{Z}_k - \mathcal{Z}_r||^2_{\widehat{W}_z} + ||R_u\mathcal{U}_k - R_{u0}u_{k-1}||^2_{\widehat{W}_{du}} + ||\Psi_{k+1}||^2_{\widehat{W}_s} \end{aligned} \tag{5.40}$$

Subject to the logical constraints in (5.39) and:

$$\begin{gathered}\mathcal{Y}_{min} - \Psi_{k+1} \leq \mathcal{Y}_{k+1} \leq \mathcal{Y}_{max} + \Psi_{k+1} \\ \mathcal{U}_{min} \leq \mathcal{U}_k \leq \mathcal{U}_{max} \\ \Delta\mathcal{U}_{min} \leq \Delta\mathcal{U}_k \leq \Delta\mathcal{U}_{max} \\ \Psi_{k+1} \geq 0\end{gathered} \tag{5.41}$$

where $\widehat{W}_* = \text{diag}(W_*)$, and

$$R_u = \begin{bmatrix} \mathcal{I} & 0 & \cdots & 0 & 0 \\ -\mathcal{I} & \mathcal{I} & \cdots & 0 & 0 \\ 0 & -\mathcal{I} & \ddots & \vdots & \vdots \\ \vdots & \vdots & \ddots & \ddots & \vdots \\ 0 & 0 & \cdots & -\mathcal{I} & \mathcal{I} \end{bmatrix};\ R_{u0} = \begin{bmatrix} \mathcal{I} \\ 0 \\ \vdots \\ 0 \end{bmatrix},\quad \Psi_{k+1} = \begin{bmatrix} \psi_{k+1} \\ \psi_{k+2} \\ \cdots \\ \psi_{k+p} \end{bmatrix}$$

$\mathcal{Y}_{r,filt}$ is the filtered output reference vector, $\mathcal{U}_r$, $\bar{\delta}_r$, and $\mathcal{Z}_r$ are the reference vectors for the inputs, auxiliary binary variables and auxiliary continuous variables respectively, as shown below:

$$\mathcal{Y}_{r,filt,k+1} = \begin{bmatrix} y_{r,filt,k+1}^T & y_{r,filt,k+2}^T & \cdots & y_{r,filt,k+p}^T \end{bmatrix}^T \tag{5.42}$$

$$\mathcal{U}_r = \begin{bmatrix} u_{r,k}^T & u_{r,k+1}^T & \cdots & u_{r,k+m-1}^T \end{bmatrix}^T \tag{5.43}$$

$$\bar{\delta}_r = \begin{bmatrix} \delta_{r,k}^T & \delta_{r,k+1}^T & \cdots & \delta_{r,k+p-1}^T \end{bmatrix}^T \tag{5.44}$$

$$\mathcal{Z}_r = \begin{bmatrix} z_{r,k}^T & z_{r,k+1}^T & \cdots & z_{r,k+p-1}^T \end{bmatrix}^T \tag{5.45}$$

By substituting (5.36) and (5.37) into (5.40) and (5.41) respectively, then rearranging the equation to separate quadratic and linear terms to formulate the problem in a standard MIQP format:

$$\min_{\xi_k} J_k \triangleq \frac{1}{2}\xi_k^T \mathcal{H} \xi_k + \mathcal{G}^T \xi_k \tag{5.46}$$

$$\mathcal{S}\xi_k \leq b \tag{5.47}$$

where ξ_k represents the manipulated variables optimized over at each sampling instant k described by:

$$\xi_k = [\mathcal{U}_k^T \ \bar{\delta}_k^T \ \mathcal{Z}_k^T \ {\Psi_k}^T]^T$$

$\mathcal{H}$ represents the quadratic terms of the MIQP optimization problem. For the optimization problem to be solvable $\mathcal{H}$ must be symmetric and positive definite or semi-definite.

$$\mathcal{H} = 2\begin{bmatrix} {\mathcal{H}_1}^T\widehat{W}_y\mathcal{H}_1 + \widehat{W}_{\Delta u} + \widehat{W}_u & {\mathcal{H}_1}^T\widehat{W}_y\mathcal{H}_2 & {\mathcal{H}_1}^T\widehat{W}_y\mathcal{H}_3 & 0 \\ {\mathcal{H}_2}^T\widehat{W}_y\mathcal{H}_1 & {\mathcal{H}_2}^T\widehat{W}_y\mathcal{H}_2 + \widehat{W}_d & {\mathcal{H}_2}^T\widehat{W}_y\mathcal{H}_3 & 0 \\ {\mathcal{H}_3}^T\widehat{W}_y\mathcal{H}_1 & {\mathcal{H}_3}^T\widehat{W}_y\mathcal{H}_2 & {\mathcal{H}_3}^T\widehat{W}_y\mathcal{H}_3 + \widehat{W}_z & 0 \\ 0 & 0 & 0 & \widehat{W}_s \end{bmatrix} \tag{5.48}$$

Additionally, the linear terms of the optimization problem are combined in

$$\mathcal{G} = 2[g_1 \ \ g_2 \ \ g_3 \ \ 0]^T \tag{5.49}$$

where

$$\begin{aligned} g_1 = {} & {X_{filt,k}}^T\Phi^T\widehat{W}_y\mathcal{H}_1 - {\mathcal{Y}_{r,filt}}^T\widehat{W}_y\mathcal{H}_1 - {\mathcal{U}_r}^T\widehat{W}_u + {\mathcal{D}_{filt,k}}^T{\mathcal{H}_d}^T\widehat{W}_y\mathcal{H}_1 \\ & - {u_{k-1}}^T({R_{u0}}^T\widehat{W}_{\Delta u}R_u + {H_{11}}^T\widehat{W}_y\mathcal{H}_1) - {\delta_{k-1}}^T{H_{21}}^T\widehat{W}_y\mathcal{H}_1 \\ & - {z_{k-1}}^T{H_{31}}^T\widehat{W}_y\mathcal{H}_1 - {d_{filt,k-1}}^T{H_{d1}}^T\widehat{W}_y\mathcal{H}_1 \end{aligned} \tag{5.50}$$

$$\begin{aligned} g_2 = {} & {X_{filt,k}}^T\Phi^T\widehat{W}_y\mathcal{H}_2 - {\mathcal{Y}_{r,filt}}^T\widehat{W}_y\mathcal{H}_2 - \bar{\delta}_r^T\widehat{W}_d + {\mathcal{D}_{filt,k}}^T{\mathcal{H}_d}^T\widehat{W}_y\mathcal{H}_2 \\ & - {u_{k-1}}^T{H_{11}}^T\widehat{W}_y\mathcal{H}_2 - {\delta_{k-1}}^T{H_{21}}^T\widehat{W}_y\mathcal{H}_2 - {z_{k-1}}^T{H_{31}}^T\widehat{W}_y\mathcal{H}_2 \\ & - {d_{filt,k-1}}^T{H_{d1}}^T\widehat{W}_y\mathcal{H}_2 \end{aligned} \tag{5.51}$$

$$\begin{aligned} g_3 = {} & {X_{filt,k}}^T\Phi^T\widehat{W}_y\mathcal{H}_3 - {\mathcal{Y}_{r,filt}}^T\widehat{W}_y\mathcal{H}_3 - {\mathcal{Z}_r}^T\widehat{W}_z + {\mathcal{D}_{filt,k}}^T{\mathcal{H}_d}^T\widehat{W}_y\mathcal{H}_3 \\ & - {u_{k-1}}^T{H_{11}}^T\widehat{W}_y\mathcal{H}_3 - {\delta_{k-1}}^T{H_{21}}^T\widehat{W}_y\mathcal{H}_3 - {z_{k-1}}^T{H_{31}}^T\widehat{W}_y\mathcal{H}_3 \\ & - {d_{filt,k-1}}^T{H_{d1}}^T\widehat{W}_y\mathcal{H}_3 \end{aligned} \tag{5.52}$$

In (5.47), equality and inequality constraints representing logical and categorical constraints in (5.39) as well as input/output constraints in (5.41) are depicted in $\mathcal{S}$ and b as follows:

$$\mathcal{S} = \begin{bmatrix} s_1 \\ s_2 \\ s_3 \\ s_4 \\ -s_3 \\ s_5 \end{bmatrix};\ s_1 = \begin{bmatrix} \mathcal{E}_1 \\ \mathcal{E}_2 \\ \mathcal{E}_3 \\ 0 \end{bmatrix}^T,\ s_2 = \begin{bmatrix} \mathcal{H}_1 \\ \mathcal{H}_2 \\ \mathcal{H}_3 \\ -I_{p(n_y)} \end{bmatrix}^T,\ s_4 = \begin{bmatrix} -\mathcal{H}_1 \\ -\mathcal{H}_2 \\ -\mathcal{H}_3 \\ -I_{p(n_y)} \end{bmatrix}^T \tag{5.53}$$

$$s_3 = \begin{bmatrix} I_{m(n_u)} & [0]_{m(n_u)\times p(n_d)} & [0]_{m(n_u)\times p(n_z)} & [0]_{m(n_u)\times p(n_y)} \\ R_u & [0]_{m(n_u)\times p(n_d)} & [0]_{m(n_u)\times p(n_z)} & [0]_{m(nu)\times p(n_y)} \end{bmatrix},\ s_5 = [0\ \ 0\ \ 0\ \ -I_{p(n_y)}]$$

$$b = \begin{bmatrix} \mathcal{E}_5 - \mathcal{E}_4\hat{X}_k - \mathcal{E}_d\mathcal{D}_k + \mathcal{E}_{41}u_{k-1} + \mathcal{E}_{42}\delta_{k-1} + \mathcal{E}_{43}z_{k-1} + \mathcal{E}_{4d}d_{k-1} - \mathcal{E}_6u_{k-1} - \mathcal{E}_7y_{k-1} \\ \mathcal{Y}_{\max} - \Phi\hat{X}_k - \mathcal{H}_d\mathcal{D}_k + H_{11}u_{k-1} + H_{21}\delta_{k-1} + H_{31}z_{k-1} + H_{d1}d_{k-1} \\ \mathcal{U}_{\max} \\ \Delta\mathcal{U}_{\max} + R_{u0}u_{k-1} \\ -\mathcal{Y}_{\min} + \Phi\hat{X}_k + \mathcal{H}_d\mathcal{D}_k - H_{11}u_{k-1} - H_{21}\delta_{k-1} - H_{31}z_{k-1} - H_{d1}d_{k-1} \\ -\mathcal{U}_{\min} \\ -\Delta\mathcal{U}_{\min} - R_{u0}u_{k-1} \\ 0 \end{bmatrix}$$

Here $n_u,\ n_d$ and n_z are dimensions of the inputs, the auxiliary binary variables δ and the auxiliary continuous variables z, respectively.

To formulate the physical activity closed-loop intervention problem based on the described *JustWalk* intervention, the following input and output vectors are used:

$$u = [u_8 \quad u_9 \quad u_{10}]^T, \quad n_u = 3 \tag{5.54}$$

$$y = [y_4 \quad y_7]^T, \quad n_y = 2 \tag{5.55}$$

$$d = [\xi_{7T} \quad \xi_{7wknd}]^T, \quad n_d = 2 \tag{5.56}$$

5.4.2 Logical and Discrete Constraints

The hybrid nature of the HMPC formulation enables constraining the manipulated variables to sets of discrete predefined values. This is particularly important for interventions that require the use of predefined values for the intervention components, like the case with medical dosages of a drug, or in smoking cessation. For a demonstration, the possible set of step *Goals* is assumed as $u_{8,k} \in U_8 = \{Cv_1, \cdots, Cv_{n_{u_8}}\}$, and the possible set of *Expected Points* is $u_{9,k} \in U_9 = \{Cv_{n_{u_8}+1}, \cdots, Cv_{n_{u_8}+n_{u_9}}\}$. Therefore, the logical and discrete auxiliary variables are defined as follows:

$$\delta_{j,k} = 1 \Leftrightarrow z_{j,k} = Cv_j, \quad j = 1, \cdots, n_{u_8} + n_{u_9} \tag{5.57}$$

To enforce this condition

$$z_{j,k} = Cv_j \delta_{j,k}, \quad j = 1, \cdots, n_{u_8} + n_{u_9} \tag{5.58}$$

Furthermore, the following constraints must be included to guarantee that only one value can be assigned to each of the manipulated variables at each sampling time:

$$\sum_{j=1}^{n_{u_8}} \delta_{j,k} = 1, \quad u_{8,k} = \sum_{j=1}^{n_{u_8}} z_{j,k} \tag{5.59}$$

$$\sum_{j=n_{u_8}+1}^{n_{u_8}+n_{u_9}} \delta_{j,k} = 1, \quad u_{9,k} = \sum_{j=n_{u_8}+1}^{n_{u_8}+n_{u_9}} z_{j,k} \tag{5.60}$$

The effect of all entries on a given day can only be quantified on the outputs past midnight (when the day is over), as the amount of steps taken on a day is recorded until 11:59 pm, then it resets to zero at the beginning of the next day. The output measurements are then shifted to be temporally aligned with their associated inputs on a given day. As the logic behind awarding the points is a part of the HMPC

formulation, it is essential to account for output measurement limitations and assure that the *Expected Points* convert to *Granted Points* at the beginning of the next day. Therefore, the auxiliary logical variable δ_{GA} on day k is set as true when the performed steps meet or exceed the given goal on the previous day $(k-1)$, as follows:

$$\delta_{GA,k} = 1 \Leftrightarrow y_{4,k-1} \geq u_{8,k-1} \tag{5.61}$$

A set of linear conditions corresponding to the logical constraints, with the same feasible set, is obtained through the application of a big-M reformulation (Martín *et al.*, 2016a). The following constraints are included to assign the suitable values of δ_{GA}:

$$y_{4,k-1} - u_{8,k-1} \leq \delta_{GA,k}\ [y_4^{max} - u_8^{min}] \tag{5.62}$$

$$y_{4,k-1} - u_{8,k-1} \geq [1 - \delta_{GA,k}]\ [y_4^{min} - u_8^{max}] \tag{5.63}$$

The *Granted Points* are represented by the auxiliary variable z_{GA}, where $u_{10,k} = z_{GA,k-1}$. At the beginning of each day, the points awarded are set to equal the amount announced on the previous day, if the goal has been met $(u_{10,k} = u_{9,k-1})$

$$u_{9,k-1} - z_{GA,k} \leq [1 - \delta_{GA,k}][u_9^{max} - u_{10}^{min}] \tag{5.64}$$

$$u_{9,k-1} - z_{GA,k} \geq [1 - \delta_{GA,k}][u_9^{min} - u_{10}^{max}] \tag{5.65}$$

No points are awarded $(u_{10} = 0)$ if the goals are not achieved.

$$z_{GA,k} \geq \delta_{GA,k} u_{10}^{min}, \quad z_{GA,k} \leq \delta_{GA,k} u_{10}^{max} \tag{5.66}$$

The constraints described above in (5.57) - (5.66) are included into the system presented in (5.16) by defining the values for matrices $E_1, E_2, E_3, E_4, E_5, E_6, E_7$, and E_d through Hysdel (Torrisi and Bemporad, 2004).

5.4.3 Maintenance Phase

The maintenance phase of the intervention is activated upon reaching and sustaining the desired target for the behavior for a determined number of days. In this phase, the HMPC algorithm is reconfigured to maintain the behavior at the desired level with minimal use of financial rewards, to avoid financial dependency in sustaining the healthy behavior. The controller algorithm should also be able to reactivate the use of the points in case of a significant relapse in the behavior. The reconfiguration of the HMPC performance is accomplished by adjusting the penalty weights in the objective function according to the considerations of each phase of the intervention.

In the initiation phase, the main aim is to achieve the desired daily step count. The reference point for the output is represented by $y_r = [y_{r4} \quad y_{r7}]^T$, where y_{r4} is the desired step target (e.g., 10,000 steps/day). Therefore, the penalty weight matrix W_y is set to impose setpoint tracking only on the behavior y_4, where $W_y = \text{diag}\{1, 0\}$. The remaining weight matrices in (5.21) are set to approximately zero in this phase.

The maintenance phase is activated when the intervention target has been consistently achieved for at least $n_s - 2$ times during the last n_s days. This is the case when the participant's behavior falls within a predefined tolerance tol_4 region from the intervention target of 10,000 steps/day. To enforce this condition, a new auxiliary logical variable $\delta_{goal}(k)$, which is not included in the general formulation of HMPC by (5.14)-(5.16), is defined as

$$\begin{gathered} \delta_{goal,k-i} = 1 \Leftrightarrow |y_{4,k-i} - y_{r4}| \leq tol_4 \\ i = 0, \cdots, n_s - 1 \end{gathered} \tag{5.67}$$

Therefore, the maintenance phase is enabled at sampling time k if

$$\sum_{i=0}^{n_s-1} \delta_{goal,k-i} \geq n_s - 2 \tag{5.68}$$

During this phase, it is necessary to reconfigure the controller to target low point usage (u_9). The input targets $u_r = [u_{r8} \quad u_{r9} \quad u_{r10}]^T$ are adjusted in this phase, where $u_{r9} = 0$, and an appropriate value must be assigned to the corresponding weight in the manipulated variables penalty weights matrix $W_u = \text{diag}\{0, w_{u_9}, 0\}$ (e.g., $w_{u_9} = 1$).

5.5 Results and Discussion

In this section, results for a closed-loop simulation for a representative *JustWalk* participant are presented. Regularized ARX model estimated from *JustWalk* experimental data in Section 5.3.2 is implemented as the controller model for the HMPC, in an effort to provide personalized interventions. Two main cases are presented in this section: A) a nominal case: where there is no mismatch between the controller and the plant model, and B) a non-nominal case: where 100 different realizations of the estimated regularized ARX model are utilized as the plant model, in a Monte-Carlo simulation to test the controller robustness under plant-model mismatch. The intervention starts at day zero with the aim to change the sedentary lifestyle of the participant, averaging 5,000 steps/day, to a more active lifestyle averaging 10,000 steps/day. This simulation scenario is inspired by the performance observed in previous physical activity interventions with similar components (King *et al.*, 2013). The manipulated variables are *Goals* (u_8), *Expected Points* (u_9), and *Granted Points* (u_{10}). The disturbances considered in the simulations are *Evironmental Context: Temperature* (ξ_{7_T}) in the form of deviations from the mean temperature, and *Evironmental Context: Weekend* ($\xi_{7_{wknd}}$) which can have a significant impact on *Behavior* (y_4). Moreover, given its importance, the system model has been augmented to include *Goal Attainment* (y_7) as a system output, which allows for constraint enforcement on this signal, as illustrated in Chapter 4 and in El Mistiri *et al.* (2022b).

HMPC tuning parameters are chosen as follows: the sampling time $T_s = 1$ day, the prediction horizon $p = 20$ days, and the move horizon $m = 10$ days. Minimum and maximum bounds for the manipulated variables are $u_{min} = [0\ 0\ 0]^T$, $u_{max} = [\infty\ 500\ 500]^T$, $\Delta u_{min} = [-\infty\ -\infty\ -\infty]^T$, $\Delta u_{max} = [\infty\ \infty\ \infty]^T$. Output constraints are $y_{min} = [0\ -100]^T$, $y_{max} = [\infty\ \infty]^T$. To assure the convexity of the optimization problem, small values are assigned to move suppression weights ($W_{\Delta u}$) in both intervention phases, while the weights for the manipulated variables matrix (W_u) are adjusted based on the intervention phase.

A target for *Expected Points* (u_{r_9}) is set at 150 points/day in the initiation phase with a penalty weight of $w_{u_9} = 0.5$, to limit the controller towards reasonable use of financial rewards. The manipulated variable reference is then adjusted to $u_{r9} = 0$ points/day in the maintenance phase with an associated weight $w_{u_9} = 1$, to pursue the target more assertively. In a departure from the approach followed in previous work where predefined categorical values were enforced for all manipulated variables, only *Expected Points* are constrained to categorical levels while *Goals* are of a continuous nature in this simulation. The categorical values of the positive reinforcement intervention component are defined by the set $U_9(k) = \{0, 50, 100, 150, 200, 250, 300, 350, 400, 450, 500\}$ with $n_{u_8} = 0$ and $n_{u_9} = 10$. Consequently, the HMPC formulation is applied to enforce the big-M logical condition for the *Granted Points* (u_{10}), and discrete values for the *Expected Points* (u_9). To trigger controller reconfiguration into the maintenance phase of the intervention, *Behavior* must fall within a tolerance region of $tol_4 = 600$ steps/day from the desired setpoint value of 10,000 steps/day for 6 days out of the last $n_s = 8$ days. The unmeasured disturbance is assumed to follow a Gaussian distribution with $d'(k) \sim \mathcal{N}(0, 300)$. Additionally, no plant-model mismatch is considered. To allow for a progressive increase on the performed steps and adequate disturbance rejection the following 3DoF

tuning parameters are selected $\alpha_r = [0.9\ 0]^T$, $\alpha_d = [0.75\ 0]^T$, $f_a = [0.6\ 0]^T$.

5.5.1 Nominal Case

Fig. 5.9 presents simulation results of the application of the HMPC controller in delivering optimal personalized PA interventions in a nominal case, without considering a plant-model mismatch. For setpoint tracking, it can be observed that the output response tracks the filtered reference closely, despite the presence of stochastic unmeasured disturbance, and measured disturbances in the form of fluctuations in temperature and the change in operating conditions between weekday and weekend. The output response reaches 95% settling time within 26 days from the beginning of the intervention, as specified by the value of $\alpha_r^1 = 0.9$ for *Behavior* (y_4). This is accomplished with reasonable use of the *Expected* and *Granted Points*, following the selected value for the target u_{r9} in the initiation phase. By day 30, the participant's performance satisfies the condition in (5.68), which activates the maintenance phase (highlighted in green). In the maintenance phase, the use of the positive reinforcement component of the intervention through financial rewards is minimal, following the set target of 0 points/day in this phase, through the higher value of its associated weight $w_{u_9} = 1$.

On day 40 of the intervention, a significant decrease in the temperature occurs, which lasts for 8 days. This pulse in the disturbance decreases the participant's step count outside of the tolerance region, leading to the re-introduction of the initiation phase to help guide the participant toward the desired setpoint. As observed in Fig. 5.9, controller reconfiguration allows for the use of the financial rewards to influence the participant's step count towards the desired level of PA (10,000 steps/day) and counter the impact of the temperature disturbance. Moreover, the benefits of the anticipation feature can be observed as the controller starts ramping up the daily

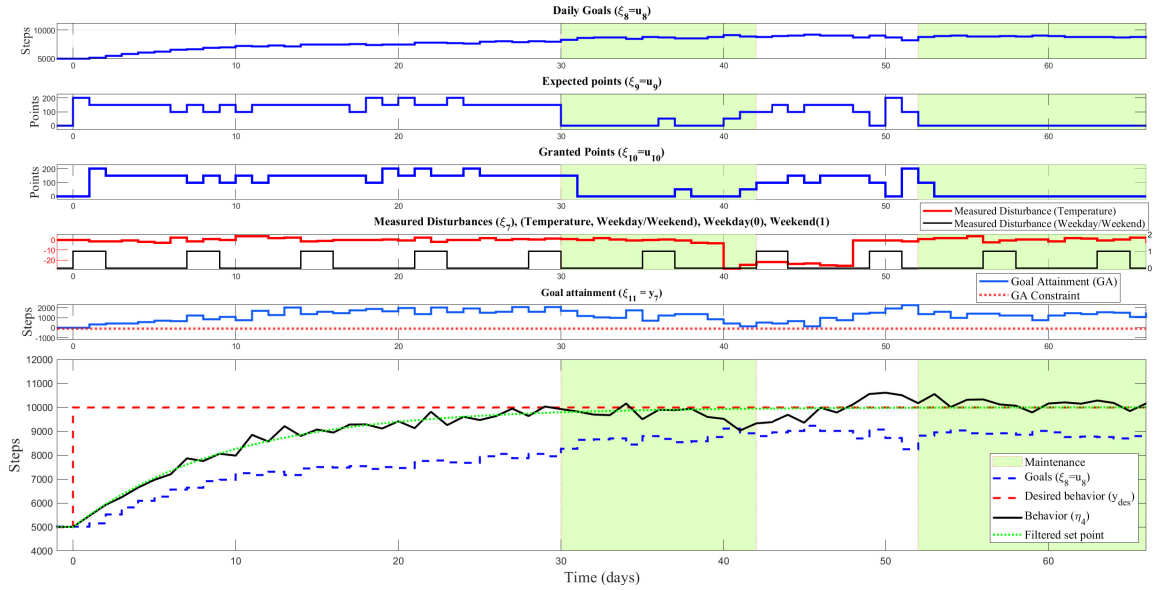

Figure 5.9: Closed-Loop Simulation Results from the Implementation of HMPC in a Personalized Intervention for a Representative *JustWalk* Participant, in the Presence of Measured Disturbances (Temperature and Weekend/Weekday) and Unmeasured Stochastic Disturbance. The Controller Tuning Parameters Are: $p = 20$, $m = 10$, $\alpha_d = [0.75 \;\; 0]^T$, $\alpha_r = [0.9 \;\; 0]^T$, $F_a = \text{diag}(0.6, 0)$, $W_y = \text{diag}(1, 0)$, $W_u = \text{diag}(0, 0.5, 0)$ (Initiation Phase), and $W_{\Delta u} = \text{diag}(0.01, 0, 0)$. The Following Constraints Were Used: $0 \leq u_8 \leq 15000$ steps/day, $0 \leq u_9 \leq 500$ points/day, $-\infty \leq \Delta u_8 \leq \infty$, $-\infty \leq \Delta u_9 \leq \infty$, $-100 \leq y_7 \leq \infty$. For the Maintenance Phase, $n_s = 8$ Days, $W_u = \text{diag}(0, 1, 0)$, and $tol_4 = 700$ steps/day.

goals delivered to the participant a day prior to the forecasted drop in the temperature (on day 39). As illustrated in the figure, the controller performs very well in terms of measured disturbance rejection, which is accomplished through the anticipation feature and the selected tuning parameters. Consequently, *Behavior* is back within the tolerance region by day 46 of the intervention and remains in this region for the next 6 days, which leads to the re-activation of the maintenance phase on day 52.

The constraint on the *Goal Attainment* (y_7) is satisfied throughout the intervention, despite the simulated exaggerated sudden decrease in temperature ($\Delta T = 25^\circ$ F). This extravagant drop in temperature is simulated to test the controller's capabilities, and it shows that the controller algorithm is capable of rejecting substantial amounts of measured and unmeasured disturbances within the defined constraints for the nominal case. However, to ensure that the controller's optimization problem is solvable without running into infeasibilities even in the presence of plant-model mismatch, slack variables are utilized as a part of the controller formulation (5.22). In this work, a slack weight of $W_s = \text{diag}(0, 10)$ is assigned so the output constraint is "soft" enough to not render the mixed integer quadratic programming (MIQP) problem infeasible, yet "hard" enough to be enforced throughout most of the intervention.

5.5.2 Robustness Analysis

In closed-loop behavioral interventions, controllers are designed to modify or guide a participant's behavior toward a desired outcome. However, due to the complexity of human behavior and the scarcity of available data, it can be challenging to accurately estimate the underlying model that governs individual responses. This uncertainty in the estimated idiographic model can lead to inaccurate predictions and reduce the effectiveness of the controller. Furthermore, behavior change systems may possess time-varying dynamics (Shiyko *et al.*, 2014), where model parameters may vary over time depending on various factors (e.g., environment, seasonality, notification fatigue, etc). This can also reduce the predictive capabilities of the estimated linear time-invariant (LTI) idiographic model, and impact the reliability of the formulated controller. Additionally, the presence of unmeasured (therefore, unmodeled) inputs to the system can substantially impact the controller's effectiveness. Therefore, discrepancies between the controller model and the actual behavior of a participant must

be considered to ensure the robustness of the controller.

In the presence of uncertainty, Monte Carlo simulation is a reliable technique to evaluate the performance of a control system in terms of stability and stochastic robustness (Ray and Stengel, 1993). Monte Carlo simulation incorporates randomness in the analysis of controller performance, by randomly sampling from the distributions of uncertainty in the estimated model parameters. This allows for the exploration of various possible scenarios, which provides a comprehensive understanding of the controller's robustness. Hence, to assess the robustness of the proposed controller formulation, tuning, and control strategy in non-nominal scenarios a Monte Carlo simulation has been implemented, and the results of which are presented in this section.

100 different realizations within one standard deviation from the deterministic equivalent of the estimated regularized ARX model (presented in Section 5.3.2) are randomly sampled utilizing the covariance matrix. The sampled realizations of the model are then implemented as the plant model, while the controller model is kept as the mean realization, creating a plant-model mismatch. The obtained results from the Monte Carlo simulation shown in Fig. 5.10 illustrate the robust performance of the controller in the presence of a mismatch. This can be observed in the response of the controlled variable (*Behavior*) as all realizations (plotted in green) are kept within a tight bound around the nominal case. This is accomplished through the array of manipulated variable responses seen in green in the figure; the controller optimally moves the manipulated variables for each realization, despite the presence of mismatch, while abiding by all the constraints and conditions specific to the problem. Consequently, there is a wide variety of observed responses in the manipulated variables, that are needed to maintain the outputs of the sampled plant realizations close to the filtered setpoint. This illustrates the success of the proposed controller formu-

lation, tuning, and control strategy in handling uncertainty and variability in model parameters, by reducing the variance in the controlled variable to a family of plant models by adjusting the manipulated variable responses based on feedback signals.

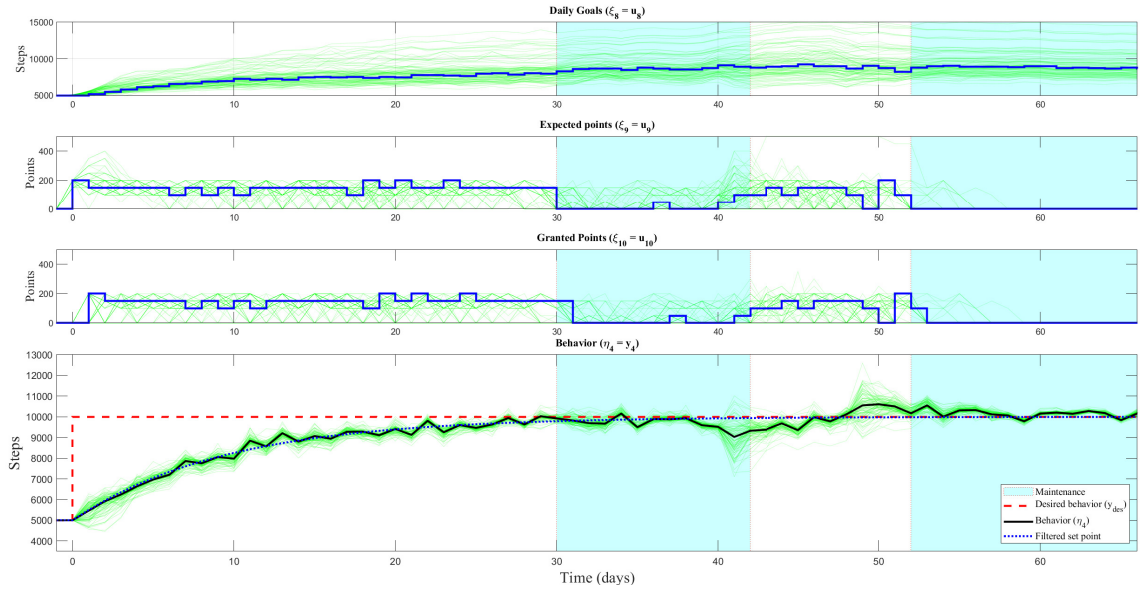

Figure 5.10: Closed-Loop Monte Carlo Simulation Results from the Implementation of HMPC in a Personalized Intervention for *JustWalk* Participant A, in the Presence of Measured Disturbances (Temperature and Weekend/Weekday) and Unmeasured Stochastic Disturbance. The Controller Tuning Parameters Are: $p = 20$, $m = 10$, $\alpha_d = [0.75 \quad 0]^T$, $\alpha_r = [0.9 \quad 0]^T$, $F_a = \text{diag}(0.6, 0)$, $W_y = \text{diag}(1, 0)$, $W_u = \text{diag}(0, 0.01, 0)$ (Initiation Phase), and $W_{\Delta u} = \text{diag}(0.01, 0, 0)$. The Following Constraints Were Used: $0 \leq u_8 \leq 15000$ steps/day, $0 \leq u_9 \leq 500$ points/day, $-\infty \leq \Delta u_8 \leq \infty$, $-\infty \leq \Delta u_9 \leq \infty$, $-100 \leq y_7 \leq \infty$. For the Maintenance Phase, $n_s = 8$ Days, $W_u = \text{diag}(0, 1, 0)$, and $tol_4 = 700$ steps/day.

More importantly, all of the presented realizations resulted in stable closed-loop responses, without running into infeasibility. It is important to note that in some of the randomly sampled scenarios the constraint on *Goal Attainment* is violated for

periods of the intervention. This is indeed the case in all realizations where the gains of the manipulated variables (especially *Goals*) are insufficient to facilitate positive *Goal Attainment*. Such scenarios demonstrate the importance of the addition of the slack variable in the controller formulation to soften constraints and render the MIQP problem feasible. Moreover, these scenarios bring into consideration the inclusion of dynamic upper constraints on *Goals* based on the average participant performance over the last 7 days, to ensure "ambitious yet achievable" goals are given, as presented in Chapter 6.

5.6 Conclusions and Future Work

This chapter presents the estimation of a dynamic model for a system that represents changes in PA levels. PA data for a representative *JustWalk* participant is divided into estimation and validation sub-experiments based on the designed multisine input signal cycles. The partitioned data is then utilized in estimating a regularized ARX model with order selection in an exhaustive search over all possible combinations of estimation and validation sub-experiments. The significance of the proposed approach to search over all the possible estimation and validation combinations is that it provides a model geared towards output prediction while maintaining a good fit throughout the overall data.

The estimated models are then utilized as the controller and plant models to test (in simulations) the proposed HMPC formulation in delivering personalized behavioral interventions promoting healthy levels of PA, specifically in the form of daily step count. Moreover, 100 realizations of the estimated model are generated by randomly sampling from the distribution of uncertainty around model parameters. The various realizations of the model are then utilized as the plant model, while the controller model is kept as the deterministic equivalent, in a Monte Carlo simulation to

examine the robustness of the controller in the presence of discrepancies between the plant model and the estimated model parameters.

Simulation results demonstrate the effectiveness of the HMPC algorithm as the decision-making framework in individualized PA behavioral interventions. The HMPC-based controller performs very well for the considered participants in terms of setpoint tracking, and disturbance rejection (measured and unmeasured) both in the nominal scenario and in the presence of a plant-model mismatch. As a part of the proposed HMPC algorithm, the controller is reconfigured to enable a maintenance phase, in which financial rewards are reduced or tuned off. Controller reconfiguration helps participants maintain healthy levels of PA in the maintenance phase, without relying on financial rewards to sustain the healthy behavior.

The work presented in this chapter is part of a series of growing applications of systems identification and control systems engineering principles in behavioral medicine, that were initially carried out as part of the *JustWalk* intervention at Arizona State University (ASU). The explored simulations are vital in the evaluation of the proposed controller formulation, and provide the means to troubleshoot and enhance the controller algorithm prior to real-world implementation. This will be carried out as a part of *YourMove* study, in one of the first of its kind closed-loop behavioral interventions promoting healthy levels of PA, which is built in collaboration between the University of California, San Diego and ASU (R01CA244777, 2020). One of the main aims of *YourMove* study is to include this framework in the design of a long-term behavioral health intervention that incorporates system identification, initiation, and maintenance phases, in what is known as the control optimization trial (COT; Hekler *et al.* (2018)), as described in the next chapter. This is an essential step towards the dissemination of user-friendly adaptive behavioral interventions on a large scale, thereby improving individual and public health.

Chapter 6

INPUT SIGNAL DESIGN, MODEL ESTIMATION, AND HYBRID MODEL PREDICTIVE CONTROL STRATEGIES IN THE CONTROL OPTIMIZATION TRIAL FRAMEWORK: ANALYSIS OF *YOURMOVE*, A PHYSICAL ACTIVITY INTERVENTION

6.1 Introduction

With the availability of temporally rich data through mHealth technologies, the study of idiographic modeling and interventions (on an individual level) has been reinvigorated. Control systems engineering methods, such as system identification and control systems design, can be used on such data to obtain dynamic models on an individual level and deliver personalized optimal adaptive behavioral interventions; these are thought to be more successful than static interventions (Hekler *et al.*, 2018). Prior work has demonstrated the value of input signal design in obtaining informative data sets to learn about the dynamics associated with behavior change (Hekler *et al.*, 2016), the ability of dynamic modeling techniques to predict dynamic responses of behavior change to perturbations in various system components (Martín *et al.*, 2020; Freigoun *et al.*, 2017), and the effectiveness of different model predictive control (MPC) strategies to deliver optimal personalized physical activity (PA) interventions guiding participants towards healthy behavior in simulation environments as presented in Chapters 4 and 5 (Martín *et al.*, 2016a; El Mistiri *et al.*, 2022b; Cevallos *et al.*, 2022). The main hurdles limiting the dissemination of PA interventions on a large scale include the lack of a thorough understanding of the dynamic processes behind behavior change, missingness arising from noncompliance

by participants, and the absence of a conceptual framework to deliver and automate interventions individualized for each participant. Building on prior work, in this chapter each of these challenges is addressed, specifically for one of the first of its kind behavior change studies implementing the concept of the control optimization trial (COT; Hekler *et al.* (2018)) framework, under the name of *YourMove*.

The aim of *YourMove* is to evaluate the effectiveness of the synergism between system identification and control systems engineering principles in delivering personalized optimal behavioral interventions, and establish a framework on which such COT-based interventions can be automated to enable their dissemination on a large scale (from model estimation to controller implementation). To accomplish this, in *YourMove* participants undergo three different stages: 1) a baseline stage, where PA levels of the participants are observed prior to being assigned daily targets; 2) a system identification experiment stage, where designed pseudo-random input signals are introduced to generate informative data to ideographically (on an individual level) estimate predictive dynamical models for PA behavior change; and 3) a closed-loop intervention stage, where a hybrid model predictive control (HMPC; El Mistiri *et al.* (2023); Khan *et al.* (2022); Cevallos *et al.* (2022); Nandola and Rivera (2013)) algorithm is the decision-making framework driving personalized optimal interventions to improve PA levels. The closed-loop intervention stage is divided into two different sub-stages: 1) an initiation phase, where the controller guides the participants towards the desired target of meaningful PA levels by adjusting daily goals and financial incentives, and 2) a maintenance phase, where the use of the financial rewards is phased off. Fig. 6.1 illustrates system identification and closed-loop stages in COT-based PA interventions like *YourMove*.

As the closed-loop intervention stage relies on the idiographic models from the system identification stage, it is essential to estimate predictive models that properly

represent each individual's behavior change dynamics to assure the personalization of the closed-loop intervention and robustness of the controller. This starts with an input signal design that provides enough excitation to the system in the frequency range of interest, thus facilitating the estimation of adequate participant-specific models for closed-loop control. Moreover, to allow the scalability of the intervention we develop a framework to estimate personalized models for over 190 participants, online, and to fit the models in a generalized structure for the HMPC-guided closed-loop phase of the intervention. Finally, to ensure the delivery of "ambitious yet achievable" in a robust and personalized manner, behavioral scientists' input is leveraged to structure controller tuning and reconfiguration in an adaptive manner, based on participant's responses.

The purpose of this chapter is to describe the challenges faced in implementing *YourMove*, detail the steps devised to overcome these challenges, and present preliminary results and findings from the first COT-based study. This chapter is organized as follows: Section 6.2 briefly describes *YourMove*. Section 6.3 presents a detailed description of the input signals designed for *YourMove*. In Section 6.4 the methods utilized to estimate participant-specific models and fit them into a generalized model structure are detailed. The algorithm followed in controller tuning and reconfiguration in the closed-loop stage of the intervention is outlined in Section 6.5. Results for three representative *YourMove* participants illustrating their performance across the three stages of the COT framework are presented and discussed in Section 6.6. Section 6.7 concludes with preliminary findings from the ongoing *YourMove* study and directions for future work.

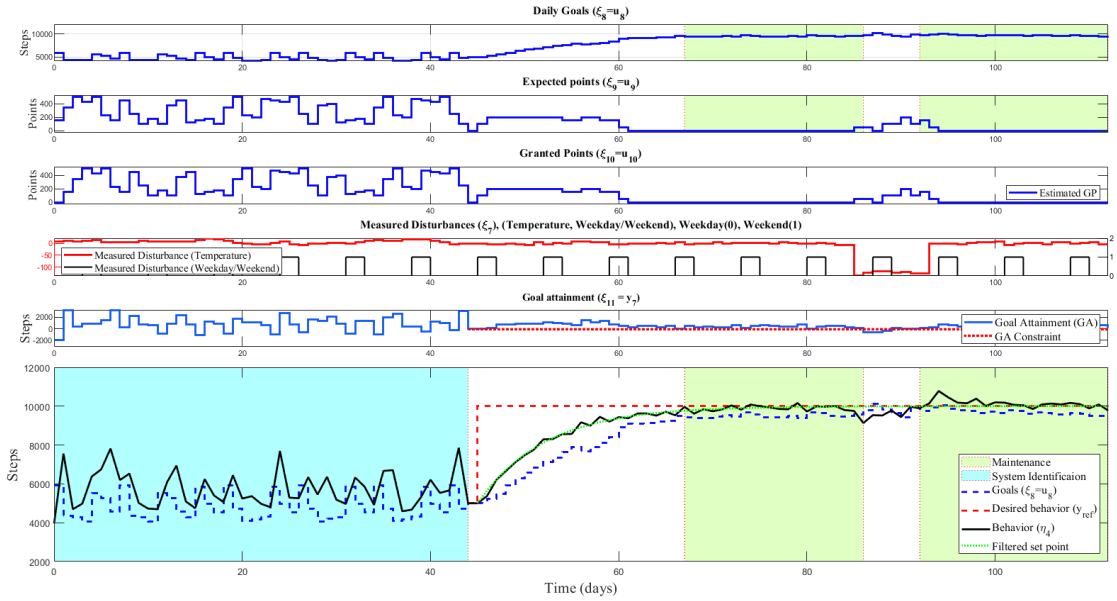

Figure 6.1: Simulation Results Illustrating the Stages of the Control Optimization Trial (COT) Behavioral Intervention, Based on a Representative Participant from *JustWalk*. Highlighted in Cyan is the System Identification Stage, and in Green is the Maintenance Phase, While the Unhighlighted Areas Represent the Initiation Phase.

6.2 *YourMove* Intervention

YourMove is a physical activity intervention based on Social Cognitive Theory (SCT; Bandura (1989)), utilizing the same intervention components in *JustWalk* as presented in Chapters 4 and 5. The purpose of the trial is to develop the framework for personalized closed-loop behavior change interventions and test their effectiveness against a control group of participants that has a fixed daily step goal of 10,000 steps per day. For a robust, personalized closed-loop intervention, an adequate understanding of the dynamics behind PA behavior change must be developed through a predictive model estimated utilizing system identification principles. For the dynamic predictive idiographic model to be informative and capture the important dynamics

for decision-making by the HMPC algorithm, the input signal design must provide enough excitation of states, encompassing the bandwidth of the system for each individual. To measure system signals, especially PA levels, smartwatch activity trackers (Fitbit Versa 3) are provided to all participants as a part of the trial. The capabilities of the Versa 3 replace the need for a mobile app, as intervention components (daily goals and points) are delivered to the participants through the watch. Each evening participants are also nudged to complete a series of daily micro ecological momentary assessments (EMA; Shiffman *et al.* (2008)) as seen in Fig. 6.2, where more than one survey question is asked per SCT construct. This should capture more variability in each construct, yielding more reliable and informative measurements. The used EMA survey questions in *YourMove* are presented in Table 6.1. In addition, using the Versa 3, other measurements such as daily resting heart rate and weather information are collected, which can be used as exogenous "disturbances" in the dynamic modeling of the behavior change system. A back-end server is used to communicate the personalized daily goals in all stages of the intervention, as well as store all the gathered data for modeling and future secondary analysis.

YourMove is a unique adaptive mHealth intervention designed to guide overweight sedentary adults towards healthy levels of PA. What distinguishes *YourMove* from previous studies is the duration and the nature of the intervention. Unlike previous studies, in *YourMove* individuals participate in the trial for a total duration of a full year, in an effort to monitor the long-term gains of the intervention and help participants sustain improvements to PA levels. Another aspect of the uniqueness of *YourMove* is that it is one of the first of its kind in terms of testing the effectiveness of closed-loop control interventions in real-world circumstances. Therefore, *YourMove* serves as a proof of concept for control engineering-based interventions. To accomplish this aim, the study is designed with three main stages. The baseline stage lasts for

(a) *YourMove* idol watch-face **(b)** EMA watch-face

Figure 6.2: Examples of the Custom Watch-Face Variations Provided to Participants in *YourMove*. (a) Shows the Idol Watch-Face Displaying the Daily Step Goal, Progress Towards the Goal, and Rewards. (b) Shows an Example of One of the Micro-EMA Survey Questions.

10 days, where the performance of the participants prior to the delivery of daily step goals is observed. This is significant in terms of establishing "ambitious but achievable" step goal ranges for each participant, and baseline average performance to quantify the benefits of the intervention after it is done. The second stage is the system identification experiment, where the designed personalized (based on median baseline performance) pseudo-random input signals are delivered to participants on a daily basis in the form of daily *Goals* (u_8) and *Expected Points* (u_9) with the aim of generating informative enough experimental data to estimate individualized dynamic models for each participant. The system identification stage is assigned to last for a total of 132 days (4.4 months). Finally, for the remainder portion of

Table 6.1: EMA Survey Questions Used in *YourMove* Study, Along with Their Respective Behavioral Constructs.

Construct	Survey Question
Self-Efficacy (η_3)	Being active is a top priority tomorrow.
	Being active is a top priority tomorrow.
	No matter what, I'm going to be active tomorrow.
Behavioral Outcomes (η_5)	Being active makes me feel more fit.
	In general, I feel energetic after being active?
	In general, I feel fatigued after being active?
Enviornmental Context ($\xi_{7Typicalness}$)	Tomorrow's schedule will help me be active.
	Circumstances will help me be active.
Perceived Barriers (ξ_5)	I expect obstacles to being active.
	Overall, being active will be hard tomorrow.

the study, the closed-loop intervention stage is deployed where participant-specific HMPC controllers are commissioned to guide each participant toward reaching the intervention target of 10,000 steps per day and maintain that level until the end of the intervention. HMPC formulation has proven to show a lot of potential as it has been previously tested in simulations on both hypothetical models (Martín *et al.*, 2016a), and idiographic models estimated from *JustWalk* experimental data for representative participants as illustrated in Chapter 5 and in Cevallos *et al.* (2022); Khan *et al.* (2022) and El Mistiri *et al.* (2023).

One of the main limitations faced in the *JustWalk* study was the burden on participants associated with answering EMA surveys on the mobile app. This hindered the ability to consistently measure SCT constructs like *Self-Efficacy* and *Behavioral Outcomes*, limiting estimation to multi-input-single-output (MISO) models with the only

output being *Behavior* (measured objectively). The use of the interactive watch-face of the Versa 3 for micro EMA delivery in *YourMove* is done to reduce the burden on participants, by seamlessly providing the EMA survey questions at the wrists of the participants, as seen in Fig. 6.2b, and allowing participants to "snooze" the surveys so they could be answered later, in case momentary circumstances do not allow a participant to immediately respond. Furthermore, the use of micro EMA survey questions, where multiple survey questions are geared towards measuring each of the important SCT constructs for the dynamic model, should yield more realiable mreasurements with higher variability. The obtained measurements of the SCT constructs of interest should enable modeling the system in a multi-input-multi-output (MIMO) structure, where all SCT constructs prominent to PA behavior change can be considered for the closed-loop intervention stage, which is important for implementing personalized control strategies like the ones proposed in Chapter 4 and in El Mistiri *et al.* (2022b). Additionally, the validation of the dynamic model presented in Section 4.2.2 through semi-physical grey-box modeling methods should be possible with the availability of consistent measurements for the key SCT construct.

Recruitment for *YourMove* is done within California, as participants need to be physically present in San Diego for baseline measurements, in a large-scale study including over 380 participants. Recruitment criteria for the intervention are defined as inactive, healthy, adults between the ages 25 to 65, living in the United States of America, who are willing to participate in the mHealth intervention for a long-term period of 365 days. In the following section, a detailed description of the input signal design process for *You Move*, utilizing the multisine design guidelines illustrated in Braun *et al.* (2002) and Rivera *et al.* (2002), is presented.

6.3 *YourMove* Input Signal Design

The pseudo-random nature of multisine signals makes them attractive to use as input signals for system identification, as their deterministic features can be specified to precisely accommodate theoretical and practical requirements, yet they mimic random noise. They can be designed to provide excitation at frequencies of interest; therefore, multisine signals are used for the manipulated inputs *Goals* and *Expected Points* for the system identification stage of *YourMove* intervention. Similar to equation (5.7), the multisine signals for the two inputs $\{u_8, u_9\}$ are defined as follows:

$$\begin{aligned} u_i(k) &= \lambda_i \sum_{j=1}^{n_s} \sqrt{2\alpha_{[i,j]}} \cos(\omega_j k T_s + \phi_{[i,j]}) \\ \omega_j &= \tfrac{2\pi j}{N_s T_s}, \quad j = 1, \ldots, n_s \end{aligned} \tag{6.1}$$

where T_s is the sampling time, λ_i is a scaling factor, n_s represents the number of excited sinusoidal harmonics, and N_s denotes the period length in terms of samples. For the j^{th} harmonic of the signal, each variable has the following meaning: $\alpha_{[i,j]}$ stands for the Fourier coefficient specifying the relative power of the harmonic, ω_j specifies the frequency, $\phi_{[i,j]}$ is the phase, i represents the input number where $i = \{8, 9\}$ for the inputs of interest, and n_u is the total number of inputs.

Following the guidelines presented in Braun *et al.* (2002), in the design of plant-friendly multisine signals the effective frequency range can be specified by selecting the design parameters based on the estimated range of the dominant time constant of the system τ_{dom}^H and τ_{dom}^L, and the user-defined parameters α_s and β_s to dictate the covered high and low-frequency content respectively, as expressed in (2.6) and (6.2).

$$\omega_* = \frac{1}{\beta_s \tau_{dom}^H} \leq \omega \leq \frac{\alpha_s}{\tau_{dom}^L} = \omega^* \tag{6.2}$$

where ω_* and ω^* represent the lower and upper bounds of the effective frequency range. To satisfy the plant-friendly design guidelines and the Nyquist-Shannon sampling

theorem, the following inequality must be satisfied.

$$N_s \geq \max(\frac{2\pi\beta_s\tau_{dom}^H n_u}{T_s}, 2n_u n_s) \tag{6.3}$$

Input signal design in system identification is an iterative process, that requires some prior knowledge of the system dynamics of interest. In this work, *a priori* knowledge from analyzing the experimental data from previous studies, particularly *JustWalk* is leveraged (see Section 5.3.2). One of the main observations from *JustWalk* data analysis is that the dynamic response of *Behavior* is quite fast for changes in the examined input variables as can be seen in Freigoun *et al.* (2017), Cevallos *et al.* (2022) and El Mistiri *et al.* (2023). For the majority of the participants in *JustWalk*, the time constant has been estimated to be at approximately 1 day. Hence, in the input signal design for *YourMove*, the selected guideline parameters for the estimated dominant time constant have been set to $\tau_{dom}^H = 1$ day $= \tau_{dom}^L$. As the decisions for the *Goals* and *Expected Points* are done on a daily level, the sampling time is set to $T_s = 1$ day. Additionally, analysis of the *JustWalk* data shows the importance of high-frequency dynamics in modeling the system, to allow the controller to make the right decisions. At the same time, the uncertainty associated with the steady-state gains for the inputs analyzed in *JustWalk* illustrates that low-frequency dynamics are significant in determining adequate gains for the manipulated variables of interest. Hence, the values for the user-defined coefficients are chosen to enforce a wide effective frequency range ($\beta_s = 3.5$ and $\alpha_s = 1$). The lower and upper bounds on the number of excited sinusoidal harmonics n_s are set based on the "plant-friendly" multisine design guidelines and the Nyquist-Shannon sampling theorem, respectively, as expressed in (6.4)

$$\cdot\frac{N_s}{2n_u} \geq n_s \geq \frac{\beta_s\alpha_s\tau_{dom}^H}{\tau_{dom}^L} \tag{6.4}$$

to abide by the guidelines, $n_s \geq 4$, the value for the excited sinusoids is selected at

$n_s = 5$, which provides excitation of state to harmonics beyond the higher bound of the effective frequency range ω^*, and allows for more power to higher frequencies.

To model the fast dynamics associated with PA behavior change, the input signals must generate dynamically informative data across all frequencies. Hence, in a departure from what was done in *JustWalk* (where the high-frequency non-excited harmonics were attenuated to have an amplitude of 0 like seen in Section 5.3.1 and Fig. 6.3). In *YourMove* the relative amplitude for non-excited high-frequency dynamics is selected as $hf = 0.5$. This provides all the remainder harmonics with a relative amplitude of 50% of the low-frequency excited harmonics, which can prove to be very significant for decision-making by the HMPC in the closed-loop intervention stage of *YourMove*. This is also important for future secondary data analysis, where MoD and other sophisticated predictive frameworks can be used to model and study higher frequency dynamics for each individual. To ensure that the input signals are optimally distributed between the maximum and minimum values of the sequence, crest factor minimization is performed following Guillaume *et al.* (1991).

The concept of statistical independence of the designed input signals to one another is very important. Uncorrelated input signals promote unbiased estimation and hence facilitate transfer functions for each input independently. There are multiple approaches to assure statistical independence of the two input signals, which are covered in detail in Rivera *et al.* (2007a) and Lee and Rivera (2006); in this work, the focus is on shifted and zippered approaches to multisine design.

6.3.1 Zippered Multisine

In the "zippered" approach the orthogonality between input signals is assured by alternating the excited harmonics for each input in the frequency domain, yielding highly uncorrelated signals (Rivera *et al.*, 2009). This is done by assigning Fourier

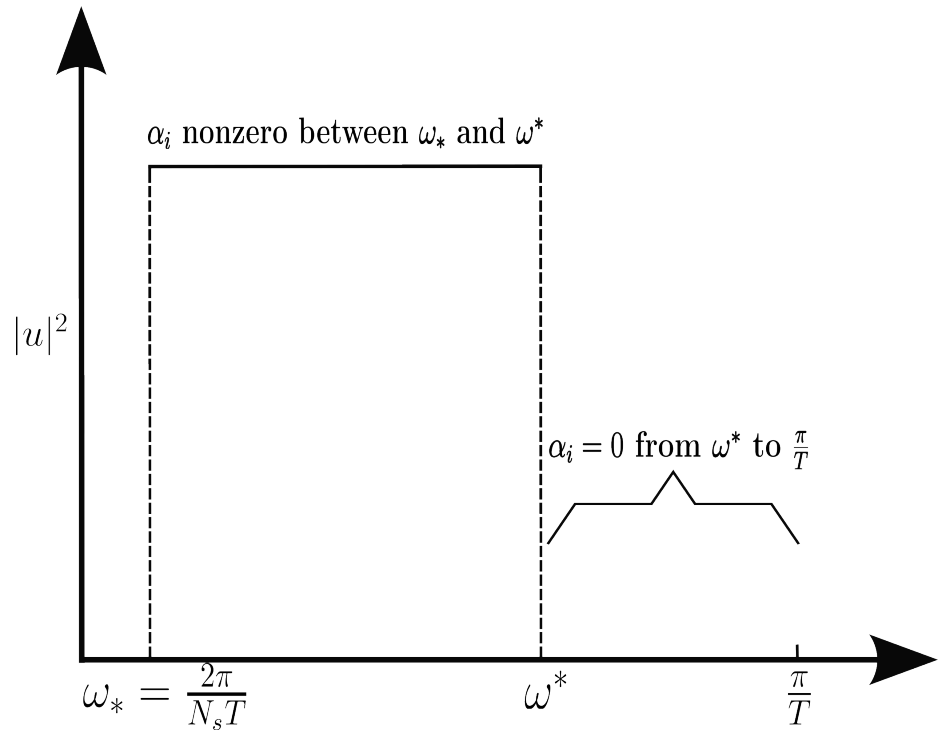

Figure 6.3: Schematic Illustrating the Common Practice in Multisine Input Signal Design Where the Relative Amplitude for Harmonics Past ω^* is 0.

coefficients ($\alpha_{[i,j]}$) to be non-zero for input i at certain frequencies, while the remainder of the inputs are assigned zero Fourier coefficients at the same frequencies, as can be seen in the spectral power density in Fig. 6.4. To independently excite $n_s = 5$ harmonics, for $n_u = 2$, the Fourier coefficients $\alpha_{[i,j]}$ are selected as follows:

$$\alpha_{[n,j]} = \begin{cases} 1 & \text{if } j = n_u(j-1) + (i-7) \\ & \text{for } j = 1, 2, \ldots, n_s \\ 0 & \text{otherwise} \end{cases} \tag{6.5}$$

To fit the excited harmonics in an alternating pattern, the zippered approach requires more low-frequency information, as can be seen by the harmonic to the left of the lower frequency bound in Fig 6.4. Therefore this approach requires a relatively

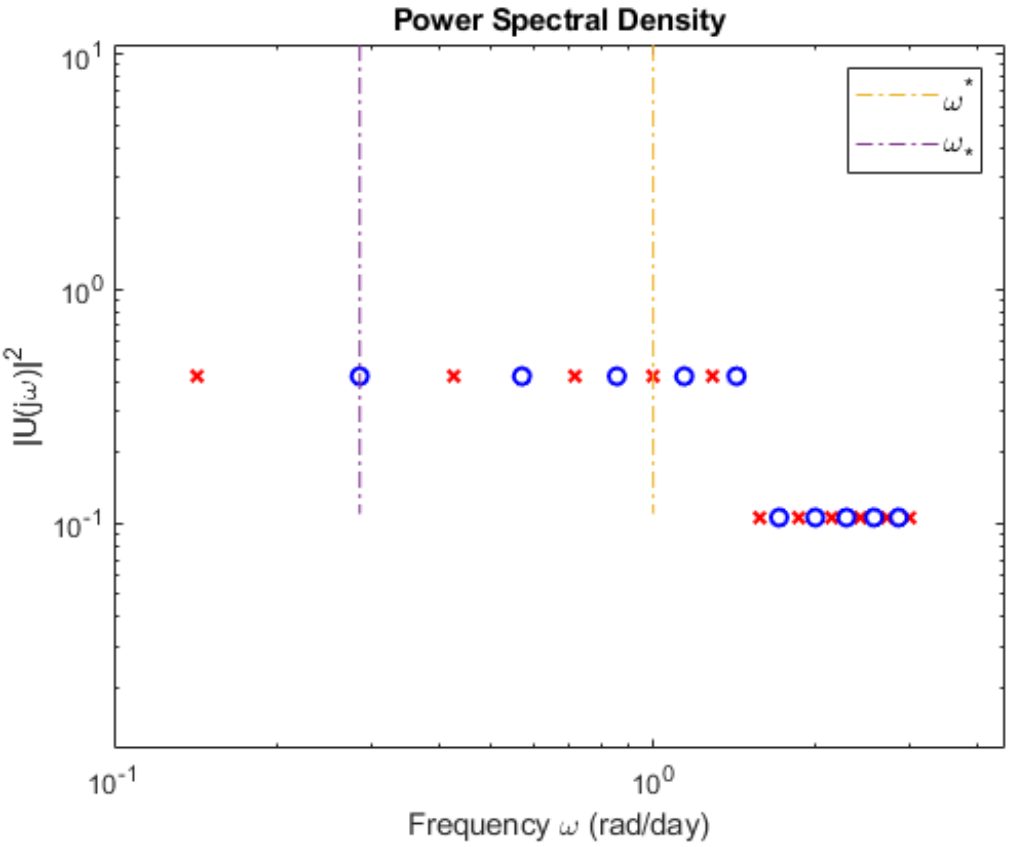

Figure 6.4: Power Spectral Density of the Designed Inputs in a Two-Channel Signal, Illustrating the Alternating Harmonics in the Zippered Spectra Approach. The Dashed Vertical Lines from Left to Right Represent the Low and High Effective Frequency Bounds ω_* and ω^* Respectively.

longer duration for each cycle, which is a disadvantage. To provide enough excitation for five independent harmonics, across two input signals, the overall duration of the signal per cycle must be $N_s \geq 44$ days according to (6.3), which could be significantly long for a behavioral intervention study. The chosen value for the duration of the period $N_s = 44$ days as can be seen in Fig. 6.5.

As expected, the orthogonality in the frequency domain produces uncorrelated inputs, which is verified by the correlation analysis shown in Fig. 6.6. It can be seen

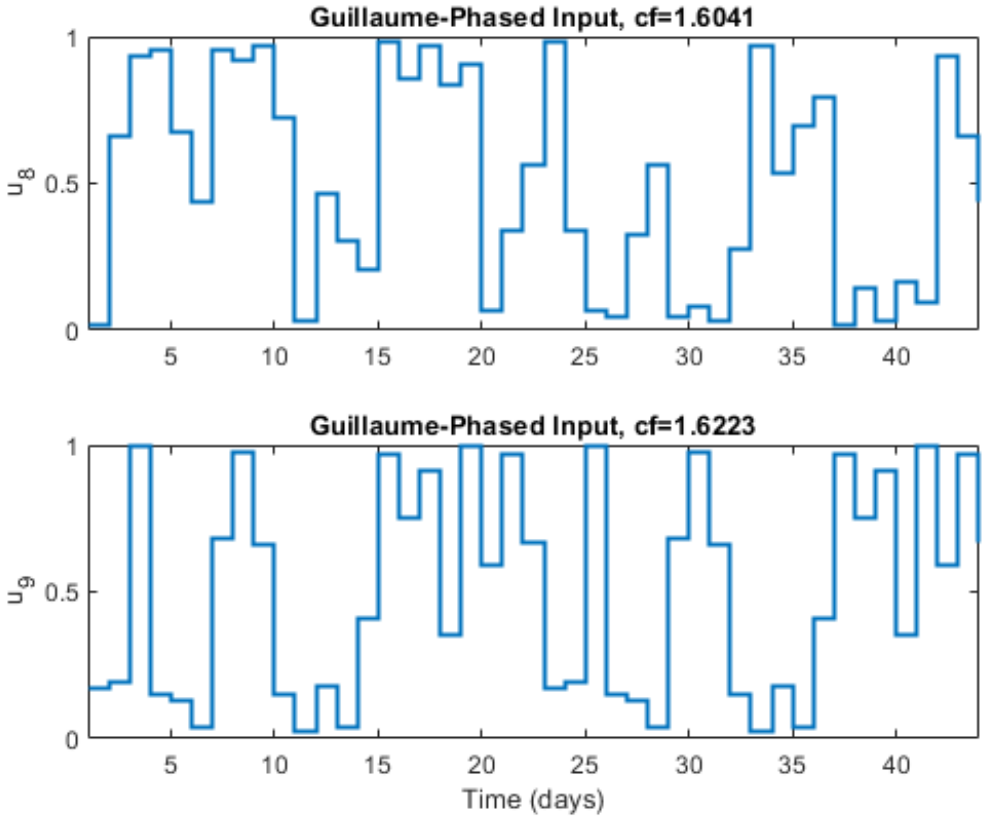

Figure 6.5: Time-domain Depiction of the Designed Zippered Input Signals (u_8, u_9) in *YourMove*. $N_s = 44$ days, $T_s = 1$ day, for $n_s = 5$ Excited Low Frequency Harmonics Per Signal.

that the correlation coefficients for all lags are negligible and well within the standard error bounds of three standard deviations (3σ), illustrating that the signals cannot, with a 99% confidence interval be distinguished from white noise.

6.3.2 Shifted Multisine

In the shifted approach, the input signal design is generated for only one input channel ($n_u = 1$), and then subsequent channels are shifted relative to the other inputs to increase statistical independence. The advantage of this approach is that it

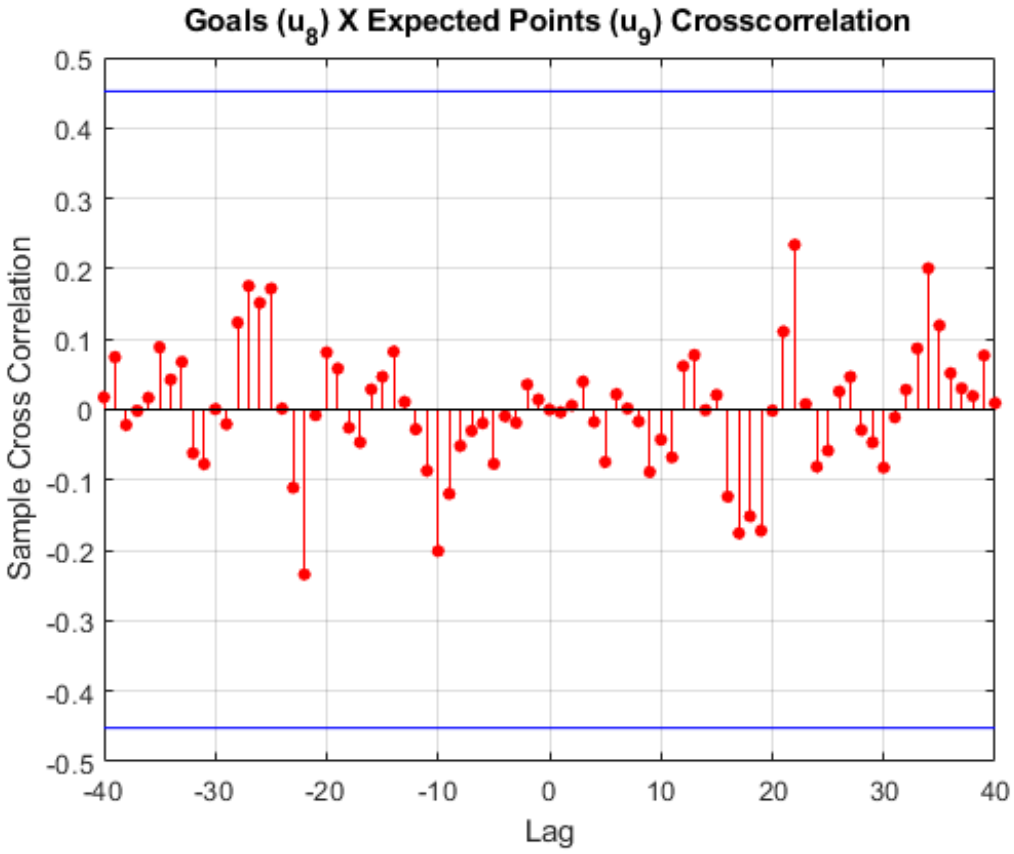

Figure 6.6: Cross-correlation Coefficients for Zippered Signals for the First 40 Lags, with Standard Error Bounds of 3σ.

results in shorter cycles, where according to (6.3) $N_s \geq 22$ days. As can be seen in Fig. 6.7, a value of $N_s = 22$ days has been selected to allow for executing more cycles within the duration of the study designated for the system identification experiment.

Shifting of the input signal introduces phase differences that promote orthogonality. Note that in the shifting process, the cross-correlation between the input signals is more likely to be prominent as the number of input signals increases. For the system of interest, only two of the inputs can be independently manipulated (*Goals* and *Expected Points*), which allows for shifting the signals by half a full cycle. This can

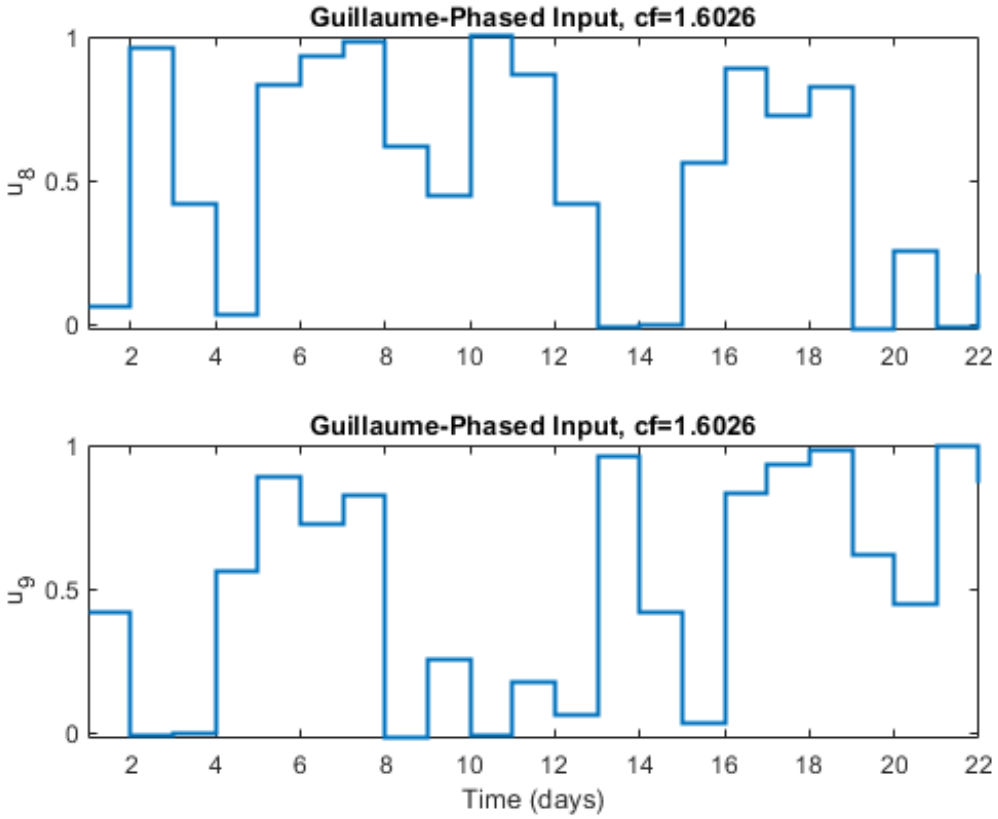

Figure 6.7: Time-domain Depiction of the Designed Shifted Signal in Two Input Channels (u_8, u_9). $N_s = 22$ days, $T_s = 1$ day, for $n_s = 5$ Excited Low Frequency Harmonics.

be observed in Fig. 6.7 where the signals are shifted by $t = N_s/2 = 11$ days. This is also evident in the correlation coefficients at lags $k = \{-11, 11\}$, where their values are relatively close to the confidence bounds of $3\sigma^2$ as seen in Fig. 6.8.

Because the signals for the two input channels are shifted copies of one another, they share the same Fourier coefficient values $\alpha_{[i,j]}$ for all harmonics. Consequently, both signals have equally excited harmonics at the same frequencies and equivalent power spectral densities, as can be seen in Fig. 6.9 by the overlapping sinusoidal harmonics.

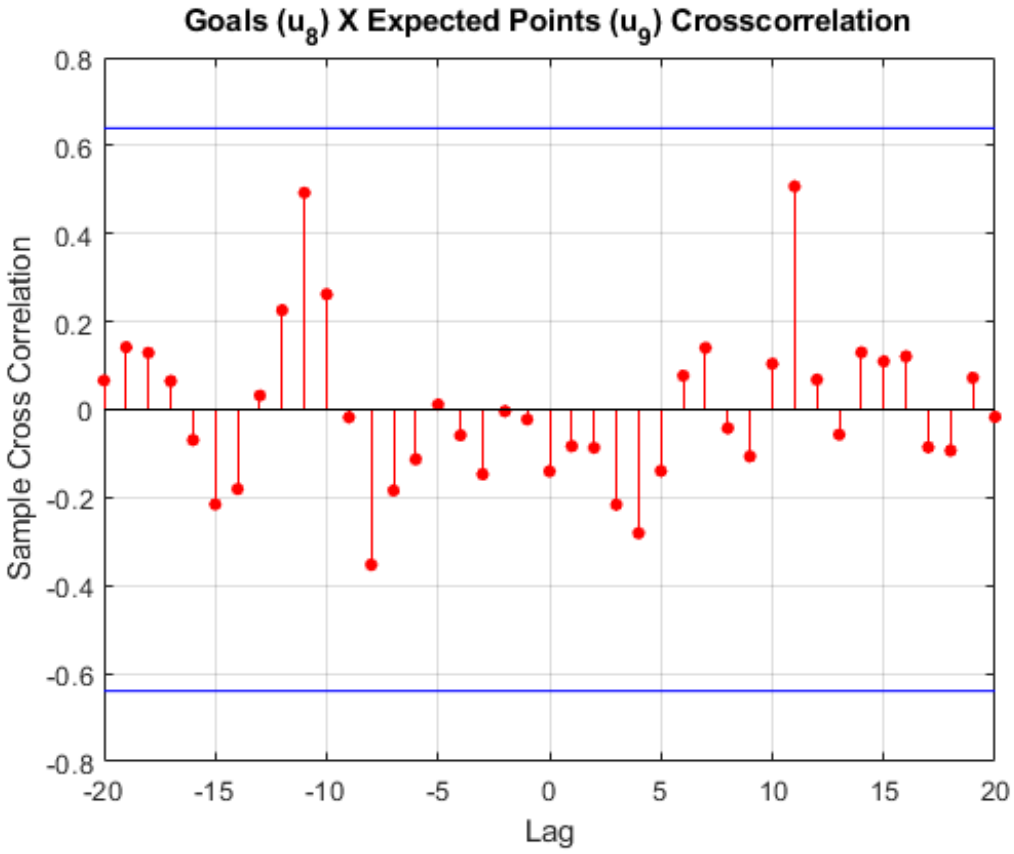

Figure 6.8: Cross-correlation Coefficients for the Designed Shifted Input Signals for the First 20 Lags, with Confidence Bounds of $3\sigma^2$.

6.3.3 Selection of Input Signal Approach

As noted in the previous subsections, each multisine design approach has its advantages and disadvantages. This trade-off exists between the statistical independence of the designed inputs and the duration of each cycle, which impacts the decision to select one approach over the other. In terms of cross-correlation of the input signals, it is clear that the zippered approach provides better signals due to the orthogonality of the signals in the frequency domain and, therefore, their guaranteed statistical independence. On the other hand, in the shifted multisine the correlation coefficients for $N_s/2$ lags in each cycle are relatively significant and can affect the estimation of

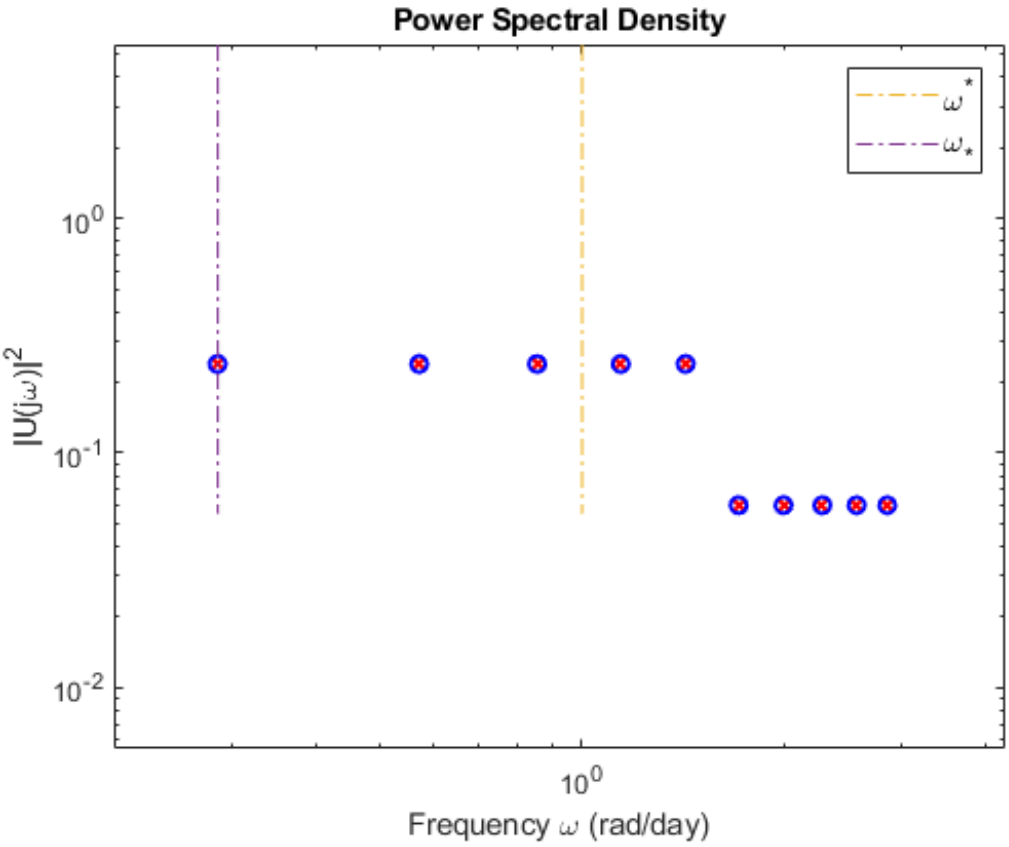

Figure 6.9: Power Spectral Density of the Designed Shifted Input Signal for Two Channels Illustrating the Overlap in the Harmonics. $N_s = 22$ days, $T_s = 1$ day, for $n_s = 5$ Excited Low Frequency Harmonics.

the impact of each input separately. The impact of such correlation coefficients on the data analysis is minimal as long as the duration of each cycle provides enough time for the responses to settle before $N_s/2 = 11$ days. This is the hypothesized case for the system of interest, where an estimated settling time between 5 to 6 days is expected based on the takeaways from *JustWalk* data analysis. Additionally, as the overall input signals are cyclical, utilizing each cycle separately for model estimation and validation can reduce the impact of the correlated input signals. Consequently, the shifted approach provides input signals that are expected to be sufficiently uncor-

related for the purpose of the experiment, with enough cycles to support meaningful cross-validation (described in the next paragraph).

One of the most important procedures in system identification is cross-validation. In cross-validation the model performance (in terms of fit percentages, such as Normalized-Root-Mean-Square-Error; NRMSE) is evaluated over data points that have not been used in the estimation step. This is significant as it provides information about how well the model is able to predict the outputs under different conditions and input changes than the ones examined in the estimation process. Traditionally in system identification, the data is split into two consecutive segments where one is utilized for estimation, and the other for validation. This approach assumes that the underlying noise characteristics in the system remain the same throughout the experiment. Based on the work done on *JustWalk* data, it is safe to assume that the noise characteristic associated with PA behavior change systems are mean-centric as seen in Section 5.3.2, however, they vary in nature over time (Freigoun *et al.*, 2017). To account for such phenomena, the approach of segmenting the data into sub-experiments based on input signal cycles allows for testing different combinations of estimation and validation data, to reach a better-performing model encompassing the stationary yet varying noise characteristics in behavior change systems.

The shifted multisine approach has the advantage in the aspect of overall signal duration, as shown in the previous subsections. Each cycle in the designed shifted multisine inputs has a duration of 22 days, which allows for executing a total of 6 cycles per the designated period for the system identification stage of 132 days. As a result, different combinations of estimation and validation data can be tested for each individual (35 combinations of three or four estimation cycles), to obtain individualized models that describe behavior change under different noise characteristics. The zippered multisine inputs inherently require more low-frequency information to ac-

commodate for the alternating excited harmonics, see Fig 6.4, which results in longer signals. Consequently, the selected design parameters yield a 44 days cycle, which allows only three cycles per the designated system identification period, and obstructs the ability to test different estimation/validation combinations. If the zippered input signals were deployed for 6 cycles, double the duration of the system identification stage would be needed, which would limit the time designated for the closed-loop control intervention stage and hinder the ability to achieve the main aim of the study (evaluating the controller performance in real-world situations). To reduce the duration of the zippered multisine signal, the low-frequency harmonics must be reduced, which would result in less informative input signals. Hence, the shifted approach is the one selected for *YourMove*, as it allows for executing more cycles in less overall time while maintaining excited harmonics in both high and low frequencies (and with acceptable cross-correlations).

6.3.4 Personalization of the Input Signals

The concept of personalization of the input signals stems from the goal of estimating participant-specific models. Unlike nomothetic approaches where a generalized model is estimated for a whole population (or subgroups of the population), in the idiographic approach a model is estimated for each individual separately. As observed in previous work, each participant can have a specific set of dynamics and gains that influence behavior change. Differences between individuals can include distinct shapes and speeds of response, as well as magnitudes and directions of steady-state gains for each considered input. Hence, it is important to design individualized input signals, that can yield participant-specific models, ultimately resulting in personalized optimal closed-loop interventions. In *YourMove* the personalization of the intervention starts from the system identification stage, where each participant is given their

own unique input signal design. This is accomplished by two measures: 1) a unique realization of the input signals is automatically generated when a new participant is recruited in the study, and 2) the baseline stage median performance is used to operationalize "ambitious yet achievable" goals for each participant. Therefore, the goals factor signal shown in Fig. 6.7 is scaled based on the baseline stage performance and then multiplied by the median baseline stage step count to define the maximum number of step goals given in the system identification stage.

$$Goals = Baseline\ Median + Scaled\ Goals\ Factor \times Baseline\ Median \tag{6.6}$$

A priori knowledge from *JustWalk* and other studies specifying PA behavioral profiles (King *et al.*, 2013; Adams *et al.*, 2013) provide guidance in selecting the amplitudes of the designed input signals, especially *Goals*. Due to physical limitations, and psychological factors the relationship between the daily step targets and the actual amount of steps walked per day is hypothesized to be nonlinear (an "inverted U" curve, as described in Martín *et al.* (2020)); there is a finite number of steps a person can walk on a certain day (similar to saturation limits in a chemical process), also a hypothesized negative impact of too ambitious daily goals on the *Self-Efficacy* of personnel and consequently their daily PA levels. To provide personalized ambitious (yet not extremely ambitious goals) the median of baseline performance for each participant is used to set both the minimum value for *Goals* given to a participant, as well as to define the individualized range for the goals signal in the system identification experiment. If the baseline stage performance median is equal to or lower than 3,000 steps per day, the goal factor is scaled to be between 0 to 1.50. A goal factor between 0 and 0.5 for a median *Behavior* in the baseline stage is between 3,000 to 5,500 steps per day. Finally, the goal factor for higher-performing participants is between 0 and 0.25. This is done in an effort to guide participants towards higher performance and

test each participant's ability to meet and exceed their baseline performance while leaving room for the controller to help the participants reach 10,000 steps per day on average. Furthermore, this gain scaling scheme should maintain the daily goals in the system identification stage close enough to the baseline performance and well below elevated values of daily goals that can have a negative impact. As per the *Expected Points*, financial constraints in the intervention limit the maximum number of points available to be rewarded is limited to 500 points, therefore, the signal is linearly scaled to span from 0 to 500 points.

The full potential of this work is reached when the estimated idiographic models are utilized in the closed-loop control for personalized optimal interventions, as a part of this unique COT study. Therefore, it is essential to devise a thorough framework to properly model an individual's behavior change dynamics and facilitate an efficient and meaningful closed-loop intervention stage. As the number of participants recruited for this study is relatively large (in comparison to other behavioral intervention studies) at 380+ participants, it is imperative to codify the proposed modeling framework, to assure repeatability across all participants and reduce human involvement in the process. These are crucial steps towards the dissemination of meaningful behavior interventions promoting healthy behavior on a large scale and benefiting public health. In the next section, the main challenges faced in optimizing the modeling framework are detailed along with approaches to overcome them.

6.4 *YourMove* Idiographic Modeling for a Generalized Intervention Structure

A practical and also fundamental challenge to the dissemination of PA behavioral interventions on a large scale (e.g., *YourMove* with 190+ intervention participants) lies in the form of the uniqueness of the responses from each individual to the diverse intervention components and exogenous factors. It is impossible to deliver an optimal

personalized intervention to individuals without an adequate understanding of system dynamics and a "good enough" model that reflects the speed and amplitude of each individual's dynamic response to the various changes in environmental, and personal factors, as well as to the intervention components. This is indeed one of the biggest challenges faced in the ongoing COT *YourMove* study, especially when it comes to finding the optimal model structure for each individual in a timely manner, to be able to seamlessly deploy the closed-loop intervention phase of the experiment. To overcome such an obstacle, different measures must be taken into account in the design and implementation of the study. In the previous section, the effort to personalize the input signals in order to generate unique signals exclusive to each participant has been explained, with the benefit of the defined "ambitious yet achievable" goal ranges for each individual, based on their baseline performance. In this section, the strategies that will be used to operationalize idiographic model estimation for the participants are discussed in detail and a road map for the deployment of such large-scale interventions is drawn.

6.4.1 DSPSA in Estimating Individualized ARX Models

Participant-specific models representing responses to the various changes in personal, and environmental factors that influence *Behavior* and other psychological constructs are not only unique in their gains and coefficients, but they are also unique in the selected inputs (features) constructing a model. For example, while some individuals might be heavily influenced by environmental factors like temperature and day (e.g., weekday vs. weekend), such factors may not have any effect on the outputs of interest for other individuals. Hence, there is a significant need for personalized models to describe each individual's dynamics. In system identification, a common practice is to apply correlation analyses for all the considered input and output combinations

to be able to determine which inputs should be selected for a model. However, such an approach is inconclusive when the duration of the available data is limited, especially if there is insufficient variability. Because of the nature and aims of *YourMove* study, budgetary and time constraints, the duration designated for the system identification experiment is limited to 132 days. With sampling carried on a daily level $T_s = 1$ day, this means only 132 data points per measurement including all the inputs and outputs are available in the best-case scenario. Moreover, lack of the ability to consistently and objectively measure all the components in the system (especially for self-reported psychoactive constructs like *Self-Efficacy*), and the high amplitude noise characteristics believed to be a part of behavior change systems, hinder the ability of correlation analyses to effectively reflect on the best input-output combinations to model the system for each individual.

In prior work, an exhaustive search method has been proposed where all possible input combinations for each individual were tested using black-box modeling techniques like ARX with order selection, which showed some promise (Freigoun *et al.*, 2017). However, a major disadvantage of this approach is how computationally and time-intensive it is; it can take hours or days to perform an exhaustive search for one participant. For instance, the total number of possible combinations of features $N_{combinations}$ for each output grows exponentially with respect to the number of considered features n, in accordance with (6.7).

$$N_{combinations} = 2^n - 1 \tag{6.7}$$

In addition to feature selection, searching over the optimal regressor order (for every selected input-output combination) significantly increases the number of possible combinations (Kha *et al.*, 2022). In the case of *YourMove*, ideally, three outputs are considered (*Self-Efficacy* η_3, *Behavior* η_4 and *Behavioral Outcomes* η_5) and 7 different

inputs/features. This renders the exhaustive search method impractical, due to the effort needed to explore all possible feature and regressor order combinations to model the system for each of the 190 participants. Hence, there is a need for hyper-heuristic search algorithms to replace exhaustively searching over all the possible combinations, and effectively optimize over model structure (in terms of included inputs and model orders associated with each input-output combination) in the limited time available for system identification. This is an essential step before commissioning the controller in *YourMove* intervention. To accomplish this, discrete Simultaneous Perturbation Stochastic Approximation (DSPSA; Wang and Spall (2011)) is utilized.

SPSA is a widely accepted non-deterministic, simulation-based optimization approach, where simultaneous stochastic perturbations of the system replace the need for traditional gradient descent methods (Spall, 1998). SPSA is particularly practical for noisy systems where an explicit solution for the objective function is not available. Variations of SPSA can be applied for binary sets (BSPSA; Aksakalli and Malekipirbazari (2016)) like the case with feature selection, and discrete variables (DSPSA; Wang and Spall (2011), and Wang and Spall (2014)), which is required to search over discrete values of regressor orders. The work done by Aksakalli and Malekipirbazari (2016) illustrates the benefits of BSPSA in feature selection, as it was found to slightly outperform other hyper-heuristic algorithms like Binary Genetic Algorithms, Sequential Backward Selection, and Sequential Forward Selection in small data sets, and the performance difference was found to be a lot more significant in favor of BSPSA in larger data sets. Additionally, in Wang and Spall (2013) DSPSA has been further examined and its rate of convergence is presented. The effectiveness of SPSA and its variations has been demonstrated in solving problems spanning various fields including public health (Wang and Spall, 2014), supply chain management (Schwartz *et al.*, 2006), and behavioral medicine (Kha *et al.*, 2022).

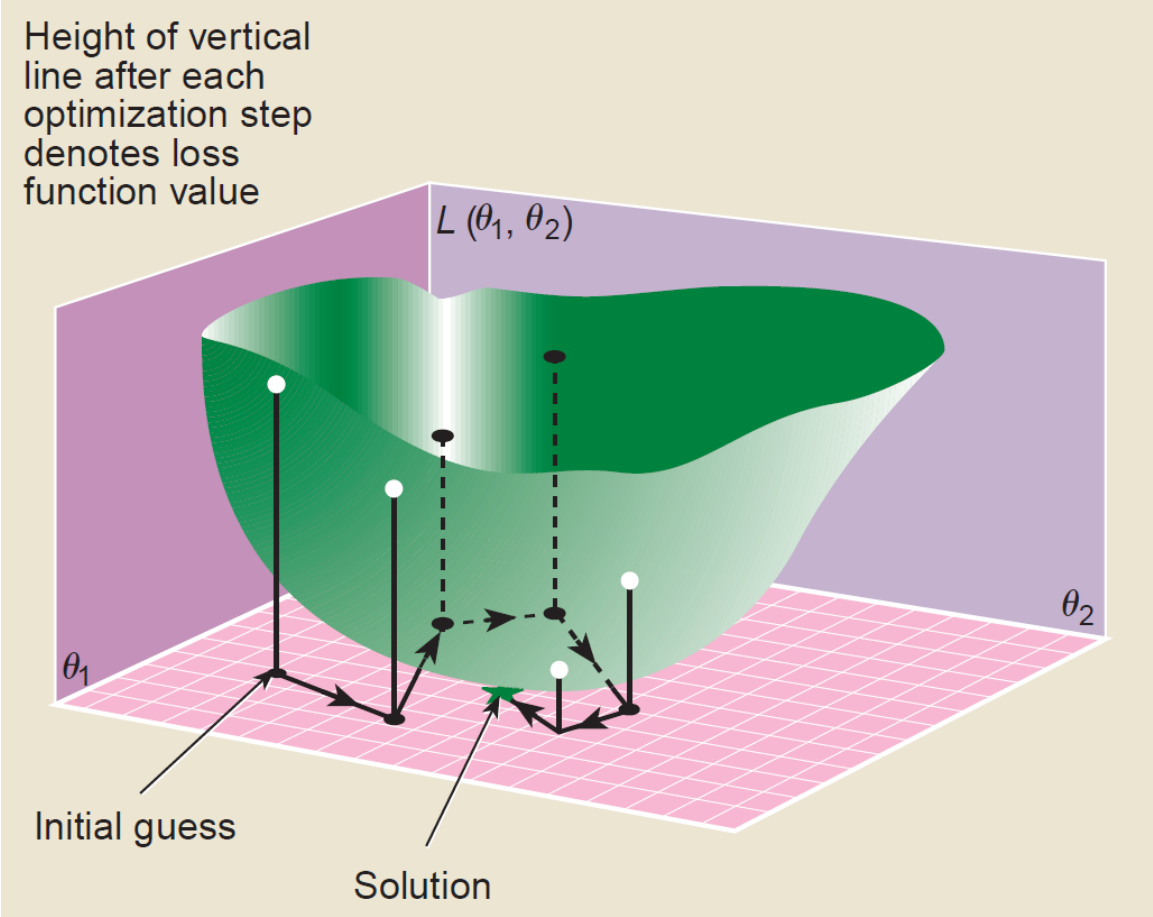

Figure 6.10: Depicts a Stochastic Algorithm Minimizing a Loss Function (Spall, 1998).

Building on the work done in Kha *et al.* (2022), DSPSA is applied to optimize over a multi-input-multi-output (MIMO) ARX structure in *YourMove*. This is done by providing an initial guess of all model parameter values, $\hat{\theta}$. To approximate a gradient for the system, the objective function $J(\hat{\theta})$ is estimated at new values for the model parameters at each iteration, which are obtained through random, opposing-directions simultaneous perturbations, similar to the example shown in Fig. 6.10. As the SPSA is applied for discrete values (binary for feature selection, and integers for regressor orders), the perturbed parameter values are bounded and rounded to the

nearest integer. The approximated gradient is then used to update parameter values at each iteration. The entire process is then repeated for a total of N iterations, which is a user-defined value. The optimization objective function of DSPSA is formatted as a loss function, L, which can be expensive to calculate at each iteration or not attainable explicitly. The available noisy measurement of the loss function can be defined as

$$J(\theta) = L(\theta) + \epsilon(\theta) \tag{6.8}$$

where $\epsilon(\theta)$ is zero mean noise. Therefore, by minimizing the expected value of the noisy measurement $E(J(\theta))$, the loss function is minimized

$$\min_{\theta \in \phi} L(\theta) = \min_{\theta \in \phi} E(J(\theta)) \tag{6.9}$$

where ϕ is the feasible values domain. Through iterating over and updating θ, SPSA follows a logic similar to the gradient descent to minimize the objective function.

To avoid over-parameterization of the ARX models, regressor orders (n_a, n_b, and n_k) must be constrained within reasonable bounds ($\{n_a^{lb}, n_a^{ub}\}$, $\{n_b^{lb}, n_b^{ub}\}$, and $\{n_k^{lb}, n_k^{ub}\}$). Additionally, as the feature selection optimization is of a binary nature, the search over features must be constrained to binary values ($\{0, 1\}$). Hence, upper and lower bounds are defined for all considered parameters ub and lb respectively, where $ub = [ub_1, ub_2, \ldots, ub_p]$, $lb = [lb_1, lb_2, \ldots, lb_p]$, and p is the total number of parameters to optimize over. In this case, a constrained DSPSA algorithm must be applied, where in each iteration k if any of the model parameter values obtained from the random perturbations is outside of its defined bounds, it is projected onto the feasible bounds. Therefore the projection operator $\Psi(\theta_k) = [\Psi_1(\theta_{k1}), \Psi_2(\theta_{k2}), \ldots, \Psi_p(\theta_{kp})]$ is defined

as follows:

$$\Psi_i(\theta_i) = \begin{cases} ub_i & \text{if } \theta_i > ub_i \\ \theta_i & \text{if } lb_i \leq \theta_i \leq ub_i \\ lb_i & \text{if } \theta_i < lb_i \end{cases} \tag{6.10}$$

A step-by-step detailed summary of the constrained DSPSA algorithm as described in Wang and Spall (2014), Aksakalli and Malekipirbazari (2016), and Kha *et al.* (2022) is presented below:

1. Provide an initial guess for parameter values $\hat{\theta}_0 \in \mathbb{Z}^p$, where $\mathbb{Z}^p$ donates the multivariate space of discrete values of p dimensions.

2. Generate the random perturbation vector for iteration k, $\Delta_k = [\Delta_{k1}, \Delta_{k2}, \ldots, \Delta_{kp}]^T$ where the probability distribution of Δ_k is specified by the user. In this case a Bernoulli ± 1 is utilized with a probability of 0.5.

3. The middle point of the hypercube $\pi(\hat{\theta}_k) = \lfloor \Psi(\hat{\theta}_k) \rfloor + \mathbf{1}_p/2$ is defined, where $\lfloor \cdot \rfloor$ is the floor operator, and $\mathbf{1}_p$ is a vector of ones of the p dimension.

4. Evaluate the objective function $J(\hat{\theta}_k)$ at directionally opposing perturbed values $\hat{\theta}_k^+ = [\Psi(\pi(\hat{\theta}_k) + c_k\Delta_k)]$ and $\hat{\theta}_k^- = [\Psi(\pi(\hat{\theta}_k) - c_k\Delta_k)]$, where $[\cdot]$ is the round operator and c_k is a user-defined sequence gains vector that can be specified for each model parameter separately.

5. Estimate the gradient $\hat{g}_k(\hat{\theta}_k)$ from the evaluated objective function at the perturbed values of parameters vector $\hat{\theta}_k^+$ and $\hat{\theta}_k^-$ as follows:

$$\hat{g}_k(\hat{\theta}_k) = \frac{J(\hat{\theta}_k^+) - J(\hat{\theta}_k^-)}{2c_k\Delta_k} \tag{6.11}$$

   The approximated gradient value is then used to update the parameters

$$\hat{\theta}_{k+1} = \hat{\theta}_k - a_k\hat{g}_k \tag{6.12}$$

where the diminishing step size $a_k = a/(1+A+k)^{\alpha}$ is specified by user's choice for coefficients $a > 0$, $A \geq 0$, $0.5 < \alpha \leq 1$.

6. Repeat steps 1 through 5 for N iterations and report the bounded and rounded parameter values $[\Psi(\hat{\theta})]$ that minimize the objective function.

This DSPSA algorithm is utilized to optimize ARX model structures for all combinations of estimation-validation data grouping, following the approach presented in Section 5.3.2). For *YourMove*, with a total of $N_{cycles} = 6$ input signal cycles, the considered combinations include three (50%) and four (66.67%) cycles for estimation, $S_e = \{3, 4\}$. Consequently, a total of $N_{ev} = 35$ combinations of estimation-validation cycles are possible, for which DSPSA is utilized to search over features and regressor orders.

$$N_{ev} = \sum_{r \in S_e} \frac{N_{cycles}!}{(r!(N_{cycles} - r)!)} \tag{6.13}$$

The Normalized Root Mean Square Error (NRMSE) is utilized to quantify the goodness of fit of the estimated ARX models for N_{ev} combinations of estimation-validation data, and it serves as the objective function for the DSPSA. As seen in equation (6.14), NRMSE is calculated by utilizing simulated output from the estimated model $\hat{Y}$, the measured output Y, and the mean of the measured output $\bar{Y}$, where $||\cdot||_2$ is the l_2-norm of the vector.

$$F(\theta) = 100 \times \left(1 - \frac{||Y - \hat{Y}||_2}{||Y - \bar{Y}||_2}\right) \tag{6.14}$$

For each estimation-validation data combination j, model fits are calculated for each cycle, then separately averaged for validation cycles $F_v^j(\theta^j)$ and for estimation cycles $F_e^j(\theta^j)$ to obtain a good sense of the performance of the model for prediction (over the validation cycles), and in fitting the dynamics observed in estimation cycles,

respectively. Furthermore, the goodness of fit of the model is calculated for the full data set by applying (6.14) to obtain an overall fit $F_o^j(\theta^j)$.

The aim of the DSPSA is to maximize the model's goodness of fit, especially for prediction (validation). Hence, a weighted average of the goodness of fit index $F_{wa}^j(\theta^j)$ is calculated as shown in (6.16) and utilized to construct the objective function utilized to approximate the gradient (6.11), for each of the available data combinations j.

$$\underset{\theta^j \in \mathbb{Z}^p}{\arg\max}\ J^j(\theta^j) = \underset{\theta^j \in \mathbb{Z}^p}{\arg\min}\ -J^j(\theta^j) \tag{6.15}$$

where

$$J^j(\theta^j) = F_{wa}^j(\theta^j) = W_v F_v^j(\theta^j) + W_e F_e^j(\theta^j) + W_o F_o^j(\theta^j) \tag{6.16}$$

W_v, W_e, and W_o represent the averaging weights for validation, estimation, and overall fit percentages, respectively. In this context, the weight for the validation fit index is the highest at $W_v = 0.6$, to prioritize the model's ability to predict each participant's response to the intervention components.

The obtained values of model structure parameters $\hat{\theta}_k^j$ are stored for each iteration in the search over the optimal model structure for each estimation-validation data combination. Additionally, all calculated fit indices are saved. Finally, the model structure that provides the highest weighted average fit F_{wa} across all DSPSA iterations, for all data combinations is selected. This process is repeated for all of the three outputs of interest.

For the sake of the repeatability of the results and secondary data analysis in *YourMove*, a unique seed number is randomly generated for each participant, which dictates the realization of the stochastic search in DSPSA. As order and feature selection search is a non-convex optimization problem, convergence is not guaranteed. Therefore, a sufficiently large number of iterations N is needed to adequately search over DSPSA parameters space. Then, the combination of orders and features with

the highest weighted average NRMSE fit F_{wa} is selected, as long as it satisfies specified conditions to ensure the operability of the controller. However, utilizing more iterations increases the computational time associated with DSPSA, while the benefit diminishes in terms of improving NRMSE fits (Kha *et al.*, 2022). Particularly for *YourMove*, computational time is quite costly with the limited period available for model estimation before initiating the controller phase. In *YourMove*, participants are enrolled automatically into the controller phase, in batches of around 1-4 participants, upon completion of the system identification phase. Model estimation and controller decisions take place on the server (online and overnight) within a limited window of four hours. Accounting for this trade-off, the default total number of iterations is set up to $N = 10$ iterations, which averages around 20 minutes per participant to estimate MISO models for all outputs of interest and construct a full model, utilizing the available computational resources on the server.

As presented in Section 5.3.2, cross-validation fits are not the only criterion for model validation. Another important criterion is the nature of the estimated dynamics, which can be represented in the characteristics of the step responses. In the context of *YourMove*, for the closed-loop intervention to be applicable, the steady-state gain between the main intervention component, *Goals* $u_8 = \xi_8$, and *Behavior* $y_4 = \eta_4$ must be positive. That is

$$P(\infty) = \lim_{s \to 0} \frac{y_4(s)}{u_8(s)} > 0 \tag{6.17}$$

Otherwise, the optimal solution of the optimization problem, based on the predictive model, would be trivial; the controller would deliver the minimum amount of *Goals* allowed within constraints. Therefore, to ensure the practicality and applicability of the controller, the selected model for each participant cannot describe a negative steady-state gain in *Behavior* with respect to *Goals*.

To satisfy this requirement, an iterative procedure is followed. In this procedure, condition (6.17) is checked for all of the 350 models estimated for *Behavior* (a model per each of the 10 iterations for 35 possible data combinations). The model that satisfies the gain condition and has the highest weighted fit average F_{wa} is selected. If none of the 200 estimated ARX models satisfies the condition in (6.17), then a new seed number is generated participant and the number of iterations is increased by 5 iterations for this participant, in an effort to expand the search space to find a better model. This procedure is repeated until a model that abides by (6.17) is reached, or the number of DSPSA iterations reaches $N = 25$. Finally, if no model is found that satisfies the gain condition, the model with the largest F_{wa} is selected and adjusted to have zero gain between *Goals* and *Behavior*.

Based on *a priori* knowledge from the *JustWalk* data analysis (see Section 5.3.2), PA behavior change systems are not of a high order (Kha *et al.*, 2022; El Mistiri *et al.*, 2023; Freigoun *et al.*, 2017). Hence, the upper and lower bounds on possible model orders for all inputs and outputs are specified as:

$$n_a^{lb} = 1, n_a^{ub} = 3 \tag{6.18}$$

$$n_b^{lb} = 1, n_b^{ub} = 3 \tag{6.19}$$

$$n_k^{lb} = 1, n_k^{ub} = 1 \tag{6.20}$$

For the initial values utilized to construct $\hat{\theta}_0$, all features are selected, and model orders are selected as $n_a = 2$, $n_b = 2$, and $n_k = 1$ for all outputs and estimation-validation data combinations. The remainder of the DSPSA user-specified parameters utilized in *YourMove* study are selected based on previous work and recommendations by Wang (2013), which are presented in Table 6.2.

In model estimation for each output, interrelationships between outputs are not considered in *YourMove*. This is done as the outputs of *Self-Efficacy* and *Behavioral*

Table 6.2: DSPSA Parameters Used in *YourMove* Study.

Parameter	Value	Parameter	Value
A	$0.10N$	a	0.25
α	0.501	c	1

Outcomes are self-reported constructs, which are subject to higher rates of missingness. Moreover, with the limited number of available data samples and the total number of considered exogenous inputs, interrelations between outputs are not considered to avoid ill-conditioned matrices. The estimated MISO models for each participant are combined in a generalized model structure to implement in the controller phase, which is described in the following subsection.

6.4.2 Generalized Predictive Model for HMPC

As mentioned in the earlier sections, the idiographic ARX models estimated through DSPSA are unique to each participant, not only in terms of dynamics but also in terms of the inputs utilized to estimate the model and the modeled outputs (based on the availability of measurements and the optimal feature selection from DSPSA). Hence, a common structure is needed to serve as the predictive model in the HMPC formulation, which provides a generalized framework to commission the controller for all participants, yet allows for the personalization of the closed-loop intervention for each participant through tuning and constraints assignment.

To accomplish this task for each participant, the estimated DSPSA ARX idiographic MISO models are converted into a minimal discrete-time state-space representation with no direct feedthrough ($n_k \neq \mathbf{0}$), then augmented into a multi-output

model:

$$x_{k+1} = A_x x_k + B\xi_k \tag{6.21}$$

$$y_k = Cx_k \tag{6.22}$$

where $\xi \in \mathbb{R}^{n_\xi}$ represents all the considered exogenous inputs, $y \in \mathbb{R}^{n_y}$ is for all the modeled outputs, and $x \in \mathbb{R}^{n_x}$ is a vector representing all the identified states. For each input-output relationship, if the particular input is not selected by DSPSA its coefficients are set to 0 in the B matrix. Then, the estimated coefficients in the state-space model are rearranged to populate the predictive model in the devised 3DoF-KF HMPC, introduced in 5.4.1.

$$x_{k+1} = A_x x_k + B_1 u_k + B_2 \delta_k + B_3 z_k + B_d d_k \tag{6.23}$$

$$y_k = C_x x_k + d'_k + v_k \tag{6.24}$$

$$E_2 \delta(k) \leq E_5 + E_4 y(k) + E_1 u(k) - E_3 z(k) - E_d d(k) \tag{6.25}$$

where $x \in \mathbb{R}^{n_x}$, and $u \in \mathbb{R}^{n_u}$ are modeled system states and manipulated variables; $y \in \mathbb{R}^{n_y}$ is the output vector; d, d', and v are modeled measured disturbance inputs, unmeasured disturbances, and measurement noise, respectively. $\delta \in \{0,1\}^{n_\delta}$ and $z \in \mathbb{R}^{n_z}$ are binary and discrete auxiliary variables that are introduced to convert discrete, logical decisions into their equivalent linear inequality constraints represented in (6.25). Variables n_x, n_u, n_{dist}, and n_y are the total number of states, controller manipulated inputs, measured disturbances, and outputs, respectively.

In a departure from prior work (Khan *et al.*, 2022; Martín *et al.*, 2016a; Cevallos *et al.*, 2022), the manipulated inputs are considered continuous, rather than fixed categorical values. This reduces the complexity of the controller formulation, as the only logical condition considered in the decision-making is for awarding the *Granted Points* through the "big-M" matrix.

The manipulated inputs for the controller are fixed in the following sequence:

$$u = [u_8 \quad u_9 \quad u_{10}]^T, \quad n_u = 3 \tag{6.26}$$

The representative coefficients for the manipulated variables in matrix B_1 follow the same sequence in a column arrangement. As per the measured disturbances, the columns in matrix B_d are ordered in accordance with the fixed arrangement of the measured disturbance inputs vector as follows:

$$d = [\xi_{7T} \quad \xi_{7wknd} \quad \xi_{7PredTypical} \quad \xi_5]^T, \quad n_d = 4 \tag{6.27}$$

In the same principle, the outputs for the system are arranged as shown in (6.28), and the corresponding coefficients in the rows of matrix C_x are organized accordingly. Note that y_7 represents the goal attainment, which is augmented into the state-space representation after the estimation of the system model, where $y_7 = y_4 - u_8$.

$$y = [y_3 \quad y_4 \quad y_5 \quad y_7]^T, \quad n_y = 4 \tag{6.28}$$

This generalized formulation provides the ability to accommodate the various models estimated for each of the participants; by assigning values of zero to the coefficients corresponding to inputs not selected by the DSPSA, and also for outputs that cannot be modeled due to a lack of adequate measurements. This generalized model structure also maintains an intuitive, straightforward scheme for constraint enforcement and tuning of the controller.

The states obtained from the minimal realization of the estimated DSPSA ARX model are arbitrary states that lack physical meaning. Furthermore, the number of states representing each output varies between participants based on the regressor orders for each modeled output. Hence, the controller formulation is geared towards the optimization of the measured output, rather than state feedback. This allows us to tune and constrain the outputs in a meaningful way that is guided by recommendations from behavioral scientists.

6.4.3 Missingness and Data Imputation

Because of the limited time available for online computations, it is not possible to implement model-based or sophisticated methods for data imputation in *YourMove*. Therefore, a simple method is utilized to impute missing data points on the server utilizing the moving average. In this method, the moving average of the last 7 days is calculated and used to replace the missing data point for the respective measurement. Both the raw signals (with missingness) and the imputed signals are stored separately in the database, for future secondary data analysis. Moreover, the imputed signals are used to impute any missing future data points. Following this approach, when a participant stops wearing their activity tracker or responding to EMA surveys, the measurement signal settles at a constant value.

6.5 Control Strategies

As illustrated in Chapters 4 and 5, judicious formulation of the optimization problem in MPC for closed-loop behavioral interventions is crucial for its success. The implementation of the 3DoF-KF HMPC formulation, in one of the first of its kind COT interventions, is the fruit of years of research and meticulous consideration. This served as the basis for the real-world implementation in the ongoing *YourMove* study. As this intervention is quite extensive in scale (190+ participants in total to be enrolled in the closed-loop intervention), a wide variety of participant-specific models and responses are encountered. Therefore, sophisticated tuning rules and logical conditions are devised, under the guidance of behavioral scientists in our team, to ensure the robustness of the controller, the automation of the intervention, and the delivery of personalized interventions that lead to meaningful behavior change. In this section, the utilized tuning rules and logical conditions in *YourMove* are described, along

with the reasoning behind them. Default tuning parameters used in the closed-loop intervention are presented in Table 6.3. The algorithm followed in adaptively adjusting controller tuning and controller reconfiguration (dubbed by behavioral scientists in the team as "digital PA coach tuning") is essential for the implementation of personalized closed-loop interventions with minimal human input and is summarized in Fig. 6.11. It is important to note that controller reconfiguration and adaptive tuning parameter adjustment are done through external conditions. They are not a part of the logical conditions in the MLD matrices in the HMPC formulation.

6.5.1 Default Tuning

In *YourMove*, default controller design parameters are chosen to provide participants with challenging, but achievable, goals and guide them toward healthy levels of PA. By design, the selected controller tuning parameters are based on the assumption that the participant is engaged in the intervention, and is capable of successfully attaining the provided daily goals as they are gradually increased toward the desired level of PA. However, if a participant finds the provided daily *Goals* extremely ambitious, or easily attainable under the default controller design, then the controller is reconfigured and the tuning parameters are adaptively adjusted. The selected parameters are the result of careful considerations, behavioral scientists' feedback, and preliminary simulations based on the estimated models of the first batch of enrolled participants.

The 3DoF-KF HMPC formulation enables independent and simplified tuning for setpoint tracking, measured disturbance rejection, and unmeasured disturbance rejection by selecting the desired closed-loop speed of response, as explained in Chapter 5. For setpoint tracking, the 3DoF-KF HMPC is formulated to track a single output, which is the measured daily step count, *Behavior* y_4. Hence, its respective weight

in the output reference tracking penalty weights matrix W_y is set to one, while the remainder of the outputs are given a weight of zero. The setpoint for *Behavior* is set at $y_{4,r} = 10,000$ steps/day, based on established CDC recommendations. Moreover, the reference filter in this case is only utilized for this output, as expressed in (6.29).

$$W_y = \text{diag}(w_{3,y}, w_{4,y}, w_{5,y}, w_{7,y}) = \text{diag}(0, 1, 0, 0) \tag{6.29}$$

$$\alpha_r = [\alpha_r^1 \;\; \alpha_r^2 \;\; \alpha_r^3 \;\; \alpha_r^4]^T = [0 \;\; 0.9 \;\; 0 \;\; 0]^T \tag{6.30}$$

For measured disturbance rejection, a Type-I filter is utilized, as only step disturbances are expected to influence the system. The selected filter parameters for the considered measured disturbances are presented in (6.31).

$$\alpha_d = [\alpha_d^1 \quad \alpha_d^2 \quad \alpha_d^3 \quad \alpha_d^4]^T = [0.5 \quad 0.2 \quad 0.4 \quad 0.4]^T \tag{6.31}$$

A Kalman filter is implemented to provide the third degree of freedom in controller tuning, which accounts for unmeasured disturbances are plant-model mismatch independently from setpoint tracking and measured disturbance rejection, as described in Section 5.4. Reliable measurements influencing controller decisions in the closed-loop intervention are *Behavior* y_4 and *Goal Attainment* y_7. Therefore, their respective weights are set according to (6.32) to correct for the difference between predicted values and actual measurements from the feedback signals.

$$F_a = \text{diag}(f_a^1, f_a^2, f_a^3, f_a^4) = \text{diag}(0, 0.2, 0, 0.5) \tag{6.32}$$

Moreover, a lower constraint is enforced y_7 to ensure the provision of moderately ambitious *Goals*. The lower bound on *Goal Attainment* is selected at $y_{7,min} = -2,500$ steps/day to define an acceptable margin by which a goal on a certain intervention day can be missed by the controller. This margin is based on the expertise of behavioral scientists in the research team, and falls within one standard deviation observed in

step count data; this constraint is "softened" through the implementation of slack (see Section 5.4). The respective slack weight for *Goal Attainment* is set by default at $W_s(4,4) = 5$ to provide the controller with room to challenge the participants. In addition, an upper constraint is also placed on *Goal Attainment* $y_{7,max} = 2,000$ steps/day, to steer the controller towards providing daily goals that can be exceeded by a significant margin based on the estimated participant-specific model. In summary,

$$y_{min} = [y_{3,min} \quad y_{4,min} \quad y_{5,min} \quad y_{7,min}]^T = [-\infty \quad -\infty \quad -\infty \quad -2,500]^T \tag{6.33}$$

$$W_s = \text{diag}(w_{3,s}, w_{4,s}, w_{5,s}, w_{7,s}) = \text{diag}(0,0,0,5) \tag{6.34}$$

$$y_{max} = [y_{3,max} \quad y_{4,max} \quad y_{5,max} \quad y_{7,max}]^T = [-\infty \quad -\infty \quad -\infty \quad 2,000]^T \tag{6.35}$$

Both *Goal Attainment* constraints and the slack weight are adaptively adjusted within the intervention for each participant, based on the participant's performance as described subsequently in this section.

In the default controller design, target reference tracking is not implemented on the manipulated variables, as the weight matrix for manipulated variables target tracking W_u is set to minimal values. W_u is not set to zero, to guarantee that the quadratic coefficients matrix in the objective function H is positive semi-definite. This is also the case for the movesize suppression penalty weight matrix $W_{\Delta u}$; see Table 6.3.

To ensure sensibility and practicality of the delivered intervention components, daily goals and financial incentives, upper and lower constraints are placed on the manipulated variables and their movesize. The lower constraints on the *Expected Points* $u_{9,min}$ and *Granted Points* $u_{10,min}$ are placed to guarantee that their values are positive, as expressed in 6.36. On the other hand, a lower constraint on *Goals* $u_{8,min}$ is enforced to guarantee that the delivered daily goals are not below a certain level, even when the participant's performance drops significantly. The level at which *Goals* are constraints for each participant depends on the participant's median performance

in the baseline phase. If the baseline median is greater than 7,000 steps/day, the participant is considered an active participant. In such cases, the lower bound on goals is selected at $u_{8,min}$ = 5,000 steps/day. The constraint is lowered to $u_{8,min}$ = 4,000 steps/day for less active participants in the baseline phase, with a median between 5,000 to 6,999 steps/day. Finally, for the least active participants in the baseline phase, with a median less than 5,000 steps/day, the lower bound is specified as $u_{8,min}$ = 3,000 steps/day.

$$u_{min} = [u_{8,min} \quad u_{9,min} \quad u_{10,min}]^T = [u_{8,min} \quad 0 \quad 0]^T \tag{6.36}$$

As for upper constraints in the manipulated variables, they are set based on physical and financial limitations. The upper bounds on *Expected Points* and *Granted Points* are set to 500 points/day, to fall within budgetary constraints for the study. On the other hand, the upper bound on *Goals* is defined as $u_{8,max} = 15,000$ steps/day, to avoid providing the participants with extremely high daily goals.

$$u_{max} = [u_{8,max} \quad u_{9,max} \quad u_{10,max}]^T = [15,000 \quad 500 \quad 500]^T \tag{6.37}$$

Upper bounds are also placed on the movesize for *Goals* $\Delta u_{8,max}$ = 2,000 steps/day, to ensure that any increase in the daily goals is gradual and allows the participant to adapt and internalize increases in PA levels:

$$\Delta u_{max} = [\Delta u_{8,max} \quad \Delta u_{9,max} \quad \Delta u_{10,max}]^T = [2,000 \quad \infty \quad \infty]^T \tag{6.38}$$

6.5.2 Maintenance Reconfiguration

The aim of the COT framework is to facilitate sustained behavior change toward healthy behaviors. An essential part of this framework is the maintenance phase, where different components of the intervention can be phased off. In *YourMove*, the financial rewards component of the intervention (i.e., *Expected Points* and *Granted*

Points) are used minimally in the maintenance phase, to avoid financial dependency. When the maintenance phase is activated, the controller is reconfigured by adjusting the target on *Expected Points* $u_{9,r}$ to 0 points/day and pursuing this target through its associated weight $w_{9,u} = 1$. The maintenance phase is activated when the participant's performance is within a predefined tolerance bound for at least $n_{tol} - 1$ times during the last n_{tol} days, as described in (6.39).

$$\delta_M \Leftrightarrow \sum_{i=0}^{n_{tol}-1} \left(|y_{4,k-i} - y_{4,r}| \leq tol\right)_i \geq n_{tol} - 1 \tag{6.39}$$

If the participant relapses and their performance does not satisfy the maintenance activation condition defined in (6.39), then the initiation face is reactivated, and the controller is reconfigured to the default formulation and tuning.

Table 6.3: Default Control Design Parameters for *YourMove*.

Parameter	**Value**	**Parameter**	**Value**
p	20	$\Delta u_{9,min}$	$-\infty$
m	10	$\Delta u_{10,min}$	$-\infty$
W_u	$\text{diag}(0, 0.01, 0)$	tol	500 steps/day
$W_{\Delta u}$	$\text{diag}(0.01, 1 \times 10^{-6}, 0)$	W_u (maintenance phase)	diag(0, 1, 0)
$\Delta u_{8,min}$	$-\infty$	n_{tol}	7 days

6.5.3 Stagnation in Disturbance Measurements

One of the issues faced in behavior change interventions in general, including *YourMove*, is the limited ability to measure important psychological constructs that should influence (or be influenced) by the intervention. Chapters 4 and 5 present a robust control strategy to overcome this challenge in regards to output constraints for

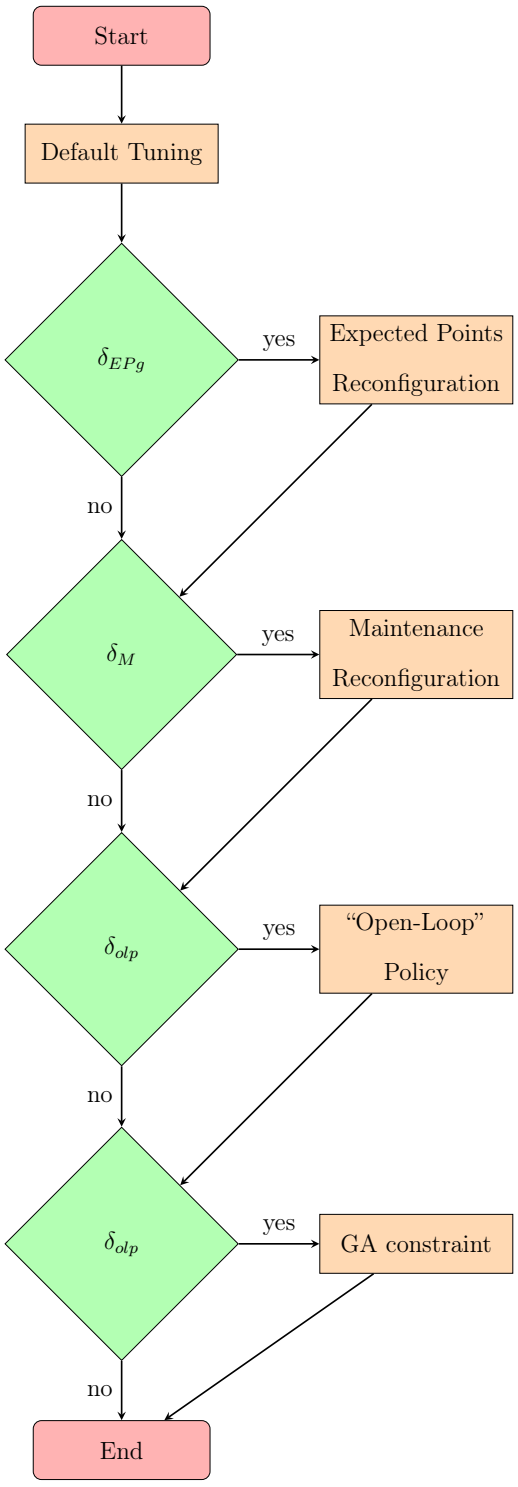

Figure 6.11: Flowchart Summarizing the Algorithm Followed in Tuning the Controller Based on the Participant's Performance.

PA interventions, which is followed in *YourMove*. However, the problem of missingness persists with EMA-measured behavioral constructs considered as disturbances in the controller model (*Perceived Barriers* ξ_5, and *Perceived Typicalness of Context* $\xi_{7Typicalness}$). Based on this observation, the control strategy utilized in *YourMove* must account for such circumstances.

In many cases for these particular constructs, participants either elect to provide the same answer to the EMA surveys or not comply with EMA measurements. In both scenarios, measurements for these constructs stagnate at a constant level that does not represent the true exogenous factors impacting the system. Consequently, behavioral scientists advise that these disturbances should not influence the closed-loop intervention decisions made by the controller. To mitigate the impact of stagnation in EMA-measured disturbances on the controller's objective function, we take advantage of the 3DoF-KF HMPC formulation and the rolling mean approach for data imputation. This is done by adjusting the initial value of the measured disturbances to equal the 7-day moving average. As a result, stagnant disturbance measurements for the mentioned behavioral constructs do not influence controller decisions.

In the 3DoF-KF HMPC formulation, deviation variables are utilized in the controller derivation (see Section 5.4). Moreover, in the implementation of the controller, all measured variables are considered in terms of deviation from initial values, which are assumed to be at steady-state. When measurements of behavioral constructs considered as measured disturbances become unreliable due to a lack of compliance from participants, their value settles at a constant level. This level is equivalent to the level a specific participant keeps on providing for EMA surveys, or the moving average value used for data imputation. In both cases, the utilization of the moving average as the initial condition for disturbances at each decision point for the controller cancels out the impact of such stagnant measurements on decision-making; the

effect of these disturbances on the system is treated as an unmeasured disturbance. As the 3DoF-KF HMPC formulation utilizes Kalman filtering to ensure robustness to unmeasured disturbances, this procedure for canceling out faulty measurements does not negatively affect the performance of the controller, however, it can reduce the degree of personalization of the closed-loop intervention.

6.5.4 "Open-Loop" Policy

As described in Chapters 4 and 5, when a low steady-state gain between *Behavior* and *Goals* exists in the predictive model, the optimal solution for MPC controller is to increase the goals as much as possible to push the participants towards more PA. As a result, extremely ambitious daily goals would be given to participants, which is not an effective way to influence sustained healthy behavior change. The devised control strategy addressed this problem, through setpoint tacking on the controlled variable (*Behavior* y_4) while constraining the readily available secondary output of GA. However, in cases of extremely low or negative steady-state gain in *Behavior* with respect to *Goals*, this formulation of the controller's objective proves ineffective. Moreover, it is observed that some of *YourMove* participants reach levels of daily steps that exceed the closed-loop setpoint of 10,000 steps/day, who can be labeled as "overachievers". For overachievers, a setpoint of 10,000 steps/day on the controller variable leads to providing lower *Goals* than the participant's performance. This defeats the purpose of the controller, as it would discourage the participant from overachieving and increasing their PA levels.

Therefore, there is a need to reconfigure the controller for such participants, to ensure the benefit of the intervention and provide "ambitious yet achievable" goals. This is done by disabling setpoint tracking on the controlled variables, $W_y = 0$. Instead, a target on *Goals* $u_{8,r}$ is set in place. This reconfiguration is applied for

both low gain and overachieving participants, with the logical conditions to activate it specified in (6.40).

$$\delta_{olp} = 1 \Leftrightarrow \delta_{lowgain} \vee \delta_{overachiever} \tag{6.40}$$

Where $\delta_{lowgain}$ is the established condition for low-gain tuning, specified by

$$\delta_{lowgain} = 1 \Leftrightarrow \lim_{s \to 0} \frac{y_4(s)}{u_8(s)} \leq 0.2 \tag{6.41}$$

and $\delta_{overachiever}$ is the condition to reconfigure the controller for overachievers, as defined by

$$\delta_{overachiever} = 1 \Leftrightarrow \left(\sum_{i=1}^{7} (y_{4,k-i} > 12,000)_i \geq 5 \right) \wedge \left(\frac{\sum_{i=1}^{7} y_{4,k-1}}{7} > 10,000 \right) \tag{6.42}$$

The levels to which the *Goals* target is adjusted depends on both the participant's model and performance. The low-gain tuning policy is activated when the modeled steady-state gain between *Behavior* y_4 and *Goals* u_8 for a given participant satisfied the condition shown in (6.41). Under this tuning policy, the target for *Goals* is set to $u_{8,r} = 10,000$ steps/day, to gear the controller towards providing daily step goals that lead the participants to more PA.

$$u_{8,r} = 10,000 \text{ steps/day}, W_u(1,1) = 1 \Leftrightarrow \delta_{lowgain} \tag{6.43}$$

On the other hand, when a participant's performance satisfies the conditions for overachievers specified in (6.42), a *Goals* target of $u_{8,r} = 13,500$ steps/day is followed. In addition, there is no need to provide financial incentives for overachievers. Hence, the financial rewards component of the intervention is turned off for participants who satisfy (6.42). This is done by adjusting the upper bound on the *Expected Points* to zero, that is $u_{max}(2) = 0$ points/day:

$$u_{8,r} = 13,500 \text{ steps/day}, u_{max}(2) = 0 \text{ points/day} \Leftrightarrow \delta_{overachiever} \tag{6.44}$$

In this tuning scheme for overachievers, the controller does not give points in contrast to the minimal use of the financial rewards approach followed in the maintenance phase. It is worth noting that in both cases of the open loop policy tuning, *Goal Attainment* y_7 constraints are enforced and adaptively tightened to ensure the delivery of achievable goals.

6.5.5 GA Constraints Tightening

A core control strategy utilized in *YourMove* is the implementation of output constraints on the *Goal Attainment* y_7 measurement to ensure the provision of "ambitious yet achievable" *Goals*. Therefore, it is crucial to carefully select constraint levels on GA to reach a balance between pushing the participants towards higher levels of PA and providing attainable goals to maintain engagement in the intervention. This is particularly relevant for cases where gains of the manipulated variables (especially *Goals*) for the estimated participant-specific models are insufficient to facilitate positive *Goal Attainment*; see Section 5.5.2. The implementation of slack to relax constraints on GA ensures the feasibility of the optimization problem. However, it allows the violation of the constraints, and consequently, the provision of very ambitious daily goals that can lead to participant dropout. To counter this effect, constraints on GA and the slack weight associated with them are dynamically adjusted in *YourMove* based on the participant's performance over the last 7 days.

The default tuning parameters utilized in *YourMove*, shown in Table 6.3, are selected to allow the controller to challenge the participants initially. The default tuning provides the controller with room to deliver ambitious goals through the selected small values for the lower constraint on GA and its corresponding slack weight.

$$y_{min}(4) = -2,500 \text{ steps/day}, W_s(4,4) = 5 \tag{6.45}$$

These selected values are the result of careful considerations and simulations, incorporating behavioral scientists' feedback. As the intervention progresses, it is important to adjust these tuning parameters based on the participant's performance. For participants who find the daily goals extremely challenging and fail to exceed them, stricter GA constraints and slack weights are gradually utilized as the number of days with negative GA increases within the last 7 days of the intervention. This is done adaptively, based on logical conditions considering the feedback signal of each participant's performance, which are presented below in the order by which they occur.

The adaptive tightening of GA constraints starts when a participant does not meet the daily goals on three out of the last 7 days, as shown in (6.46). In this case, the lower bound on GA and the slack weight are increased to $y_{min}(4) = -2,000$ steps/day and $W_s(4,4) = 25$, respectively.

$$\delta_{GA-3} = 1 \Leftrightarrow \sum_{i=1}^{7} (y_{7,k-i} < 0)_i = 3 \tag{6.46}$$

$$y_{min}(4) = -2,000 \text{ steps/day}, W_s(4,4) = 25 \Leftrightarrow \delta_{GA-3} = 1 \tag{6.47}$$

In addition, based on the expertise of behavioral scientists in the research team, the most recent days are more reflective of the participant's conditions and ability to achieve the provided goals. Hence, a higher emphasis should be placed on the participant's performance on the most recent days. Therefore, a higher slack weight is utilized when the goals are not achieved in the last three days, in accordance with (6.48)-(6.49), to "harden" GA constraints further:

$$\delta_{GA-3r} = 1 \Leftrightarrow \sum_{i=1}^{3} (y_{7,k-i} < 0)_i = 3 \Rightarrow W_s(4,4) = 30 \tag{6.48}$$

$$W_s(4,4) = 30 \Leftrightarrow \delta_{GA-3r} = 1 \tag{6.49}$$

In a similar manner, a tighter GA constraint enforcement is implemented when

Goal Attainment is negative for four out of the last 7 days, as shown in (6.50)-(6.53).

$$\delta_{GA-4} = 1 \Leftrightarrow \sum_{i=1}^{7} (y_{7,k-i} < 0)_i = 4 \tag{6.50}$$

$$y_{min}(4) = -1,500 \text{ steps/day}, W_s(4,4) = 35 \Leftrightarrow \delta_{GA-4} = 1 \tag{6.51}$$

Note that in this case the slack weight on GA constraints is significantly increased when the goals are not achieved for the last four consecutive days prior to the decision point k.

$$\delta_{GA-4r} = 1 \Leftrightarrow \sum_{i=1}^{4} (y_{7,k-i} < 0)_i = 4 \tag{6.52}$$

$$W_s(4,4) = 55 \Leftrightarrow \delta_{GA-4r} = 1 \tag{6.53}$$

In cases where *Goal Attainment* remains negative despite the adjustments made to controller tuning, a more aggressive approach is followed to ensure the attainability of the daily step goals, by adjusting input and output constraints as well as slack weights:

$$\delta_{GA-5g} = 1 \Leftrightarrow \sum_{i=1}^{7} (y_{7,k-i} < 0)_i \geq 5 \tag{6.54}$$

$$y_{min}(4) = -1,000 \text{ steps/day} \Leftrightarrow \delta_{GA-5g} = 1 \tag{6.55}$$

What distinguishes this approach is the enforcement of significantly stricter constraints, especially on the manipulated variable *Goals* u_8. In this approach, the upper constraint on u_8 is dynamically adjusted based on the average of the participant's performance for the last 7 days, as expressed in (6.56):

$$u_{max}(1) = \frac{\sum_{i=1}^{7} y_{4,k-1}}{7} + 2,000 \Leftrightarrow \left(\delta_{GA-5g} \wedge \frac{\sum_{i=1}^{7} y_{4,k-1}}{7} + 2,000 < 15,000 \right) \tag{6.56}$$

To provide the optimization problem with feasible constraints, the lower constraint on bound *Goals* is also reduced

$$u_{min}(1) = 1,000 \text{steps/day} \Leftrightarrow \delta_{GA-5g} \tag{6.57}$$

Moreover, the penalty weight for slack is gradually increased as the number of days with negative *Goal Attainment* increases, as described in (6.58)-(6.60).

$$W_s(4,4) = 65 \Leftrightarrow \left(\delta_{GA-5g} \wedge \sum_{i=1}^{7} (y_{7,k-i} < 0)_i = 5 \right) \tag{6.58}$$

$$W_s(4,4) = 75 \Leftrightarrow \left(\delta_{GA-5g} \wedge \sum_{i=1}^{7} (y_{7,k-i} < 0)_i = 6 \right) \tag{6.59}$$

$$W_s(4,4) = 100 \Leftrightarrow \left(\delta_{GA-5g} \wedge \sum_{i=1}^{7} (y_{7,k-i} < 0)_i = 7 \right) \tag{6.60}$$

Furthermore, the implementation of an upper constraint on *Goal Attainment* can be utilized to ensure the provision of ambitious daily goals. This is done for cases where a participant consistently outperforms the provided *Goals* by a significant margin, without satisfying the condition for overachievers defined in (6.42). Multiple reasons can lead to such circumstances, including plant-model mismatch. To account for such scenarios, an upper output constraint is placed on GA when the participant overachieves Goals by at least a 3,000 steps/day margin for more than four out of the last 7 days. Additionally, the upper constraint on GA is dropped, as expressed in (6.61)-(6.62).

$$\delta_{GA+5} = 1 \Leftrightarrow \sum_{i=1}^{7} (y_{7,k-i} \geq 3,000)_i \geq 5 \tag{6.61}$$

$$y_{min}(4) = -\infty,\ y_{max}(4) = 300 \text{ steps/day} \Leftrightarrow \delta_{GA+5} = 1 \tag{6.62}$$

6.5.6 Expected Points Reconfiguration

It is observed that the DSPSA ARX estimated models for some participants might not select *Expected Points* as a relevant input for the participant. Moreover, some models characterize negative steady-state gain between *Behavior* y_4 and *Expected Points* u_9. Under such circumstances, the controller is reconfigured by adjusting the

target on *Expected Point* $u_{9,r}$ and its associated penalty weight.

$$\delta_{lowEPgain} = 1 \Leftrightarrow \lim_{s \to 0} \frac{y_4(s)}{u_9(s)} \leq 0 \tag{6.63}$$

$$u_{9,r} = 250 \text{ points/day}, W_u(2,2) = 1 \Leftrightarrow \delta_{lowEPgain} \tag{6.64}$$

This is done to steer the controller towards offering financial incentives, in the form of *Expected Points*, to motivate the participants to engage in more PA.

6.5.7 Transitioning Back to Default Tuning

Participants' engagement in PA and compliance with wearing the activity-tracking device can vary tremendously within the span of the study. For instance, the effect of wearing a new activity tracker can lead to a temporary increase in the number of steps a person takes per day at the beginning of the intervention. In addition, participants' ability to engage in PA may decrease at different periods of the intervention due to various life events (e.g., undergoing surgery, or getting a new job). Therefore, a participant's average performance can drop at any time. Similarly, a participant's average performance can bounce back abruptly, once the life events subside or the participant adapts to them (e.g., recovering to good health, or adapting to a new work schedule). When such life events unfold, they can render the transition to default tuning and controller formulation infeasible, because of unrealizable default constraints on the manipulated variable *Goals* u_8.

The infeasibility in this case is caused by conflicting upper movesize constraint $\Delta u_{8,max}$ and the lower input constraint $u_{8,min}$. To guarantee the feasibility of the controller's objective function and a smooth transition back to the default controller configuration, the movesize constraint for *Goals* Δu_8 is adaptively adjusted as expressed in (6.65)-(6.66). Relaxing the movesize constraint in this manner guarantees the feasibility of delivering a daily goal for the participant that reflects the observed

bounce back in the participant's *Behavior* levels.

$$\delta_{ms} = 1 \Leftrightarrow u_{8,k-1} + \Delta u_{8,max} \leq u_{8,min} \tag{6.65}$$

$$\Delta u_{8,max} = u_{8,min} - u_{8,k-1} + 500 \Leftrightarrow \delta_{ms} \tag{6.66}$$

6.6 Preliminary Results

The *YourMove* is currently still underway (Spring 2024), with 94 participants enrolled in the controller phase. The final results of this study will be analyzed in future work, once the year-long study is over for the entire study cohort. A total of 380+ participants are to be enrolled in the study. Half of the participants in *YourMove* are randomly selected in the COT intervention group receiving the closed-loop intervention. The other half of the cohort is assigned to the control group, receiving a fixed 10,000 steps/day daily step goal throughout the intervention. In this section, preliminary results for representative participants in the COT group are presented and discussed.

YourMove is the first COT study implemented in collaboration with the Herbert Wertheim School of Public Health and Human Longevity Science at the University of California San Diego. The implementation of an automated personalized closed-loop optimal PA intervention on a large scale has brought about challenges, exposed bugs, and uncovered many technical issues. A bug in the code base affected the DSPSA ARX model estimation step for the first few batches of participants, but this was corrected. The bug led to the selection of the highest weighted average NRMSE fit model out of the DSPSA models estimated only for the last iteration in each combination of estimation-validation data, rather than selecting the model with the highest weighted average NRMSE fit across all estimated models. This bug was caught and fixed on September 22nd, 2023, and has impacted every participant

who was enrolled in the controller phase before that date (approximately 30% of the intervention group) to a varying extent. DSPSA ARX model estimation was re-executed during the closed-loop stage of the intervention for affected participants. Two out of the three representative participants presented in the subsequent section were affected by this technical issue.

6.6.1 Participant A

Participant A is an example of an adherent participant who is engaged in the intervention. This participant was able to wear their watch throughout the observed study days, averaging 1,319 minutes/day of fitbit wear-time throughout the intervention. As can be seen in Fig. 6.12, in the baseline stage this participant did well, averaging approximately 6,647 steps/day with a median of 6,405 steps/day. Consequently, a scaled goals factor between 0 to 0.25 was utilized to personalize the input signals realizations for this participant, as described in Section 6.3.4. As a result, the range covered by *Goals* u_8 in the system identification stage is between 6,405 and 8,005 steps/day. On the 11th day of the intervention, the participant received the first daily step goal at the beginning of the system identification stage. This initial participant engagement in the intervention is evident in the noticeable increase in *Behavior* y_4 levels upon the introduction of the intervention components.

In the first cycle of the system identification stage of the intervention, this participant's *Behavior* peaked at the highest level observed throughout this stage at 19,632 steps/day, significantly outperforming the provided goals. As seen in Fig. 6.12, *Behavior* y_4 decreased off that peak and settled at a level slightly higher than the range covered by the personalized *Goals* signal. This participant managed to reach or exceed the daily goals for all but one day out of the 132 days in the system identification stage. Moreover, the average step count for this participant over the system identi-

fication is 9,485 steps/day, which is 1,480 steps/day higher than the maximum goal given in that period. This can indicate that the provided daily goals were not adequately challenging for this participant, which can lead to a mismatch between the estimated dynamics from the system identification data and the plant dynamics during the closed-loop intervention (when more challenging goals were provided). One of the possible causes of this issue is the short duration of the baseline stage; the use of the median of 10 days might not be a good representation of the participant's baseline. Secondary data analyses, including cross-participant analyses, will help explore such possibilities and guide future COT experiments, by revising and improving the logic utilized in the personalization of the input signal design to deliver "ambitious yet achievable" goals.

The presented model dynamics for this participant are the result of the corrected DSPSA ARX model estimation done on September 22nd, 2023. The DSPSA ARX algorithm did not select *Temperature* ξ_{7T}, *Expected Points* u_9, and *Granted Points* u_{10} as relevant inputs for the model estimated for this participant; only *Weekend* ξ_{7wknd}, *Perceived Barriers* ξ_5, *Perceived Typicalness* $\xi_{7Typicalness}$, and *Goals* u_8 were selected, as illustrated by the unit step responses in Fig. 6.13. The model with the highest weighted average NRMSE fit F_{wa} was estimated utilizing data from the first four cycles (66.67%). Goodness-of-fit NRMSE indices for the estimated model are 9.30% over validation data, 3.87% over estimation data, and 10.15% across the overall dataset collected in the system identification stage. While the fit percentages of the estimated model for this participant are not significantly high, some important system dynamics are explained by the estimated model. For instance, one of the noticeable characteristics of the observed *Behavior* for this participant in the system identification stage is that the majority of the days with a significantly high daily step count occur on weekends, and on days where *Perceived Typicalness* ξ_7 is high.

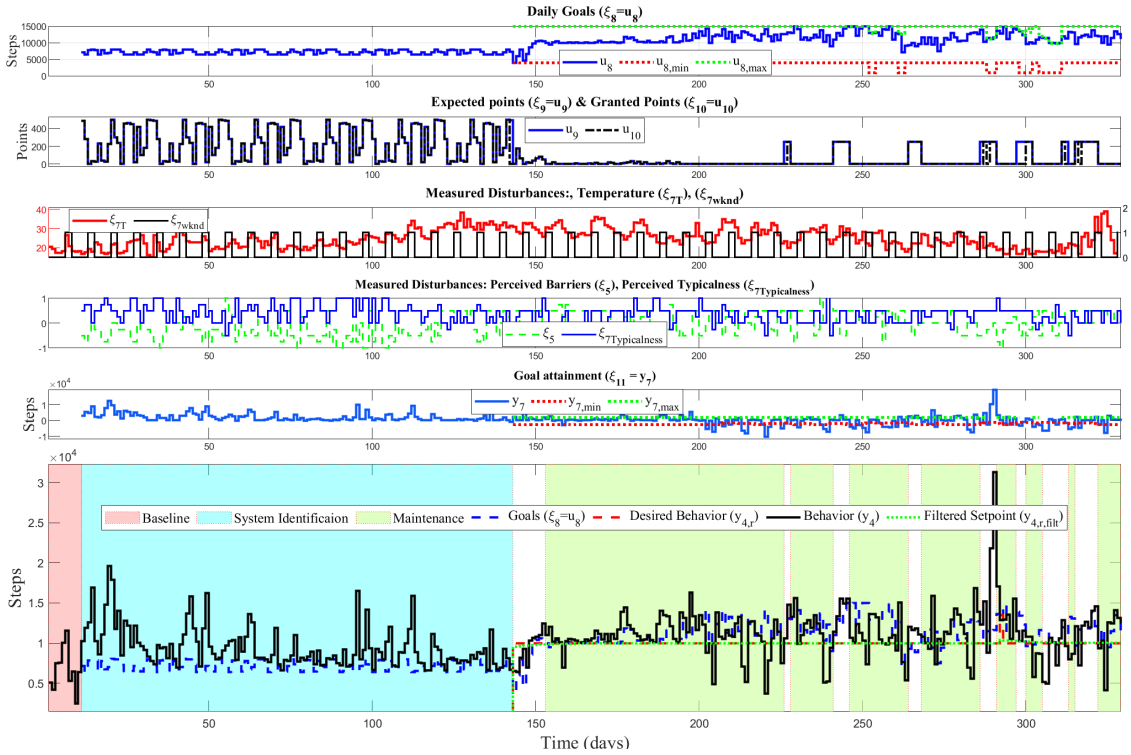

Figure 6.12: Participant A Data for the Three COT Stages of *YourMove* Study. The Open-Loop Stages (Consisting of Baseline and System Identification Stages) Are Highlighted in Red and Cyan, Respectively. The Closed-Loop Stage of the Controller Consists of the Initiation Phase (Unhighlighted), and the Maintenance Phase (Highlighted in Green).

On the other hand, the participant does not significantly exceed the daily goals on weekdays, or when ξ_7 is low. As observed in Fig 6.13, the magnitude of the steady-state gains for these two inputs are the highest in the estimated participant-specific model. Moreover, the inverse response estimated for the impact of *Weekend* ξ_{7wknd} contribute to the peaks observed in the participant's *Behavior* in response to the pulses representing weekends in the input signals. Finally, due to the range of the provided *Goals* u_8 during the system identification experiment, the model is most likely underestimating the impact of higher goals on the participant's response. While

the gain between *Goals* u_8 and *Behavior* y_4 is positive at 0.337, the implemented *Goals* range most likely did not produce a dataset informative of the dynamics between the outputs and *Goals* at a level where the provided goals are more challenging for the participant. The work done by Martín *et al.* (2020) proposes that the relationship between *Goals* u_8 and daily step count y_4 is nonlinear, following an inverted U shape. Under such an assumption, extremely ambitious and not sufficiently ambitious goals can lead to the underestimation of the impact of adequately challenging *Goals* on the participant's response.

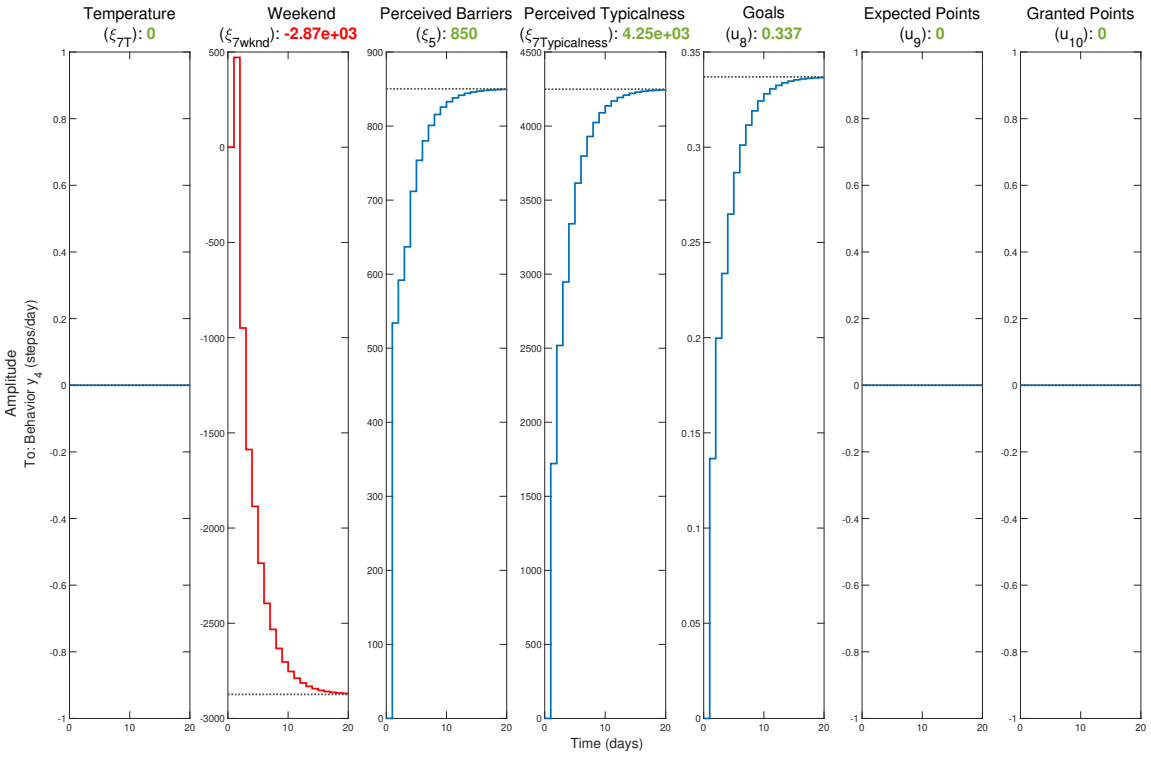

Figure 6.13: Unit Step Responses for the Estimated Model Dynamics for Participant A, Along with Their Respective Steady-state Gains.

Despite the challenges faced in model estimation, the re-estimation of this participant's model due to the reported bug in the code, and the low goodness-of-fit

for the estimated participant-specific model, the performance of the controller in the closed-loop phases of the intervention is excellent, and matches expectations based on previous work and simulations. On the 143rd day of the intervention, the closed-loop stage of the intervention started as illustrated by the introduction of the setpoint reference $y_{4,r}$ and filtered setpoint reference $y_{4,r,filt}$. The controller was commissioned under default tuning in the initiation phase for the first 10 days of the closed-loop stage of the intervention. As illustrated in Fig. 6.12, during this period the controller guided the participant towards the desired setpoint of 10,000 steps/day by gradually increasing *Goals* u_8 and utilizing *Expected Points* u_9. By the 153rd day of the intervention, the participant's performance was consistently within the tolerance region and met the condition for maintenance, described in (6.39), activating the maintenance phase. Consequently, the controller is reconfigured and the use of the financial rewards (u_9 and u_{10}) was phased off. The controller provided the participant with "ambitious yet achievable" goals consistently, while *Behavior* y_4 remained within the healthy behavior zone consistently from the activation of the maintenance phase. As observed in Fig 6.12, *Goal Attainment* y_7 constraints were satisfied on most days within this period of the intervention, the only violation of the lower constrain $y_{7,min}$ happened on day 158 and was within an acceptable margin. On the 193th day of the intervention, the DSPSA ARX model estimation algorithm was rerun for this participant after fixing the bug. As a result, a new participant-specific model was estimated and then utilized for the remainder of the closed-loop stage of the intervention. The introduction of a new participant-specific model did not have a visible impact on the controller's performance. It did not cause transient or abrupt changes in the manipulated variables for this participant.

By the 200th day of the intervention, a shift in the participant's behavior possibly occurred. This is evident in the sudden change in the participant's *Behavior* y_4 levels

on weekdays; the participant's step count was significantly lower on weekdays than their average performance thus far in the intervention as can be seen in Fig. 6.12. This shift in the participant's behavior could possibly be attributed to a change in system dynamics, which can be attributed from a behavioral science perspective to a change in life rhythms (e.g., starting a new job, change in work or school schedule, etc). Moreover, despite the change in the daily step count behavior from this participant, levels of EMA-measured disturbances included in the system model remain within the same range observed in the days prior to this behavioral shift. This indicates that another possible cause for the shift in the participant's behavior can be an unmeasured disturbance that started taking effect on day 200. In either case, the implemented 3DoF-KF HMPC formulation is robust to both plant-model mismatch and unmeasured disturbances through the Kalman filter implementation. Exist interviews at the end of the intervention will help in identifying the possible root cause for such a shift in behavior through qualitative survey questions. After day 200, the participant did not achieve the given daily goals on the observed weekdays with low step counts which led to the violation of the lower constraint on the *Goal Attainment*. During these periods of low participant performance on weekdays, the controller initially increased the daily goals to push the participant toward a higher level of PA. However, when the participant did not respond well, GA constraints were tightened through controller reconfiguration, as described in Section 6.5.5. Consequently, upper and low constraints on *Goal Attainment* $y_{7,max}$ and $y_{7,min}$ were adjusted based on the participant's performance and more achievable *Goals* were delivered to the participant by the controller, as can be seen in Fig 6.12.

Due to the low *Behavior* levels for this participant on weekdays after the 200th day of the intervention, the condition for maintenance was not met consistently. As a result, the initiation phase was reactivated whenever the condition in (6.39) was not

satisfied. This allowed the controller to utilize *Expected Points* u_9 and *Granted Points* u_{10}, to motivate the participant to engage in more PA each time the initiation phase was reactivated and GA levels remained negative. Note that *Expected Points* use followed the manipulated variable target $u_{9,r} = 250$ point/day, as described in (6.63)-(6.64), because of the zero steady-state gain between *Behavior* and *Expected Points* in the participant-specific model estimated on day 193. The participant responded well to the reactivation of the initiation phase. Each time the initiation phase was reactivated, *Behavior* y_4 level improved and rose back to the healthy behavior zone, which reintroduced the maintenance phase, as illustrated in Fig. 6.12. Additionally, after the 200th day of the intervention, the participant reached significantly high *Behavior* levels after every dip in their performance. This can be attributed to the participant compensating for missing the provided *Goals* on the previous days.

The presented results illustrate the effectiveness of the 3DoF-KF HMPC-based closed-loop intervention for this participant. The average level of the participant's *Behavior* in the closed-loop stage of the intervention is 11,383 steps/day, which is above the desired setpoint for the daily step count and higher than the average of the baseline and the system identification stages. In addition, the judicious formulation of the controller's objective function through the implementation of adaptive controller tuning and reconfiguration led to the provision of "ambitious yet achievable" goals for the majority of the intervention. This robustness of the 3DoF-KF HMPC formulation proved to be effective, even when the utilized participant-specific model did not have high goodness-of-fit indices, and in the presence of a plant-model mismatch. This is particularly illustrated by the consistent controller performance, despite the change in the predictive model that occurred on day 193 of the intervention for this participant.

6.6.2 Participant B

Participant B is another adherent participant in *YourMove*; this participant averaged 1,265.5 minutes/day of wear-time over the presented days of the study. Since the beginning of the intervention, Participant B has been very active. This is evident in their performance in the baseline stage. Participant B averaged 15,500 steps/day over the 10 baseline days with a median of 14,964 steps/day. Hence, the scaled goals factor signal was scaled to be between 0 and 0.25, resulting in a *Goals* u_8 range of 3,741 steps/day in the system identification stage (between 14,964 to 18,705 steps/days). On the first day of the system identification stage, the participant did not meet the daily goal. However, the participant responded to the high daily *Goals* well at first by increasing their *Behavior* levels and reaching daily step counts as high as 23,530 steps/day in the first system identification cycle, as illustrated in Fig.6.14.

Despite the best efforts to adjust to the elevated *Goals* range, it proved to be very challenging for this participant. As evident in Fig. 6.14, the participant was not able to meet the provided ambitious daily goals and maintain high levels of *Behavior* after the first goals cycle. Matter of fact, this participant achieved positive *Goal Attainment* only on 57 days out of the 132 days system identification stage (48.18%). Furthermore, the average *Behavior* level for this participant over the system identification stage is 15,506 steps/day. This indicates that the daily goals provided in this were extremely challenging for the participant, which can lead to underestimating the impact of adequately challenging *Goals* on *Behavior*, causing a mismatch between the dynamics of the model estimated based on system identification stage data and the real system dynamics. The challenging *Goals* signal range in the system identification phase provided to this participant affirms the need for improvements to the personalization of the input signals; the provided daily *Goals* in the system identification experiment

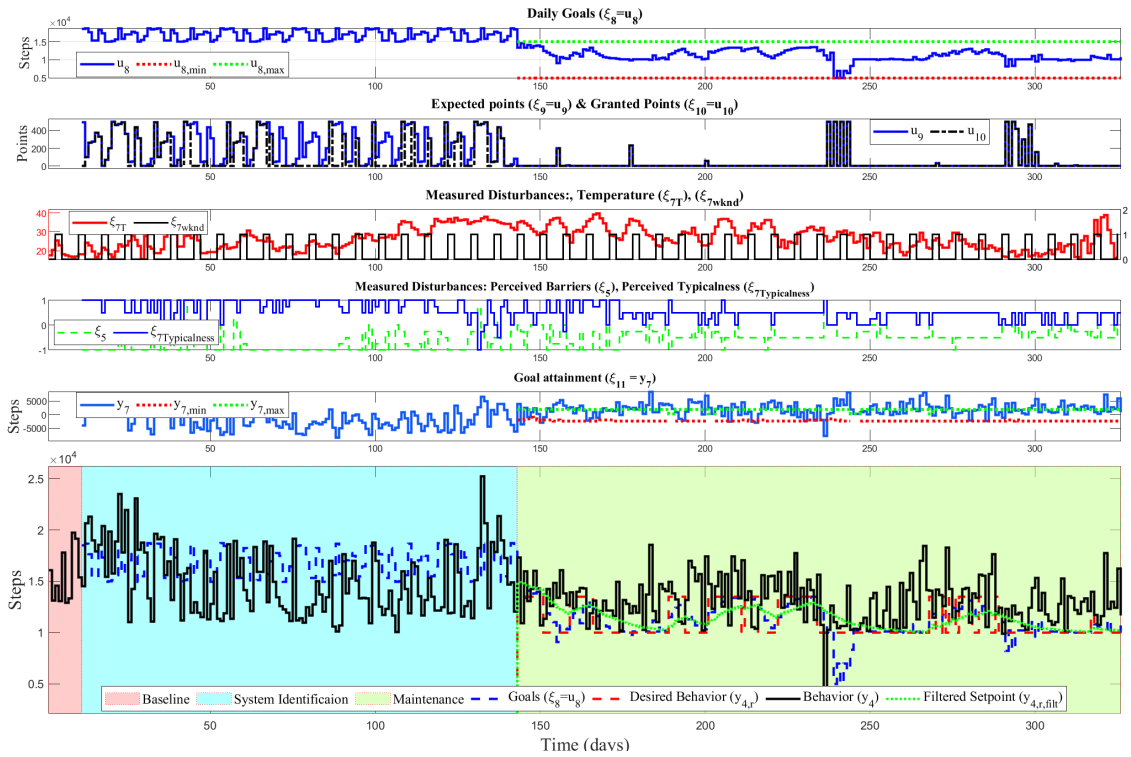

Figure 6.14: Participant B Data for the Three COT Stages of *YourMove* Study. The Open-Loop Stages (Consisting of Baseline and System Identification Stages) Are Highlighted in Red and Cyan, Respectively. The Closed-Loop Stage of the Controller Consists of the Initiation Phase (Unhighlighted), and the Maintenance Phase (Highlighted in Green).

should capture the response of the participant to "ambitious yet achievable" goals.

The examined model for this participant is the result of the corrected DSPSA ARX model estimation done on September 22nd, 2023. All seven considered inputs were selected DSPSA ARX algorithm as demonstrated in the unit step responses presented in Fig. 6.15. The order of the ARX model for this participant is $n_a = 3$, $n_b = [1\ 3\ 1\ 1\ 2\ 3\ 2]$, and $n_k = [1\ 1\ 1\ 1\ 1\ 1\ 1]$. Four out of the six system identification cycles (66.67%) were utilized to estimate this model. The four cycles used as estimation sub-experiments for this participant are the first, second, fourth, and

sixth cycles. The estimated participant-specific model yielded NRMSE goodness-of-fit indices of 15.86%, 14.17%, and 17.38% over the validation, estimation, and overall data, respectively. Note that the steady-state gain between *Goals* u_8 and *Behavior* y_4 is at 0.139, which is low enough to place this participant in the "open-loop" control policy in the closed-loop stage of the intervention, see Section 6.5.4. This is the result of the elevated *Goals* levels provided to the participant in the system identification stage. Contrary to Participant A, Participant B was less active over weekend days; Participant B walked 1,423 steps/day less on weekends compared to weekdays over the system identification stage. This is reflected in the unit step response dynamics for *Weekend* ξ_{7wknd}, presented in Fig. 6.15, where the inverse underdamped response captures the immediate decrease in *Behavior* levels on weekends.

Closed-loop data for Participant B showcases another successful personalized closed-loop 3DoF-KF HMPC-based intervention, as demonstrated in Fig.6.14. Because of the high daily step count for this participant at the end of the system identification stage, the condition for maintenance was met from the first day of the closed-loop stage of the intervention. As a result, this participant entered the closed-loop stage directly in the maintenance phase, and there was no need for an initiation phase. Therefore, the use of the financial rewards component of the intervention was minimal after day 143. Additionally, the high performance of Participant B at the end of the system identification stage satisfied the condition for overachievers in the "open-loop" control policy, where the target reference tracked by the controller objective function is on the manipulated variables, see Section 6.5.4. Therefore, the controller was reconfigured to follow a target of $u_{8,r} = 13{,}500$ steps/day each time the condition in (6.42) was satisfied. In addition, because of the low gain between *Behavior* and *Goals* in the estimated participant-specific model, Participant B satisfied the low gain condition (6.41) in the "open-loop" control policy as well. Consequently, each time

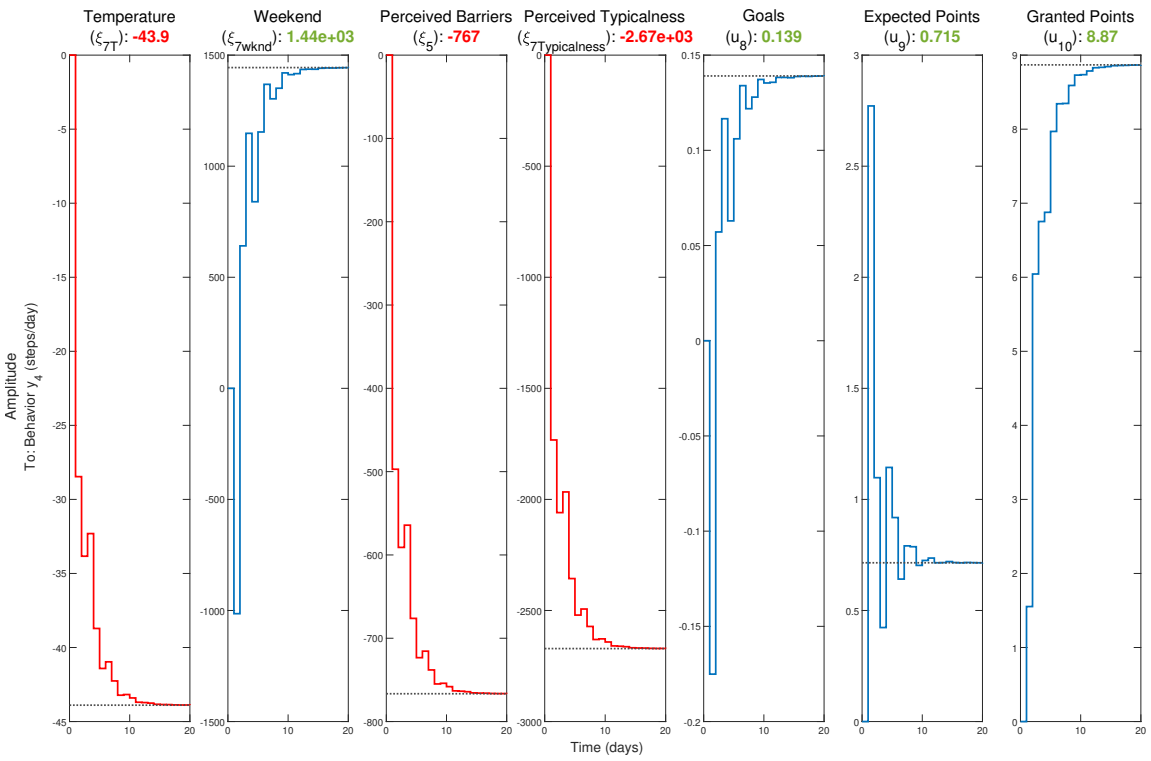

Figure 6.15: Unit Step Responses for the Estimated Model Dynamics for Participant B, Along with Their Respective Steady-state Gains.

this participant's *Behavior* y_4 levels did not satisfy the condition for overachievers, the controller was reconfigured to the low-gain tuning in the "open-loop" policy by adjusting the target on *Goals* to $u_{8,r} = 10{,}000$ steps/day.

The results for Participant B illustrate the effectiveness of the maintenance reconfiguration in helping participants sustain healthy levels of PA. As observed in Fig. 6.14, Participant B enrolled in the controller stage directly in the maintenance phase, and remained in the maintenance phase throughout the presented 189 days of the closed-loop 3DoF-KF HMPC-based part of the intervention. The average daily step count for this participant over the presented closed-loop stage of the intervention is 13,087 steps/day, approximately 2,000 steps/day lower than the average *Behavior*

level in the system identification stage. However, the average over the closed-loop stage is considerably higher than the 10,000 steps/day level recommended by various health agencies, including the CDC. This participant walked more than 10,000 steps/day on all but two days out of the observed 189 days of the closed-loop stage. This was achieved through the provision of "ambitious yet achievable" goals throughout the closed-loop stage of the intervention. As evident in the *Goal Attainment* y_7 signal in Fig. 6.14, Participant B met or exceeded the given *Goals* on most of the days in the closed-loop stage. Additionally, the lower constraint on *Goal Attainement* $y_{7,min}$ was violated on four days only in this stage. In three out of those four occurrences, the margin for violation of the constraint was negligible. The only significantly negative *Goal Attainment* in the closed-loop for Participant B occurred on day 236 of the intervention, where the participant was more than 8,000 steps/short of achieving the goal. This is believed to be an outlier that could have been possibly caused by technical issues in data collection, which will be investigated further in secondary data analyses after the experiment is over for all participants. The predictive model for Participant B was re-estimated on day 190 of the intervention, after correcting the described bug in the DSPSA ARX code base. The presented closed-loop data in Fig. 6.14 do not show that the introduction of the new model on day 190 caused transient or had a negative impact on the controller's decisions. The only observed anomaly in the *Goals* provided by the controller happened between days 239 to 241 of the intervention, where the given *Goals* were very low. These low levels of *Goals* are believed to be caused by technical issues that impacted measurements on day 236 of the intervention, especially for EMA-measured disturbances.

Closed-loop results for Participant B further affirm the robustness of the 3DoF-KF HMPC formulation and the effectiveness of the "digital PA couch tuning" rules in implementing personalized PA behavior change interventions, facilitating the adop-

tion and maintenance of healthy levels of PA. Even when the conditions of the system identification experiment were not ideal, the estimated participant-specific model did not have high NRMSE fit indices, technical issues were faced, and the participant-specific model was changed during the closed-loop stage, the judicious and robust formulation of the controller's objective function managed to deliver "ambitious yet achievable" daily goals and assisted Participant B in sustaining healthy PA levels.

6.6.3 Participant C

Participant's C adherence is on par with the previously presented participants. Participant C wore their Fitbit device every day of the reported intervention days, averaging 1,267 minutes/day of wear-time. As illustrated in Fig. 6.16, Participant C was active during the baseline stage, over which this participant averaged 9,920 steps/day with a median of 10,132 steps/day. Consequently, the *Goals* input signal was scaled utilizing a scaled goals factor between 0 and 0.25, as described in Section 6.3.4. Therefore, the personalized *Goals* signal in the system identification stage covered the range between 10,132 and 12,665 steps/day. Following the baseline stage, the system identification stage was introduced on the 11th day of the intervention, in which the participant responded well to the level of the delivered *Goals*.

During the system identification stage of the intervention, the covered *Goals* u_8 range proved to be adequately challenging for Participant C. This is evident in Participant's C performance throughout this stage, where they were able to meet or exceed the daily *Goals* on 72 out of the 132 days of the system identification stage, reaching 54.6% positive *Goal Attainment* throughout that period. Additionally, the average *Behavior* y_4 level for Participant C is 11,179 steps/day which is higher than their baseline average. This indicates that this participant responded well and was engaged with the *Goals* intervention component during this stage. As a result, the

participant's average performance in this stage exceeded the CDC-recommended daily step count of 10,000 steps/day. Another interesting observation about Participant C's engagement in the intervention is noted in the EMA-measured disturbances. As can be seen in Fig. 6.16, Participant C responded to EMA surveys in the system identification stage in a different manner than in the closed-loop stage. On the majority of the system identification days, Participant C responded with the same answer to almost all EMA survey questions or did not respond at all. This can indicate that Participant C was not very engaged with daily micro-EMA surveys during this stage. The lack of variability in the EMA-measured exogenous signals can lead to the misrepresentation of real system dynamics in the estimated dynamic model, because of the lack of persistence of excitation in the signals (Ljung, 1999). On the other hand, in the closed-loop stage, especially after day 180 of the intervention, Participant C started providing varying answers to EMA survey questions. This may indicate a possible shift in the participant's behavior and engagement in the intervention, particularly in EMA surveys, during the closed-loop stage which can cause plant-model mismatch.

The implementation of the DSPSA search algorithm in ARX model estimation yielded the highest NRMSE goodness-of-fit index in model cross-validation out of the three representative participants presented in this work. NRMSE fit percentages for Participant C are 26.47%, 13.40%, and 7.57% for validation, estimation, and overall data, respectively. The orders of the DSPSA selected model with the highest weighted average fit percentage F_{wa} are $n_a = 2$, $n_b = [2\ 1\ 3\ 3\ 3\ 2\ 2]$, and $n_k = [1\ 1\ 1\ 1\ 1\ 1\ 1]$. Data for the first, second, third, and fifth input signal cycles were utilized as estimation sub-experiments (66.67% estimation data), whereas the fourth and sixth sub-experiments were used in cross-validation (33.33% validation data). As demonstrated in Fig. 6.17, DSPSA selected all features in the estimated ARX model

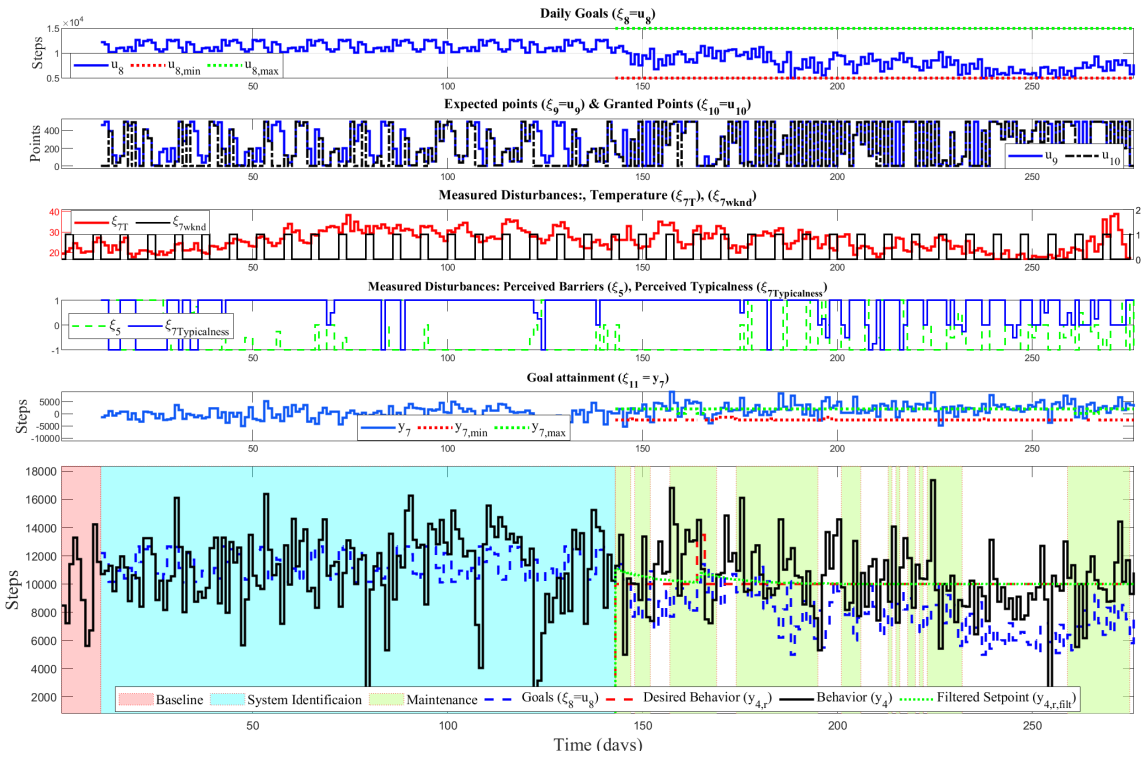

Figure 6.16: Participant C Data for the Three COT Phases of *YourMove* Study. Baseline, System Identification, and Maintenance Phases Are Highlighted in Red, Cyan, and Green, Respectively.

for Participant C.

The dynamics and steady-state gain between *Behavior* y_4 and *Goals* u_8 in the estimated participant-specific model for Participant C reflect their response to "ambitious yet achievable" daily goals, based on the covered *Goals* range and the participant's performance in the system identification stage. The steady-state gain in *Behavior* with respect to a unit step change in *Goals* is 0.672, as illustrated in Fig. 6.17. One of the interesting dynamics in the model estimated for Participant C is observed in the unit step response for *Expected Points* u_9. The inverse initial response and the negative direction of the gain imply that the participant-specific model predicts that *Behavior* y_4 will slightly increase initially upon receiving *Expected Points* before

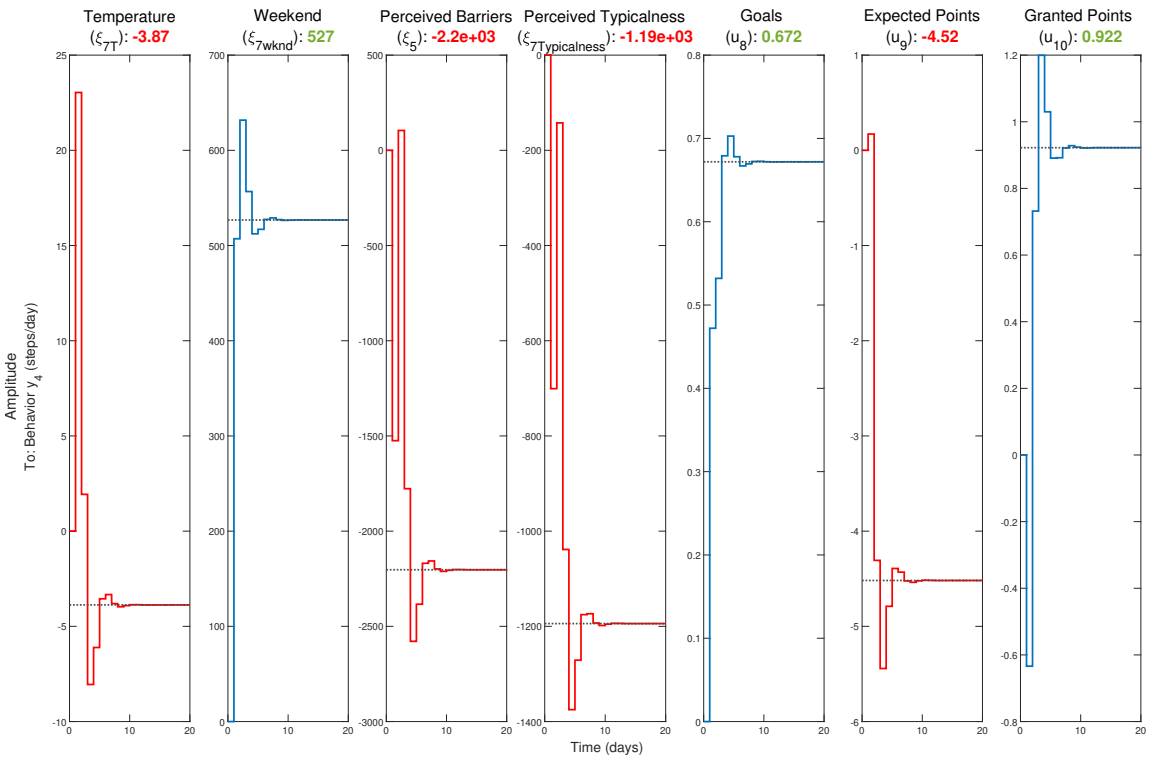

Figure 6.17: Unit Step Responses for the Estimated Model Dynamics for Participant C, Along with Their Respective Steady-state Gains.

significantly decreasing and settling at a lower level. It is important to analyze the response to *Expected Points* u_9 in unison with the unit step response to *Granted Points* u_{10}, as both signals form the financial rewards positive reinforcement component of the intervention. It is noteworthy to highlight that by the superposition principle, the combined steady-state gain of the financial rewards component is negative. This means that the participant-specific model predicts that Participant C will walk less upon receiving *Expected Points*, whether the participant is granted the points upon achieving the given goal or not. This is contrary to the aim of the positive reinforcement component of the intervention and can be indicative that the estimated model might not represent the actual dynamics of the financial rewards intervention com-

ponent for this participant. Additionally, the negative steady-state gain for *Expected Points* in the estimated participant-specific model had implications on the controller implementation, as it led to controller reconfiguration following section 6.5.6.

On day 143 of the intervention, the controller was commissioned as the participant entered the closed-loop stage of the intervention. Participant C concluded the system identification stage with high *Behavior* levels, therefore, the maintenance phase was activated from the first day of the closed-loop stage, as demonstrated in Fig. 6.16. On the second day of the closed-loop stage, Participant C missed the given goal with a significant margin due to low Fitbit wear-time, which violated the lower constraint on *Goal Attainment* $y_{7,min}$. In response, the controller delivered lower *Goals*. Participant C returned to wearing their Fitbit watch consistently, therefore the measured *Behavior* increased back to levels within the tolerance region. However, the maintenance condition was violated due to underperformance on day 145. As a result, the initiation phase was activated for one day, on day 147, and then the maintenance phase was reactivated. Fluctuations in Participant C's *Behavior* levels caused the controller to deactivate and reactivate the maintenance phase throughout the closed-loop stage based on the condition defined in (6.39). While this was intended by design, the rapid switching from one configuration to another is not desired. To counter this effect, a longer number of previous data points n_{tol} or a higher tolerance region should be utilized in the maintenance condition in future studies.

The switch in Participant C's engagement and responses to EMA surveys after day 180 of the intervention impacted the controller's decisions, as illustrated in Fig. 6.16. The dynamics captured in the participant-specific model were estimated based on the data gathered in the system identification stage, which showed different characteristics in terms of EMA-measured disturbances variability and levels. As a result, the predicted controlled variable values over the prediction horizon in the 3DoF-KF

HMPC algorithm at each decision point were low. Consequently, the controller delivered lower *Goals* to not violate constraints on the *Goal Attainment* over the prediction horizon. Despite plant-model mismatch, the controller adjusted the delivered *Goals* based on the feedback signal and guided Participant C back to the healthy behavior zone every time the participant relapsed. The controller's response could be made more aggressive through intuitive adjustments to tuning parameters. For instance, a higher value for the Kalman filter coefficient f_a^2 corresponding to *Behavior* would lead to more aggressive moves in the manipulated variables through feedback error correction, as expressed in the 3DoF-KF HMPC formulation in Section 5.4.1. Another possible approach to deal with scenarios where EMA-measured disturbances negatively impact prediction accuracy is by reducing the speed of response to such measured disturbances. This can be done through the 3DoF formulation, by increasing the filter coefficients corresponding to EMA-measured disturbances (α_d^3 and α_d^4).

Moreover, the observed chattering in the *Expected Points* u_9 is attributed to the estimated characteristics of the dynamics response of *Behavior* to changes in *Expected Points*. Based on the negative steady-state gain for *Expected Points*, the controller was reconfigured to target a manipulated variable reference of $u_{9,r} = 250$ points/day. However, the predicted negative effect of this manipulated variable on the *Behavior* y_4, based on the participant-specific model, conflicted with the objective of reaching setpoint reference for *Behavior* $y_{4,r}$. Therefore, the controller fluctuated the expected points in the observed manner to balance between the targets in the objective function and mitigate the impact of *Expected Points*. To counter this effect in future implementations, the penalty weight on the manipulated variable reference $w_{9,u}$ should be lowered, giving the target on the controlled variable a higher priority.

The closed-loop intervention results for Participant C demonstrate the effectiveness of the 3DoF-KF HMPC formulation in delivering a personalized behavioral inter-

vention, assisting the participant toward reaching and maintaining healthy behavior. This is demonstrated in the way the controller guided the participants back towards a healthy level of daily step counts each time the participant relapsed. Moreover, the provided daily goals to Participant C were achievable and challenged the participant as needed to bring them back to the set reference. The lower constraint on the *Goal Attainment* $y_{7,min}$ was only violated on a few occasions, which was negligible margins. On the other hand, the upper constraint $y_{7,max}$ was violated on a majority of the closed-loop intervention stage, indicating that the provided *Goals* could have been more challenging. To make the *Goals* more challenging in future COT studies, constraint tightening should be performed on the upper constraint in a similar manner to the lower constraint tightening in the "digital PA coach tuning". Nonetheless, over the observed 143 days of the closed-loop stage of the intervention, Participant C averaged a *Behavior* level of 10,307 steps/day.

6.7 Preliminary Findings & Future Work

As the *YourMove* study is still ongoing at the time of writing this dissertation, it is important to note that the presented results and findings are specific to the considered participants with high Fitbit wear time and cannot yet be generalized. Future data analysis, after the conclusion of the study, will shed light on the effectiveness of the proposed COT intervention framework and the 3DoF-KF HMPC formulation in delivering PA behavioral interventions on a population level, in contrast to the control group which was given a constant daily goal of 10,000 steps/day. However, the COT framework is geared toward personalized optimal behavioral interventions. Hence, analyzing idiographic results is crucial to understanding the shortcomings in *YourMove* and improving the effectiveness of personalized optimal closed-loop behavioral interventions in another essential step towards their implementation on a large scale.

The real-world implementation results of the COT framework in *YourMove* offer an unprecedented opportunity to evaluate the unique nature by which each participant responds and interacts with the intervention components, throughout the three stages of the intervention. The learned lessons for each stage of the COT will form the foundation and provide needed *a priori* knowledge for future COT interventions. From analyzing the data of the three presented participants in this work, it is clear that revisions are needed to the personalization of the input signal design for the system identification stage. While the utilized procedure in *YourMove* yielded an adequately defined "ambitious yet achievable" *Goals* range for Participant C, that was not the case for the other presented participants. The delivered *Goals* in the system identification stage were not challenging enough for Participant A, and extremely challenging for Participant B. This has negative implications from both behavioral science and control systems engineering perspectives. From a behavioral science point of view, extremely or insufficiently challenging daily goals can lead to participant dissociation with intervention components, even participant dropout. Additionally, the collected system identification data in such cases does not represent the true participant-specific dynamics when the delivered daily goals are challenging and push the participant toward healthy behavior. We propose the utilization of an adaptive input signal personalization approach in future work, which can be done by utilizing the participant's average *Behavior* level over the one cycle to define the *Goals* range for the next cycle similar to work presented in Chapter 2 and in El Mistiri *et al.* (2022a).

In *YourMove* a black-box model estimation method is applied, specifically ARX, with DSPSA to search over model features and orders for each participant. While this approach proved to be sufficient in estimating participant-specific models, it has its limitations. For instance, this approach does not allow explicit constraint

enforcement on the direction of the estimated model steady-state gains. Consequently, some of the estimated model dynamics do not capture the expected outcomes from the intervention components (e.g., negative steady-state gains between *Behavior* and *Expected Points* for Participant C). While this is desirable in exploratory analysis aiming to understand the causal ideographic effect of each intervention component, it has ramifications on the closed-loop intervention implementation. Measures were taken in *YourMove* to mitigate the impact of estimated participant-specific models with negative steady-state gain between *Behavior* and *Goals* on the personalized closed-loop stage of the intervention. This came at a computational cost in the model estimation step, by expanding the search space for the DSPSA as explained in Section 6.4.1. It also led to the delivery of less personalized closed-loop interventions for such participants, through the utilization of the "open-loop" control policy.

Furthermore, the estimated idiographic models based on the system identification stage data are linear and do not capture any possible time or parameter-varying system dynamics. This results in a more significant plant-model mismatch in cases where a participant's behavior shifts, based on the participant's context and conditions in the closed-loop stage of the intervention (e.g., Participant A and Participant C). Therefore, we recommend the utilization of either "physics informed" modeling approaches to enable imposing constraints on the estimated steady-state gains, or other approaches that capture context-varying dynamics for each participant, e.g., Linear Parameter Varying (LPV; Mohammadpour and Scherer (2012)) and Model-on-Demand (MoD; Stenman (1999)). Additionally, there is a need to update the data set used in model estimation to include data points encompassing the new system dynamics, after the shift in the participant's behavior. This introduces new challenges that need to be studied and addressed before the next COT study. For instance, there is a need for a reliable algorithm to detect and flag possible shifts

in the participant's behavior. Once a shift in behavior is identified, the controller is decommissioned and a new stage of the system identification can be initiated for at least one cycle. An alternative option is to detune the controller in a new closed-loop system identification stage. Upon the end of the new identification stage, the data set is updated and the model is re-estimated in approaches like semi-physical modeling and LPV, whereas for MoD updating the estimation database is sufficient.

One of the main takeaways from *YourMove* is the robustness of the 3DoF-KF HMPC algorithm and its ability to deliver personalized interventions even when the estimated participant-specific models had low NRMSE fits. The estimated model for each participant does not need to be perfect, it just needs to be good enough to allow the controller to make informed decisions specific to the participant. This is evident in the presented closed-loop data for the three representative participants in this work. However, this does not mean that there is no added benefit from having more idiographic models that estimate participant-specific dynamics; better participant-specific models lead to more personalized closed-loop interventions. The successful implementation of optimal personalized closed-loop intervention for each of the presented participants is the result of the judicious formulation of the HMPC objective function, the robust 3DoF-KF structure which allows intuitive tuning, and adaptively tuning and reconfiguring the controller based on each participant's response. One of the possible improvements to the devised control strategies is the addition of upper constraint tightening on GA, in order to provide participants with more challenging daily goals when they significantly outperform the given *Goals* for consecutive days. Another possible improvement to the controller reconfiguration for overachievers is abandoning reference tracking for both controlled and manipulated variables. Instead, the objective function should be formulated to constraint the controller variable (*Behavior* y_4) within a region based on the moving average of the performance of the

participant, to ensure the delivery of challenging *Goals* for overachievers

YourMove serves as a proof of concept for the effectiveness of the COT framework in delivering behavior change interventions, in general, and PA interventions in particular. Based on the presented results in this work, the closed-loop stage within the COT framework yielded the desired outcomes for engaged participants, who abided by wearing their Fitbit watches and put in efforts toward achieving the delivered goals. *YourMove* is the first COT intervention to our knowledge, in which control systems engineering principles were used to deliver closed-loop interventions. The unique data collected in your *YourMove* move, the lessons learned from the real-world implementation of the 3DoF-KF HMPC formulation, and the insights gained from full data analysis after the conclusion of the study provide the base over which future COT interventions will be built.

Chapter 7

MODELING AND SYSTEM IDENTIFICATION OF USER ENGAGEMENT IN MHEALTH INTERVENTIONS USING A BAYESIAN APPROACH FOR MISSING DATA IMPUTATION

7.1 Introduction

Digital behavior change interventions (DBCIs) such as Just-In-Time Adaptive Interventions (JITAIs) have demonstrated efficacy in addressing a range of health behaviors including physical activity (Nahum-Shani *et al.*, 2015). A meta-analysis of 22 studies comprising of 1,757 adults found that DBCIs increased total physical activity among participants in randomized controlled trial (RCT) studies (n = 8) (SMD = 0.28, 95% CI: 0.01 - 0.56, p = 0.04) and pre-post design studies (n = 6) (SMD = 0.25, 95% CI: 0.09 - 0.41, p = 0.002). The increase in moderate-to-vigorous physical activity (MVPA) was found to be 52 minutes per week on average (SMD = 0.47, 95% CI: 0.32 - 0.62, $p < 0.001$) and a reduction in sedentary time of 58 minutes per day (SMD = -0.45; 95%CI: -0.69, -0.19, $p < 0.001$) (Stockwell *et al.*, 2019). However, despite the demonstrated effectiveness of DBCIs to positively impact physical activity, this effectiveness is heavily impacted by user engagement with DBCIs. Participants who fail to engage with the technology used to deliver and tailor interventions (e.g., smartphone-based app, wearable activity tracker) will have limited exposure to the behavior change techniques within the technological system (Cole-Lewis *et al.*, 2019). A recent 2021 meta-analysis of 11 studies using physical activity-focused DBCIs found a significant association between DBCI engagement and increased physical activity (0.08, 95% CI: 0.01 -0.14, SD 0.11). This association

was found to be consistent across three measures including the number of activities completed by the user, the number of unique logins, and subjective measures of the users' experience of engagement (Mclaughlin *et al.*, 2021).

DBCI engagement can be conceptualized as a multi-faceted construct that includes affective and cognitive dimensions, which are typically captured through the user's self-reported subjective experience. Additionally, behavioral dimensions of DBCI engagement typically manifest through the user's distinct interactions with the system and are primarily measured passively by the technology itself. Behavioral measures of engagement are often the most readily observable aspect of engagement in mobile health interventions as they typically result in a variety of digital traces (e.g., the number of application page views, the amount of time spent using an application, the number of self-report questions completed, etc. (Perski *et al.*, 2017; Yardley *et al.*, 2016)). Engagement with DBCIs is thus an inherently dynamic process as it will change over time based on several factors including ever-changing contextual conditions and various psychological states. These influences on DBCI engagement are often difficult to detect. However, by leveraging mobile technology, information on exogenous or environmental factors (e.g., temperature, precipitation, location) can be collected passively via mobile sensors. Additionally, the use of ecological momentary assessment (EMA; Shiffman *et al.* (2008)) can be leveraged to capture real-time psychological measures (e.g., perceived busyness, commitment) via self-report methods. The combination of these data streams provides a unique opportunity for the development of dynamic computational process models that can specify and test dynamic hypotheses of the relationships between DBCI engagement and these influences over time.

Despite the dynamic nature of DBCI engagement, the majority of the literature on this topic focuses on engagement as a static phenomenon, primarily using cross-

sectional measures (Spruijt-Metz *et al.*, 2015b). This approach also follows the current paradigm in behavioral science of focusing on modeling behavior change processes through group-level (nomothetic) studies and analyses. Typically, this methodology utilizes between-participant studies aiming to estimate the effect of an intervention at a population or group level, or, to identify associations between predictors and the behavior of interest. While this methodology can potentially identify if there is a relationship between variables, these approaches fail to explain the dynamic nature of the change between variables over time and in context. Therefore, insights gained from these approaches cannot inform decision-making when it comes to the optimal intervention approach for a specific individual in a given context, instead of what works best on average for a given population (Just-in-Time Adaptive Interventions (JITAIs; Perski *et al.* (2022); Klasnja *et al.* (2015); Nahum-Shani *et al.* (2015))). In this work, the focus is instead on individual-level (idiographic) analytic approaches. The utilization of system identification methods to model mobile health application use as an engagement-related behavior is studied. Models and results are presented based on data from *HeartSteps II*, a year-long micro-randomized trial (MRT) in the physical activity domain (Spruijt-Metz *et al.*, 2022).

Missing data remains a persistent problem in the analysis of health and behavioral data and is a prominent feature of the *HeartSteps II* study data (Rioux and Little, 2021; Hayati Rezvan *et al.*, 2015). If not addressed properly, missing data can potentially introduce bias into conclusions or negatively impact statistical inference. A review of randomized controlled trials (RCTs) published between July and December 2013 in BMJ, JAMA, Lancet, and the New England Journal of Medicine found that 95% of the reviewed studies (n = 73/77) reported some missing outcome data. Among those studies, the most commonly used approach was complete case analysis (45%, n = 33/77) (Bell *et al.*, 2014b). In fact, complete case analyses and similar deletion

approaches are the most commonly used methods for handling missing data across health and behavioral science studies (Karahalios *et al.*, 2012; Lang and Little, 2018). In this chapter, we take a Bayesian approach to model-based imputation of missing data based on Markov Chain Monte Carlo (MCMC) methods (Hoffman *et al.*, 2014).

7.2 Materials and Methods

7.2.1 HearSteps II

This work relies on data from a year-long micro-randomized trial (MRT), the *HeartSteps II* trial (Spruijt-Metz *et al.*, 2022). MRTs are closely related to just-in-time adaptive interventions (JITAIs), but use a randomized selection of intervention components to yield data for the purpose of optimizing the intervention components for eventual delivery as a JITAI. The goal of the *HeartSteps II* intervention is to encourage walking and other types of physical activity (Spruijt-Metz *et al.*, 2022). The *HeartSteps II* intervention components are based on self-determination theory (SDT; Deci and Ryan (2012)). In behavior change theories like SDT changes in behavior are hypothesized to occur due to interactions between behavior, psychological, and environmental factors.

As one of the main objectives of *HeartStep II* is to understand the impact of context and timing on intervention delivery, intervention components were designed to influence participants' physical activity related behaviors across several timescales:

- Within-day, participants are provided with two types of contextually tailored activity suggestions: anti-sedentary messages and walking suggestions.
- On a daily basis, *HeartSteps II* delivers motivational messages designed to promote commitment to exercise and self-monitoring of step count and minutes of activity.

- Once per week, *HeartSteps II* provides an opportunity for self-reflection on the participants' current physical activity routine including creating or reviewing physical activity plans and goals for the following week.

All of the above components were available on-demand. The detailed description of *HeartSteps II* study protocol including inclusion and exclusion criteria is presented in (Spruijt-Metz *et al.*, 2022).

In addition to delivering intervention components, the *HeartSteps II* smartphone application collects responses to a wide range of self-report questions prompted at a variety of frequencies. Further, *HeartSteps II* uses a Fitbit wearable activity tracker to collect step count and activity duration data. *HeartSteps II* recruited participants who were overweight, but otherwise healthy adults between the ages of 18-65 located in the greater Los Angeles County region (n=96).

A primary focus of this modeling effort was to analyze the impact of an individual's contextual conditions (e.g., psychological and environmental) on engagement related behaviors. While engagement with digital behavior change interventions (DBCIs) is comprised of multidimensional factors including affective, cognitive, and behavioral components, this study operationalized engagement through the total of daily application page views. App page views is a key indicator of app engagement as higher app page view counts indicate a potentially higher level of exposure and opportunity for engagement with intervention content including activity planning and activity suggestions. The number of unique app page views was collected passively via the smartphone based *HeartSteps II* app and then was aggregated to the daily level representing the sum total app page views per day.

The *HeartSteps II* app passively measured several indicators of behavior and context-specific information such as the number of intervention messages received by the participant each day as well as the daily average temperature in the partic-

ipant's location. Other mobile sensors like the Fitbit device passively recorded the participant's step count as the primary measure of daily physical activity. The Fitbit also provided a passive measure of the daily wear time; both were computed as a daily sum of minute-level measurements. Finally, the day of the week was captured as an important activity-related variable due to weekly activity patterns and trends. More specifically, this study focused on weekday/weekend as an indicator variable. These constructs are summarized in Table 7.1 along with the variable names used to represent each construct in the hypothetical models.

Table 7.1: *HeartSteps II* Construct and Variables.

Construct	**Variable**
Inventory levels (system outputs)	
App Engagement	η_1
Perceived Exercise Commitment	η_2
Step Count	η_3
Inflows/Outflows (system inputs)	
Perceived Busyness	ξ_1
Perceived Restedness	ξ_2
Messages Received	ξ_3
Weekend	ξ_4
Wear Time	ξ_5
Temperature	ξ_6

The use of ecological momentary assessment (EMA) provided an opportunity to collect daily self-reported information on an individual's level of commitment to ex-

ercise, their projected level of busyness, and their perceived level of restedness that day. These data were captured via daily questionnaires delivered by the *HeartSteps II* app. The questions respectively were, “How committed do you feel this morning to be physically active today?,” “How busy is your day going to be today?,” and "How well rested do you feel this morning?" Each of these constructs is measured using a single self-report question with responses on a five-point Likert scale.

7.2.2 Theory-Based Dynamic Modeling

The application of fluid analogies in behavioral medicine has provided a framework to translate prominent behavior change theories (e.g., Social Cognitive Theory, Theory of Planned Behavior) into dynamical models that can be utilized to guide the design of personalized behavioral interventions combating unhealthy behaviors such as physical inactivity, and smoking (Rivera *et al.*, 2018). Moreover, fluid analogies have been proposed as a tool to help behavioral scientists hypothesize new behavior change models and derive dynamic models based on such hypotheses. In this work, dynamic hypotheses are proposed to explain changes in engagement over time of a representative participant from the *HeartSteps II* intervention.

In fluid analogies, output variables are modeled as inventory levels, whereas exogenous variables are represented as inflows/outflows to the inventories. In Fig. 7.1, we provide a graphical representation of a hypothesized exercise commitment model describing connections between app engagement, exercise commitment, and Fitbit step count. It is hypothesized in this model that engagement with the intervention app (*App Engagement*, η_1), operationalized as the number of app page views per day, increases the participant's commitment to participate in physical activity as a part of the intervention. Reciprocally, an increase in participant's *Perceived Exercise Commitment* (η_2) leads to a proportional increase in *App Engagement*. Moreover, the

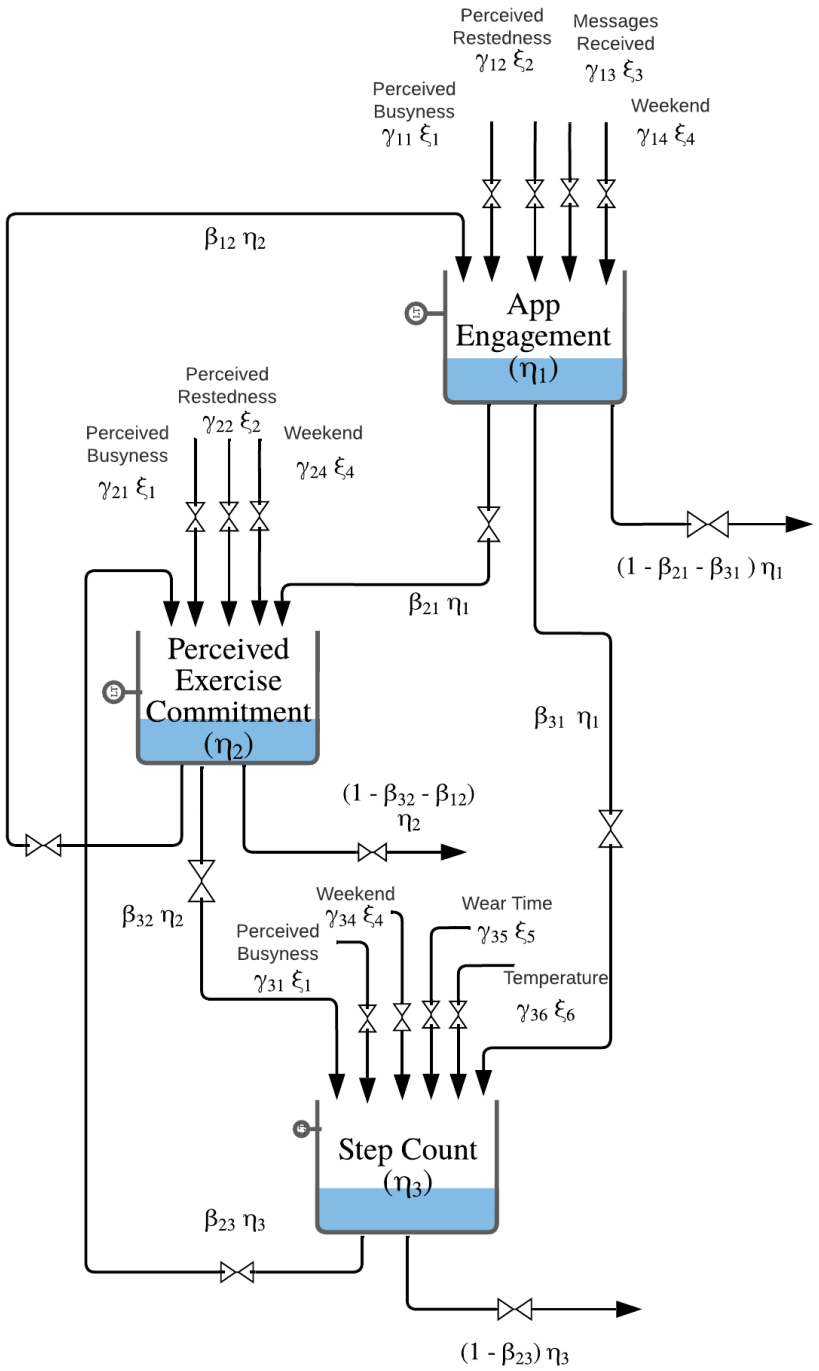

Figure 7.1: Fluid Analogy Representation of the Hypothesized DBCI App Engagement Model.

reciprocal interaction between *Perceived Exercise Commitment* and the daily levels of physical activity, operationalized by the *Step Count* (η_3), is also captured in the exercise commitment loop presented in Fig. 7.1. Finally, exogenous variables that are hypothesized to significantly impact the system including *Perceived Busyness* (ξ_1), *Perceived Restedness* (ξ_2), *Messages Received* (ξ_3), *Weekend* (ξ_4: as a binary variable indicating whether an intervention day is on the weekend of not), *Wear Time* (ξ_5) of the Fitbit device, and *Temperature* (ξ_6) are specified in the model.

By applying the principle of conservation of total mass to each inventory, an ordinary differential equation representation of the hypothesized system dynamics is obtained as shown below:

$$\tau_1 \frac{d\eta_1}{dt} = \gamma_{11}\ \xi_1(t) + \gamma_{12}\ \xi_2(t) + \gamma_{13}\ \xi_3(t) + \gamma_{14}\ \xi_4(t) + \beta_{12}\ \eta_2(t) - \eta_1(t) \tag{7.1}$$

$$\tau_2 \frac{d\eta_2}{dt} = \gamma_{21}\xi_1(t) + \gamma_{22}\xi_2(t) + \gamma_{24}\xi_4(t) + \beta_{21}\eta_1(t) + \beta_{23}\eta_3(t) - \eta_2(t) \tag{7.2}$$

$$\tau_3 \frac{d\eta_3}{dt} = \gamma_{31}\xi_1(t) + \gamma_{34}\xi_4(t) + \gamma_{35}\xi_5(t) + \gamma_{36}\xi_6(t) + \beta_{31}\eta_1(t) + \beta_{32}\eta_2(t) - \eta_3(t) \tag{7.3}$$

where τ_i and η_i represents the time constant for inventory i, respectively. γ_{ij} represents the gain between inventory i and the inflow/outflow ξ_j, β_{iz} denotes the gain in inventory i for changes in inventory z, and ζ_i is for unmeasured disturbances, where i, j, z are integers.

7.2.3 Bayesian-Based Data Imputation

To impute missing data in this study, model-based Bayesian inference in Dynamic Bayesian Networks models (DBNs; Murphy *et al.* (2002)) is utilized (van de Schoot *et al.*, 2021). Specifically, we constructed a discrete-time dynamic Bayesian network model, as shown in Fig. 7.2, with a structure based on that of the fluid analogy model presented in the previous section. The exogenous variables (inputs) with missing

data points (*Perceived Busyness* and *Perceived Restedness*) are assumed to have a normally distributed first-order autoregressive dynamic structure, where the mean depends linearly on the previous measurement with an unknown but time-invariant standard deviation. On the other hand, all the endogenous system variables (outputs) are considered to be normally distributed with means that are dependent on a linear combination of current and previous values of variables (e.g., nodes), as presented in Fig. 7.2, also with a time-invariant unknown standard deviation. Weights in the linear combinations are given normal prior distributions, while the unknown standard deviations are assumed to have exponential prior distributions. The corresponding probabilistic model is described below.

$$\eta_{1,k} \sim \mathcal{N}(w_{11}\eta_{1,k-1} + w_{12}\eta_{2,k} + g_{11}\xi_{1,k} + g_{12}\xi_{2,k} + g_{13}\xi_{3,k} + g_{14}\xi_{4,k} + c_{e1}, s_{e1}) \tag{7.4}$$

$$\eta_{2,k} \sim \mathcal{N}(w_{22}\eta_{2,k-1} + g_{21}\xi_{1,k} + g_{22}\xi_{2,k} + g_{24}\xi_{4,k} + c_2, s_2) \tag{7.5}$$

$$\eta_{3,k} \sim \mathcal{N}(w_{33}\eta_{3,k-1} + w_{31}\eta_{1,k} + w_{32}\eta_{2,k} + g_{31}\xi_{3,k} + g_{34}\xi_{4,k} + g_{35}\xi_{5,k} + c_3, s_3) \tag{7.6}$$

where

$$\xi_1 \sim \mathcal{N}(d_1\xi_{1,k-1} + c_{i1}, s_{i1}) \tag{7.7}$$

$$\xi_2 \sim \mathcal{N}(d_2\xi_{2,k-1} + c_{i2}, s_{i2}) \tag{7.8}$$

$$w_*, g_*, c_* \sim \mathcal{N}(0,1) \text{ and } s_* \sim Exp(0.1) \tag{7.9}$$

In this work, we use Markov chain Monte Carlo (MCMC) methods to sample from the joint posterior distribution of the DBN's unknown model parameters and missing data variables conditioned on the observed variables (Hoffman *et al.*, 2014).

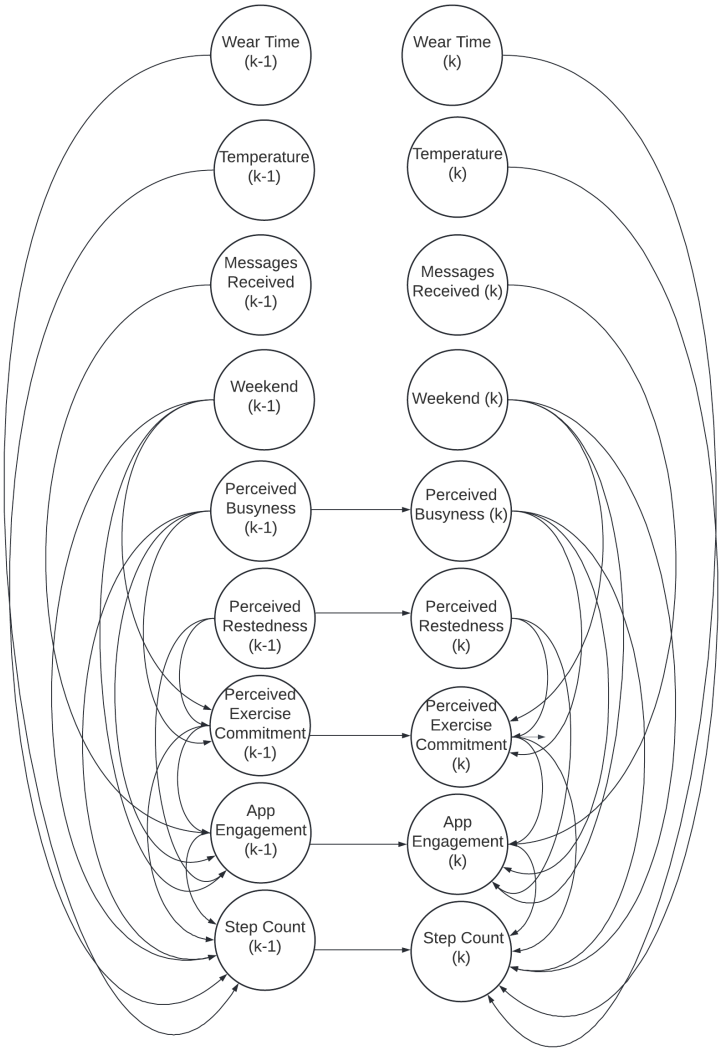

Figure 7.2: Graphic Representation of the Dynamic Bayesian Network Model Representation of the Hypothesized Model, Used to Impute Missing Data Points in a Markov Chain Monte Carlo Sampling Approach.

The sampled model parameters are then discarded and the sampled missing data values are retained. This process results in multiple imputations of the missing data variables. As this approach utilizes MCMC methods, the number of samples obtained from this process can be specified. The DBN model is implemented and inference is performed using the BayesLDM toolbox (Tung *et al.*, 2022).

7.2.4 Data Analysis

The *HeartSteps II* data set consists of time series of sensor-based and self-reported measurements for all of the variables used in the proposed model. However, all variables are subject to some amount of missingness. An exclusion criterion was defined based on missingness of the constructs presented in Table 7.1, where participants with missingness exceeding 40% were excluded. A representative participant with the least amount of missingness (30.05%) was selected for the data analysis presented in this chapter.

The data set for the representative participant was then segmented into sequences with at least 7 consecutive data points, which allowed enough data in each segment to fit the expected regressor structures for black-box modeling techniques. Furthermore, a maximum of 5 consecutive missing data points were allowed between sequences. Given that this participant's engagement with the application and intervention components was poor in the first 99 days of the intervention, data pre-processing and model estimation were implemented on data points from day 100 to the end of the intervention. This resulted in a total of five data segments of varying lengths that were designated as sub-experiments. The sub-experiments were grouped into validation and estimation groups, where 28.9% of the data was assigned for validation and the remainder for estimation, as seen in Fig. 7.4. This procedure reduced the total available data to 252 days, with missing data points on 10 days (3.97% missingness).

This data set is referred to as the "raw data" in this work.

Next, the data was standardized using the means and standard deviations of the available data points. Missing data values in the standardized raw data were then imputed using the BayesLDM toolbox, based on the model structure in Fig. 7.2 and assumptions provided in Section 7.2.3. As the data of interest is ordinal by nature, the imputed data set was de-standardized, and then the imputed data points were rounded to the nearest integer. Data points representing the behavioral constructs of interest (*Perceived Exercise Commitment, Perceived Busyness, Perceived Restedness*) were projected onto the upper and lower constraints of the five-point Likert scale used for such measurements. 1,000 different imputed data sets were generated, each of which represented a different realization of the sampled missing data points. The mean of the 1,000 sampled imputed data sets was obtained, rounded, and then bounded to the ordinal values. Lastly, 100 realizations of the data sets were randomly selected and re-standardized to perform black-box model estimation utilizing Auto Regressive with eXogenic inputs (ARX; Ljung (1999)) structure.

To evaluate the performance of the Bayesian inference approach, other standard imputation methods were also considered: backward-fill pandas development team (2022), forward-fill Team (2022), and linear interpolation. Backward and forward fill methods produce ordinal values, within the measurement ranges. On the other hand, the data set imputed with linear interpolation was also rounded to integer values, based on the range of possible measurements for the behavioral constructs. Furthermore, all imputed data sets were segmented into sub-experiments consistent with the sequences of the non-imputed data. For the imputed data, each sub-experiment period started on the same time (day) index as its equivalent in the raw data, however, each sub-experiment is slightly longer (by two sampling instances on average) as a consequence of data imputation. All imputed data sets were utilized to estimate

ARX models.

ARX models belong to the family of parametric black-box model estimation techniques that utilize input-output measurements to estimate the dynamics between the measurements, without knowing the causal structure behind them. These models can be used to confirm relationships between the variables of interest, which can be essential in the confirmation of hypothesized models and the estimation of semi-physical models. ARX time series models are a linear representation of a dynamic system in discrete time, as shown in (7.10).

$$y\left(k\right)+\sum_{l=1}^{n_a}a_l y\left(k-l\right)=\sum_{j=1}^{n_\xi}\sum_{i=0}^{n_{b_j}-1}b_{(i+1)(j)}\xi_j\left(k-n_{k_j}-i\right)+e\left(k\right) \tag{7.10}$$

where $y(k)$ represents the measured output, $\xi_j(k)$ is the measured input j, and $e(k)$ represents the prediction error. k represents the time step. a_l represent autoregressive model parameters up to the output regressor order n_a and $b_{(i)(j)}$ denotes model coefficient for regressor i up to the regresor order n_{b_j}, for input j. n_{k_j} represents the delay in each input. Model parameters are estimated using least squares regression as shown in (7.11) where $\hat{\theta}$ represents a vector of model parameters as arranged in regressor space.

$$\hat{\theta}=\arg\min_{\theta}\frac{1}{N}\sum_{t=1}^{N}(y(t)-\hat{y}(t|\theta))^2 \tag{7.11}$$

One of the advantages of utilizing ARX models lies in the simplicity of their linear structure, which makes the optimization problem in (7.11) readily solvable. This allows the use of various algorithms to optimize over model structure through order and input selection (Banerjee *et al.*, 2024a). Consequently, more insight regarding the dynamic nature of the relationships between variables of interest can be gained and used to validate/falsify hypotheses and guide future dynamic hypotheses generation regarding the causal dynamics of a system, particularly behavior change systems.

An order selection algorithm was applied on the standardized raw data set, where

all the possible order combinations are searched over from a select range of orders for each variable. The combination that minimizes the mean square error (MSE) over validation data was ultimately selected. The specified order sets were $n_a, n_{b_j} \in \{1, 2, 3\}$ for all inputs and the output of interest, while $n_{k_j} \in \{0, 1\}$. The selected order was then utilized to estimate parameters for models from the raw data, every realization of the Bayesian inference imputed data, and the other considered standard interpolation methods. By fixing the order of all the estimated models to the one obtained from the raw data, we were able to compare the same number of model parameters across all estimated models. Additionally, because the Bayesian inference approach follows MCMC methods, the uncertainty propagates to the various realizations of the sampled imputed data points under the assumptions made about distributions, as well as to the estimated ARX model parameters. This approach yielded 105 estimated models, which were then further analyzed and vetted in terms of their fit percentage over the validation data, step responses, gains, and uncertainties. The approach can be extended to quantify the uncertainty in regressor orders as well, by performing order selection on the various realizations of the imputed data sets.

To further examine the BayesLDM performance in comparison to the considered traditional interpolation methods, additional data points were withheld at random in the input variables prone to missingness (*Perceived Exercise Commitment, Perceived Busyness, Perceived Restedness*). This provides "ground truth" to evaluate the error in the imputed data points. This is done by calculating the root mean square error (RMSE) to obtain a measure of how close the imputed data points are to the actual values. Values for the variables mentioned above were withheld for 75 days from the raw data, resulting in an overall missingness of 33.73% (85 days with missingness out of the total 252 days). The data analysis procedure mentioned above was then repeated, from data imputation to model estimation based on the regressor structure

obtained from order selection on the raw data. The results obtained are presented and discussed in the ensuing sections.

To quantify model fits, we use normalized root mean square error (NRMSE) fit index. The standard NRMSE statistic is shown in (7.12) where $y(k)$ is the measured output, $\hat{y}(k)$ is the model output, $\bar{y}$ is the mean of all measured $y(k)$ values, and $||\cdot||_2$ indicates a vector l_2-norm.

$$F = 100 \times \left(1 - \frac{||y(k) - \hat{y}(k)||_2}{||y(k) - \bar{y}||_2}\right) \tag{7.12}$$

The NRMSE fit index is calculated for each of the segmented sub-experiments separately and then averaged over the sub-experiments designated for validation and estimation data. Due to the differences in the duration of each sub-experiment, each sub-experiment is weighted by the ratio of its duration to the length of the overall data to ensure its impact on the fit index for validation and estimation is proportionate to its size. Lastly, to provide all estimated models with the exact same conditions, only the raw data set is utilized to evaluate model fits.

7.3 Results

The ARX regressor orders obtained from the implementation of the order selection algorithm on the raw data was $n_a = 3$, $n_b = [3\ 1\ 2\ 3\ 2]$, and $n_k = [0\ 1\ 0\ 1\ 1]$ which yields a total of 14 parameters to be estimated. To validate the estimated models, two criteria are considered:

- Model cross-validation where the performance of the models was assessed in terms of the normalized root mean square error (NRMSE) over validation data that was not used in model estimation.
- The characteristics of the step responses of the estimated models (steady-state gains, directional, speed, and shape of response).

The step responses of the model estimated from the raw data are shown in Fig. 7.3, along with their steady-state gains, and the NRSME fit over the entire raw data set. Simulation results of the estimated model in comparison with the raw data are presented in Fig. 7.4, which shows data segmented into sub-experiments highlighted based on their grouping (estimation in grey; validation in light-blue) along with their weighted average fit index.

Table 7.2: Performance of the Four Examined Imputation Methods: Mean Realization of the Bayesian Inference Approach, Forward-fill, Backward-fill, and Linear Interpolation. The Presented Values Are in Terms of the RMSE, Based on the Difference Between the Imputed Values and the Actual Withheld Values for 75 Randomly Selected Intervention Days for *Perceived Busyness* (ξ_1), *Perceived Restedness* (ξ_2), and *Perceived Exercise Commitment* (η_2).

Method	ξ_1	ξ_2	η_2
Bayesian Inference	1.35	1.27	1.44
Forward-fill	1.95	1.83	2.91
Backward-fill	1.94	1.80	2.41
Linear Interpolation	1.58	1.51	2.35

The performance of the BayesLDM toolbox in imputing values for the withheld data points is presented in Table 7.2. In this table, the root mean square error (RMSE) values for each of the examined imputation methods show how close the imputed data points are to the actual values of the variables prone to missingness.

For the sake of visual clarity and brevity, simulation results and fit indices of only one realization of the Bayesian inference imputed data points are shown and compared to the other imputation methods. The considered realization to represent

Table 7.3: Summary of the Fit Indices of the ARX Models Estimated from the Raw Data and Data Imputed By Four Different Methods.

Method	Estimation Fit (%)	Validation Fit (%)	Overall Fit (%)
10 missing data points (3.97% missingness)			
Raw Data	51.11	36.55	46.89
Bayesian Inference	51.07	36.68	46.91
Forward-fill	51.04	36.67	46.88
Backward-fill	51.11	36.72	46.95
Linear Interpolation	51.07	36.70	46.92
data withheld for 75 days (33.73% missingness)			
Bayesian Inference	50.91	37.05	46.90
Forward-fill	51.29	35.99	46.87
Backward-fill	50.03	36.28	46.05
Linear Interpolation	50.93	36.58	46.75

BayesLDM imputed data is the mean of the 1,000 sampled data points, whereas, the remainder 100 realizations are utilized to illustrate the propagation of uncertainty into the estimated model parameters. Table 7.3 below provides a summary and a comparison of the model fits estimated from data imputed by the four considered imputation methods. Simulation results of the ARX model estimated from the mean realization of the Bayesian imputation approach are shown in Fig. 7.4 and Fig. 7.5 for the cases of 3.97% and 33.73% missingness, respectively.

The step responses of all the estimated models (from the various imputation methods and realizations and the raw data) are shown in Fig. 7.6 and Fig. 7.7, for 3.97% and 33.73% missingness, respectively. In these figures, the step responses of the mod-

els reported in Table 7.3 are shown in opaque lines, whereas the step responses of models estimated based on the 100 randomly selected BayesLDM imputed data realizations are plotted in transparent green lines to highlight the propagated uncertainty into estimated model dynamics.

7.4 Discussion

The model orders obtained through minimizing the MSE fits for the raw validation data, over the specified order ranges, confirm the presence of relationships between the examined variables as specified by the fluid analogy model presented in Section 7.2.2. While the ODE directly describing the relationship between the inputs and *App Engagement* (7.1) is of a first-order, the overall dynamics of the ODEs system (7.1)-(7.3) is of a third-order. Hence, it falls well within expectations of the hypothesis to have third-order dynamics between the specified inputs and *App Engagement* (η_1). Furthermore, the obtained cross-validation fit percentages of the estimated ARX model (36.55% validation, and 46.89 % overall as shown in Table 7.3) are considered very good for noisy systems associated with behavior change. This increases confidence in the estimated models and the obtained regressor orders.

The observed dynamics of the step responses (shown in Fig.7.3 and Fig.7.6) further asserts confidence in the estimated models, and by extension, in the hypotheses about the system dynamics; they agree with literature in terms of the direction of the gains between the selected inputs and the modeled output. One of the interesting observations in the step responses is the lead-lag dynamics between *Perceived Busyness, Messages Received* and *App Engagement*. This indicates the fast nature of the effect of such inputs on the output of interest, which shows that the impact of messages sent in the intervention happens within day and affirms the need for studying the multi-timescale dynamics in behavior change systems. Consequently, a higher sampling rate

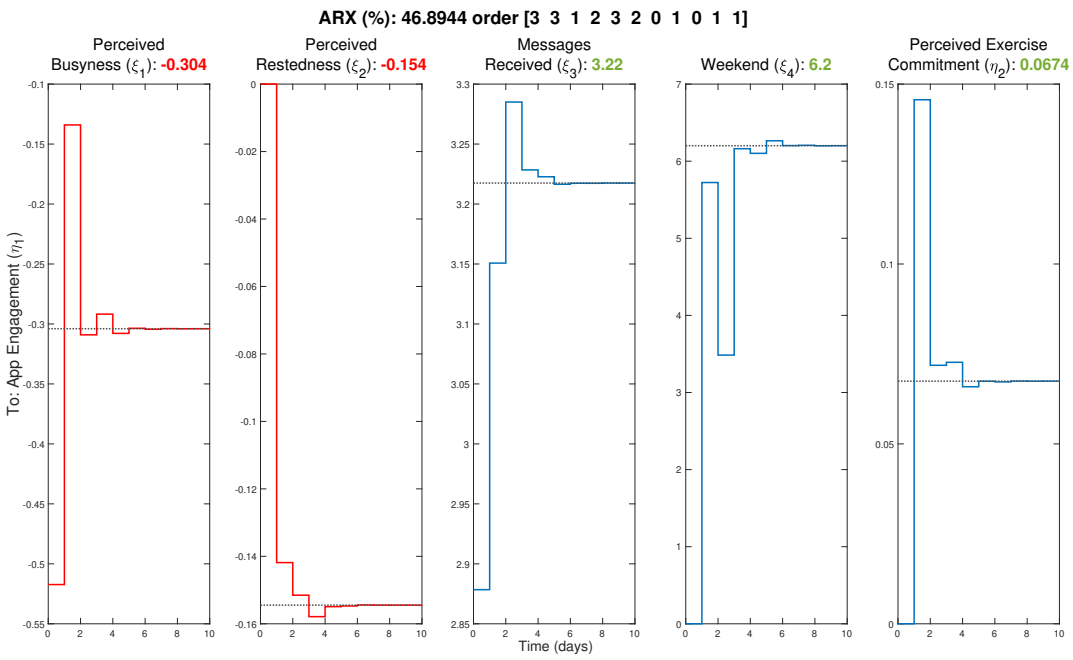

Figure 7.3: Unit Step Responses of the 5-Input ARX Model Estimated from the Raw Data, Along with Their Steady-State Gains. The Step Responses Are Arranged Left to Right as *Perceived Busyness*, *Perceived Restedness*, *Messages Received*, *Weekend*, and *Perceived Exercise Commitment* with Gains of -0.304, -0.154, 3.22, 6.20, 0.0674 Respectively.

is needed to properly estimate the dynamic relationship between the mentioned variables. In addition, lead-lag dynamics translate to direct feed-through conditions in state-space representation of the model, which requires special accommodations when implementing model-based control schemes like Model Predictive Control (MPC) to automate personalized behavioral interventions. This is particularly the case as the direct feed-through exists between the potential manipulated and controlled variables in closed-loop conditions (*Messages Received* and *App Engagement* respectively).

Simulation results of the models estimated from the raw data, and the mean of 1,000 realizations of the data imputed through Bayesian inference, shown in Fig. 7.4

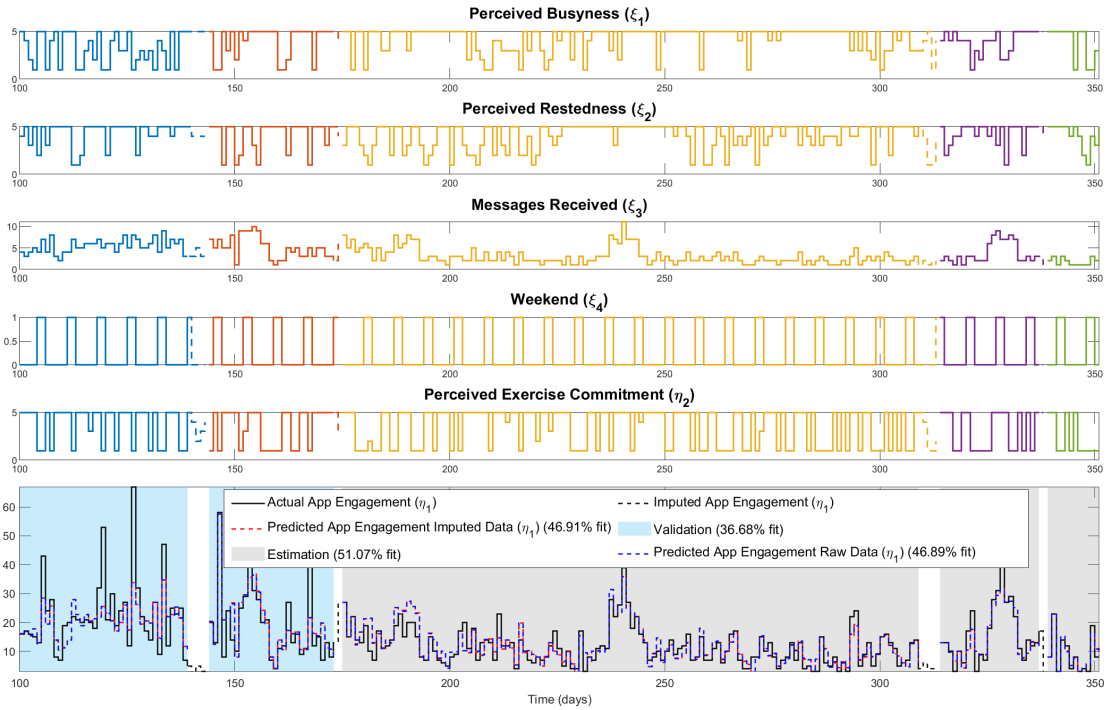

Figure 7.4: Time Series Plot Representing the Results of the Estimated ARX Models for a Representative *HeartSteps II* Participant Utilizing Raw Data and the Mean Realization of the Bayesian Inference Imputation for the Case of 3.97% Missingness. Five Input Sequences Corresponding to Exogenous Variables (*Perceived Busyness*, *Perceived Restedness*, *Messages Received*, and *Weekend*) and Endogenous Variable (*Perceived Exercise Commitment*) Are Shown. The Bottom Plot Includes Actual and ARX Predicted `App Page Views in Views/day. Estimation and Validation Data Regions Are Highlighted in Magenta and Cyan, Respectively. The ARX Models Are Estimated Through Least-Squares Regression, Based on the Model Order Obtained Through Order Selection $n_a = 3$, $n_b = [3\ 1\ 2\ 3\ 2]$, and $n_k = [0\ 1\ 0\ 1\ 1]$.

and Fig. 7.5 for the cases of 3.97% and 33.73% missingness respectively, illustrate that the estimated models do a decent job of tracking the actual *App Engagement* throughout the peaks and troughs in the data. The estimated models under-predict sudden significant increases in *App Engagement*, which can be attributed to unmea-

sured inputs to the system. From an initial look at the presented results, it may seem that the benefit of the imputed data points is incremental, especially when comparing the fit indices presented in Table 7.3. However, this is exactly the intended result, as data imputation is only meant to provide more data points while maintaining the integrity of the dynamics in the data. This is also evident in the step responses shown in Fig. 7.6; the examined imputation methods yield models with similar results in terms of the shape of responses and gains.

Case deletion is an acceptable approach only when missingness is low. However, as the amount of missing data points increases case deletion becomes impractical, especially for idiographic modeling. For instance, in the scenario of withholding data on 75 days of the intervention, only 49 data points were left to perform model estimation after segmenting the data into sequences with at least 7 consecutive data points. This high rate of missingness (88.56%) made it impossible to estimate an informative model if the data set with holdouts was treated as the raw data set. The BayesLDM toolbox provides a powerful model-based approach to data imputation through MCMC methods, which enables us to perform data analysis and model estimation even when missingness is high. Moreover, the added benefit of the Bayesian inference approach to imputation is the ability to propagate and quantify the combined uncertainty from data imputation and data scarcity. This can have important applications for closed-loop optimal behavioral interventions, where the estimated uncertainty can be utilized to ensure the robustness of the designed controllers and their ability to account for the various sources of uncertainty.

As can be observed in Fig. 7.6, the models estimated from the randomly selected realizations of the Bayesian inference sampled data (highlighted in transparent green) span a range of possible step responses around the mean realization. The range spanned by these realizations covers all the results obtained from the standard

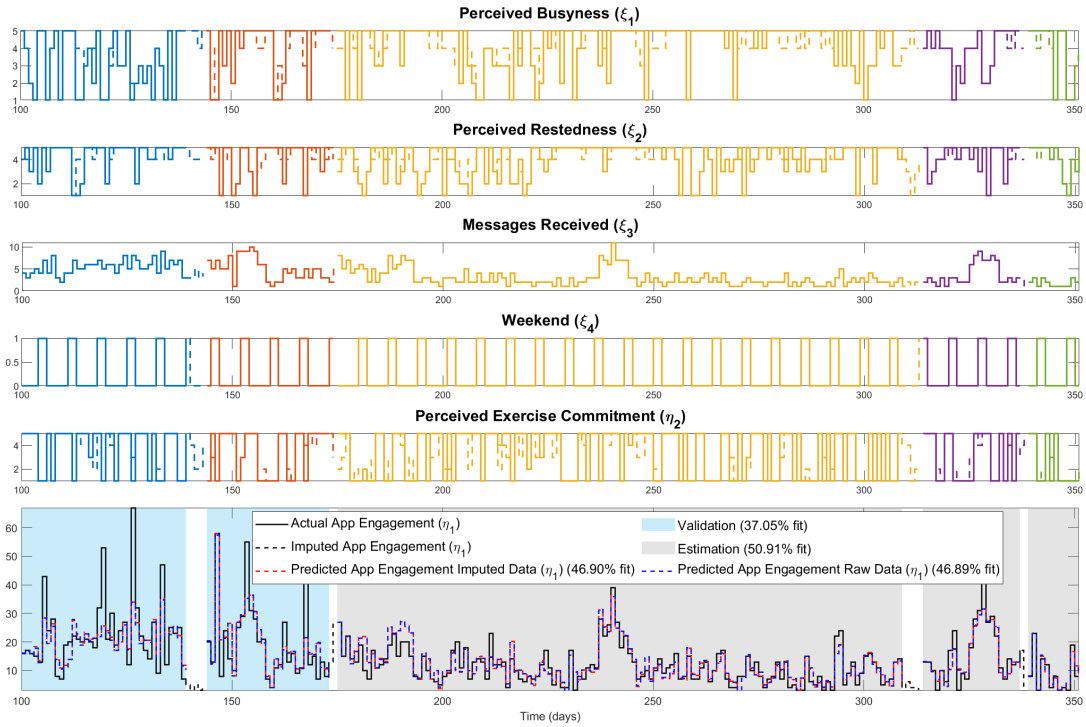

Figure 7.5: Time Series Plot Representing the Results of the Estimated ARX Models for a Representative *HeartSteps II* Participant Utilizing Raw Data and the Mean Realization of the Bayesian Inference Imputation for the Case of 33.73% Missingness (Withholding Data Points on 75 Days). Five Input Sequences Corresponding to Exogenous Variables (*Perceived Busyness*, *Perceived Restedness*, *Messages Received*, and *Weekend*) and Endogenous Variable (*Perceived Exercise Commitment*) Are Shown. The Bottom Plot Includes Actual and ARX Predicted `*A*pp Page Views in Views/day. Estimation and Validation Data Regions Are Highlighted in Magenta and Cyan, Respectively. The ARX Models Are Estimated Through Least-Squares Regression, Based on the Model Order Obtained Through Order Selection $n_a = 3$, $n_b = [3\ 1\ 2\ 3\ 2]$, and $n_k = [0\ 1\ 0\ 1\ 1]$.

imputation methods shown in the Figure. Moreover, notice that the variation in the gains is lower for passively measured variables: *Messages Received* and *Weekend*.

Such variables are measured continuously and do not suffer from missingness. Hence, their values are used in the BayesLDM approach to impute the missing data points of the other considered variables in the DBN model. Additionally, it is important to consider the fact that the step response dynamics and gains of the model estimated from the raw data fall within the span of credible interval uncertainty quantified by the Bayesian inference imputation realizations for the majority of the examined inputs. The only exceptions to this outcome are observed in the step responses to the *Perceived Restedness* and *Received Messages*, as can be seen in Fig. 7.6. The main reason behind this observation is the interactions and correlations between the model parameters. In the presence of more data points, the dynamics of the system can be better explained by a different combination of model parameters, which yields different sets of gains for the considered inputs. This falls within the trade-off between bias and variance in model estimation.

The advantages of the Bayesian inference approach to data imputation can be especially seen in the case of data holdouts (33.73% missingness). This is particularly evident in Table 7.2, where the performance of the model-based BayesLDM approach outshines traditional interpolation methods. The calculated MSE values for the mean realization of the Bayesian inference sampled data are the lowest amongst the examined imputation methods, which indicates that BayesLDM imputation estimated the closest values, by significant margins, to the true withheld values of the EMA measured behavioral constructs of interest. Therefore, the BayesLDM approach performs very well even in cases where the missingness in the data is high.

This observation is further illustrated by the step responses for this case, shown in Fig. 7.7, where only the step responses of the model estimated from the mean realization of the Bayesian inference imputed data coincide with those estimated from the raw data (with 3.97% missingness). This is evident in the shape and speed of

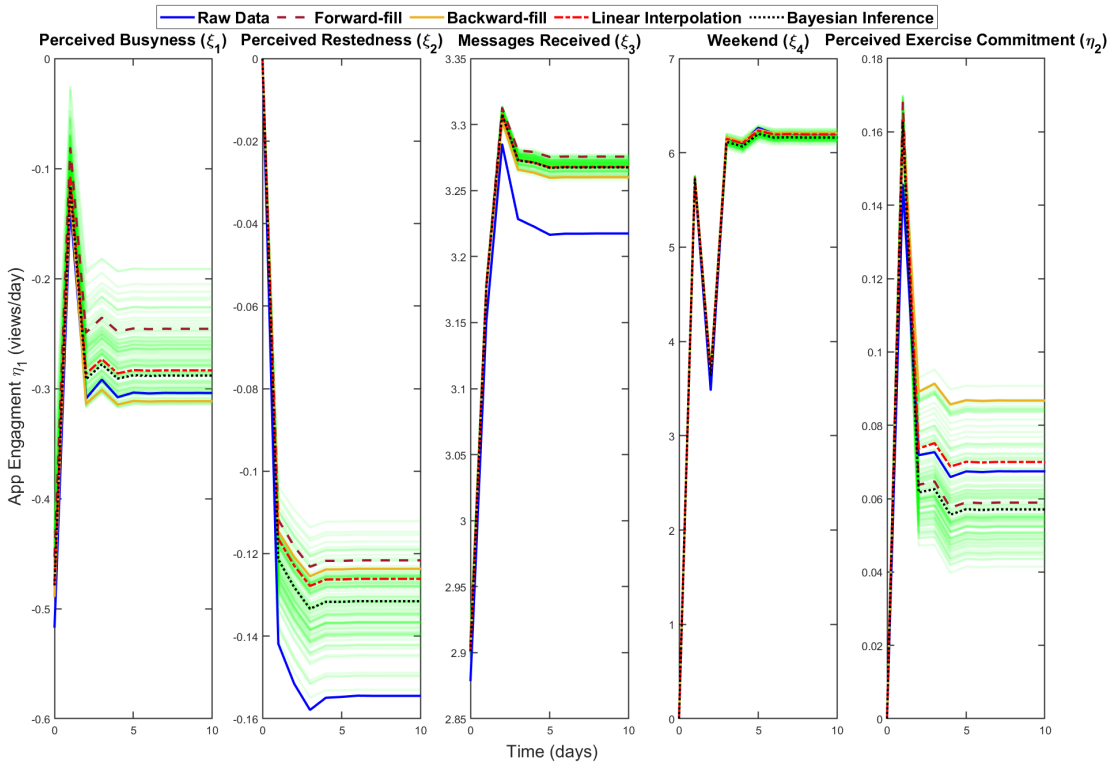

Figure 7.6: Unit Step Responses of the 5-Input ARX Models Estimated from the Raw Data and the Imputed Data Sets in the Case of 3.97% Missingness. Step Responses of the Main Estimated Models Are Shown in Opaque Lines. The Captured Uncertainty from 100 Randomly Selected Bayesian Inference Imputed Data is Highlighted in Transparent Green.

response, as well as the direction of the gains for all considered inputs. On the other hand, the models estimated from the data imputed through traditional interpolation methods do not agree with the step responses of the ARX model estimated from the raw data for some of the considered inputs. This is particularly noticeable, in varying degrees, in the step responses for *Perceived Busyness* and *Perceived Restedness*, as demonstrated in Fig. 7.7. Moreover, as more data points are imputed in this case, the propagated uncertainty due to data imputation is higher. This observation is

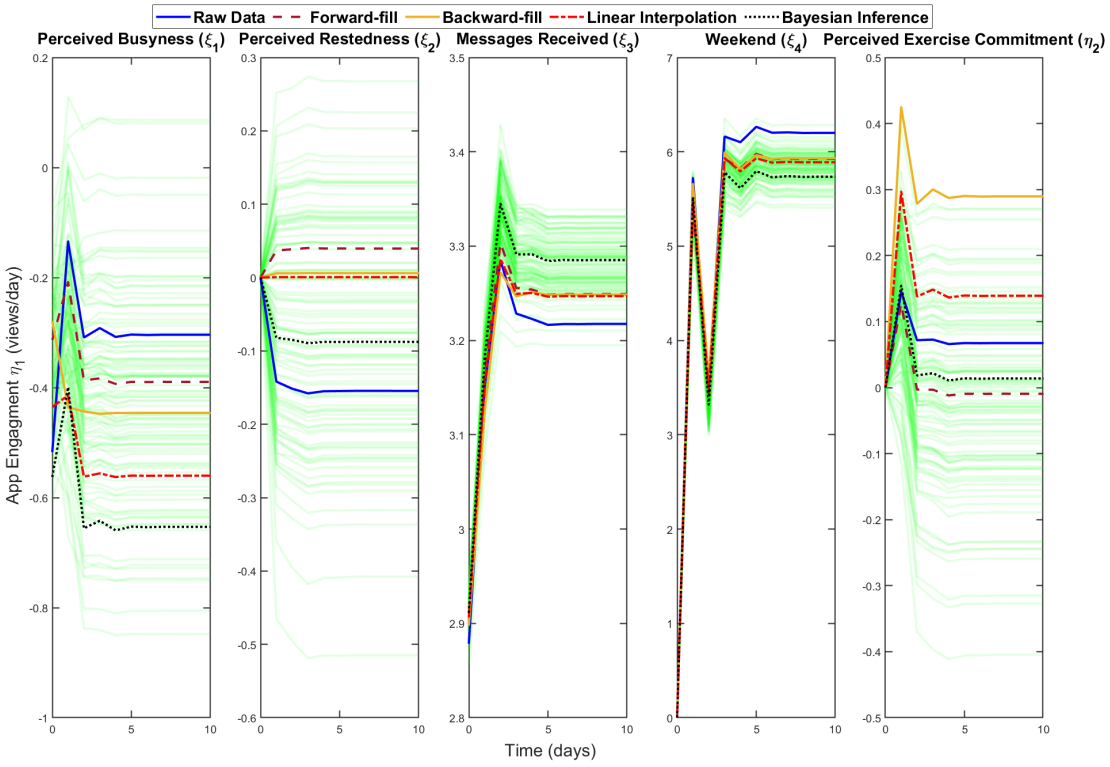

Figure 7.7: Unit Step Responses of the 5-Input ARX Models Estimated from the Raw Data and the Imputed Data Sets in the Case of 33.73% Missingness. Step Responses of the Main Estimated Models Are Shown in Opaque Lines. The Captured Uncertainty from 100 Randomly Selected Bayesian Inference Imputed Data is Highlighted in Transparent Green.

illustrated by the wider span of uncertainty (highlighted in transparent green) for all considered inputs. The obtained results demonstrate that the BayesLDM toolbox provides a powerful approach to performing model-based data imputation while maintaining the integrity of the dynamics in the data and propagating the uncertainty from data imputation into the estimated model of the system in a quantifiable manner. Consequently, the obtained optimal solutions in well-established robust control schemes, such as stochastic model predictive control (SMPC; Mesbah (2016)), can

differ significantly based on the provided probabilistic uncertainty distribution.

7.5 Conclusions

In this chapter, we introduce a theory-driven dynamic hypothesis describing the changes in participant engagement in *HeartSteps II* study over time, translate the hypothesis to a dynamic model using engineering principles in a fluid analogy, and tackle the ubiquitous issue of missingness faced in such studies. We propose the implementation of model-based Bayesian inference methods to impute the missing data points and illustrate its benefits over traditional interpolation methods. Longitudinal data from *HeartSteps II* for a representative participant is utilized to test the proposed imputation approach, and examine the suggested dynamic hypothesis. The findings in this chapter confirm some of the assumptions underlying the proposed dynamic hypotheses, particularly the influence of the examined inputs on *App Engagement*, which ultimately provides more insight into the dynamic nature of engagement in DBCIs. The proposed theory-based, semi-physical engagement model remains unfalsified. The insights gained from this chapter will lead to future efforts in designing more informative experiments to validate the model, with the ultimate aim of better understanding the dynamics of engagement in DBCIs and improving their efficiency.

The findings in this chapter also demonstrate the benefits of using a model-based Bayesian inference approach for data imputation, especially in terms of estimating the model uncertainty due to missing data. Because the Bayesian inference approach follows MCMC methods, it allows for quantifying uncertainty in missing data points by propagating it into the estimated models. This can have significant applications in the implementation of closed-loop behavioral interventions, ensuring the robustness of the designed controller, and contributing to the dissemination of optimal personalized closed-loop interventions on a large scale.

Chapter 8

SUMMARY, CONCLUSIONS AND FUTURE WORK

8.1 Summary and Conclusions

This dissertation has demonstrated the effectiveness of applying system identification and control systems engineering principles in behavioral interventions, with physical activity interventions presented as a proof of concept. Mobile health (mHealth) interventions have gained traction in recent years. This is particularly the case for physical activity interventions, because of the availability of temporally dense data through advances in wearable technology (e.g., smartwatches, activity trackers). While the efficacy of behavioral interventions in promoting healthy behaviors has been demonstrated during active intervention periods, the sustained impact of such interventions remains limited. This is mainly because full knowledge of the dynamic nature of behavior change on an individual level is not available and a framework to personalize and automate the delivery of such interventions over long periods is lacking. System identification and control system engineering principles provide a synergistic approach to address these gaps in knowledge and facilitate the delivery of personalized interventions (Hekler *et al.*, 2016; Rivera *et al.*, 2018). This dissertation builds on previous work by establishing and validating the control optimization trial (COT) framework.

The main challenges limiting the dissemination of physical activity interventions on a large scale include the absence of a validated first-principle model structure describing the dynamics of behavior change. Previous work by Martín *et al.* (2020) proposed a dynamical systems model based on Social Cognitive Theory (SCT; Ban-

dura (1986)), which served as the basis for the design of a system identification experiment under the name of *JustWalk*. This work extends the previously postulated model to include separate and possibly competing dynamics of different facets of SCT behavioral constructs, particularly fatigue and fitness as measurable behavioral outcomes. Additionally, the enhanced model is used to formulate improved Model Predictive Control (MPC) strategies for closed-loop interventions and test these in simulated settings ahead of real-world implementation. The strategies developed address important limitations faced in behavioral interventions, such as unreliable measurements for behavioral constructs that may result from poor participant adherence (see Chapter 4).

Control strategies for physical activity interventions presented in this work are expressed in a Three Degrees-of-Freedom by means of Kalman Filtering Hybrid Model Predictive (3DoF-KF HMPC) formulation. HMPC relies on a Mixed Logical Dynamics (MLD) framework that incorporates categorical and logical conditions into the controller objective as linear inequality constraints, resulting in a mixed integer quadratic programming (MIQP) problem. In this dissertation, the HMPC formulation is improved to incorporate conditions based on decisions made in previous instances and feedback from the participant's responses. This allows for incorporating decisions relating to intervention components over the move horizon (e.g., having positive reinforcement with financial rewards), improving the efficiency of the control strategy. This dissertation evaluates the performance and the robustness of the 3DoF-KF HMPC controller in delivering personalized interventions in Monte Carlo simulations for a representative *JustWalk* participant, utilizing black-box Auto Regressive with eXogenic inputs (ARX; Ljung (1999)) model estimation, as presented in Chapter 5. The use *JustWalk* data in validating the devised 3DoF-KF HMPC formulation for physical activity interventions is instrumental in the development of

the first COT study *YourMove* (R01CA244777, 2020).

Additionally, this dissertation has leveraged findings and knowledge gained from analyzing *JustWalk* data in improving input signals design for two separate studies *YourMove* and *JustWalk Just-In-Time-Adaptive-Intervention (JITAI)* (R01LM013107, 2020). For *YourMove*, *a priori* knowledge from *JustWalk* guided the use of multi-sines signals for the two components of the intervention (goal-setting and positive reinforcement). In particular, the time constants obtained from models estimated for representative *JustWalk* participants are used to define parameters in input signal design based on "plant-friendly" guidelines Deshpande *et al.* (2014). Furthermore, the insights gained from *JustWalk* data analysis provided the basis for selecting the effective frequency range for the designed input signals, using more excited harmonics, and utilizing a relative amplitude for non-excited high-frequency harmonics of 0.5 (see Chapter 6).

In *YourMove*, the input signals are personalized in two ways: 1) different realizations of the design input signals are generated for each participant on the first day of the system identification stage, and 2) the maximum and minimum values of the delivered goals in the goal-setting component of the intervention for each participant are dictated by the participant's median performance in the baseline stage. In addition, to estimate personalized ARX models in *YourMove*, Discrete Stochastic Perturbation Simultaneous Approximation (DSPSA; Wang and Spall (2011)) is used to optimize model structure (online and overnight) for each participant, in terms of model orders and selected features, as presented in Chapter 6.

The work summarized above formed the pillars over which the first COT study was built, under the name of *YourMove*. Based on monitoring *YourMove* closed-loop results the utilized control strategies are updated, generating the "digital PA coach tuning" algorithm for adaptive controller tuning and controller reconfiguration based

on each participant's performance. This dissertation presents unprecedented closed-loop intervention results for representative *YourMove* participants, illustrating the effectiveness of the devised control strategies and robustness of the 3DoF-KF HMPC formulation in real-world experimental settings. As *YourMove* is still underway, the findings presented in this dissertation remain to be generalized. However, these show significant potential for the efficacy of personalized optimal closed-loop intervention in guiding participants towards healthy levels of daily steps and helping them sustain this healthy behavior over extended periods of time.

In addition, the work in this dissertation explores multi-timescale dynamics of behavior change processes in the context of just-in-time (JIT) states, forming the groundwork for the development closed-loop just-in-time adaptive interventions (JITAIs; Perski *et al.* (2022); Klasnja *et al.* (2015); Nahum-Shani *et al.* (2015)). JIT states are conceptualized as conditions over which the participant would respond favorably to support provided as a part of the intervention. Therefore, support provided in JIT states can contribute to adaptations over time that result in sustained behavior change. To further understand these concepts, a comprehensive system identification and signal processing approach is researched in one of the first empirical studies of JIT states based on system identification principles under the name of *JustWalk JITAI*.

In this dissertation, innovative input signals are designed and implemented in *JustWalk JITAI*, providing informative data sets through the excitation of harmonics at frequencies of interest, while operationalizing JIT states as one of the intervention components, as described in Chapter 2. Moreover, advanced data-driven signal processing and modeling approaches are evaluated on a representative *JustWalk JITAI* participant. Specifically, singular spectrum analysis (SSA; Elsner and Tsonis (2013)) is used for noise reduction and to study the separability of the measured behavior signal into uncorrelated components describing behavior change dynamics at different

frequencies. In addition, the use Model-on-Demand (MoD; Stenman (1999)) is explored as a technique that can capture nonlinearities associated with behavior change systems in context of JIT states. MoD is a data-driven approach that estimates local models based on data in a neighborhood in regressor space around each operating point under a global structure. The results presented in Chapter 3 in this dissertation demonstrate the efficacy of the input signal design in providing dynamically informative data; the effectiveness of SSA in systematically filtering noise in behavior signals and decomposing physical activity behavior signals into signals that explain the overall trend and cyclicality; and the benefit of MoD as a modeling approach that can explain idiosyncrasies of behavior change within JIT context.

Finally, the work in this dissertation leverages data from the *HearSteps II* study in examining dynamical process models for engagement in physical activity interventions, and addressing the ubiquitous problem of data missingness in mHealth interventions. Fluid analogies developed in collaboration with behavioral scientists are used to conceptualize a model for engagement in *HeartSteps II*, and consequently translate it into a computational model. This computational model is transferred to a Dynamic Bayesian Network representation that serves as the basis for a Bayesian inference technique for data imputation, utilizing Markov Chain Monte Carlo methods to sample from the joint posterior distribution of model parameters and missing data points given the observed variables through the BaysLDM toolbox (Tung *et al.*, 2022). This method allows for informed data imputation by incorporating underlying assumptions about system dynamics into the posterior distribution capturing uncertainty due to both data scarcity and missingness. Consequently, multiple realizations of the sampled data are obtained. ARX model estimation is performed on the different realizations of the imputed data sets, propagating the uncertainty into the estimated system dynamics, as presented in Chapter 7.

Overall, this dissertation contributes to a legacy of continuous innovations in the application of system identification, signal processing, and control systems engineering principles in behavioral medicine. The culmination of years of research has come to fruition in the implementation and clinical evaluation of one of the first-of-its-kind closed-loop behavioral interventions following the COT framework, in another step toward improving the efficiency and accessibility of mHealth interventions. The tools developed, data generated, and findings in this research work provide a strong foundation and provide necessary knowledge for future COT interventions, in diverse application settings.

8.2 Future Research Directions

This dissertation has presented preliminary results from the first COT study (*YourMove*) demonstrating the potential of personalized optimal behavioral interventions based on control system engineering principles. The tools and approaches developed, and lessons learned in this work can be extended toward developing future COT interventions, including the currently under-development Healthy Moms Zone 2.0 study (HMZ 2.0; R01DK134863 (2020)). Furthermore, data from *YourMove* and *JustWalk JITAI* provides many research opportunities for scientific exploration and furthering the understanding of the dynamic nature of behavior change systems.

8.2.1 Within-day Models

In the presented work, SSA and MoD have been implemented on daily-level data. To better understand the dynamic responses of participants to notifications sent within a day, this approach can be applied to data where the accumulative step count on each day is sampled at a higher rate (e.g., 3-hour window). This produces significantly longer data sets, however, measurement noise should increase. In addi-

tion, within-day signals contain oscillatory behavior due to resetting the accumulative step count to zero at the beginning of every day. Therefore, SSA can be used to decompose this signal into components, separating the overall trend from daily periodic patterns and discarding noisy components. As a result, multi-timescale models can be estimated by modeling each group of correlated components separately.

MoD can also be used to estimate models for each SSA decomposed component of the accumulative step count signal. With the implemented input signal design and the available inputs, the obtained models should be able to capture short-term and long-term dynamic responses of notifications sent at different conditions, including JIT states. This is especially the case, as longer databases will allow including more exogenous inputs (e.g., day of the week, time of the day, etc) in the MoD estimator's database, to better define conditions of the operating point in regressor space.

8.2.2 YourMove JITAI

The algorithms and methods developed and explored throughout this work can be combined to deliver a closed-loop JITAI, following the COT framework, which can be called *YourMove JITAI*. To conduct such a study, the input signal design presented in this work can be refined and improved after secondary data analysis of experimental *JustWalk JITAI* data for all participants. In this extension of *YourMove*, data imputation can be handled utilizing the Bayesian inference techniques presented in this work (see Chapter 7) based on a DBN representation of the OLSE subsystem of the SCT model (see Chapter 4), instead of utilizing the moving average over the last observed data points.

Optimization over intervention components in JITAIs can be formulated as a multi-timescale dynamic problem, which provides opportunities to investigate methods to judiciously formulate such a complex closed-loop problem. For instance, de-

cisions regarding sending notifications need to be made within-day. On the other hand, decisions pertaining to goal-setting, expected points, and which decision rules to use for notifications must be made on a daily level. Two approaches are proposed to accomplish this task, which can be applied using the different tools and methods evaluated in this dissertation:

Daily Level Control

This approach is the simpler approach of the two. In this approach, only one controller is commissioned for decision-making on all intervention components on a daily level, while actuation on sending notifications within day is left to the same algorithm implemented in *JustWalk JITAI*. The decision rules by which notifications are actuated are considered as a categorical manipulated variable. The controller can be formulated by integrating MoD within the 3DoF-KF HMPC structure (illustrated in Fig. 8.1), allowing it to make personalized optimal decisions while considering the impact of conditions at the operating point, including JIT states.

To construct the database for the MoD optimizer, SSA can be used to reduce measurement noise in the daily step count signal. Another possible implementation to investigate is the utilization of the accumulative daily step count signal, sampled at a higher rate (e.g., 3-hour window). SSA can be used to decompose this signal into its components, and then reconstruct the signal excluding high-frequency components. Consequently, a smoothed signal of the accumulative daily step count can be obtained, which then can be resampled on a daily level and used in the MoD estimator's database.

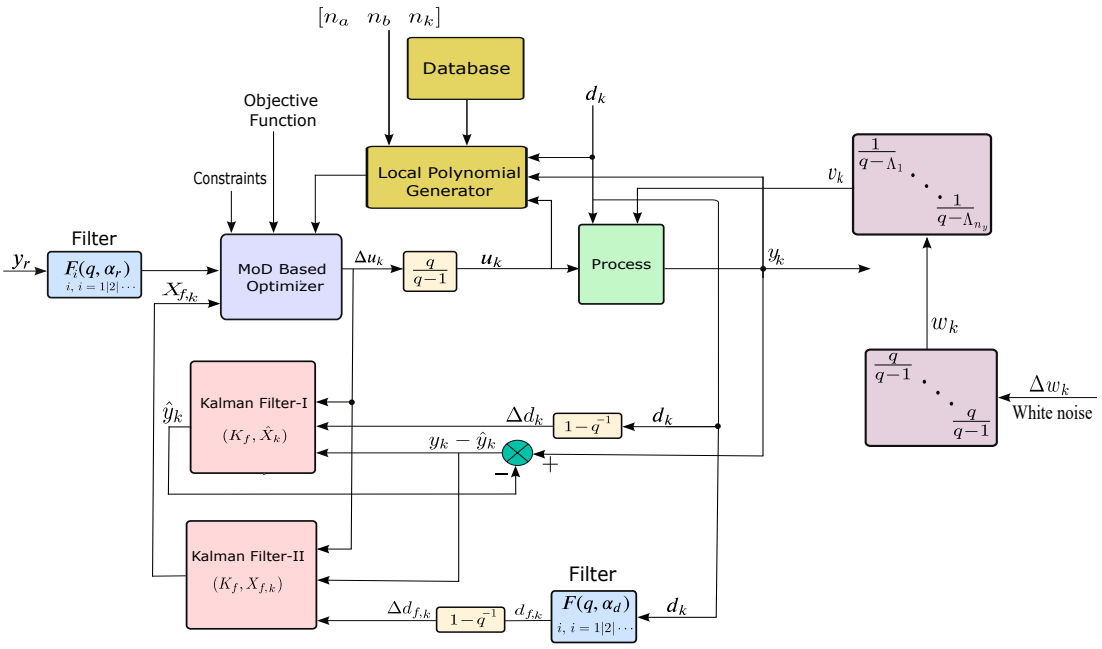

Figure 8.1: Block Diagram Schematic Representing a Proposed MoD-Based 3DoF-KF MPC for Setpoint Tracking of a Process Subject to Constraints, Measured and Unmeasured Disturbances. Logical and Categorical Decisions Can Be Included Through the Hybrid Formulation, By Utilizing MLD Matrices and Mixed Integer Quadratic Programming (Banerjee *et al.*, 2024b).

Hierarchical Control

This approach is an extension of the previous one, in which the control problem is broken down into two separate optimization problems. The outer controller can be formulated following Section 8.2.2, allowing it to manipulate intervention components on a daily level, including providing daily goals and expected points, as well as selecting the decision rules followed in sending notifications. The inner controller handles decision-making on an intraday level, including granting points upon achieving the goal given on a certain day and whether to send notifications or not, at each decision point within the day. The HMPC formulation can be used to translate the logical con-

ditions defined by the decision rules manipulated variable, selected by the daily-level controller, into linear inequality constraints for the inner controller. Additionally, MoD optimizer can be used to estimate a local predictive model for the controller at each decision point, following 3DoF-KF MOD-HMPC structure. The MoD optimizer database for the intraday controller can be constructed by applying SSA on the 3-hour sampled accumulative daily step count as proposed in Section 8.2.1.

8.2.3 Semiphysical Modeling

First-principle models based on fluid analogies have been proposed to generate dynamic hypotheses and translate conceptual theories of behavior change into computational models explaining the dynamic nature of behavior change (Hekler *et al.*, 2016; Rivera *et al.*, 2018). In this work, a fluid analogy SCT-based dynamic process system model is presented and used as the basis for the design of *YourMove* and *JustWalk JITAI* studies. Data from both studies has been used to estimate participant-specific utilizing black-box modeling techniques. The obtained models partially validate some aspects of the proposed dynamical process system SCT model, however, further research and investigation are needed to fully validate the model structure. The informative datasets obtained from both studies (*YourMove* and *JustWalk JITAI*) provide opportunities to accomplish this task and further the understanding of the dynamic nature of behavior change. Grey-box modeling methods can be used to leverage the experimental data from these studies in validating the first-principle model of SCT derived from the fluid analogy and estimating participant-specific model parameters.

As demonstrated in this dissertation, the application of system identification, signal processing, data science, and control systems engineering in behavioral medicine is of great promise. Prospects include furthering the understanding of the dynamic nature of behavior change through the lens of dynamical process systems, analyzing

and estimating models that capture idiosyncrasies within a population and idiosyncrasies for individuals in context, and automating the delivery of optimal personalized behavioral interventions. All of these contribute to the paradigm shift in behavioral medicine and serve the purpose of the dissemination of preventive interventions on a large scale to improve individual and public health.

Adams, M. A., J. F. Sallis, G. J. Norman, M. F. Hovell, E. B. Hekler and E. Perata, "An adaptive physical activity intervention for overweight adults: A randomized controlled trial", PloS one **8**, 12, e82901 (2013).

Ahn, A. C., M. Tewari, C.-S. Poon and R. S. Phillips, "The limits of reductionism in medicine: could systems biology offer an alternative?", PLoS medicine **3**, 6, e208 (2006).

Aksakalli, V. and M. Malekipirbazari, "Feature selection via binary simultaneous perturbation stochastic approximation", Pattern Recognition Letters **75**, 41–47 (2016).

Australian Government Department of Health, "About physical activity and exercise", URL `https://www.health.gov.au/health-topics/physical-activity-and-exercise/about-physical-activity-and-exercise?utm_source=health.gov.au&utm_medium=callout-auto-custom&utm_campaign=digital_transformation` (2021).

Bandura, A., "Self-efficacy: toward a unifying theory of behavior change", Psychological Review **84**, 191–215 (1977).

Bandura, A., *Social Foundations of Thought and Action: A Social Cognitive Theory* (Prentice-Hall series in social learning theory, 1986).

Bandura, A., "Human agency in social cognitive theory.", American Psychologist **44**, 9, 1175–1184 (1989).

Bandura, A. and R. H. Walters, *Social Learning and Personality Development* (New York : Holt, Rinehart and Winston, 1963).

Banerjee, S., R. T. Kha, D. E. Rivera and E. B. Hekler, "Predicting goal attainment in control-oriented behavioral interventions using a data-driven system identification approach", Journal of Process Control In-Press (2024a).

Banerjee, S., O. Khan, M. El Mistiri, N. N. Nandola and D. E. Rivera, "Data-Driven Control of Highly Interactive Systems using 3DoF Model-On-Demand MPC: Application to a MIMO CSTR", in "IFAC Symposium on System Identification (SYSID 2024)", (IFAC, 2024b), In Press.

Bell, M. L., M. Fiero, N. J. Horton and C.-H. Hsu, "Handling missing data in rcts; a review of the top medical journals", BMC Medical Research Methodology **14**, 1, 1–8 (2014a).

Bell, M. L., M. Fiero, N. J. Horton and C.-H. Hsu, "Handling missing data in RCTs; a review of the top medical journals", BMC Med. Res. Methodol. **14**, 1, 118 (2014b).

Bender, C. G., J. C. Hoffstot, B. T. Combs, S. Hooshangi and J. Cappos, "Measuring the fitness of fitness trackers", in "2017 IEEE Sensors Applications Symposium (SAS)", pp. 1–6 (IEEE, 2017).

Bohlin, T., "A case study of grey box identification", Automatica **30**, 2, 307–318 (1994).

Bollen, K. A., *Structural Equations with Latent Variables* (New York : Wiley, 1989), 1st edn.

Booth, F. W., C. K. Roberts and M. J. Laye, "Lack of exercise is a major cause of chronic diseases", Comprehensive physiology **2**, 2, 1143 (2012).

Bordons, C. and E. F. Camacho, *Model Predictive Control* (Springer Verlag London Ltd, 2007).

Braun, M., R. Ortiz-Mojica and D. Rivera, "Application of minimum crest factor multisinusoidal signals for "plant-friendly" identification of nonlinear process systems", Control Engineering Practice **10**, 3, 301–313 (2002).

Braun, M. W., *Model-on-demand nonlinear estimation and model predictive control: Novel methodologies for process control and supply chain management* (Arizona State University, 2001).

Braun, M. W., D. E. Rivera and A. Stenman, "A Model-on-Demand identification methodology for nonlinear process systems", Int. J. Control **74**, 18, 1708 – 1717 (2001).

Carver, C. S. and M. F. Scheier, *On the Self Regulation of Behavior* (Cambridge University Press, 1998).

Centers for Disease Control and Prevention, "Adult physical inactivity prevalence maps by race/ethnicity", URL `https://www.cdc.gov/physicalactivity/data/inactivity-prevalence-maps/index.html` (2021).

Cevallos, D., C. A. Martín, M. El Mistiri, D. E. Rivera and E. Hekler, "Un esquema de decisiones para intervenciones adaptativas comportamentales de actividad física basado en control predictivo por modelo híbrido: ilustración con Just Walk", Revista Iberoamericana de Automática e Informática Industrial **19**, 3, 297–308 (2022).

Cloutier, M. and E. Wang, "Dynamic modeling and analysis of cancer cellular network motifs", Integrative Biology **3**, 7, 724–732 (2011).

Cole-Lewis, H., N. Ezeanochie, J. Turgiss *et al.*, "Understanding health behavior technology engagement: pathway to measuring digital behavior change interventions", JMIR formative research **3**, 4, e14052 (2019).

Collins, L. M., S. A. Murphy and K. L. Bierman, "A conceptual framework for adaptive preventive interventions", Prevention science **5**, 3, 185–196 (2004).

Conroy, D. E., S. Elavsky, A. L. Hyde and S. E. Doerksen, "The dynamic nature of physical activity intentions: a within-person perspective on intention-behavior coupling", Journal of Sport & Exercise Psychology **33**, 6, 807 (2011).

de Wit, C. C., B. Siciliano and G. Bastin, *Theory of robot control* (Springer Science & Business Media, 2012).

Deci, E. L. and R. M. Ryan, "Self-determination theory", Handbook of theories of social psychology **1**, 20, 416–436 (2012).

Department for Digital Culture, "Sporting future - first annual report", URL `https://www.gov.uk/government/publications/sporting-future-first-annual-report` (2017).

Deshpande, S., N. N. Nandola, D. E. Rivera and J. W. Younger, "Optimized treatment of fibromyalgia using system identification and hybrid model predictive control", Control Engineering Practice **33**, 161–173 (2014).

Dong, Y., *A novel control engineering approach to designing and optimizing adaptive sequential behavioral interventions*, Ph.D. thesis, Chemical Engineering, Arizona State University (2014).

Dong, Y., S. Deshpande, D. E. Rivera, D. S. Downs and J. S. Savage, "Hybrid model predictive control for sequential decision policies in adaptive behavioral interventions", in "Proceedings of the American Control Conference", pp. 4198–4203 (2014).

Dong, Y., D. E. Rivera, D. S. Downs, J. S. Savage, D. M. Thomas and L. M. Collins, "Hybrid model predictive control for optimizing gestational weight gain behavioral interventions", in "Proceedings of the American Control Conference", pp. 1973 – 1978 (2013).

Dong, Y., D. E. Rivera, D. M. Thomas, J. E. Navarro-Barrientos, D. S. Downs, J. S. Savage and L. M. Collins, "A dynamical systems model for improving gestational weight gain behavioral interventions", in "Proceedings of the American Control Conference", pp. 4059–4064 (2012).

Downs, D. S., J. S. Savage, D. E. Rivera, J. M. Smyth, B. J. Rolls, E. E. Hohman, K. M. McNitt, A. R. Kunselman, C. Stetter, A. M. Pauley *et al.*, "Individually tailored, adaptive intervention to manage gestational weight gain: protocol for a randomized controlled trial in women with overweight and obesity", JMIR research protocols **7**, 6, e9220 (2018).

El Mistiri, M., O. Khan, D. E. Rivera and E. Hekler, "System identification and hybrid model predictive control in personalized mhealth interventions for physical activity", in "2023 American Control Conference (ACC)", pp. 2240–2245 (IEEE, 2023).

El Mistiri, M., D. E. Rivera, P. Klasnja, J. Park and E. Hekler, "Enhanced Social Cognitive Theory dynamic modeling and simulation towards improving the estimation of 'just-in-time' states", in "2022 American Control Conference (ACC)", pp. 468–473 (2022a).

El Mistiri, M., D. E. Rivera, P. Klasnja, J. Park and E. Hekler, "Model predictive control strategies for optimized mHealth interventions for physical activity", in "2022 American Control Conference (ACC)", pp. 1392–1397 (2022b).

Elsner, J. B. and A. A. Tsonis, *Singular spectrum analysis: a new tool in time series analysis* (Springer Science & Business Media, 2013).

Eren, U., A. Prach, B. B. Koçer, S. V. Raković, E. Kayacan and B. Açıkmeşe, "Model predictive control in aerospace systems: Current state and opportunities", Journal of Guidance, Control, and Dynamics **40**, 7, 1541–1566 (2017).

Fielding, J. E., "Smoking: health effects and control", New England journal of medicine **313**, 9, 555–561 (1985).

Ford, A. and F. A. Ford, *Modeling the environment: an introduction to system dynamics models of environmental systems* (Island press, 1999).

Freigoun, M. T., C. A. Martín, A. B. Magann, D. E. Rivera, S. S. Phatak, E. V. Korinek and E. B. Hekler, "System identification of just walk: A behavioral mhealth intervention for promoting physical activity", in "2017 American Control Conference (ACC)", pp. 116–121 (2017).

Gaikwad, S. and D. Rivera, "Control-relevant input signal design for multivariable system identification: Application to high-purity distillation", IFAC Proceedings Volumes **29**, 1, 6143–6148, URL `https://www.sciencedirect.com/science/article/pii/S1474667017586668`, 13th World Congress of IFAC, 1996, San Francisco USA, 30 June - 5 July (1996).

Galvanin, F., M. Barolo and F. Bezzo, "Online redesign of clinical tests for the identification of type 1 diabetes models in the presence of continuous glucose monitoring systems", IFAC Proceedings Volumes **44**, 1, 8328–8333 (2011).

García, C. E., D. M. Prett and M. Morari, "Model predictive control: Theory and practice—a survey", Automatica **25**, 3, 335–348, URL `https://www.sciencedirect.com/science/article/pii/0005109889900022` (1989).

Golyandina, N., V. Nekrutkin and A. A. Zhigljavsky, *Analysis of time series structure: SSA and related techniques* (CRC press, 2001).

Gondhalekar, R., E. Dassau and F. J. Doyle III, "Periodic zone-mpc with asymmetric costs for outpatient-ready safety of an artificial pancreas to treat type 1 diabetes", Automatica **71**, 237–246 (2016).

Guillaume, P., J. Schoukens, R. Pintelon and I. Kollar, "Crest-factor minimization using nonlinear Chebyshev approximation methods", IEEE Transactions on Instrumentation and Measurement **40**, 6, 982–989 (1991).

Guo, P., *System Identification, State Estimation, And Control Approaches to Gestational Weight Gain Interventions*, Ph.D. thesis, Arizona State University (2018).

Guo, P., D. E. Rivera, J. S. Savage, E. E. Hohman, A. M. Pauley, K. S. Leonard and D. S. Downs, "System identification approaches for energy intake estimation: Enhancing interventions for managing gestational weight gain", IEEE Transactions on Control Systems Technology **28**, 1, 63–78 (2020).

Hassani, H. and A. Zhigljavsky, "Singular spectrum analysis: methodology and application to economics data", Journal of Systems Science and Complexity **22**, 372–394 (2009).

Hayati Rezvan, P., K. J. Lee and J. A. Simpson, "The rise of multiple imputation: a review of the reporting and implementation of the method in medical research", BMC Med. Res. Methodol. **15**, 1, 30 (2015).

Hekler, E., "*Just Walk* Study", `http://justwalkstudy.weebly.com/`, [Online; accessed September-23-2020] (2015).

Hekler, E., personal communication (2021).

Hekler, E. B., P. Klasnja, W. T. Riley, M. P. Buman, J. Huberty, D. E. Rivera and C. A. Martin, "Agile science: creating useful products for behavior change in the real world", Translational Behavioral Medicine **6**, 2, 317–328, URL `https://doi.org/10.1007/s13142-016-0395-7` (2016).

Hekler, E. B., P. Klasnja, V. Traver and M. Hendriks, "Realizing effective behavioral management of health: the metamorphosis of behavioral science methods", IEEE pulse **4**, 5, 29–34 (2013).

Hekler, E. B., D. E. Rivera, C. A. Martin, S. S. Phatak, M. T. Freigoun, E. Korinek, P. Klasnja, M. A. Adams and M. P. Buman, "Tutorial for using control systems engineering to optimize adaptive mobile health interventions", Journal of Medical Internet Research **20**, 6, e8622 (2018).

Hoffman, M. D., A. Gelman *et al.*, "The no-u-turn sampler: adaptively setting path lengths in hamiltonian monte carlo.", J. Mach. Learn. Res. **15**, 1, 1593–1623 (2014).

Jakobsen, J. C., C. Gluud, J. Wetterslev and P. Winkel, "When and how should multiple imputation be used for handling missing data in randomised clinical trials–a practical guide with flowcharts", BMC medical research methodology **17**, 1, 1–10 (2017).

Karahalios, A., L. Baglietto, J. B. Carlin, D. R. English and J. A. Simpson, "A review of the reporting and handling of missing data in cohort studies with repeated assessment of exposure measures", BMC Med. Res. Methodol. **12**, 1, 96 (2012).

Kessler, R. and R. E. Glasgow, "A proposal to speed translation of healthcare research into practice: dramatic change is needed", American journal of preventive medicine **40**, 6, 637–644 (2011).

Kha, R. T., D. E. Rivera, P. Klasnja and E. Hekler, "Model personalization in behavioral interventions using model-on-demand estimation and discrete simultaneous perturbation stochastic approximation", in "2022 American Control Conference", pp. 671–676 (IEEE, 2022).

Khan, O., M. El Mistiri, D. E. Rivera, C. A. Martin and E. B. Hekler, "A Kalman filter-based hybrid model predictive control algorithm for mixed logical dynamical systems: Application to optimized interventions for physical activity", in "61st IEEE Conference on Decision and Control - Dec. 6-9, 2022", pp. 2586–2593 (IEEE, 2022).

King, A. C., E. B. Hekler, L. A. Grieco, S. J. Winter, J. L. Sheats, M. P. Buman, B. Banerjee, T. N. Robinson and J. Cirimele, "Harnessing different motivational frames via mobile phones to promote daily physical activity and reduce sedentary behavior in aging adults", PLoS ONE **8**, 4, e62613 (2013).

Kitano, H., "Systems biology: a brief overview", science **295**, 5560, 1662–1664 (2002).

Klasnja, P., personal communication (2021).

Klasnja, P., E. B. Hekler, S. Shiffman, A. Boruvka, D. Almirall, A. Tewari and S. A. Murphy, "Microrandomized trials: An experimental design for developing just-in-time adaptive interventions", Health Psychology **34**, 1220–1228, URL `http://login.ezproxy1.lib.asu.edu/login?url=https://www-proquest-com.ezproxy1.lib.asu.edu/scholarly-journals/microrandomized-trials-experimental-design/docview/1749218507/se-2?accountid=4485` (2015).

Klein, A. P., K. Yarbrough and J. W. Cole, "Stroke, smoking and vaping: the no-good, the bad and the ugly", Annals of public health and research **8**, 1 (2021).

Korinek, E. V., S. S. Phatak, C. A. Martin, M. T. Freigoun, D. E. Rivera, M. A. Adams, P. Klasnja, M. P. Buman and E. B. Hekler, "Adaptive step goals and rewards: a longitudinal growth model of daily steps for a smartphone-based walking intervention", Journal of behavioral medicine **41**, 1, 74–86 (2018).

Kurzhanski, A. and I. Vályi, *Ellipsoidal calculus for estimation and control* (Springer, 1997).

Lang, K. M. and T. D. Little, "Principled missing data treatments", Prev. Sci. **19**, 3, 284–294 (2018).

Lee, H. and D. E. Rivera, *A plant-friendly multivariable system identification framework based on identification test monitoring*, Ph.D. thesis, Arizona State University, URL `http://login.ezproxy1.lib.asu.edu/login?url=https://www.proquest.com/dissertations-theses/plant-friendly-multivariable-system/docview/305357968/se-2?accountid=4485` (2006).

Lee, J. H., M. Morari and C. E. García, "State-space interpretation of model predictive control", Automatica **30**, 4, 707 – 717 (1994).

Lee, J. H. and Z. H. Yu, "Tuning of model predictive controllers for robust performance", Comput. Chem. Eng. **18**, 1, 15 – 37 (1994).

Leonard, D., N. Van Long and V. L. Ngo, *Optimal control theory and static optimization in economics* (Cambridge University Press, 1992).

Liu, X., Y. Zhang and K. Y. Lee, "Robust distributed mpc for load frequency control of uncertain power systems", Control Engineering Practice **56**, 136–147 (2016).

Ljung, L., "From Data to Model: A Guided Tour", in "International IEE Conference on Control", pp. 422–430 (Warwick, England, 1994).

Ljung, L., *System Identification: Theory for the User* (Upper Saddle River, NJ: Prentice Hall PTR, 1999), 2nd edn.

Ljung, L., R. Singh and T. Chen, "Regularization features in the system identification toolbox", IFAC-PapersOnLine **48**, 28, 745–750, URL `https://www.sciencedirect.com/science/article/pii/S2405896315028438`, 17th IFAC Symposium on System Identification SYSID 2015 (2015).

Loeber, S., B. Croissant, A. Heinz, K. Mann and H. Flor, "Cue exposure in the treatment of alcohol dependence: Effects on drinking outcome, craving and self-efficacy", British Journal of Clinical Psychology **45**, 4, 515–529 (2006).

Lopez, L. M., E. E. Tolley, D. A. Grimes and M. Chen-Mok, "Theory-based interventions for contraception", The Cochrane database of systematic reviews **3**, CD007249 (2011).

Luenberger, D. G., *Introduction to dynamic systems: Theory, models, and applications* (J. Wiley & Sons, 2012).

Martín, C. A., S. Deshpande, E. B. Hekler and D. E. Rivera, "A system identification approach for improving behavioral interventions based on Social Cognitive Theory", in "Proceedings of the American Control Conference", pp. 5878–5883 (2015a).

Martín, C. A., D. E. Rivera and E. B. Hekler, "Design of informative identification experiments for behavioral interventions", in "Proceedings of the 17th IFAC Symposium on System Identification", pp. 1325–1330 (2015b).

Martín, C. A., D. E. Rivera and E. B. Hekler, "An identification test monitoring procedure for MIMO systems based on statistical uncertainty estimation", in "Proceedings of the 54th IEEE Conference on Decision and Control", pp. 2719–2724 (2015c).

Martín, C. A., *A system identification and control engineering approach for optimizing mHealth behavioral interventions based on social cognitive theory*, Ph.D. thesis, Arizona State University (2016).

Martín, C. A., D. E. Rivera and E. B. Hekler, "A decision framework for an adaptive behavioral intervention for physical activity using hybrid model predictive control", in "2016 American Control Conference (ACC)", pp. 3576–3581 (2016a).

Martín, C. A., D. E. Rivera and E. B. Hekler, "An enhanced identification test monitoring procedure for mimo systems relying on uncertainty estimates", in "2016 IEEE 55th Conference on Decision and Control (CDC)", pp. 2091–2096 (2016b).

Martín, C. A., D. E. Rivera, E. B. Hekler, W. T. Riley, M. P. Buman, M. A. Adams and A. B. Magann, "Development of a control-oriented model of social cognitive theory for optimized mhealth behavioral interventions", IEEE Transactions on Control Systems Technology **28**, 2, 331–346 (2020).

Martín, C. A., D. E. Rivera, W. T. Riley, E. B. Hekler, M. P. Buman, M. A. Adams and A. C. King, "A dynamical systems model of Social Cognitive Theory", in "2014 American Control Conference", pp. 2407–2412 (2014).

McGinnis, J. M., P. Williams-Russo and J. R. Knickman, "The case for more active policy attention to health promotion", Health Affairs **21**, 2, 78–93 (2002).

Mclaughlin, M., T. Delaney, A. Hall, J. Byaruhanga, P. Mackie, A. Grady, K. Reilly, E. Campbell, R. Sutherland, J. Wiggers and L. Wolfenden, "Associations between digital health intervention engagement, physical activity, and sedentary behavior: Systematic review and meta-analysis", J. Med. Internet Res. **23**, 2, e23180 (2021).

Mesbah, A., "Stochastic model predictive control: An overview and perspectives for future research", IEEE Control Systems Magazine **36**, 6, 30–44 (2016).

Mohammadpour, J. and C. W. Scherer, *Control of linear parameter varying systems with applications* (Springer Science & Business Media, 2012).

Morari, M. and E. Zafiriou, *Robust Process Control* (Prentice-Hall International, 1989).

Murphy, K. P. *et al.*, "Dynamic bayesian networks", Probabilistic Graphical Models, M. Jordan **7**, 431 (2002).

Nacev, A., A. Komaee, A. Sarwar, R. Probst, S. H. Kim, M. Emmert-Buck and B. Shapiro, "Towards control of magnetic fluids in patients: directing therapeutic nanoparticles to disease locations", IEEE Control Systems Magazine **32**, 3, 32–74 (2012).

Nahum-Shani, I., E. B. Hekler and D. Spruijt-Metz, "Building health behavior models to guide the development of just-in-time adaptive interventions: A pragmatic framework", Health Psychology **34**, 1209–1219, URL `http://login.ezproxy1.lib.asu.edu/login?url=https://www-proquest-com.ezproxy1.lib.asu.edu/scholarly-journals/building-health-behavior-models-guide-development/docview/1749218476/se-2?accountid=4485` (2015).

Nandola, N. N. and D. E. Rivera, "An improved formulation of hybrid model predictive control with application to production-inventory systems", IEEE Transactions on Control Systems Technology **21**, 1, 121–135 (2013).

Navarro-Barrientos, J.-E., D. E. Rivera and L. M. Collins, "A dynamical model for describing behavioural interventions for weight loss and body composition change", Mathematical and Computer Modelling of Dynamical Systems **17**, 2, 183–203 (2011).

Norman, G. J., M. F. Zabinski, M. A. Adams, D. E. Rosenberg, A. L. Yaroch and A. A. Atienza, "A review of eHealth interventions for physical activity and dietary behavior change", American Journal of Preventive Medicine **33**, 4, 336–345.e16 (2007).

Ogunnaike, B. and W. H. Ray, *Process Dynamics, modeling and Control* (Oxford University Press, 1995).

Olson, R. D., K. L. Piercy, R. P. Troiano, R. M. Ballard, J. E. Fulton, D. A. Galuska, S. Y. Pfohl, A. Vaux-Bjerke, J. B. Quam, S. M. George, K. Sprow, S. A. Carlson, E. T. Hyde and K. Olscamp, "Physical activity guidelines for americans 2nd edition", (2018).

O'Shea, P., "Future medicine shaped by an interdisciplinary new biology", The Lancet **379**, 9825, 1544–1550 (2012).

pandas development team, T., "pandas.dataframe.bfill", `https://pandas.pydata.org/pandas-docs/stable/reference/api/pandas.DataFrame.bfill.html#pandas.DataFrame.bfill` (2022).

Park, J., M. Kim, M. El Mistiri, R. Kha, S. Banerjee, L. Gotzian, G. Chevance, D. E. Rivera, P. Klasnja, E. Hekler *et al.*, "Advancing Understanding of Just-in-Time States for Supporting Physical Activity (Project JustWalk JITAI): Protocol for a System ID Study of Just-in-Time Adaptive Interventions", JMIR Research Protocols **12**, 1, e52161 (2023).

Payne, H. E., C. Lister, J. H. West and J. M. Bernhardt, "Behavioral functionality of mobile apps in health interventions: A systematic review of the literature", JMIR mHealth and uHealth **3**, 1, e20 (2015).

Perski, O., A. Blandford, R. West and S. Michie, "Conceptualising engagement with digital behaviour change interventions: a systematic review using principles from critical interpretive synthesis", Transl. Behav. Med. **7**, 2, 254–267 (2017).

Perski, O., E. T. Hébert, F. Naughton, E. B. Hekler, J. Brown and M. S. Businelle, "Technology-mediated just-in-time adaptive interventions (JITAIs) to reduce harmful substance use: A systematic review", Addiction **117**, 5, 1220–1241 (2022).

Phatak, S. S., M. T. Freigoun, C. A. Martín, D. E. Rivera, E. V. Korinek, M. A. Adams, M. P. Buman, P. Klasnja and E. B. Hekler, "Modeling individual differences: A case study of the application of system identification for personalizing a physical activity intervention", Journal of Biomedical Informatics **79**, 82–97 (2018).

Phatak, S. S., E. B. Hekler, D. E. Rivera, C. A. Martín and M. T. Freigoun, "Building a Dynamical Model to Predict "Ambitious but Doable" Daily Step Goals", in "Annual Meeting of the Society of Behavioral Medicine", (United States, Washington DC, 2016).

Pillonetto, G., F. Dinuzzo, T. Chen, G. De Nicolao and L. Ljung, "Kernel methods in system identification, machine learning and function estimation: A survey", Automatica **50**, 3, 657–682 (2014).

Prett, D. M. and C. E. García, *Fundamental Process Control* (Butterworths, 1988).

R01CA244777, "Optimizing individualized and adaptive mhealth interventions via control systems engineering methods", URL `https://reporter.nih.gov/search/g7QkpEP3VUS-bXgSgfT-GA/project-details/10051197`, R01CA244777: National Institute of Health, National Cancer Institute (2020).

R01DK134863, "Efficacy of a novel digital platform to scale-up a personalized prenatal weight gain intervention using control systems methodology", URL `https://reporter.nih.gov/search/sP5vehxwF0eFufURM2PsnQ/project-details/10764906`, R01DK134863: National Institute of Diabetes and Digestive and Kidney Diseases (2020).

R01LM013107, "Sch: Control systems engineering for counteracting notification fatigue: An examination of health behavior change", URL `https://reporter.nih.gov/search/0RVNErIwH0atwhKP77LVkA/project-details/10359062`, R01LM013107: National Institute of Health, National Cancer Institute (2020).

Åström, K. J. and R. M. Murray, *Feedback systems: An introduction for scientists and Engineers* (Princeton University Press, 2021).

Ray, L. R. and R. F. Stengel, "A monte carlo approach to the analysis of control system robustness", Automatica **29**, 1, 229–236 (1993).

Riley, W. T., C. A. Martín, D. E. Rivera, E. B. Hekler, M. A. Adams, M. P. Buman, M. Pavel and A. C. King, "Development of a dynamical systems model of social cognitive theory", Translational Behavioral Medicine: Practice, Policy and Research pp. 1 – 13, URL `http://link.springer.com/article/10.1007/s13142-015-0356-6`, published online: 09 November 2015 (2015).

Riley, W. T., C. A. Martin, D. E. Rivera, E. B. Hekler, M. A. Adams, M. P. Buman, M. Pavel and A. C. King, "Development of a dynamic computational model of Social Cognitive Theory", Translational behavioral medicine **6**, 4, 483–495 (2016).

Rioux, C. and T. D. Little, "Missing data treatments in intervention studies: What was, what is, and what should be", International journal of behavioral development **45**, 1, 51–58 (2021).

Rivera, D., M. Braun and H. Mittelmann, "Constrained multisine inputs for plant-friendly identification of chemical processes", IFAC Proceedings Volumes **35**, 1, 425–430, URL `https://www.sciencedirect.com/science/article/pii/S1474667015389035`, 15th IFAC World Congress (2002).

Rivera, D. E., E. B. Hekler, J. S. Savage and D. Symons Downs, "Intensively adaptive interventions using control systems engineering: Two illustrative examples", in "Optimization of Behavioral, Biobehavioral, and Biomedical Interventions", edited by L. M. Collins and K. C. Kugler, pp. 121–173 (Springer, 2018).

Rivera, D. E., H. Lee, H. D. Mittelmann and M. W. Braun, "High-purity distillation", IEEE Control Systems Magazine **27**, 5, 72–89 (2007a).

Rivera, D. E., H. Lee, H. D. Mittelmann and M. W. Braun, "Constrained multisine input signals for plant-friendly identification of chemical process systems", Journal of Process Control **19**, 4, 623–635 (2009).

Rivera, D. E., C. A. Martín, K. P. Timms, S. Deshpande, N. N. Nandola and E. B. Hekler, "Control systems engineering for optimizing behavioral mhealth interventions", Mobile Health: Sensors, Analytic Methods, and Applications pp. 455–493 (2017).

Rivera, D. E., M. D. Pew and L. M. Collins, "Using engineering control principles to inform the design of adaptive interventions: A conceptual introduction", Drug and Alcohol Dependence **88**, S31–S40 (2007b).

Saint-Maurice, P. F., R. P. Troiano, D. R. Bassett, B. I. Graubard, S. A. Carlson, E. J. Shiroma, J. E. Fulton and C. E. Matthews, "Association of daily step count and step intensity with mortality among us adults", The Journal of the American Medical Association **323**, 12, 1151–1160 (2020).

Schoeppe, S., S. Alley, W. Van Lippevelde, N. A. Bray, S. L. Williams, M. J. Duncan and C. Vandelanotte, "Efficacy of interventions that use apps to improve diet, physical activity and sedentary behaviour: a systematic review", International Journal of Behavioral Nutrition and Physical Activity **13**, 1, 1–26 (2016).

Schwartz, J. D., W. Wang and D. E. Rivera, "Simulation-based optimization of process control policies for inventory management in supply chains", Automatica **42**, 8, 1311–1320, URL `https://www.sciencedirect.com/science/article/pii/S0005109806001464` (2006).

Shannon, C. E., "Communication in the presence of noise", Proceedings of the IRE **37**, 1, 10–21 (1949).

Shiffman, S., A. A. Stone and M. R. Hufford, "Ecological momentary assessment", Clinical Psychology **4**, 1, 1–32 (2008).

Shiyko, M. P., J. Burkhalter, R. Li and B. J. Park, "Modeling nonlinear time-dependent treatment effects: an application of the generalized time-varying effect model (tvem).", Journal of consulting and clinical psychology **82**, 5, 760 (2014).

Spall, J. C., "An overview of the simultaneous perturbation method for efficient optimization", Johns Hopkins APL Technical Digest **19**, 4, 482–492 (1998).

Spruijt-Metz, D., E. Hekler, N. Saranummi, S. Intille, I. Korhonen, W. Nilsen, D. E. Rivera, B. Spring, S. Michie, D. A. Asch, A. Sanna, V. T. Salcedo, R. Kukakfa and M. Pavel, "Building new computational models to support health behavior change and maintenance: new opportunities in behavioral research", Transl. Behav. Med. **5**, 3, 335–346 (2015a).

Spruijt-Metz, D., E. Hekler, N. Saranummi, S. Intille, I. Korhonen, W. Nilsen, D. E. Rivera, B. Spring, S. Michie, D. A. Asch, A. Sanna, V. T. Salcedo, R. Kukakfa and M. Pavel, "Building new computational models to support health behavior change and maintenance: new opportunities in behavioral research", Transl. Behav. Med. **5**, 3, 335–346 (2015b).

Spruijt-Metz, D., B. M. Marlin, M. Pavel, D. E. Rivera, E. Hekler, S. De La Torre, M. El Mistiri, N. M. Golaszweski, C. Li, R. Braga De Braganca, K. Tung, R. Kha and P. Klasnja, "Advancing behavioral intervention and theory development for mobile health: The HeartSteps II protocol", Int. J. Environ. Res. Public Health **19**, 4, 2267 (2022).

Stenman, A., *Model on demand: Algorithms, analysis and applications* (Citeseer, 1999).

Stockwell, S., P. Schofield, A. Fisher, J. Firth, S. E. Jackson, B. Stubbs and L. Smith, "Digital behavior change interventions to promote physical activity and/or reduce sedentary behavior in older adults: A systematic review and meta-analysis", Exp. Gerontol. **120**, 68–87 (2019).

Team, T. P. D., "pandas.dataframe.ffill", `https://pandas.pydata.org/docs/reference/api/pandas.DataFrame.ffill.html` (2022).

Tham, M. T., G. A. Montague, A. J. Morris and P. A. Lant, "Soft-sensors for process estimation and inferential control", Journal of Process Control **1**, 1, 3–14 (1991).

Timms, K. P., *A novel engineering approach to modelling and optimizing smoking cessation interventions*, Ph.D. thesis, Biological Design, Arizona State University (2014).

Timms, K. P., C. A. Martín, D. E. Rivera, E. B. Hekler and W. T. Riley, "Leveraging intensive longitudinal data to better understand health behaviors", in "Proceedings of the 36th Annual International Conference of the IEEE Engineering in Medicine and Biology Society", pp. 6888 – 6891 (2014a).

Timms, K. P., D. E. Rivera, L. M. Collins and M. E. Piper, "Understanding and optimizing smoking cessation interventions", in "Proceedings of the American Control Conference", pp. 1967–1972 (2013).

Timms, K. P., D. E. Rivera, L. M. Collins and M. E. Piper, "Continuous-time system identification of a smoking cessation intervention,", International Journal of Control **87**, 7, 1423–1437 (2014b).

Timms, K. P., D. E. Rivera, L. M. Collins and M. E. Piper, "A dynamical systems approach to understanding self-regulation in smoking cessation behavior change", Nicotine and Tobacco Research, Special Issue on New Methods for Advancing Research on Tobacco Dependence Using Ecological Momentary Assessments **16**, Suppl 2, S159–S168 (2014c).

Timms, K. P., D. E. Rivera, M. E. Piper and L. M. Collins, "A hybrid model predictive control strategy for optimizing a smoking cessation intervention", in "Proceedings of the American Control Conference", pp. 2389 – 2394 (2014d).

Torrisi, F. D. and A. Bemporad, "Hysdel-a tool for generating computational hybrid models for analysis and synthesis problems", IEEE transactions on control systems technology **12**, 2, 235–249 (2004).

Tung, K., S. De La Torre, M. El Mistiri, R. B. De Braganca, E. Hekler, M. Pavel, D. Rivera, P. Klasnja, D. Spruijt-Metz and B. M. Marlin, "Bayesldm: A domain-specific modeling language for probabilistic modeling of longitudinal data", in "2022 IEEE/ACM Conference on Connected Health: Applications, Systems and Engineering Technologies (CHASE)", pp. 78–90 (IEEE, 2022).

US Department of Health and Human Services and others, "The health consequences of smoking—50 years of progress: a report of the surgeon general", (2014).

van de Schoot, R., S. Depaoli, R. King, B. Kramer, K. Märtens, M. G. Tadesse, M. Vannucci, A. Gelman, D. Veen, J. Willemsen *et al.*, "Bayesian statistics and modelling", Nature Reviews Methods Primers **1**, 1, 1 (2021).

Wang, Q., *Optimization with Discrete Simultaneous Perturbation Stochastic Approximation Using Noisy Loss Function Measurements*, Ph.D. thesis, Johns Hopkins University (2013).

Wang, Q. and J. C. Spall, "Discrete simultaneous perturbation stochastic approximation on loss function with noisy measurements", in "Proceedings of the 2011 American Control Conference", pp. 4520–4525 (IEEE, 2011).

Wang, Q. and J. C. Spall, "Rate of convergence analysis of discrete simultaneous perturbation stochastic approximation algorithm", in "2013 American Control Conference", pp. 4771–4776 (IEEE, 2013).

Wang, Q. and J. C. Spall, "Discrete simultaneous perturbation stochastic approximation for resource allocation in public health", in "2014 American Control Conference", pp. 3639–3644 (IEEE, 2014).

Yardley, L., B. J. Spring, H. Riper, L. G. Morrison, D. H. Crane, K. Curtis, G. C. Merchant, F. Naughton and A. Blandford, "Understanding and promoting effective engagement with digital behavior change interventions", Am. J. Prev. Med. **51**, 5, 833–842 (2016).

APPENDIX A

CONSENT FOR ACADEMIC USE OF COLLABORATIVE WORK

This statement serves as a formal declaration that all co-authors of the collaborative work in the body of this dissertation document have granted their full permission for the inclusion of the collaborative work as part of this dissertation.

This collaborative transdisplinary work represents a significant portion of the research efforts undertaken by our team and its inclusion in this dissertation is essential for the representation of the complete body of work. Each co-author has been properly informed and has consented to the use of the collaborative material for academic purposes, including but not limited to, its integration, publication, and presentation within the context of the aforementioned dissertation. The co-authors understand that the work will be used for academic purposes, which may include presentations, publications, and other forms of academic dissemination.